Multi-Carrier Code Division Multiple Access

Richard Stirling-Gallacher

A thesis submitted for the degree of Doctor of Philosophy.

The University of Edinburgh.

- August 1997 -

Abstract

The topic of this thesis is the use of multi-carrier modulation with code division multiple access (CDMA). The motivation of this work is to establish if the combination of multi-carrier modulation with CDMA has a performance advantage over a conventional direct sequence CDMA (DS-CDMA) communication system.

In this thesis three types of multi-carrier CDMA are identified and the main work is concentrated on one particular combination, which is referred to as a one chip per carrier multi-carrier CDMA system. This system itself, however, can be split into different variations and an examination of two of these is made.

The first of these one chip per carrier multi-carrier CDMA systems utilises the same number of carriers as the spreading sequence length. The carriers overlap and adjacent chips of the spreading sequence modulate adjacent carriers. There is no guard interval and therefore intercarrier interference occurs. If the receiver is synchronised and has a perfect estimate of the channel, it is shown that this multi-carrier CDMA system has comparable performance to a DS-CDMA system of the same bandwidth. It is further shown that it is simple to compute the minimum mean square error criteria as the equaliser consists of N one tap equalisers, where N is the number of carriers.

The second system utilises many overlapping low data rate orthogonal carriers. The orthogonality of the carriers is maintained due to a cyclically extended guard interval and the number of carriers is much higher than the spreading sequence length. After spreading, the data streams are interleaved onto the carriers to maximise diversity. A practical form of maximum likelihood detection for 64 users is described. It is shown from simulation results that when the system is used in conjunction with 1/2 rate (constraint length 7) coding and equal gain combining the system can support 64 users at 6 dB E_b/N_0 for a bit error rate of 2×10^{-3}. This compares with an equivalent DS-CDMA system which can only support 16 users for the same bit error rate and E_b/N_0. These results assume perfect channel knowledge and synchronisation. It is further shown that to provide high spectral efficiency in a coded system a high rate convolutional coding scheme is needed. A combined decoder/canceller is also presented.

Finally, techniques to achieve synchronisation and channel estimation algorithms are presented. These algorithms are considered in conjunction with the second system. In the framework of synchronisation, methods are presented for frequency and timing synchronisation. For channel estimation, simulation results are presented for a simple channel estimator.

Declaration of originality

This thesis was composed entirely by myself. The work reported herein was conducted exclusively by myself in the Department of Electrical Engineering at the University of Edinburgh.

Richard Stirling-Gallacher
August 1997

Acknowledgements

I would like to thank the following people for their invaluable assistance during the course of this PhD:

- Dr. Gordon Povey and Prof. Peter Grant, my supervisors, for their continous support and guidance. Also for reading this thesis.
- Everyone in the Signals and System group for their tremendous support throughout my time at Edinburgh. I would like in to thank in particular the people who read my thesis, including Ian Band, Iain Scott, Gunther Auer, Rudy Tanner, John Thompson and Sascha Spangenberg.
- Dr. Ed Warner currently at DRA for much help and assistance at the beginning of my PhD.
- Peter Hulbert and Steve Wales of Roke Manor Research Ltd. for providing me with two interesting summer placements.
- Roke Manor Research Ltd. and EPSRC for for providing me with financial support.

Contents

List of Figures

List of Tables

Abbreviations

ACF	auto correlation function
AMPS	advanced mobile telephone system
AWGN	additive white Gaussian noise
BER	bit error rate
BPSK	binary phase shift keying
CC	convolutional code
CCF	cross correlation function
CD	compact disc
CDMA	code division multiple access
DAB	digital audio broadcasting
DAPSK	differential amplitude phase shift keying
DAT	digital audio tape
DECT	digital European cordless telephone
DFT	discrete Fourier transform
DPC	differential phase combining
DPSK	differential phase shift keying
DS	direct sequence
DS-CDMA	direct sequence code division multiple access
DS-SS	direct sequence spread spectrum
DQPSK	differential quaternary phase shift keying
DVB	digital video broadcasting
EGC	equal gain combining
ETSI	European Telecommunications Standards Institute
FH	Frequency hopping
FM	frequency modulation
FDM	frequency division multiplexing
FDMA	frequency division multiple access

FFT	fast Fourier transform
GSM	Groupe Speciale Mobile (or Global system for mobile communications)
HSDL	high speed digital subscriber line
IC	Interference cancellation
ICI	Inter carrier interference
IDFT	Inverse discrete Fourier transform
IFFT	Inverse fast Fourier transform
ISI	Inter symbol interference
LFSR	linear feedback shift register
LMS	least mean square
MC-CDMA	multi carrier code division multiple access
MCM	multi carrier modulation
MLD	maximum likelihood detection
MMSE	minimum mean square error
MPEG	motion pictures experts group
MRC	maximum ratio combining
MSE	mean square error
NMT	nordic mobile telephone
OFDM	orthogonal frequency division multiplexing
OFDM-CDMA	orthogonal frequency division multiplexing code division multiple access
O-QAM	offset quaternary amplitude modulation
PCC	punctured convolutional code
PCM	pulse coded modulation
PDF	probability density function
PG	processing gain
PN	pseudo noise
QAM	quaternary amplitude modulation
QASK	quaternary amplitude shift keying
RDS	radio data system
RLS	recursive least square
SFN	single frequency network
SNR	signal to noise ratio
SQAM	staggered quadrature amplitude modulation
TACS	total access communication system
TDMA	time division multiple access
TH	time hopping
UMTS	Universal mobile telecommunication system
W-CDMA	Wideband - CDMA

List of principal symbols

α_{kl}	complex gain for the lth path of the kth symbol
a_i	real part of received sampled complex received signal x_i before FFT (OFDM-CDMA)
$a_k(n)$	equaliser coefficient for symbol k on carrier n (MC-CDMA)
B	Bandwidth
B_m	message bandwidth
B_{ss}	spread spectrum bandwidth
BW_1	bandwidth of one carrier from MC-CDMA system (Kondo and Milstein)
BW_m	bandwidth of m carriers from MC-CDMA system (Kondo and Milstein)
b_m	data bit for user m (OFDM-CDMA)
b_{km}	kth transmitted symbol for user m (MC-CDMA)
C	Channel capacity
$C_{linear}(y)$	linear correlator function as a function of offset y
$C_{sign}(y)$	sign only correlator function as a function of offset y
$\mathbf{c}_m$	spreading code vector for user m
D	Number of multipath components
D'	Frequency diversity
D_s	Delay spread
d_m	differentialy encoded data bit for user m
d_{min}	minimum free distance of convolutional code
F	guard interval length (in seconds)
E	Error signal for frequency tracking loop
f_d	Doppler frequency
$f_{d_{max}}$	maximum Doppler frequency
f_{offset}	frequency offset
$\widehat{f}_{offset}$	frequency offset estimate
f_i	frequency offset for carrier i
$\mathbf{G}$	diagonal equaliser matrix (OFDM-CDMA)

g_l	Equaliser coefficent for the lth row and lth column of matrix $\mathbf{G}$ (OFDM-CDMA)
$\mathbf{H}$	diagonal channel matrix (OFDM-CDMA)
h_l	channel coefficent for the lth row and lth column of matrix $\mathbf{H}$ (OFDM-CDMA)
J	spacing of sub-carriers MC-CDMA
K	constriant length
L	spreading sequence length (OFDM-CDMA)
L_{error}	number of guard interval samples used for tracking
L_f	number of pilot tones in the frequency domain
M	size of serial to parallel converter (OFDM-CDMA)
$\mathbf{M}_n$	Hadamard matrix
m	mobile user index
N	spreading sequence length = number of carriers (MC-CDMA)
N_a	spreading sequence length (MC-CDMA, one sequence per carrrier type a)
N_b	spreading sequence length (MC-CDMA, one sequence per carrier type b)
N_c	spreading sequence length (MC-CDMA, one sequence per carrier type c)
N_u	number of users
$N_{u_{max}}$	maximum number of users
N_g	guard interval length (in samples)
$\mathbf{n}$	received noise vector
P	number of parallel data streams (MC-CDMA)
$P(d)$	probability that the wrong path at distance d is selected
p	puncturing period for punctured convolutional coding
p_{thres}	threshold for controlled equalisation
Q	size of sub-system (OFDM-CDMA)
$R_c = k/n$	code rate of convolutional code
$\mathbf{r}$	received signal vector after the FFT (OFDM-CDMA)
S	parallel streams (MC-CDMA)
$S_m(t)$	continous time representation of baseband signal produced by the mth user
$S_m(i)$	discrete time representation of baseband signal produced by the mth user
S_{pilots}	number of data symbols between pilot tones
$\mathbf{s}$	sent signal vector (OFDM-CDMA)
T_b	data bit duration
T_c	chip duration (DS-CDMA)
T_c'	chip duration (MC-CDMA)
T_{data}	useful data section for adaptive algorithm (MC-CDMA)

T_s	symbol duration
T_{train}	training time for adaptive algorithm (MC-CDMA)
T_u	useful part of transmitted symbol (OFDM-CDMA)
$t_j(l)$	value of transmitted pilot tones on carrier j for symbol l
$\mathbf{u}$	received signal vector after equalisation (OFDM-CDMA/MC-CDMA)
v_j	soft output from MLD despreader (OFDM-CDMA)
$\mathbf{v}$	possible sent sequence vector (OFDM-CDMA)
W	length of window for Viterbi deocder
$x(t)$	received signal before FFT (OFDM-CDMA)
x_i	sampled received signal before FFT (OFDM-CDMA)
$x_k(n)$	sampled received signal before FFT for data bit k (MC-CDMA)
x_{lk}	deccorelated symbol for the kth symbol on the lth path (DS-CDMA)
y	offset for timing
$y_k(n)$	composite transmitted signal (DS-CDMA)
z_i	imaginary part of sampled received x_i before FFT (OFDM-CDMA)
β_l	power of path l
δ_j^2	distance between received sequence $\mathbf{r}$ and sent sequence $\mathbf{v}_j$
Δ_j^i	difference in Euclidean distance between the ith possible and the chosen jth MLD sequence.
$(\Delta f)_c$	coherence bandwidth
$(\Delta f)_{c1}$	coherence bandwidth (Prasad)
$(\Delta f)_{c2}$	coherence bandwidth (Proakis)
$(\Delta f)_{c3}$	coherence bandwidth (Lee)
τ_l	delay of path l
μ	step size for LMS algorithm
ω_d	distance spectra of convolutional code at distance d
$(\Delta t)_c$	coherence time
σ_f^2	frequency estimation variance
λ	forgetting factor of RLS algorithm

Chapter 1
Introduction

This thesis will consider a communication system based on combining multi-carrier modulation techniques with code division multiple access (CDMA). These two different techniques have historically evolved from different fields. CDMA is a technique for providing communication for multiple users using spread spectrum techniques and is used for high capacity commercial cellular communication systems such as IS-95 [1]. Multi-carrier modulation has evolved from frequency division multiplexing in the 1950s to its use in digital television and audio broadcasting systems of today.

This chapter will commence by summarising the current state of the art in wireless technology. It will examine cellular technology and explain why the proposed multi-carrier code division multiple access system is of interest. Following this, a brief summary of the main areas of research covered in the thesis will be presented and the thesis structure described.

1.1 Cellular systems

In recent years, there has been an explosion of wireless communication services. This has occurred due to the demand of communicating without the constraints of a fixed network and the advances in microelectronics to provide such a system. A wireless communication system provides a flexible link using different forms of data. The most widely used wireless communication networks are personal communications networks (PCN) which are based on cellular networks. Other wireless communication networks include wireless area networks (both local and wide area), paging systems, cordless system and satellite systems. Each of these will be described before discussing in more detail cellular networks.

Wireless area networks are designed for low data rate communication and are based on low mobility operation in an office (local area) or a mobile user (wide area). Cordless systems allow the user limited mobility by providing a communication link between the users terminal and a base station connected to a fixed network. Standard telephone calls can therefore be accomplished but with increased mobility. Two standards which have been developed for achieving this are CT2 and DECT [2]. Paging systems are very different from either cordless or wireless area networks and only provide communication in one direction, transmitting short messages to a given user. The advantage of this is that only a simple and therefore cheap receiver is required. Wireless communication system based on satellite systems are relatively rare for commercial applications due to the high cost. There are, however, many planned future satellite systems. Most of these systems intend to provide services using spread spectrum techniques (Motorola's Iridium system is an exception to this) to enable communication in regions of low population or supplement existing cellular networks coverage.

The focus of this thesis is wireless communication networks based on cellular networks. A cellular network is one in which the required area of coverage is split into a number of cells. Each cell is assigned a base station and every user (or mobile) located within the cell communicates to this base station. Handover occurs when the user moves from one cell to another or the received signal strength of another base station is greater than the one the user is presently communicating with. There are two links in cellular networks, the uplink and the downlink. The uplink is the link from the mobile to the base station and the downlink is the link from the base station to the mobile. The first such networks were pioneered in the late 1970s and included the advanced mobile phone system (AMPS) implemented in the USA, the total access communication systems (TACS) in the UK and other systems implemented throughout Europe such as the nordic mobile telephone (NMT) system and the C-Netz (implemented in Germany). All these systems used analogue technology and are collectively called first generation systems. None of these systems are compatible with each other and therefore roaming between countries (and different systems) is therefore not possible.

To provide a cellular network to an increasing number of users and to establish compatibility with digital fixed networks, GSM was established in the 1980s. GSM is a digital European cellular system which is now operational in most European countries in the 900 MHz band. Each user generates coded speech data at 22.8 kbits/s and after time multiplexing, channel coding and insertion of training bits the total transmitted data rate is 270.833 kbits/s. Due to the high data rate and corresponding intersymbol interference an equaliser is needed at the receiver. A modified version of GSM, DCS-1800, is also in operation in the 1800 MHz band. As GSM and DCS-1800 are international standards within European, users have the ability to roam between countries.

In the USA, a digital cellular standard IS-54 (sometimes referred to as digital AMPS) has also been established which is compatible with AMPS. Since IS-54 was standardised however, DCS-1900 (a variation on DCS-1800 in the 1900 MHz band) and a CDMA system known as IS-95 has also been developed. Due to the presence of different standards, it is more difficult in the USA to achieve roaming.

For future cellular communication in Europe, research, is focussed on providing high data rate services (up to 2 Mbits/s) so video and Internet services can be supported. The goal of this research is to establish a third generation cellular system under the title universal mobile telecommunications system (UMTS) [3] which is backwardly compatible with GSM. To achieve this goal there are several European funded research projects [4] such as CODIT and ATDMA.

Multi-carrier techniques and CDMA are not new techniques, however, the combination of the two is a relatively new idea. The first published research work on multi-carrier code division multiple access was by Fazel [5] and Chouldy et al. [6] in 1993. Both these papers consider a downlink single cell system.

1.2 Main research areas

The main topic of this thesis is to investigate the combination of multi-carrier modulation with CDMA. There are a number of different combinations for achieving this, but the research presented here is

restricted to one of these combinations. The purpose of this is to ascertain if the combination of multi-carrier modulation with CDMA for a single cell downlink cellular system has a performance advantage over traditional direct sequence CDMA techniques.

There are a number of different aspects to this investigation. In particular two variations of the multi-carrier CDMA combination will be separately studied. The performance of these systems will be examined for coherent and noncoherent modulation techniques, different detection schemes and various channel coding schemes. Synchronisation and channel estimation issues will also be addressed.

1.3 Thesis structure

After this brief introduction, Chapter 2 will describe in detail spread spectrum techniques, multipath fading channels and orthogonal frequency division multiplexing. This chapter therefore explains concepts which are fundamental to understanding the thesis.

Chapter 3 discusses and reviews the different arrangements for combining CDMA with multi-carrier modulation to form a multi-carrier CDMA system. This chapter is split into three sections corresponding to the three different combinations. At the end of the chapter a summary is made which discusses the advantages and disadvantages of the different approaches. One of these arrangements is then selected and forms the basis for the next three chapters. This arrangement is referred to as a one chip per carrier MC-CDMA system.

The subject of Chapter 4 is an investigation of a proposed one chip per carrier multi-carrier CDMA system which is similar to one investigated by Linnartz [7]. This is compared against a DS-CDMA system of the same bandwidth. Both coherent and non-coherent modulation schemes are investigated, in addition to adaptive receiver architectures.

Chapter 5 examines another one chip per carrier CDMA system originally proposed by Fazel [5]. This chapter is split into three sections. The first section investigates the performance of different detection schemes. One of these schemes is then selected in the second section in conjunction with different coding schemes. In the last section a combined decoder and interference canceller is introduced and its performance compared to other architectures.

The analysis in chapters 4 and 5 assumes the multi-carrier receivers are perfectly synchronised and have perfect knowledge of the channel. As such the results represent lower bounds on BER performance. In Chapter 6 we therefore investigate synchronisation and channel estimation algorithms. These algorithms are investigated with particular emphasis on the system described in Chapter 5.

Finally, Chapter 7 draws conclusions on the work that has discussed in this thesis. In this chapter, the achievements and limitations of the results obtained are discussed. Suggestions for further work are also presented.

Chapter 2
Background

In this chapter concepts are introduced which are used throughout this thesis. It is important to discuss these concept before an examination of multi-carrier techniques with code division multiple access (CDMA) is conducted. This chapter is split into three sections. Section 2.1 introduces the concept of spread spectrum and its use in a CDMA communication system. Section 2.2 describes the characteristics of a mobile radio channel and channel modelling methods. Finally in section 2.3, we introduce orthogonal frequency division multiplexing (OFDM) and describe its role in digital broadcasting.

2.1 Spread spectrum

The capacity of a channel with bandwidth B can be specified in terms of the Hartley-Shannon law [8],

$$C = B\log_2(1 + \text{SNR}) \tag{2.1}$$

where SNR represent the signal-to-noise ratio. The capacity C can be regarded as the maximum data rate possible. If the bandwidth required to transmit a message is defined as B_m and this bandwidth is increased the same capacity (or bit rate) can be supported at a lower SNR. This reduction in required SNR is very advantageous for a communications system and can be represented as a processing gain (PG)

$$PG = \text{SNR}_{normal} - \text{SNR}_{spread} \tag{2.2}$$

$$PG \approx 10\log_{10}\left(\frac{B_{ss}}{B_m}\right) \tag{2.3}$$

where B_{ss} is the spread spectrum bandwidth. This expansion of the bandwidth has a number of other advantages including interference and multipath rejection. The are, however, a number of techniques which cause bandwidth expansion but which are not spread spectrum systems. It is therefore important to define a spread spectrum system.

A spread spectrum system must satisfy two basic criteria [9]. First the bandwidth of the transmission must be much greater than the information bandwidth. Secondly, the transmission bandwidth must be determined by a function which is independent of the message and known at the receiver. Both of these

criteria must be satisfied for a communication system to be considered as a spread spectrum system. The expansion of bandwidth in a spread spectrum system is normally achieved by a spreading sequence and this is in most cases a pseudo noise (PN) sequence.

Spread spectrum systems can be categorised by techniques used in the signal spreading and despreading processes. Four distinct categories, [1] can be identified:

- Frequency hopping (FH)
- Chirp
- Time hopping (TH)
- Direct sequence (DS)

of these techniques, DS and FH are those most often used for conventional or military spread spectrum communication systems. Chirp spread spectrum systems are used mainly in radar applications. TH is less common and is mainly used in hybrid systems. These techniques can be further split into two groups which describe how the systems reject interference. These two groups are avoidance and averaging. An averaging system is one in which the reduction of the interference occurs because the interference is averaged over a large period of time. In contrast an avoidance system is one in which interference is reduced because the interferer and wanted signal are frequency or time separated for large periods of time. From the list seen above the DS system is the only averaging system, the other systems are avoidance systems. It is useful to discuss some of the basic aspects of the different systems identified above.

2.1.1 Frequency hopping

Frequency hopping causes the frequency of transmission to change according to a set of predetermined values. These values are determined by the PN sequence. Frequency hopping was originally developed for the military to avoid jamming or eavesdropping. If the hopping is sufficiently fast it is very difficult for the jamming transmitter or eavesdropping receivers to follow the signal.

A fast hopping system is one in which the frequency of transmission changes at a faster rate than the information rate, otherwise it is termed a slow hopping system. To facilitate synchronisation, it is normal for each frequency to occur only once in the hopping sequence. During synchronisation the receiver can thus search for the beginning of the hopping sequence.

[1] These categories do not include any combination of spread spectrum with multi-carrier techniques. This will be covered in Chapter 3

2.1.2 Chirp

Chirp modulation changes the carrier frequency of the transmitted signal within a time period. In this sense, it is similar to frequency hopping. In contrast however, the frequency change does not occur in discrete steps but is continuous and monotonic over a range. This is normally achieved in a linear fashion for radar applications. This system is not based on the use of a spreading sequence (or PN code), but the transmission bandwidth is much larger than the information bandwidth and is determined by a function independent of the message. Chirp modulation, therefore, satisfies the two criteria to qualify as a spread spectrum system.

The receiver for a chirp system makes use of the fact that different frequencies have different delays when passed through a filter. This effect which is normally minimised in filter design is used to cause the chirp energy to gather into one pulse.

2.1.3 Time hopping

To achieve time hopping, the data bits are sent in frames. Each frame is subdivided into time slots. The particular time slot that is chosen to send the required data bit is determined by the PN sequence. In most time hopping systems only one data bit is sent per frame. The required data bit, therefore, changes its position in each frame for every subsequent frame that is sent. Although time hopping is the least utilised of the spread spectrum techniques, it is a useful method of enciphering time division multiple access (TDMA) communications.

2.1.4 Direct sequence

Direct sequence is the most common spread spectrum technique and is used in almost all of the commercial spread spectrum systems. To produce a direct sequence spread spectrum (DS-SS) signal the bits of the PN sequence ('chips') modulate the data bits. The period of the PN sequence [1] is normally the same as the information bits. By modulating the information sequence by a higher rate code, the date rate is increased and the bandwidth correspondingly increases.

At the receiver the signal is decorrelated by multiplying the received signal by a copy of the PN sequence, causing the large bandwidth to be reduced to the bandwidth of the information signal.

If the period of the PN sequence is the same as the information bit, the power spectral density of a DS spread spectrum signal can be approximated by

[1] It is also possible to use a PN sequence which is longer than the information bit. This system has greater security but also requires more complicated synchronisation.

$$S(\omega) = T_c \text{sinc}^2\left(\frac{\omega T_c}{2}\right) \tag{2.4}$$

where T_c is the chip duration. The bandwidth of the DS spread spectrum signal between zero crossing is $2/T_c$.

2.1.5 Code division multiple access

Traditionally to provide a communication link for a number of simultaneous users (multi-access communications) the available bandwidth has been split either into a number of frequency bands or a number of time slots. If the system bandwidth is split into a number of frequency bands, each user occupies the assigned frequency band for all of the time. This system is referred to as frequency division multiple access (FDMA). If the system bandwidth is available to all of the users on a time slot basis, the system is referred to as time division multiple access (TDMA).

It is also possible to form a multi-access communication system using spread spectrum techniques. This system is referred to as code division multi-access (CDMA). CDMA is a spread spectrum system where the users, each with their unique spreading sequence, communicate simultaneously over the same frequency band. Total interference in CDMA is dependent on the processing gain (PG), the larger the PG, the larger the necessary bandwidth and the greater the number of users that can be supported. Almost all multi-access CDMA systems use DS-SS as the spread spectrum technique. Such a system is, therefore, referred to as a DS-CDMA system.

There are some advantages of spread spectrum which may enable a cellular system based on CDMA to have a performance advantage over cellular systems based on TDMA or FDMA techniques. One of these is that CDMA is less susceptible to multipath fading than TDMA or FDMA because a RAKE receiver [10] can be used to resolve the different multipath components and combine them coherently providing diversity. A cellular CDMA system [11] can also utilise voice activity detection and antenna sectorisation to decrease the interference from other users.

The main advantage, however, of CDMA over TDMA or FDMA for cellular systems is the frequency reuse of the frequency spectrum in each cell. Each user in a CDMA system has a unique spreading spreading sequence and all users utilise the same bandwidth. This bandwidth can be reused in neighbouring cells, causing a small performance degradation (depending on the attenuation factor). A similar reuse pattern in FDMA or TDMA is not possible since it causes severe performance degradation. The frequency reuse available in CDMA improves the spectral efficiency or system capacity of the system.

The capacity of a CDMA system, however, depends on the discrimination of the different users which is determined by the orthogonality of the PN codes used. The choice of the PN codes for a particular CDMA system is therefore extremely important. There is a considerable amount of research conducted in techniques used at the receiver for improving the discrimination of users. Most of this research is

based on interference cancellation or adaptive signal processing techniques. For the purpose of this introduction, however, a discussion of these techniques will not be made. We will instead examine properties of different PN codes which are used throughout this thesis.

2.1.6 Pseudo noise (PN) sequences

There are many kinds of PN sequences, but there are two properties which are important when selecting a given PN code for a particular spread spectrum or CDMA system. The first of these is the autocorrelation function (ACF) which is the correlation of a given code with a time shifted version of itself. An ideal ACF would have a peak at zero time offset and would be zero elsewhere. This is desirable to facilitate synchronisation at the receiver. ACF values for non-zero time offsets are often referred to as off peak ACF values.

For multi-user communications the cross correlation (CCF) of the codes is particularly important. The CCF is a measure of the orthogonality of a code with another code from the same family. It is desirable to have codes with a low CCF so more users can be supported for a given bit error rate (BER).

2.1.6.1 Walsh codes

A Walsh code is obtained by selecting the rows of a Hadamard matrix. A Hadamard matrix is a $n \times n$ matrix, denoted by $\mathbf{M}_n$, containing 1s and 0s with the property that any row differs from any other row in exactly $n/2$ positions. One row of the matrix contains all zeros. The other rows contain $n/2$ zeros and $n/2$ ones.

The base matrix $\mathbf{M}_2$ is given by

$$\mathbf{M}_2 = \begin{bmatrix} 0 & 0 \\ 0 & 1 \end{bmatrix}$$

For any Hadamard matrix of size n, $\mathbf{M}_n$, the Hadamard matrix $\mathbf{M}_{2n}$ can be generated,

$$\mathbf{M}_{2n} = \begin{bmatrix} \mathbf{M}_n & \mathbf{M}_n \\ \mathbf{M}_n & \overline{\mathbf{M}}_n \end{bmatrix}$$

where $\overline{\mathbf{M}}_n$ is the inverse of the matrix $\mathbf{M}_n$. In this way, any Hadamard matrix can be iteratively generated from the base matrix. For a Walsh code of length N, there are N distinct Walsh codes corresponding to the N rows of the Hadamard matrix. Walsh codes are particularly useful, because they are orthogonal to each other. Their orthogonality is, however, destroyed when used in a CDMA communication system in multipath channels. Orthogonality is maintained, however, in Gaussian or single path fading

channels.

2.1.6.2 m-sequences

m-sequences are by far the most widely known PN sequence. To generate a m-sequence a length m linear feedback shift register (LFSR) is used. Such a shift register is shown in Figure 2.1. The sequences generated are periodic with period n where $n = 2^m - 1$. Each period contains 2^{m-1} ones and $2^{m-1} - 1$ zeros.

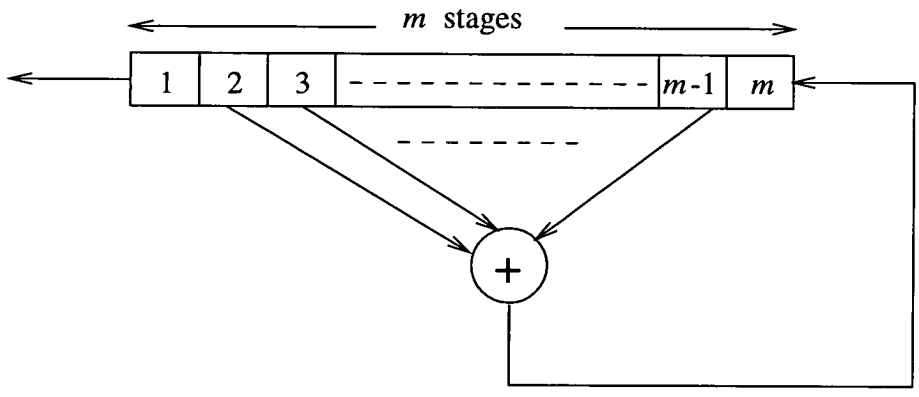

Figure 2.1: Linear feedback shift register (LFSR)

For any LFSR of length m there are a number of possible feedback connections. Not all of these connections, however, produce m-sequences. Mathematically, the connections and the state of the shift register can be described as polynomials. To produce an m-sequence the polynomial describing the feedback connections must be irreducible[1]. Table 2.1 shows the number of valid m-sequences that can be produced for LFSRs of length 3 to 8.

Table 2.1: *Valid m-sequences*

shift register length m	code length $n = 2^{m-1}$	Number of m sequences
3	7	2
4	15	2
5	31	6
6	63	6
8	255	16

m-sequences have peak CCF values which are higher than Gold codes of the same length [14]. In certain types of multipath channels, however, m-sequences have lower average CCF values than Walsh codes but higher than Gold codes [2]. The off peak ACF of an m-sequence is -1 for all time offsets greater than one chip duration.

[1] The feedback connector polynomial is defined as irreducible if the operation of dividing the shift register state polynomial by the connector polynomial always produces a remainder.

[2] This is has been shown by private research.

2.1.6.3 Gold codes

Gold [12] has shown that by using certain pairs of m-sequences of length n and combining them using modulo 2 addition, another sequence can be formed. This new sequence is known as a Gold code. It is also possible to obtain a set of Gold codes of length n by cyclically shifting one of the selected m-sequences by a given number of chips. In this way n Gold codes of length n can be formed. By including the original m-sequences a total of $n + 2$ Gold codes can be formed. Gold codes have a lower peak CCF [14] than m-sequences and are therefore more useful in CDMA applications. Gold codes do, however, have a three value off peak ACF. (This compares to m-sequences which only have one.) Synchronisation for Gold codes is, therefore, more complicated.

2.1.7 Proposed CDMA systems

Although spread spectrum techniques have been used for many years for military communications, it is only in the last 10 years that spread spectrum techniques have been considered for commercial applications. A DS-CDMA cellular communication system known as IS-95 [1] has been standardised. The system was originally proposed by Qualcomm Inc. and is presently in operation in the USA and Korea, while trials are also being conducted in other countries. The system uses a combination of Walsh codes and m-sequences on the downlink (base station to mobile). All base stations are assigned the same pair of m-sequences (length 2^{15}-1) for inphase and quadrature channels. Different phase offsets of the code sequence are used for different base stations. This phase offset is made sufficiently long to ensure there is no confusion between received signals from different base stations. To identify mobiles on the downlink, each mobile is assigned a Walsh code of length 64 which is then combined with the m-sequence. The downlink also uses a pilot tone for carrier and PN code synchronisation. In the uplink, (mobile to base station) each user is assigned a unique code obtained from a long PN code (length 2^{42}-1) through a masking procedure. The transmitted data is convolutionally encoded and the output of the coder is taken 6 bits at a time to select one of 64 Walsh functions. The system is claimed to have a higher capacity than the European Groupe speciale mobile (GSM) (TDMA/FDMA) cellular system.

A variation of IS-95 called wideband CDMA (W-CDMA) has been proposed for the universal mobile telecommunication system (UMTS). Different CDMA cellular systems have also been the subject of many European research programmes such as CODIT.

2.2 Mobile radio channel

An important aspect of every communication system is the communication channel. To optimise the performance of a given communication system or a receiver architecture it is important to understand how the mobile channel affects the transmitted signal. In this section we shall discuss some of the basic aspects of mobile radio channels.

There are two types of channels discussed in this thesis: a Gaussian channel and a multipath channel.

The Gaussian channel or additive white Gaussian noise (AWGN) channel is a basic model to which other results can be compared. The Gaussian channel simply adds white noise with a Gaussian probability density function (pdf) to the transmitted signal. The mobile radio channel is, however, more sophisticated than a Gaussian channel due to multipath propagation, channel time variations and industrial interference. The multipath channel model, however, includes the effects of multipath propagation and channel time variation and is, therefore, a realistic representation of a mobile radio channel. To understand this model it is important to understand multipath propagation.

Multipath propagation in the channel is caused by obstacles between the transmitter and receiver. These obstacles cause scattering, reflections and diffractions of the transmitted signal. The received signal, therefore, consists of several components, each one corresponding to a particular path between the transmitter and receiver. Depending upon the instantaneous amplitudes and delays of each component, constructive or destructive interference occurs. Since the phase difference between these components depends on the frequency of propagation, some frequencies will be attenuated and others will pass through the channel with very little attenuation. A channel with such properties is referred to as a frequency selective channel.

Theoretical studies [13] have shown that multipath propagation can be modelled as shown in Figure 2.2. The delays τ_i originate from the various specular reflections, while the factors $A_i(t)$ are the consequences of local scattering. If the number of the scattered components is large enough, $A_i(t)$ can be modelled as a complex Gaussian variable since the the addition of many independent variables sum to a Gaussian variable. The modulus of $A_i(t)$ has Rayleigh statistics if the real and imaginary components of $A_i(t)$ have a zero mean. If the mean of the real and imaginary is not zero (as in the case of one of the specular components dominating) the modulus of $A_i(t)$ is Ricean.

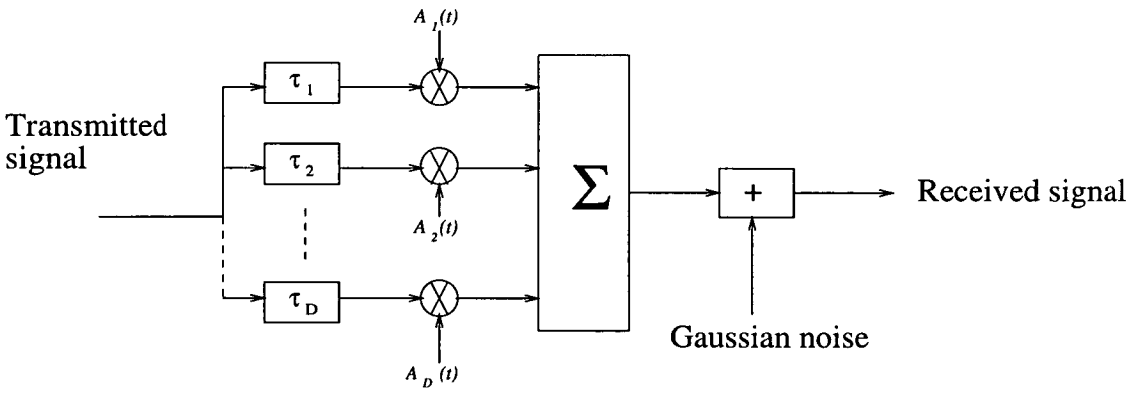

Figure 2.2: General mobile radio channel

The power spectrum of $A_i(t)$ can be determined from the relationship between the incidence of the multipath components and the direction of the moving mobile. If we assume this distribution is uniform, the power spectrum of $A_i(t)$ when translated to baseband, can be written as

$$S_A(f) = \frac{\sigma_i^2}{\pi\sqrt{f_{d_{max}}^2 - f_d^2}} \quad -f_{d_{max}} \leq f_d \leq f_{d_{max}} \tag{2.5}$$

where σ_i^2 is the power of path i, f_d is the Doppler frequency and $f_{d_{max}}$ is the maximum Doppler frequency. This power spectral density is referred to as the classic Doppler spectrum. Other important power spectral densities commonly used are Ricean and Gaussian [13]. For the purpose of this Thesis, we shall only consider the classic Doppler spectrum.

As stated previously, frequency selectivity is due to the spread of the channel impulse response. A measure of frequency selectivity for a channel is given by the coherence bandwidth (Δf_c) which is the range of frequencies for which fading can be considered to be correlated. There are different definitions for this (see Appendix B), but they are all related to the reciprocal of the channel delay spread. The most common definition for coherence bandwidth is given by Proakis [14],

$$(\Delta f)_c \approx \frac{1}{\tau_d} \tag{2.6}$$

where τ_d is the maximum delay spread. If the signalling interval $T \gg \tau_d$ the channel introduces a negligible amount of intersymbol interference (ISI) and the channel can be considered as a single path fading channel. (For a DS-SS signal the signalling interval is T_c.) This condition implies that $1/T \ll (\Delta f)_c$ and the channel is referred to as a frequency non-selective channel.

Another important aspect of the multipath channel is the variation of the parameter $A_i(t)$ with time. This is defined as the time coherence $(\Delta t)_c$ which is defined as

$$(\Delta t)_c \approx \frac{1}{f_{d_{max}}} \tag{2.7}$$

A channel is defined as slowly fading or time non-selective if the attenuation and phase shift for each multipath component are fixed for the duration of the signalling interval T. This condition can be expressed as $T \ll (\Delta t)_c$ which implies $f_{d_{max}}.T \ll 1$.

2.3 Orthogonal frequency division multiplexing

In this section we shall describe the principles of orthogonal frequency division multiplexing (OFDM) and the techniques used in digital broadcasting. It is important, however, to first discuss multi-carrier techniques and its historical development into OFDM.

2.3.1 History of Multi-carrier modulation and basic principles

Multi-carrier modulation (MCM) is a form of frequency division multiplexing (FDM), the basic principles of which are shown in Figure 2.3. Input data at a rate of A bits/s (duration T_b seconds) are grouped into a block of N bits. These N bits are passed to a serial to parallel converter so that each parallel stream has a bit rate of A/N bits/s. Each output stream then modulates a carrier of frequency f_n. There are N carriers which are spaced Δf apart. f_n is given by,

$$f_n = f_c + n\Delta f \quad n = 1, 2, 3, \ldots, N \tag{2.8}$$

where f_c is the lowest frequency of the transmitted signal.

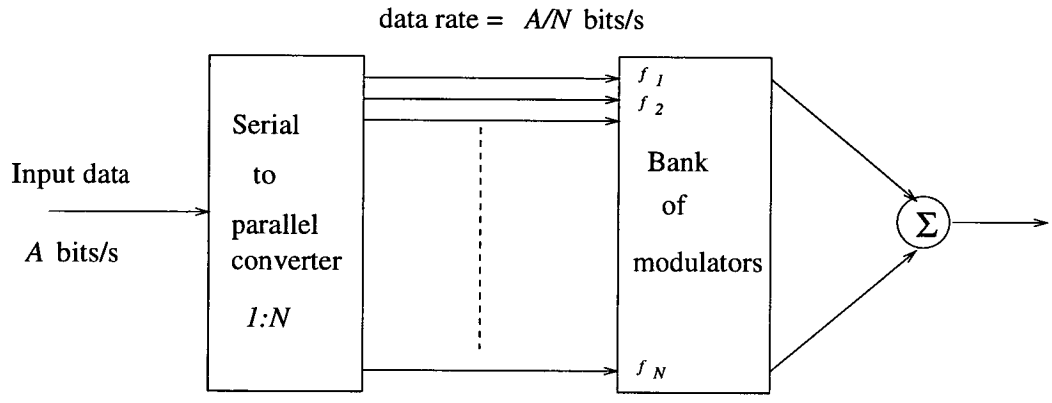

Figure 2.3: Multi-carrier transmitter

The modulated carriers are then summed for transmission. As can be seen from Figure 2.4, the duration of the symbol is lengthened by a factor of N. When compared to a single carrier system transmitting the same data stream, the delay spread of the channel becomes a much smaller proportion of the symbol duration. In this way MCM reduces intersymbol interference (ISI). In addition, it is more robust against burst errors caused by the rapid deep Rayleigh fading, because the long symbols become slightly distorted by the fade as opposed to several adjacent symbols being completely destroyed.

The principle of MCM was first used almost 40 years ago by the Collins Kineplex system [15]. Early MCM systems borrowed technology from conventional FDM systems and used filters to separate the bands. As sharp filters are very difficult to implement, there was an excess bandwidth due to the separation between the carriers.

An improvement of the bandwidth usage was made by Salzberg [16] in 1967 by using staggered quadrature amplitude modulation (SQAM). In this scheme, the carriers still used an excess bandwidth but they overlapped at the -3dB points. The orthogonality of the carriers was maintained by staggering the data on alternate inphase and quadrature sub-channels. This modulation scheme is sometimes referred to as offset quadrature amplitude modulation (O-QAM). As the data is staggered, the filtering requirements

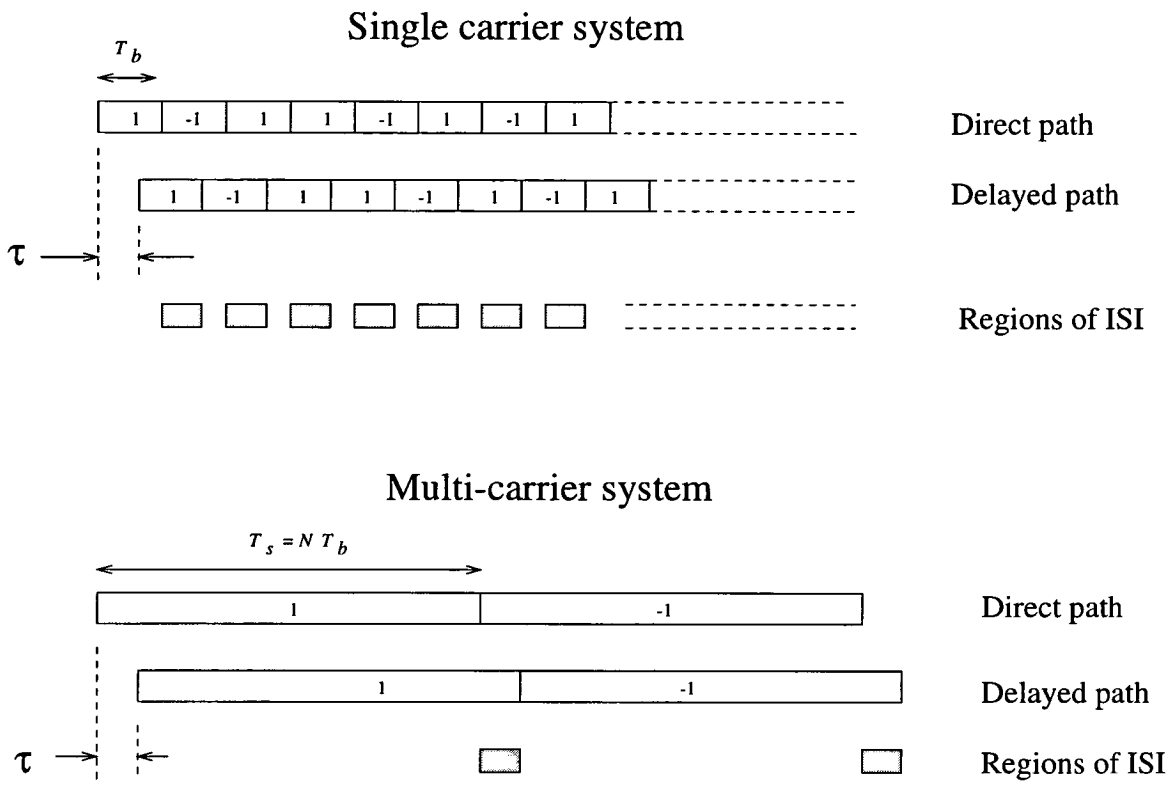

Figure 2.4: The reduction of ISI from multi-carrier transmission

are also not as stringent.

For a large number of carriers, the array of sinusoidal generators and coherent demodulators required becomes unreasonably complex and for the system considered above, more than 20 carriers is impractical. In 1971 Weinstein and Ebert [17] showed that a bank of coherent modulators (with a sinc power spectral density) could be produced by an inverse fast Fourier transform (IFFT). Likewise, the corresponding bank of demodulators could be implemented by a fast Fourier transform (FFT). This principle forms the basis of an orthogonal frequency division multiplexing (OFDM) [1] system in which the carriers are spaced in frequency by the reciprocal of the date rate and overlap resulting in the optimum bandwidth efficiency. The power spectral density of 8 carriers arranged in this way is seen in Figure 2.5.

2.3.2 Principles of OFDM

OFDM is a special kind of multi-carrier modulation. In common with MCM, the data (of rate A and duration T_b) required to be transmitted is passed to a serial to parallel converter (1:N) producing N parallel streams of rate A/N. These parallel streams modulate N sub-carriers which are separated in frequency by A/N where B is the transmission bandwidth. The carriers are generated by an N point

[1] This multi-carrier system is not an OFDM system in the strict sense. This is because no cyclic extension is used. The carriers will, however, remain orthogonal in a Gaussian channel.

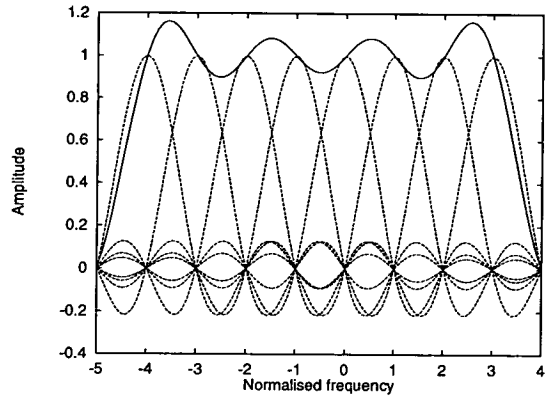

Figure 2.5: 8 Overlapping sinc functions (composite sum shown as continuous line)

IFFT whose output is passed to an interpolation filter.

Due to multipath propagation in the channel, ISI still exists (see Figure 2.4) in this transmission system, although reduced to a large extent. To eliminate the effects of ISI completely with OFDM and to maintain the orthogonality of the carriers in a multipath channel a cyclically extended guard interval (of duration F) is inserted into the transmitted signal. This cyclically extended guard interval is a repeat of the last samples from the IFFT and so the output signal is extended backwards in time. This is shown in Figure 2.6. At the receiver only the useful part of the symbol is passed to the FFT and so the received symbol is not subject to ISI. As the transmitted symbol is cyclically extended backwards, the carriers remain orthogonal. Depending upon the instantaneous amplitudes and delays of the multipath components some of the sub-carriers will experience deep fading.

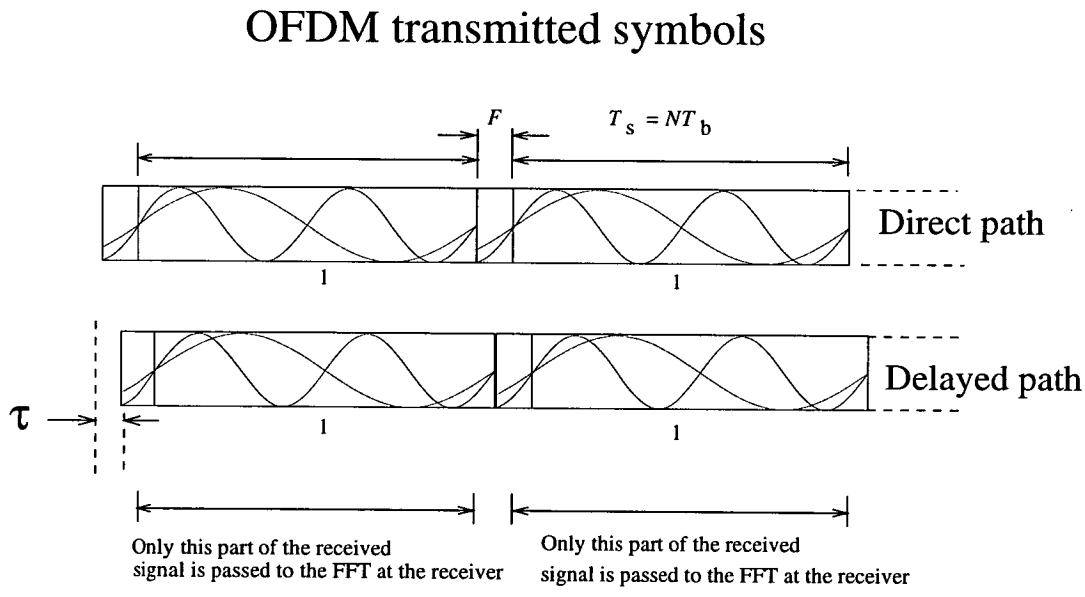

Figure 2.6: OFDM transmitted symbols (Only two carriers shown for clarity, N carriers are present)

If the guard interval F is greater than the maximum delay spread τ_d and if the symbol time $T_s = NT_b$ in

each subcarrier is smaller than the time coherence of the channel ($1/f_{d_{max}} \gg T_s$), the transfer function $H(f,t)$ of the channel may be regarded as being quasi-constant in time and frequency. Therefore, each sub-channel will appear like a slow flat fading channel. Over the bandwidth B, this results in a high order of diversity which is considered ideal for a mobile receiver.

The condition $1/f_{d_{max}} \gg T_s$, however, poses an upper limit on the number of carriers that can be used. The addition of the guard period, although eliminating the effects of ISI causes a mismatch between the duration of the transmitted signal ($T_s + F$) and the duration of the received symbol (T_s) which causes a power loss (in dB) of log (T/T_s) where $T = T_s + F$. This means that the ratio of F/T_s has to be maintained at a low level.

Denoting the frequency of the kth transmitted carrier by f_k where $f_k = f_c + k/T_s$ for $k = 0, 1, \ldots, N-1$, the time domain representation of the kth carrier can be written as $\phi_k(t)$,

$$\phi_k(t) = \begin{cases} e^{j2\pi f_k t} & -F \leq t < T_s \\ 0 & \text{otherwise} \end{cases}$$

For data bit n the time domain representation of the carrier can be written as $\psi_{n,k}$,

$$\psi_{n,k}(t) = \phi_k(t - n(T_s + F)) \tag{2.9}$$

It can be shown that the carriers satisfy the orthogonality conditions:

$$n \neq n' or k \neq k' : \int_{t=0}^{T_s} \psi_{n,k}(t)\psi^*_{n't'}(t)dt = 0 \tag{2.10}$$

$$\text{and} \int_{t=0}^{T_s} |\psi_{n,k}(t)|^2 dt = T_s \tag{2.11}$$

In the last five years multi-carrier modulation in the form of OFDM has received considerable attention. OFDM has been considered as a transmission technique for high rate digital subscriber lines (HSDL), audio and video broadcasting, cellular radio systems and spread spectrum systems. In the next section, we will discuss the application of OFDM for digital broadcasting. This is followed by a discussion of different combinations of multi-carrier modulation with spread spectrum techniques in the next chapter.

2.3.3 Digital broadcasting

In the early 1980s, broadcasting companies in Europe re-examined broadcasting principles so that programmes could be received at a much higher quality. This was influenced by the higher quality available

from other media (such as compact disc (CD) and digital audio tape (DAT)) and also by the availability of high performance digital signal processing integrated circuits which could make digital broadcasting a practical reality. The broadcasting industry decided to adopt OFDM as the transmission technique for digital broadcasting as it facilitates the transmission of high data rates in a spectrally efficiency manner. Further, one of the advantages of the OFDM system over the traditional FM broadcast system is the ability to use a single frequency network (SFN). Traditionally, national broadcasting (both radio and television) is accomplished by transmitting programmes on a regional basis. Each region transmits its programmes on a certain set of frequencies and adjacent regions choose frequencies which are sufficiently far apart to reduce interference problems. This means that when a user is moving from one region to another the user must change frequency to continue to receive the same program [1]. Due to the guard interval in OFDM, if the time difference between received transmissions is shorter than the guard interval, all nearby transmitters can transmit on the same frequency. In this way, the signals received from different transmitters on the same frequency do not interfere with each other and a single frequency network can provide national coverage.

2.3.3.1 Audio broadcasting

Digital audio broadcasting (DAB) using OFDM transmissions has been standardised by the European Telecommunications Standards Institute (ETSI). The DAB standard is ETSI standard ETS 300 401 [18]. The OFDM transmission system for digital audio broadcasting is designed to be totally flexible. There are four modes of operation. The key features of each mode is shown in Table 2.2. As can be seen from Table 2.2 the number of active carriers ranges from 192 to 1536 with a corresponding guard interval length from 32 μs to 246 μs. For all modes the modulation scheme is $\pi/4$ differential quaternary phase shift keying ($\pi/4$ DQPSK) which alleviates the requirement for channel estimation and equalisation. For all modes, motion picture experts group (MPEG) coding is used which processes the pulse coded modulated (PCM) audio signal and produces a compressed audio bit stream. The resulting multiplexed data stream ranges from 8 kbits/s to 384 kbits/s. The data is convolutionally encoded using a punctured convolutional code of constraint length 7. Both time and frequency interleaving are incorporated. The coded data is transmitted in frames (see row 1 of Table 2.2 for different frame length). There are 3 blocks for each frame: the synchronisation block, the fast information block and the main service block. The synchronisation block contains 2 symbols. The first symbol is a null symbol which is used to identify the start of the frame. The second symbol is used as a phase reference for the DQPSK modulation. The fast information block transmits data about the present mode and chosen coding scheme. The main service block transmits the useful information.

[1] This problem has been solved in recent years by the radio data system (RDS). An RDS receiver will automatically change its frequency when the user moves one region to another

Table 2.2: *Different DAB modes*

	Mode 1	Mode 2	Mode 3	Mode 4
Frame length	96 ms	24 ms	24 ms	48 ms
Number of active carriers	1536	384	192	768
Carrier spacing	1 kHz	4 kHz	8 kHz	2 kHz
Symbol duration	1.246 ms	312 μs	157 μs	623 μs
guard interval length	246 μs	62 μs	32 μs	123 μs
Reccomended use	SFN	Local services	Services below 3 GHz and cable	Local services and SFN in L-Band

2.3.3.2 Television broadcasting

Digital Terrestrial Television Broadcasting (DTTB) using OFDM transmission has also been standardised by ETSI. The DTTB standard is ETSI standard ETS 300 744 [19]. In the same way as DAB the DTTB system is designed to be flexible. There are two defined modes of operation, a 2K mode and a 8K mode. The 2K mode uses 1705 active carriers and is recommended for single transmitter operation and for small SFN's with limited transmitter distances. The 8K mode uses 6817 active carriers and is recommended for large SFNs. For both modes, all the data carriers in one frame are either modulated by QPSK, 16 level QAM, 64 level QAM or non-uniform 64 level QAM. Various pilot tones are used for frame synchronisation, channel estimation and transmission mode identification. The length of the guard interval can be selected from 7μs to 1.12 ms depending on the mode of the transmission.

The coding scheme is a concatenated coding scheme using a Reed-Solomon code as the outer code and a punctured convolutional code as the inner code. The maximum transmitted date rate supported is 31.67 Mbits/s.

There has been much research work conducted on OFDM for digital television broadcasting and we will summarise here some of the most recent research activities.

Sari [20] has compared the performance of an OFDM system with a single carrier system which has a frequency domain equaliser. Both systems use IFFTs and FFTs except in the case of the single carrier system the IFFT and FFT are moved further down the communication chain. In the absence of channel coding, the single carrier system with frequency domain equaliser substantially outperforms the OFDM system. The main conclusion of this work is that the OFDM system does not perform well without coding. When both systems were compared with concatenated coding it has been shown by Polley [21] that the OFDM system outperforms the single carrier system with frequency domain equaliser.

Several schemes for digital broadcasting have been proposed which do not require channel estimation or equalisation. The first of these is differential quaternary phase shift keying (DQPSK) which has been proposed by Saito [22]. Saito investigates the performance of the DQPSK scheme in the presence of multipath, ghosting and the influence of non-linear amplifiers.

Another idea for alleviating the requirement for channel estimation and channel equalisation is a 64-level differential amplitude phase shift keying (DAPSK) scheme suggested by Rohlings [23]. In this scheme, 4 bits from every 6 bits are used to represent the amplitude and the other 2 bits represent the phase. This is done in a cyclical fashion so differential coding can be used. The difference in performance between 64-level DAPSK and 64-level QAM (coherent) is analysed. The 64-level DAPSK system is shown to require an E_b/N_0 4.5 dB higher than that of the 64-level QAM system at a BER of 1×10^{-4}.

A third method for channel estimation for coherent demodulation schemes has been suggested by Mignone [24]. This scheme, which is called CD3-OFDM, uses the synchronisation frame of the OFDM transmitted signal to obtain an initial channel estimate. The received data after channel decoding is re-encoded and remodulated to form a sequence. This sequence is compared to a delayed version of the received sequence (before demodulation) in a feedback loop to form subsequent channel estimates. The scheme has been shown by Mignone to have no cost in the required carrier to noise (C/N) ratio for a given bit rate compared to a system with pilot tones.

2.4 Summary

In this chapter concepts has been introduced which are used throughout this thesis. In particular spread spectrum, channel modelling techniques and OFDM have been discussed. The spread spectrum section has discussed different spreading techniques, DS-CDMA systems and the generation and properties of commonly used spreading sequences. The channel modelling section has discussed channel models used throughout this thesis. Important characteristics of multipath fading channels, such as coherence bandwith and coherence time have also been introduced. Finally, the last section has described multi-carrier techniques, the principles of OFDM and the role of OFDM in digital audio and television broadcasting systems.

Chapter 3
Review

3.1 Introduction

In this chapter we will discuss and review some of the different arrangements for combining CDMA with multi-carrier modulation (MCM) to form a multi-carrier CDMA (MC-CDMA) system. This chapter is split into three sections corresponding to the three different types of MC-CDMA.

In section 3.2 we consider MC-CDMA systems in which each carrier in the multi-carrier multiplex is modulated by a short length PN sequence. This is followed in section 3.3 by a discussion of the second form of MC-CDMA in which the individual carriers are modulated by one chip of the spreading sequence. Thus the PN sequence is spread in the frequency domain and the number of carriers is greater than or equal to the length of the spreading code. Finally in section 3.4 we will describe a MC-CDMA system in which the data is first passed to an OFDM multiplex and then spread by a PN sequence. In each section we will describe the principles and discuss some of the possible advantages/disadvantages that the particular system may have over DS-CDMA.

3.2 One PN sequence per carrier

Sourour and Nakagawa [25] have devised a multi-carrier CDMA system in which a small number of carriers, M, are used and the data on each carrier is spread by a short length PN code. The carriers are spaced by $1/T_c'$ where T_c' is the chip duration. The transmitter for user m is shown in Figure 3.1. Here the incoming data stream $b(t)$ is multiplied by the higher rate PN code $PN_m(t)$. Interleavers are used on every stream which reorder the data bits and hence provide diversity since the same data bit is not transmitted on all of the carriers simultaneously. The transmitted spectrum is shown in Figure 3.2.

The bandwidth of transmission is given by,

$$B = \frac{M+1}{T_c'} \tag{3.1}$$

As the bandwidth of a traditional DS-CDMA system is given by

$$B = \frac{2}{T_c} \tag{3.2}$$

the length, N_a, of the PN spreading sequence $PN_m(t)$ for the system to occupy the same bandwidth as an equivalent DS-CDMA system is given by,

$$N_a = \frac{2}{M+1}N \tag{3.3}$$

where N is the length of the spreading sequence for an equivalent DS-CDMA system.

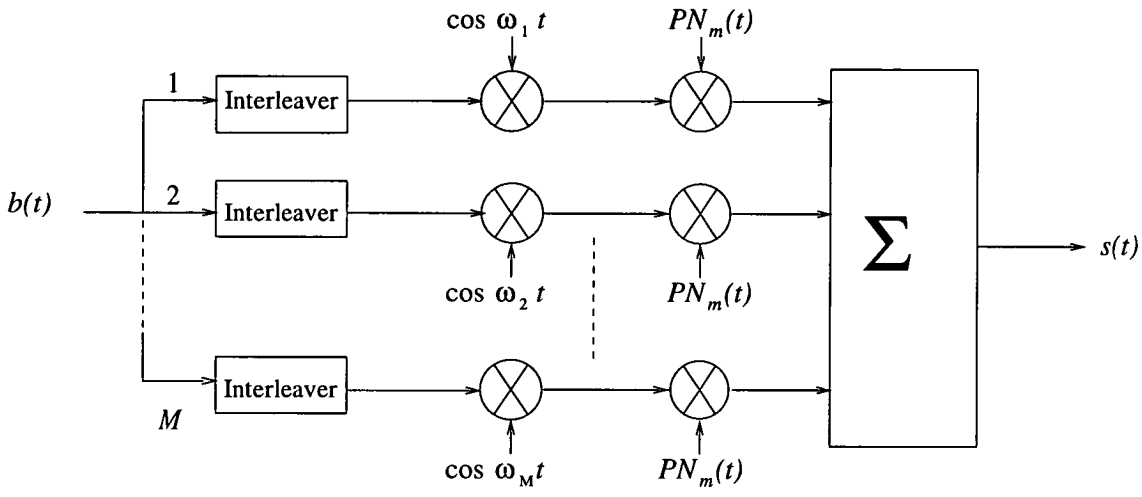

Figure 3.1: Multi-carrier CDMA from Sourour and Nakagawa [25]

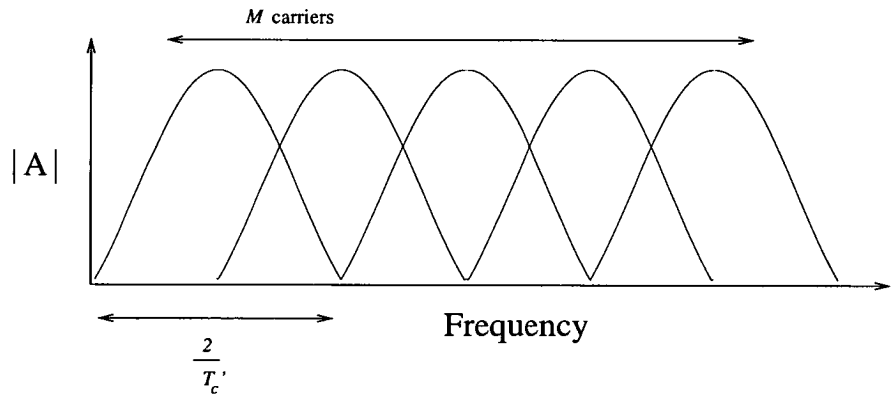

Figure 3.2: Spectrum of transmitted signal from multi-carrier CDMA shown in Figure 3.1 [25]

To reduce the data rate on individual carriers, the incoming data can be converted from a serial stream into M parallel data streams. This reduces the ISI because the sent symbol duration is longer. A longer PN sequence can also be used for the same transmission bandwidth. A system of this type has been suggested by Sourour and Nakagawa [26] and is shown in Figure 3.3. The length of the equivalent PN code is given by

$$N_b = \frac{2M}{M+1}N \tag{3.4}$$

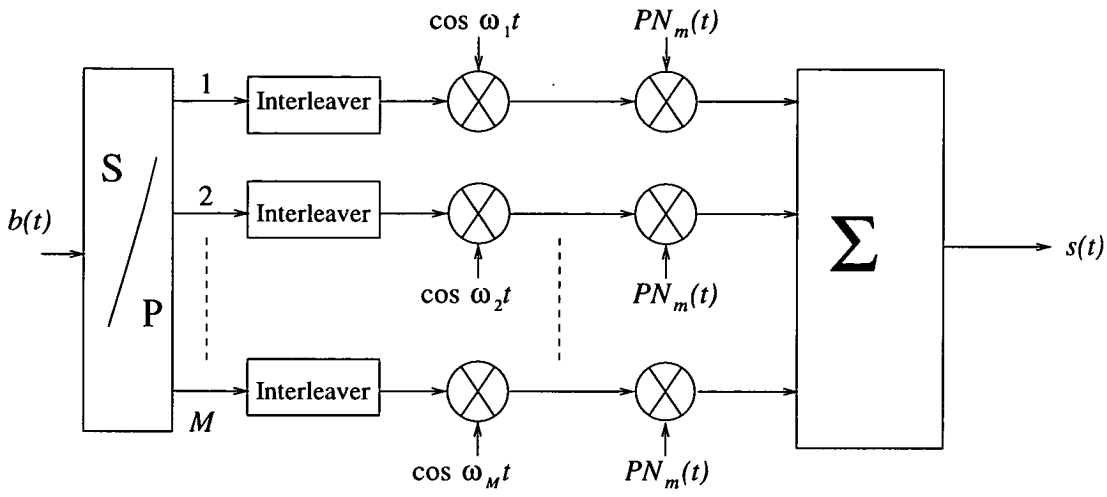

Figure 3.3: Multi-carrier CDMA from Sourour and Nakagawa [26]

Comparing these two systems, the system of Figure 3.1 provides the greater diversity as the same data bit is transmitted on several different carriers.

To combine both of these systems Sourour and Nakagawa [27] devised the system of Figure 3.4. Here the incoming bit stream with duration T_b is serial to parallel converted into P parallel data streams with duration $T = PT_b$. Each stream is then branched into S parallel streams with the same data bit. The PS carriers are again spaced by the $2/T_c'$, and the frequency separation between the S identical bit carriers is maximised to obtain diversity. (See Figure 3.5.) To obtain the same transmitted bandwidth as an equivalent DS-CDMA system, the length of the spreading sequence can be shown to be [27]

$$N_c = \frac{2P}{PS+1}N \tag{3.5}$$

Interleaving is also incorporated. It has been shown by Sourour and Nakagawa [27] that as the number of carriers increases and the transmission bandwidth is kept constant each carrier experiences only flat fading. This occurs when

$$PS > D - 2 \tag{3.6}$$

where D is the number of resolvable paths for a comparable DS-CDMA system. Nakagawa and Sourour have investigated the performance of this system by varying S, the number of identical bit carriers and the size of the serial to parallel converter P. The best performance was achieved by using a RAKE receiver on every received carrier, when each carrier was subject to 2-path fading. The performance of this receiver was shown to be superior to a standard DS-CDMA system of the same bandwidth using a RAKE receiver. This performance is achieved at the expense of receiver complexity. If the carriers of the MC-CDMA system shown in Figures 3.1 and 3.3 are subject to flat fading, the suggested MC-

CDMA is at a disadvantage compared to the RAKE receiver because the multipath components are not resolvable and thus cannot be combined over the subchannels.

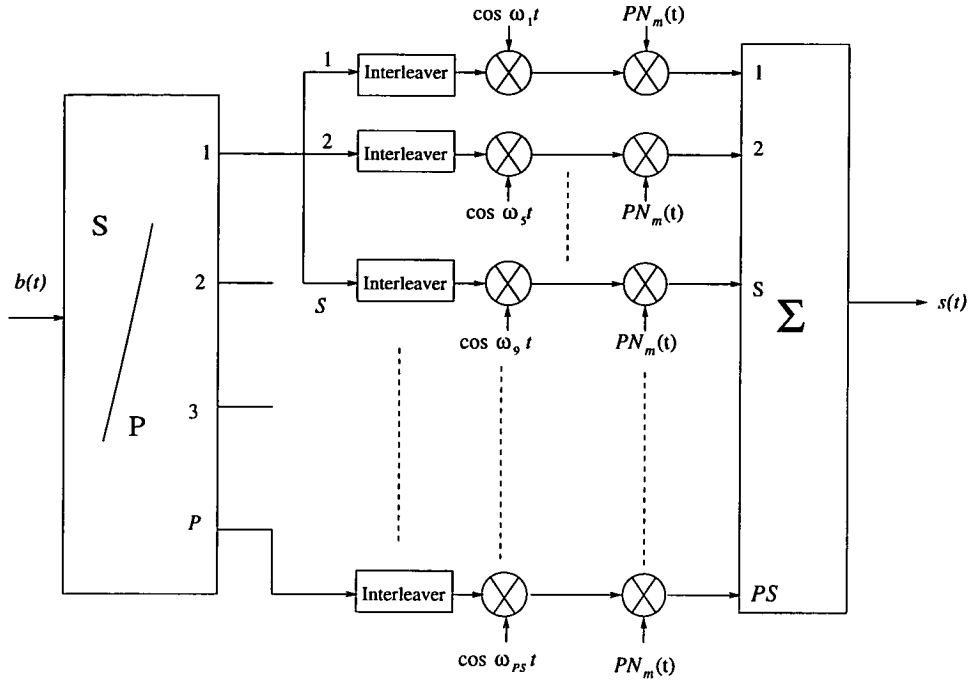

Figure 3.4: Multi-carrier CDMA from Sourour and Nakagawa [27]

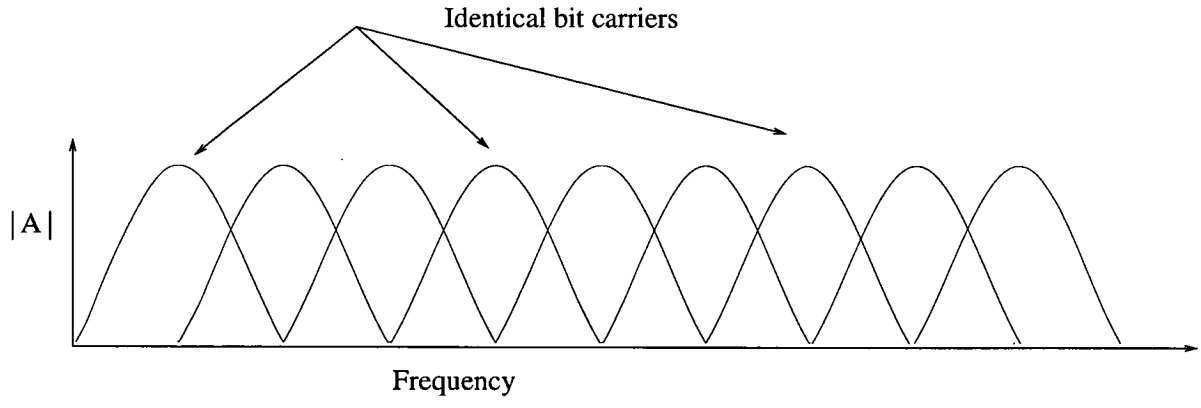

Figure 3.5: *Spectrum of transmitted signal from multi-carrier CDMA system shown in Figure 3.4 [27] (P=3, S=3)*

Sousa and Chen [28] have investigated a system as seen in Figure 3.1 where the chip duration is longer than the channel delay spread and thus the carriers are subject to flat fading. The main motivation for this is to facilitate the synchronization process. As the chip duration is longer than the equivalent DS-CDMA system, synchronisation is easier. Instead of resorting to the scheme seen in Figure 3.4 to obtain frequency diversity, they used a Reed-Muller code with soft decision decoding. The results [28] show that although the uncoded single carrier DS-CDMA system with a RAKE receiver can outperform the suggested uncoded multi-carrier DS-CDMA due to diversity benefits, the multi-carrier DS-CDMA with Reed-Muller coding outperforms the DS-CDMA RAKE receiver with the same coding scheme. It

is also interesting to note that the performance of the multi-carrier DS-CDMA is less affected by the variation in the number of users than the single carrier DS-CDMA system and thus more suitable to a system where the service demands are relatively unstable.

Sousa and Chen [29] have also investigated a sub-channel hopping technique for the scheme shown in Figure 3.3, to obtain diversity without the time delays and complexities of coding. In the proposed system M PN sequences are assigned for each user (same as the number of carriers), so that every data stream is uniquely identified by a spreading sequence. In contrast to previous methods where one sub-stream is sent over each sub-channel, sub-streams can hop to any of the sub-channels depending on the fading parameters. This is especially suitable when operating over channels with very slow time variations which are often encountered in environments with slow moving vehicles or pedestrians. This system has been shown to perform better than a conventional RAKE and the proposed scheme proposed by Sousa and Chen [28] with Reed-Muller coding.

Kondo and Milstein [30, 31] have investigated a multi-carrier system similar to that of Figure 3.3. In this particular system all carriers have the same spreading sequence and the bandwidth of the carriers are disjoint as seen in Figure 3.6. The overall transmission null to null bandwidth BW_m is given by,

$$BW_m = BW_1 M \tag{3.7}$$

where M is the number of carriers and BW_1 is the bandwidth of the individual carriers given by,

$$BW_1 = \frac{2}{MT_c'} \tag{3.8}$$

where MT_c' is the chip duration of the multi-carrier system.

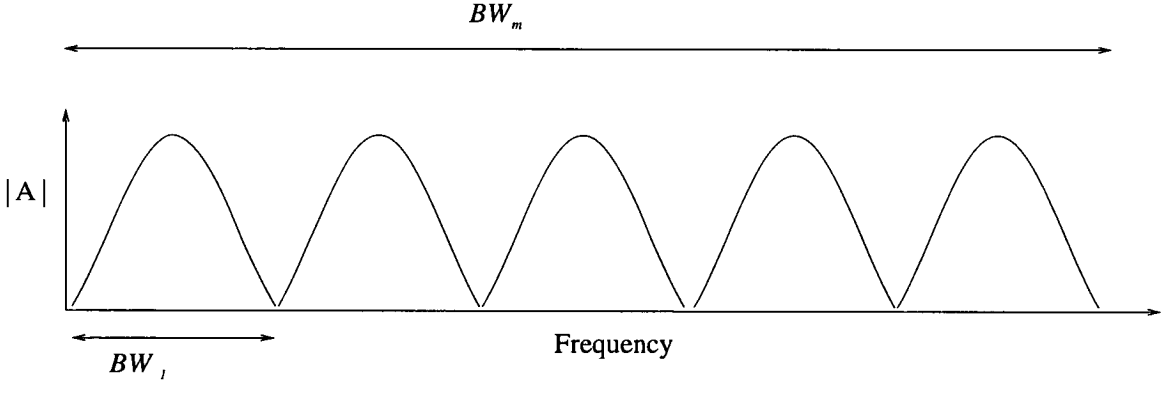

Figure 3.6: Spectrum of transmitted signal from Kondo and Milstein multi-carrier CDMA [30]

In the analysis by Kondo and Milstein, a comparison is made between the proposed multi-carrier system and a RAKE receiver with the same diversity. To ensure the same energy per bit in both the multi-carrier

and single carrier systems, the energy per carrier in the multi-carrier system is reduced by a factor of M. In multipath fading channels both systems are shown to have the same performance against increasing levels of multi-user interference. The multi-carrier system does however have superior performance with narrow band interference. This scheme has therefore been suggested by Kondo and Milstein as a candidate for an DS-CDMA scheme overlaying a traditional FDMA system.

3.3 One PN chip per carrier

In this section we will consider systems in which the processing gain of each carrier is one and the value of one chip of the spreading sequence (and the data content) modulate the carrier. Some of these systems combine OFDM with CDMA.

Some of the first research work of combining multi-carrier techniques with CDMA in this way has been conducted by Chouldy *et al.* [6]. In this system a DS-CDMA system is combined with an OFDM system. All of the users' DS signals are summed together, frequency interleaved and then sent in parallel through the channel at symbol rate. Intersymbol interference is absorbed by a guard interval. The minimum mean square error (MMSE) criteria is used at the receiver and the performance of the system is compared to a DS-CDMA system. The performance of the OFDM-CDMA system is shown to be superior to that of the DS-CDMA system in multipath channels.

Linnartz *et al.* [7, 32, 33] have proposed a multi-carrier CDMA system in which a single data symbol is replicated into N parallel copies. Each branch of the parallel stream is multiplied by one chip of the spreading code of length N and modulates a sub-carrier. There are N sub-carriers in total. The spacing between the sub-carriers is J/T_b where J is an integer and T_b is the bit duration. When J=1 the transmit bandwidth is minimised and the carriers overlap in the same way as an OFDM system.

Linnartz *et al.* have investigated the performance of the system when the frequency separation of the sub-carriers is greater than the coherence bandwidth and thus the individual carriers experience independent fading so that diversity is maximised. Various detection schemes at the receiver are investigated including equal gain combining (EGC), maximal ratio combining (MRC), the Wiener filter solution [32], controlled equalisation [7] and a decorrelating interference canceller [33]. The main drawback of this technique is that to obtain the performance increase due to diversity, the carriers have to be separated by a distance greater than the coherence bandwidth. The overall transmission bandwidth of the system is therefore greater than a conventional DS-CDMA system to achieve these improvements.

Fazel [5] has proposed an OFDM-CDMA system which uses a combination of DS-CDMA with OFDM as seen in Figure 3.7. In this system, 64 users' signals are split into a number of DS-CDMA subsystems. (Eight subsystems are shown.) The data bit in each sub-system is spread by a Walsh code of length 8. From each sub-system 8 data bits are serial to parallel converted producing 64 output streams at a rate which is 8 times lower than the data rate. In this way ISI is reduced. These streams are sent to the frequency interleaver which scrambles all of the outputs and passes them to an OFDM modulator. The frequency interleaver scrambles all the outputs in order to achieve independent fading between

adjacent subcarriers. A guard interval is inserted here which is longer than the channel dispersion and absorbs any ISI. Pilot tones are also further added here periodically in frequency and time to estimate the channel. If dispersion in the channel is sufficient, chips from the same data bit experience single path independent fading. This is because the chips are separated in frequency at a distance greater than the coherence bandwidth.

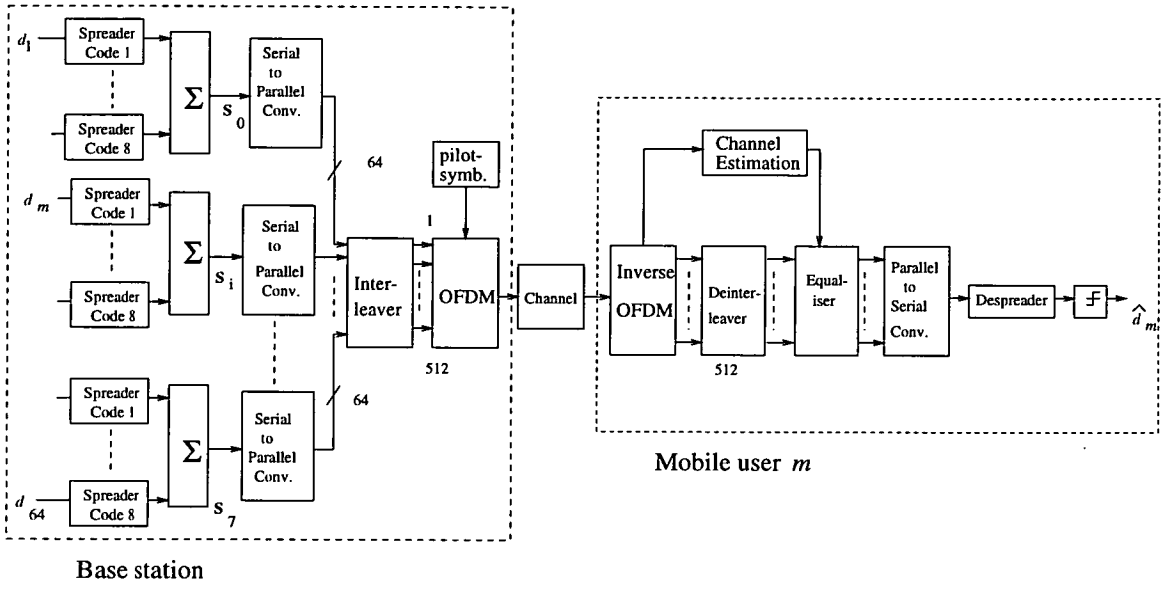

Figure 3.7: OFDM-CDMA from Fazel [5]

This system has two key advantages over the multi-carrier system proposed by Linnartz,

1) The data rate on the individual carriers is reduced by a factor of 8 and the number of carriers is increased by the same factor. In this way all sub-system outputs can be multiplexed onto the carriers enabling diversity to be achieved without increasing the transmission bandwidth.

2) In each sub-system, short (8 chip) Walsh sequences are used. This enables the use of detection schemes which would otherwise be impractical, such as maximum likelihood detection (MLD).

The performance of this OFDM-CDMA system has been shown [34,35] to provide superior spectral efficiency performance compared to a maximal ratio combining (MRC) RAKE receiver for a DS-CDMA system of the same bandwidth. The performance of this OFDM-CDMA system has also been investigated by Kaiser [36,37] in conjunction with EGC, MRC, MMSE and MLD detection techniques. Several interference cancellers have also been investigated. A single stage interference canceller using EGC has been suggested by Fazel [5] and a two stage canceller using MMSE as the first stage and EGC as the second stage has been investigated by Kaiser [37]. A two stage canceller has also been investigated by Kalofonos [38] using a threshold orthogonal restoring detector (TORC) as the first stage and MRC as the second stage.

Fazel [39] has investigated the performance of the system with a soft output from the MLD detector, so

the output can be passed to a soft decision Viterbi decoder. The performance of the resulting punctured convolutional coded MLD OFDM-CDMA is shown to be far superior to a coded DS-CDMA system. Kaiser [40] has also investigated the performance of the system with a soft output from a MMSE detector and a MLD detector in conjunction with turbo coding. The turbo coded MLD OFDM-CDMA system is shown to have improved performance over the punctured convolutional coded MLD OFDM-CDMA system.

Fazel has also investigated the performance of the system in the presence of narrow band interference [41]. By using a null symbol in the OFDM frame, an interference estimate is made so that a "soft-erasure" or "soft-switching off" of the carriers is made to notch filter the interference. The results show that narrow band interference rejection can easily be accomplished with this OFDM-CDMA system. The system is shown to be robust even if the interference represents 50 % of the transmitted bandwidth.

3.4 One PN sequence per OFDM multiplex

Wiel and Vandendrope [42–45] have investigated a multitone direct sequence spread spectrum CDMA system in which the multitone modulation is performed first, and then DS-SS is added as seen in Figure 3.8. The incoming data, of duration T_b, is passed to an M output serial-to-parallel converter, producing M output streams of duration MT_b. These streams modulate M carriers which are orthogonally spaced at $1/MT_b$. The multiplex output is then multiplied by the PN sequence which has chip duration $T_c^{'}$. The output bandwidth is controlled by $T_c^{'}$, so if the number of carriers are increased, the data rate on the individual carriers can be reduced, enabling a longer spread sequence to be used without an increase in bandwidth.

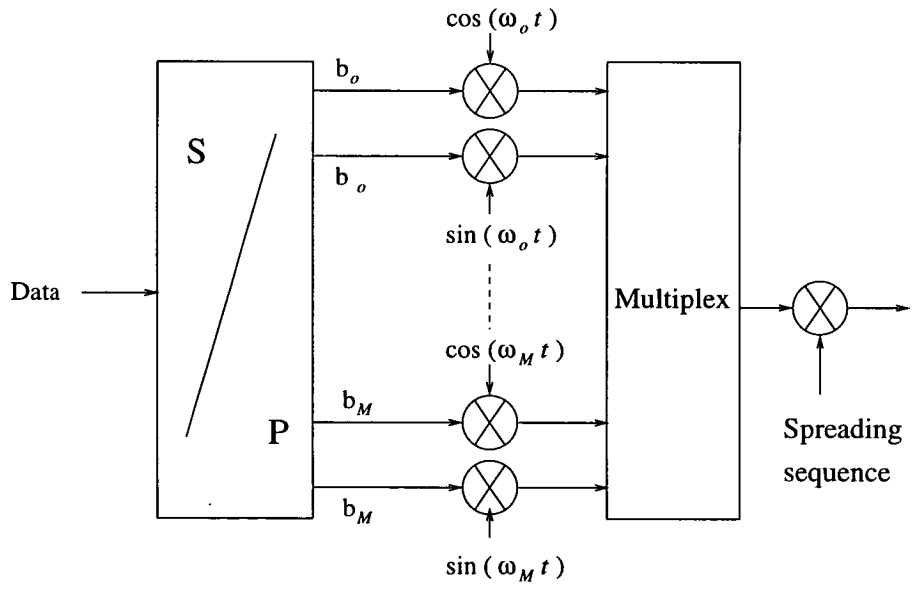

Figure 3.8: Multitone DS-CDMA from Wiel and Vandendrope [43]

In this way the system can accommodate more users than the traditional DS-CDMA system. However, the multitone DS-SS CDMA system suffers from inter-carrier interference which increases with the

number of sub carriers. In channels where the capability to use longer spreading sequence is more dominant than the inter-carrier interference, the multitone DS-CDMA can outperform a DS-CDMA system.

Prasad and Hara [46] have compared the performance of this system in a 2-path channel with other MC-CDMA systems and DS-CDMA. The considered multitone system has 4 carriers and a 2-path RAKE receiver for every carrier in the receiver. Prasad and Hara showed that the system has worse performance than the DS-CDMA system for low number of users and only has slightly better performance than the DS-CDMA system when the DS-CDMA system is fully loaded.

To combat the ISI and ICI encountered by this system in a multipath channel, various equalisers have been examined. Wiel and Vandendrope have investigated bidimensional (linear and non-linear) adaptive filters [43, 44], decision feedback joint detection [47] and an interference canceller [45].

3.5 Summary

After reviewing some of the research work on the three different forms of multi-carrier CDMA, we shall summarise some of the main features of these systems. The advantages and disadvantages over DS-CDMA are shown in Table 3.1. The typical number of required carriers M for each system is also shown. This is expressed in terms of the spreading sequence length N. As each system has many variations, we have chosen the best of each access scheme to show the possible advantages/disadvantages that each system may have.

Table 3.1: *Summary of different MC-CDMA systems*

Access Scheme	No. of Carriers M	Advantages	Disadvantages
PN Sequence per carrier (section 3.2)	$< N$	- If each carrier is subject to multipath, better performance than DS-CDMA. - T_c longer, $\Rightarrow$ easier synchronisation.	- High receiver complexity M RAKE receivers.
PN Chip per carrier (section 3.3)	$\geq N$	- Spectral efficient system. - No ISI, ICI. - Simple receiver architectures. - Practical MLD possible.	- Only coherent demodulation possible. - High no. of carriers $\Rightarrow$ Increased sensitivity to phase noise and intermodulation. [1]
PN Sequence per multiplex (section 3.4)	$< N$	- Longer PN sequence $\Rightarrow$ Possible higher capacity	- Severe inter-carrier interference, increasing with M. - Higher capacity only realisable in certain channels.

[1] Intermodulation is the effect by which 2 or more carriers mix due to the non-linear characteristic of the amplifier forming harmonically related sum and difference spurious products.

It can be seen that all systems have possible performance advantages over DS-CDMA. The PN sequence per carrier system, achieves these advantages at the expense of receiver complexity requiring M RAKE's for each receiver. The PN sequence per multiplex system has the advantage, that longer PN sequence are possible. However, due to the inter-carrier interference this possible high capacity advantage is only realisable in certain types of channels.

The PN chip per carrier systems uses many more carriers than the other two systems with a much lower data rate on each carrier. The system has no ISI or ICI (due to the guard interval), a high spectral efficiency and much simpler receiver architectures. Also a full MLD is possible. To obtain these advantages many closely spaced carriers are used. This requires a high quality local oscillator at the receiver due to the increased sensitivity to phase noise [48]. At the transmitter, a linear amplifier is needed, due to the increased number of intermodulation (IM) products which are produced by the larger number of carriers [49]. It is also important to note that in this scheme only coherent demodulation is possible (see section 4.4) and therefore channel estimation has to be performed using pilot tones.

Chapter 4
Multi-carrier CDMA

4.1 Introduction

In this chapter we investigate the performance of an uncoded multi-carrier CDMA system (MC-CDMA) similar to the one proposed by Linnartz [7]. In our study we will examine the performance of the system when the carriers overlap in the OFDM sense (see Figure 2.5) to reduce the transmission bandwidth. In this way, we compare the performance of this MC-CDMA system with an DS-CDMA system using the same bandwidth.

In section 4.2 we describe the MC-CDMA system. In section 4.3 we discuss binary phase shift keying (BPSK) for the MC-CDMA system and two combining techniques at the receiver. An equivalent DS-CDMA system is then described utilising a RAKE receiver. A performance comparison of these BPSK systems in a multipath channel is then made. In section 4.4 the MC-CDMA system with differential phase shift keying (DPSK) is described and the concept of the frequency domain RAKE receiver is introduced. We then describe an equivalent DPSK DS-CDMA receiver and present a performance analysis of these DPSK systems. In section 4.5 we examine the performance of this MC-CDMA system using adaptive receiver architectures. A summary is then made in section 4.6.

4.2 System description

The MC-CDMA system we consider in this chapter is a variation of the system proposed by Linnartz *et al.* [7]. The system proposed by Linnartz duplicates the data symbol into N parallel copies. Each branch of the parallel stream is then multiplied by a chip from a spreading code of length N. The output of these multipliers then modulates a set of N carriers which are separated in frequency at a distance greater than the coherence bandwidth. Diversity is achieved in this way. To obtain this diversity, however requires a large separation between the carriers and a large transmission bandwidth (of the order of N times the coherence bandwidth) and so the resulting spectral efficiency is low.

The system we consider here is one in which the N carriers are spaced in frequency by $1/T_b$, where T_b is the bit duration. Therefore, the system requires the minimum bandwidth for transmission as in the normal OFDM system. Contrary to the traditional OFDM system, we will investigate the performance of the system without a guard interval and therefore the carriers will not remain orthogonal in multipath. Further the received amplitudes and phases of adjacent sub-carriers are correlated but become less so, if the channel dispersion is large.

4.3 BPSK modulation

The MC-CDMA transmitter is seen in Figure 4.1. The continuous time representation of the signal produced by the mth user is given by,

$$S_m(t) = b_{km} P_{T_b}(t - kT_b) \sum_{n=0}^{N-1} c_m(n) \cos(2\pi(f_c + \frac{n}{T_b})t) \tag{4.1}$$

where b_{km} is the kth symbol transmitted from the mth user and $c_m(n)$ is the nth chip from the mth user. $P_{T_b}(t)$ is a unit amplitude pulse which is non-zero in the interval of $[0, T_b]$ and f_c is the carrier frequency of the system. We will only consider baseband signals and thus f_c is zero.

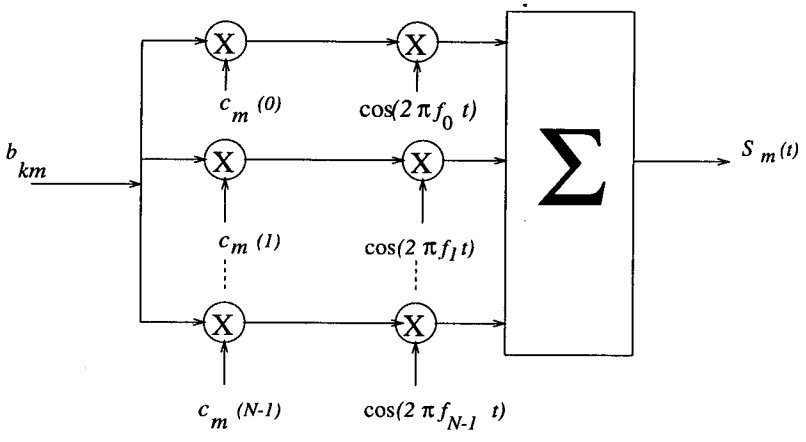

Figure 4.1: MC-CDMA transmitter

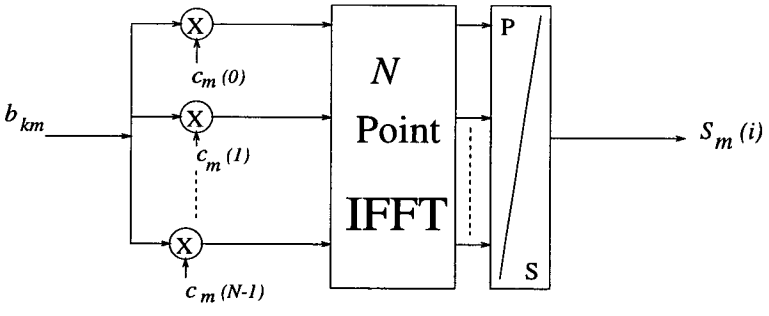

Figure 4.2: MC-CDMA digital transmitter

To reduce the number of RF mixers required, the bank of mixers can be implemented by sampling the signal and using the inverse fast Fourier transform (IFFT). This is shown in Figure 4.2. The discrete time representation of the baseband signal produced by the mth user in the system is given by,

$$S_m(i) = b_{km} P_{T_b}(i - kN) \operatorname{Re}\left[\sum_{n=0}^{N-1} c_m(n) e^{j2\pi \frac{ni}{N}}\right] \tag{4.2}$$

The received MC-CDMA signal is downconverted to baseband and sampled at the chip rate to form the incoming signal $x_k(n)$ which represents the nth chip from the kth transmitted bit. The signal is then serial to parallel converted. These parallel samples are the inputs to an N point FFT. The outputs of the FFT operation are multiplied by the receiver spreading code and the equaliser coefficients $a_k(n)$ to form $u_{k0}(n)$ which represents the nth decorelated chip from the kth symbol for user 0.

$$u_{k0}(n) = a_k(n) c_0(n) \sum_{m=0}^{N-1} x_k(n-m) e^{-j2\pi \frac{mn}{N}} \qquad n \in \{0..N-1\} \tag{4.3}$$

These signals are then summed to form the kth decision variable $\widehat{b}_{k0}$

$$\widehat{b}_{k0} = \operatorname{sgn} \sum_{n=0}^{N-1} u_{k0}(n) \tag{4.4}$$

The receiver for user 0 is shown in Figure 4.3. The equaliser coefficients $a_k(n)$ are calculated from the channel response $h_k(n)$. The channel response $h_k(n)$ can be estimated using pilot tones inserted into the channel.

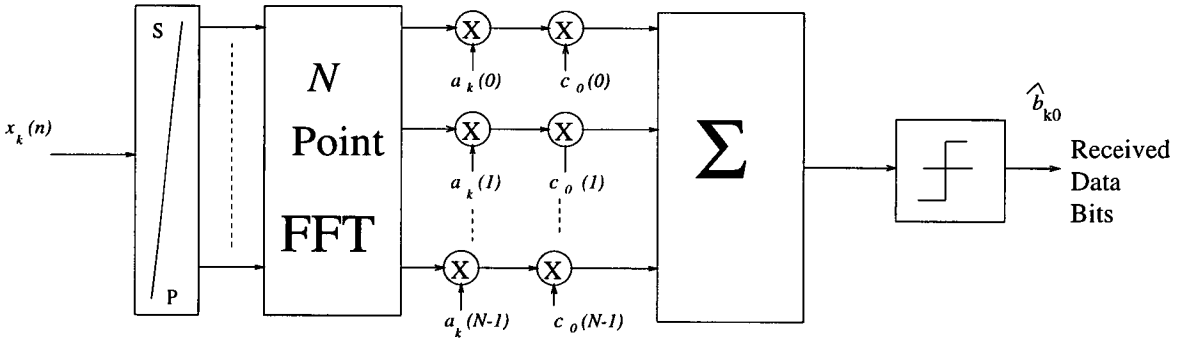

Figure 4.3: MC-CDMA receiver

For the purposes of this work, we shall assume we have a perfect channel estimate. In this way, the results represent a lower bound on performance. In section 3.4 the performance of this system will be compared to a BPSK DS-CDMA system of the same bandwidth which also uses perfect channel knowledge. The equaliser coefficients can be calculated from $h_k(n)$ in several ways and we shall investigate maximal ratio combining (MRC) and equal gain combining (EGC).

MRC is based on correcting the phases and weighting the received signal with the amplitude of fading.

$$a_k(n) = h_k(n)^* \tag{4.5}$$

EGC is sometimes called phase equalisation and is based on correcting the phase shift only.

$$a_k(n) = \frac{h_k(n)^*}{|h_k(n)|} \tag{4.6}$$

4.3.1 BPSK DS-CDMA RAKE

For comparative purposes we examine a synchronous DS-CDMA system with N_u users where each user has a spreading code of length N chips. The resulting transmitted signal is given by,

$$y_k(n) = \sum_{m=0}^{N_u-1} b_{km}c_m(n) \quad n \epsilon \{0..N-1\} \tag{4.7}$$

where $y_k(n)$ is the composite output signal at chip n within bit k. b_{km} is the kth transmitted bit from the mth user. $c_m(n)$ is the nth chip from the mth user.

If the multipath channel has a delay spread, D_s, a DS-CDMA RAKE receiver can resolve and combine $1 + D_s/T_c$ multipath components, where T_c represents the duration of the chip. In this analysis we shall use a channel with a delay spread of $3T_c$. This is shown in Figure 4.5. (The channel is explained in more detail in section 4.3.2.1 .) The BPSK DS-CDMA RAKE can therefore resolve 4 paths. A BPSK DS-CDMA system utilising a RAKE receiver is shown in Figure 4.4. For MRC the received signal is multiplied by delayed versions of the spreading sequence and complex channel gain α_{kl}. The kth received data bit for user 0, b_{k0} is therefore given by

$$\widehat{b}_{k0} = \text{sgn} \sum_{l=0}^{D-1} x_{l0}(k)\alpha_{kl}^* \tag{4.8}$$

where α_{kl} is the complex gain for the lth path of the kth bit and $x_{l0}(k)$ is the kth decorrelated symbol for mobile 0 from the lth path. D is the number of multipath components. $x_{l0}(k)$ is given by,

$$x_{l0}(k) = \sum_{n=0}^{N-1} x_k(n)c_m(n - \tau_l) \tag{4.9}$$

where τ_l is the delay of the lth path.

The complex gain α_{kl} is given by,

$$\alpha_{kl} = \rho_{kl} e^{-j\theta_{kl}} \tag{4.10}$$

where ρ_{kl} is the channel attenuation and θ_{kl} is the phase of the lth path for the kth bit.

For EGC the received signal is given by,

$$\widehat{b}_{k0} = \text{sgn} \sum_{l=0}^{D-1} x_{l0}(k) e^{j\theta_{kl}} \tag{4.11}$$

In this simulation we will consider the case of $D = 4$ corresponding to a 4-path channel.

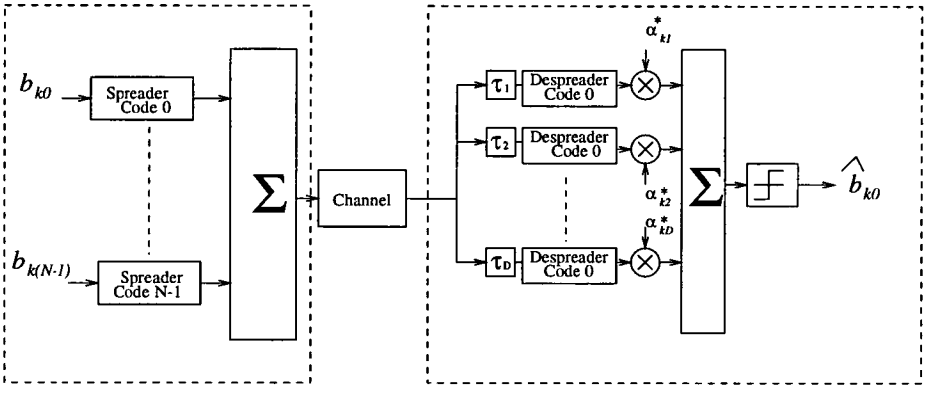

Base station

Mobile station

Figure 4.4: DS-CDMA BPSK RAKE receiver

4.3.2 BPSK performance evaluation

Monte Carlo simulations were conducted for the MC-CDMA and DS-CDMA systems. Both systems use a length 31 Gold code as the spreading sequence. A 32 point IFFT and FFT were used in the case of the MC-CDMA with the last point zero padded.

The baseband data rate in both system is 8 kbits/s yielding a chip rate of 248 kbits/s for the DS-CDMA system.

4.3.2.1 Fading channel

For the multipath channel simulation we have adopted a 4-path channel model with additive white Gaussian noise (AWGN). The mean power for all channels is assumed to be 1. The 4-path channel model is seen in Figure 4.5. In this model the scaling factors are set to $a_1 = a_2 = a_3 = a_4 = 0.5$. In the four path channel the tap delays are equally spaced at the chip duration, T_c, with independent Rayleigh fading on each path. The Rayleigh fading is characterised by the presence of the Doppler filter, Figure 4.6. A classical Doppler spectrum [13] is used with a maximum Doppler rate of 300 Hz which corresponds to a mobile speed of 162 km/h for a carrier frequency of 2 GHz.

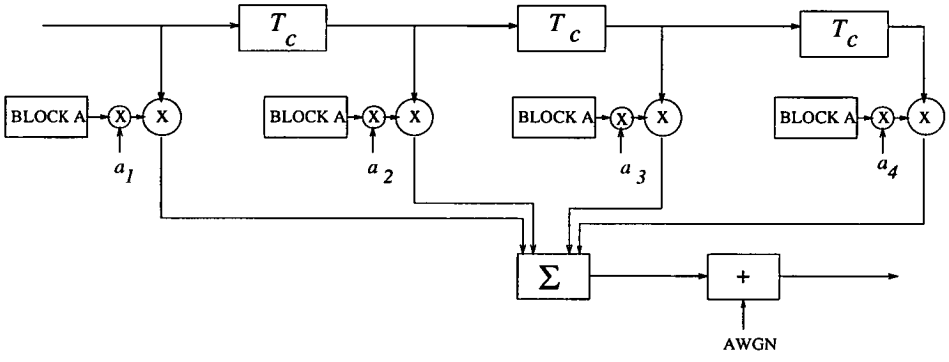

Figure 4.5: 4-path channel

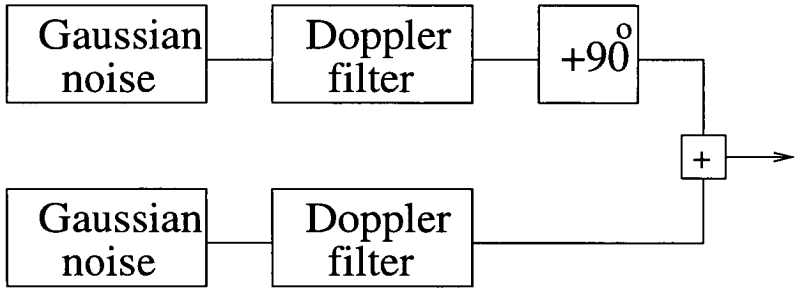

Figure 4.6: Block A for Figure 4.5

4.3.2.2 DS-CDMA

The performance of the MRC RAKE receiver is shown in Figure 4.7. Both the theoretical and Monte Carlo results are shown. For the results obtained from Monte Carlo simulations at least 10,000 errors were logged for every data point. The theoretical BER for a RAKE receiver using MRC has been derived by Fazel [34],

$$\text{BER} \approx \left(\frac{1}{2} - \frac{1}{2}\sqrt{\frac{2(N_u-1)}{3ND} + \frac{N_0}{DE_b} + 1}\right)^D \cdot \sum_{j=0}^{D-1} \binom{D-1+j}{j} \cdot \left(\frac{1}{2} + \frac{1}{2}\sqrt{\frac{2(N_u-1)}{3ND} + \frac{N_0}{DE_b} + 1}\right)^j \tag{4.12}$$

where D is the number of multipath components, N_u is the number of users and N is the length of the spreading sequence.

The EGC Monte Carlo results are shown in Figure 4.8. It can be seen that the MRC method performs better than the EGC method. For the single user at 8 dB E_b/N_0 a BER of 5×10^{-3} is achieved for MRC compared to 7×10^{-3} for EGC. At a load of 30 users and 17 dB E_b/N_0 the MRC technique achieves a BER of 5×10^{-2} compared to 8×10^{-2} for EGC. It is generally accepted that MRC is the preferred combining technique for a DS-CDMA RAKE receiver [14].

4.3.2.3 MC-CDMA

The MC-CDMA Monte Carlo results are shown in Figures 4.9 and 4.10 for MRC and EGC respectively. It can be seen for the case of a single user, that there is no difference between using MRC and EGC for MC-CDMA. For multiple users, however, EGC is the preferred technique. At a load of 30 users and 17 dB E_b/N_0, EGC achieves a BER of 3×10^{-2} compared to 0.1 for MRC. This is due to the amplitudes of the MRC equaliser coefficients affecting the orthogonality of the spreading sequence. This is in agreement with results from Yee and Linnartz [7].

By comparing the results of the EGC MC-CDMA system with that of the MRC DS-CDMA system we can see that the MC-CDMA system has a performance advantage for multiple users. For a load of 10 users at a BER of 5×10^{-3} the MC-CDMA system requires only 12 dB E_b/N_0 compared to the DS-CDMA system which requires 17 dB E_b/N_0. The DS-CDMA system does however have a performance advantage for the case of a single user.

This is an important result for this MC-CDMA system. In the system proposed by Linnartz [7] high performance was achieved because adjacent carriers were separated at a distance greater than the coherence bandwidth to achieve diversity. Further there was no inter-carrier interference due to the large carrier to carrier separation. In the MC-CDMA described here, the carriers overlap and the transmission bandwidth is minimised. As we do not use a guard interval there is inter-carrier interference. Despite this, we still achieve better performance for multiple users than an equivalent DS-CDMA system.

In this analysis however, we have not taken into account the overhead needed for channel sounding using pilot tones. (This will be dealt more in Chapter 5). When this is taken into consideration, it is expected that the difference in spectral efficiency between the two systems may be smaller than these

results suggest.

To alleviate the necessity for using pilot tones we shall examine the use of DPSK modulation for MC-CDMA in the next section.

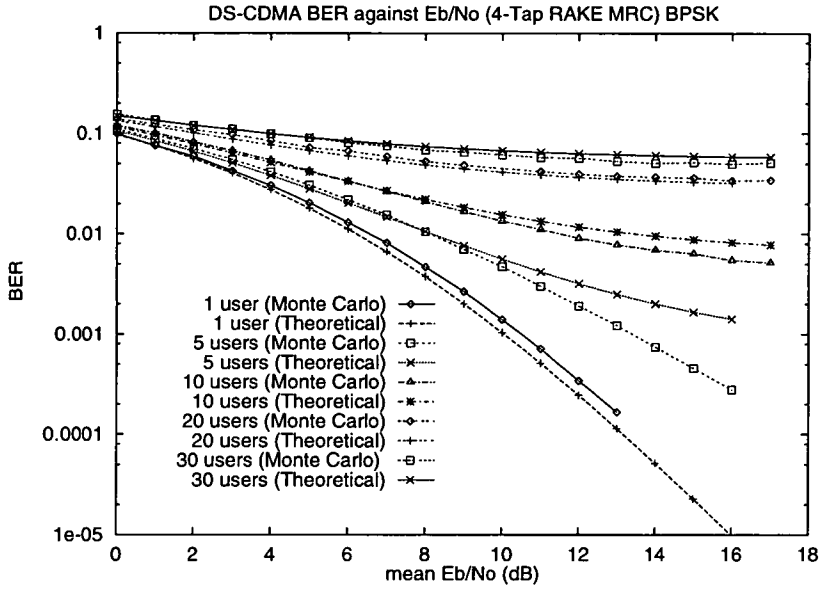

Figure 4.7: DS-CDMA MRC RAKE 4-paths

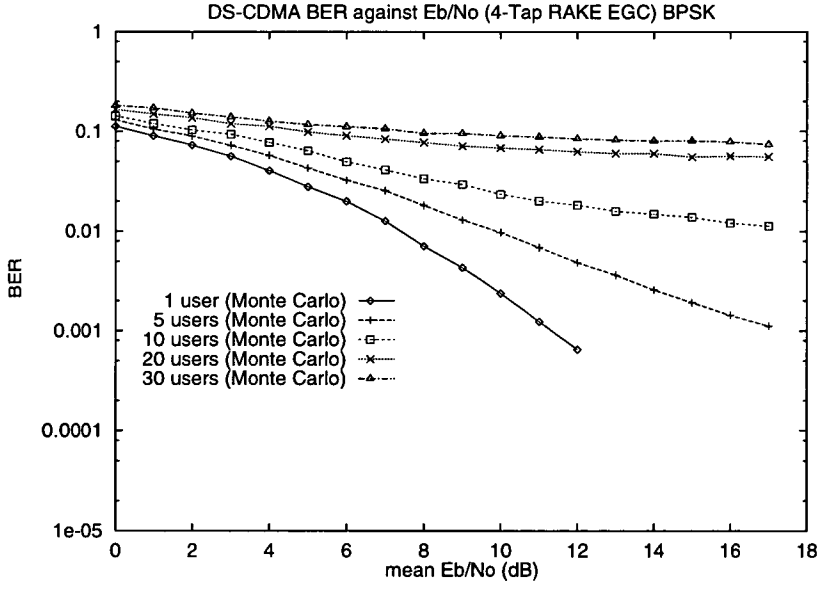

Figure 4.8: DS-CDMA EGC RAKE 4-paths

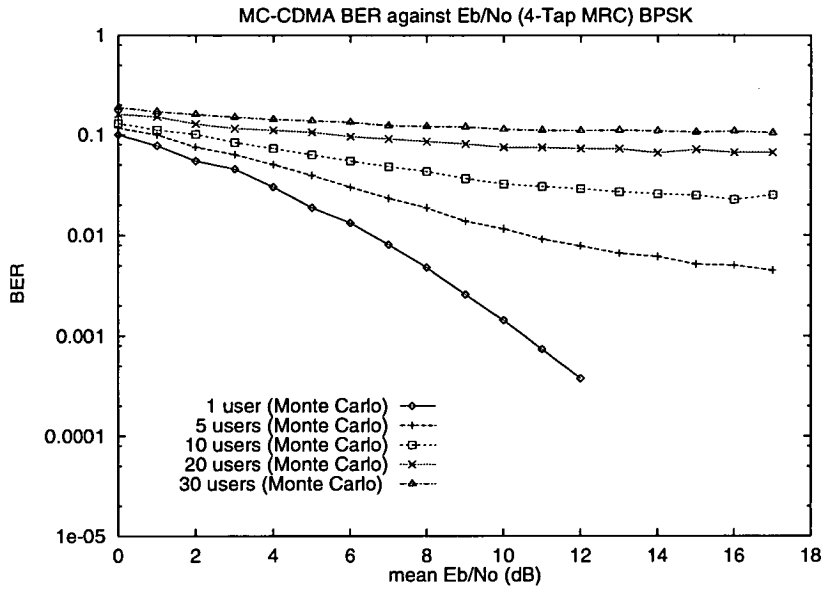

Figure 4.9: MC-CDMA MRC 4-paths

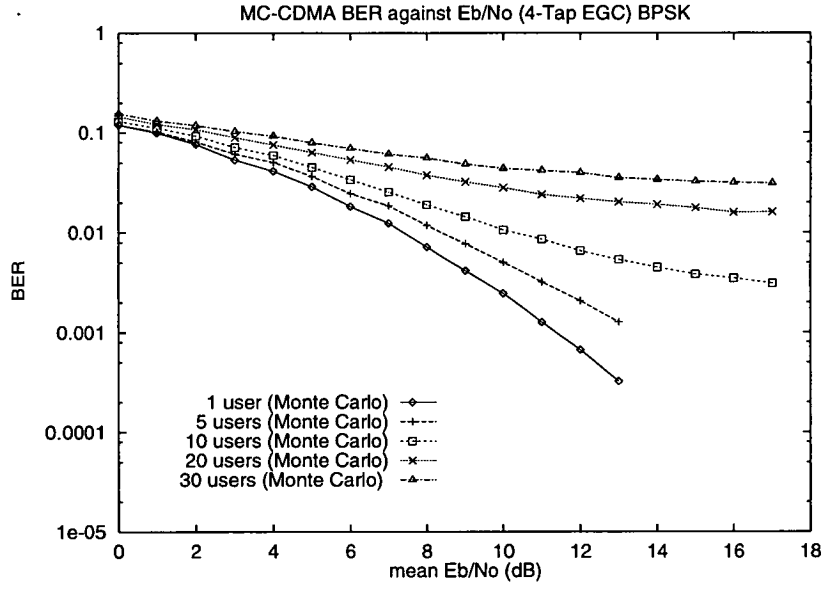

Figure 4.10: MC-CDMA EGC 4-paths

4.4 DPSK modulation

DPSK modulation has been suggested for an OFDM digital audio broadcasting (DAB) mobile receiver [50–52] as it alleviates the requirement for channel estimation. DPSK differentially encodes the data

$$d_k = b_k d_{k-1} \quad \{d_k, b_k\} \ \epsilon \ \{1, -1\} \tag{4.13}$$

where b_k is the kth information bit, and d_k is the kth differentially encoded bit. The received signal in

the presence of noise is therefore given by

$$r_k(n) = d_k(n)h_k(n) + n_k(n) \tag{4.14}$$
$$= d_k(n)\rho_k(n)e^{j\theta_k(n)} + n_k(n) \tag{4.15}$$

where $d_k(n)$ is the kth differentially encoded bit on carrier n. $h_k(n)$ is the complex fading on the nth carrier for the kth bit. The complex fading can be represented by an attenuation and phase, $\rho_k(n)$ and $e^{j\theta_k(n)}$ respectively. $n_k(n)$ is the noise term. The equalised signal corresponding to $r_k(n)$ is given by,

$$z_k(n) = r_k(n)r_{k-1}(n)^* \tag{4.16}$$
$$= \rho_k(n)^2 d_k(n)d_{k-1}(n)^* + n_k(n)' \tag{4.17}$$

where $n_k(n)'$ is the sum of two signal $\times$ noise products and one noise $\times$ noise products. If the phase of the channel does not significantly vary over two consecutive FFT frames the detector recovers the original sequence.

For our MC-CDMA system we will consider DPSK modulation on a per carrier and per symbol basis. The performance of these DPSK MC-CDMA systems will be compared to a DPSK DS-CDMA system using a RAKE receiver.

4.4.1 DPSK per data bit

The DPSK per data bit MC-CDMA receiver is shown in Figure 4.11. The output of the FFT operation

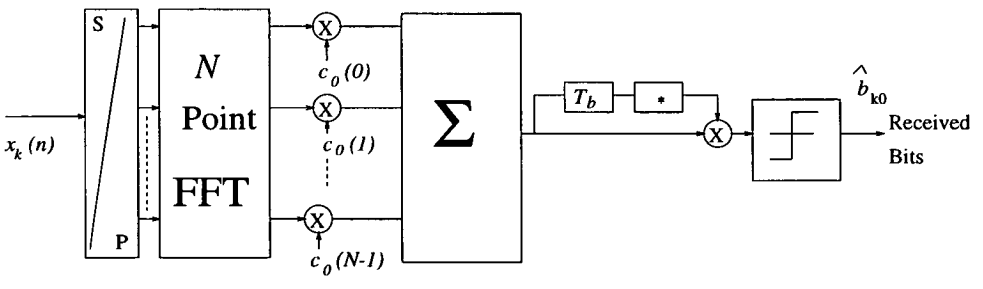

Figure 4.11: DPSK per data bit MC-CDMA receiver

is multiplied by the receiver spreading code to form u_{k0} which represents the decorrelated chips from the kth symbol from user 0.

$$u_{k0}(n) = c_0(n) \sum_{m=0}^{N-1} x_k(n-m) e^{-j2\pi \frac{mn}{N}} \quad n \in \{0..N-1\} \tag{4.18}$$

where $x_k(n)$ is the received signal sampled at chip rate. The signals are then summed to form the kth decorelated signal $z_0(k)$

$$z_0(k) = \sum_{n=0}^{N-1} u_{k0}(n) \tag{4.19}$$

The decision variable is therefore obtained by multiplying $z_0(k)$ by $z_0^*(k-1)$, the complex conjugate of $z_0(k-1)$,

$$\widehat{b}_{k0} = \text{sgn}\left[\text{Re}\{z_0(k) z_0^*(k-1)\}\right]. \tag{4.20}$$

4.4.2 DPSK per carrier (Frequency domain RAKE)

The DPSK per carrier MC-CDMA receiver is shown in Figure 4.12. The received signal is downconverted to baseband and sampled at the chip rate to form the incoming signal $x_k(n)$. These parallel

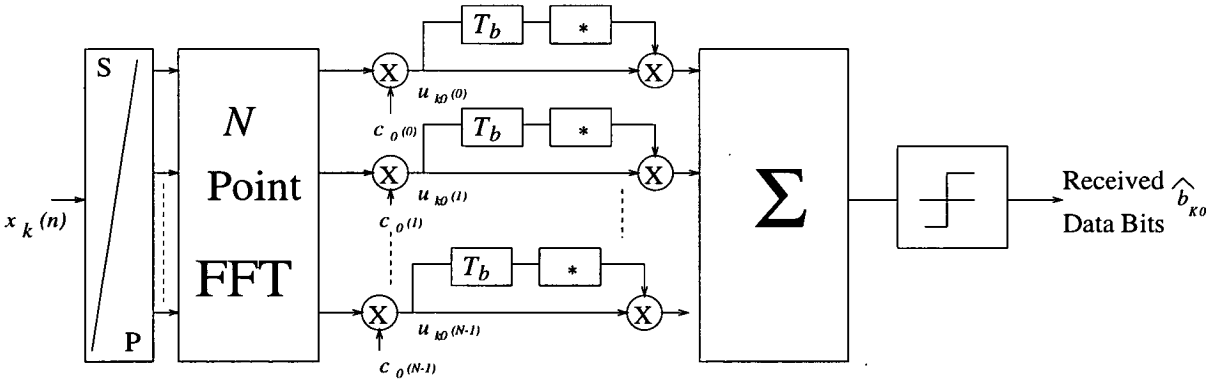

Figure 4.12: DPSK per carrier MC-CDMA receiver

samples are the inputs to a N-point FFT. The outputs of the FFT operation are multiplied by the receiver spreading code. The effects of the multipath channel are then equalised by multiplying each chip sample (sent on a different carrier) of the kth transmitted symbol $u_{k0}(n)$, by its previous value $u_{(k-1)0}(n)$. In this way a soft DPSK demodulation is performed for each carrier and the effects of the channel are

equalised, once the signals are combined. If the channel does not change between two successive received bits, the results of this operation yield a value with no imaginary component (ignoring the effects of noise). In a frequency selective channel, different carriers will experience different attenuations. The results of the DPSK soft decisions are summed to form the decision variable,

$$\widehat{b}_{k0} = \text{sgn}\left[\sum_{n=0}^{N-1} \text{Re}\{u_{k0}(n)u^*_{(k-1)0}(n)\}\right] \tag{4.21}$$

where u_{k0} is given by equation (4.18)

4.4.3 DPSK DS-CDMA RAKE

For comparative purposes we shall examine a synchronous DS-CDMA system in a multipath channel as described in section 4.3.2.1. In this section however we will examine a DS-CDMA system with DPSK modulation. The RAKE receiver for a DPSK DS-CDMA system is shown in Figure 4.13. The received

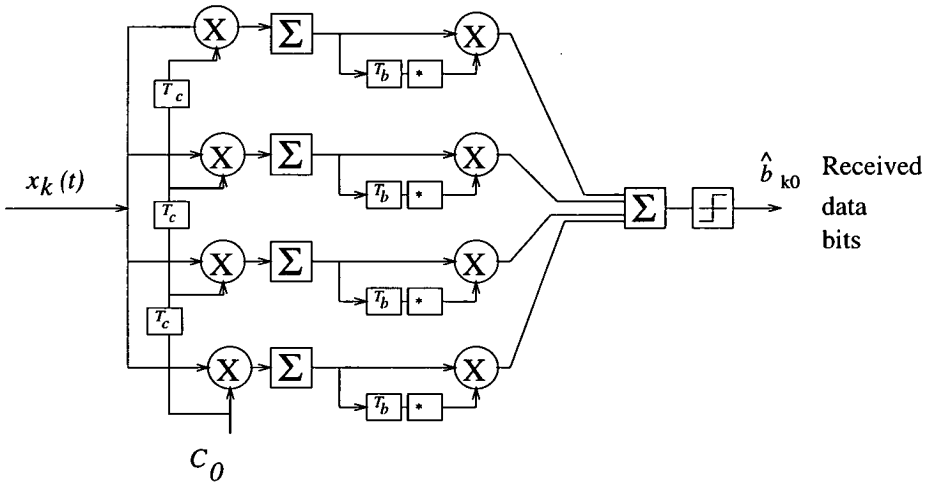

Figure 4.13: DS-CDMA DPSK RAKE receiver

signal is multiplied by delayed versions of the local spreading code, each version is delayed by the respective path delay. The received data for user 0 is given by,

$$\widehat{b}_{k0} = \text{sgn}\sum_{l=0}^{D-1} [\text{Re}\{x_{l0}(k)x^*_{l0}(k-1)\}] \tag{4.22}$$

where $x_{l0}(k)$ is the kth decorrelated symbol for user 0 on the lth transmitted path. D is the total number of taps contained in the RAKE receiver. In this way the multipath signals after decorrelation are combined using differential phase combining (DPC) [14, 53]. In this simulation we will consider D=4 corresponding to a 4 path channel.

4.4.4 DPSK performance evaluation

Monte Carlo simulations were conducted under the same conditions as those described in section 4.3.2. The three DPSK systems are simulated in the presence of Gaussian noise and multi-user interference. Multi-path simulations were also conducted and the multipath channel is the same as that described in section 4.3.2.1.

4.4.4.1 Gaussian noise channel

The results for the DPSK DS-CDMA system and DPSK per data bit are shown in Figure 4.14. The DPSK per carrier MC-CDMA system is shown in Figure 4.15. As can be seen by examining the graphs the DPSK per data bit MC-CDMA and the DPSK DS-CDMA systems both perform identically in the presence of Gaussian noise. The performance of the DPSK per carrier MC-CDMA system for the single user is however approximately 5 dB worse than the other two architectures. The irreducible BER of 3×10^{-1} has already been reached at an E_b/N_0 value of 7 dB with only 2 users. For a single user the DPSK per carrier receiver performs worse than other DPSK receivers, because the 31 'soft' decision DPSK demodulators produce excess noise. The orthogonality of the code sequence is also destroyed. We will however show that the performance improves in a multipath channel.

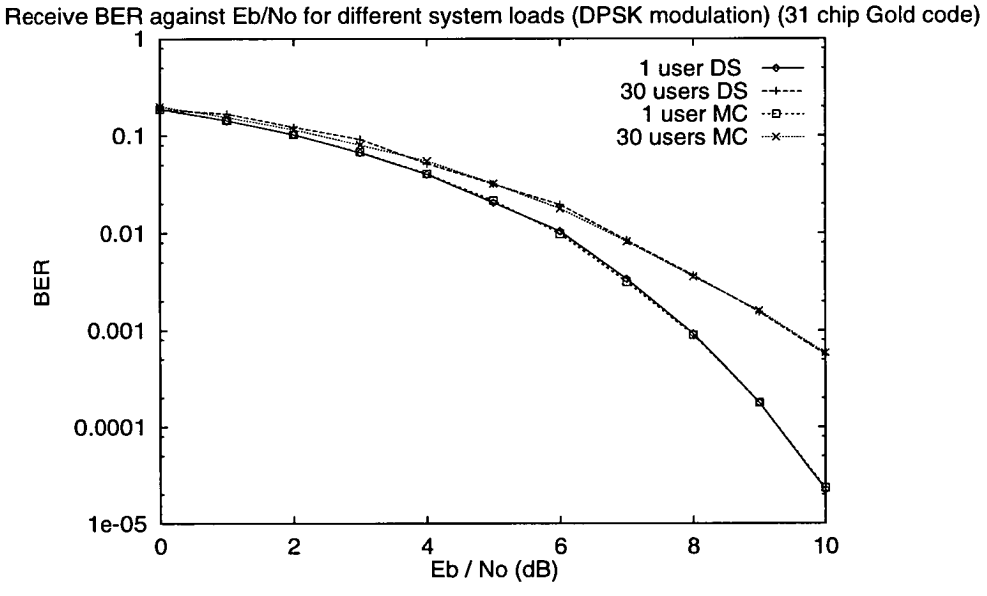

Figure 4.14: *DPSK per data bit MC-CDMA and DPSK DS-CDMA receivers in Gaussian noise channel*

4.4.4.2 Multipath channel

BER results for the DPSK DS-CDMA, DPSK per data bit and DSPK per carrier MC-CDMA systems are shown in Figures 4.16, 4.17 and 4.18 respectively.

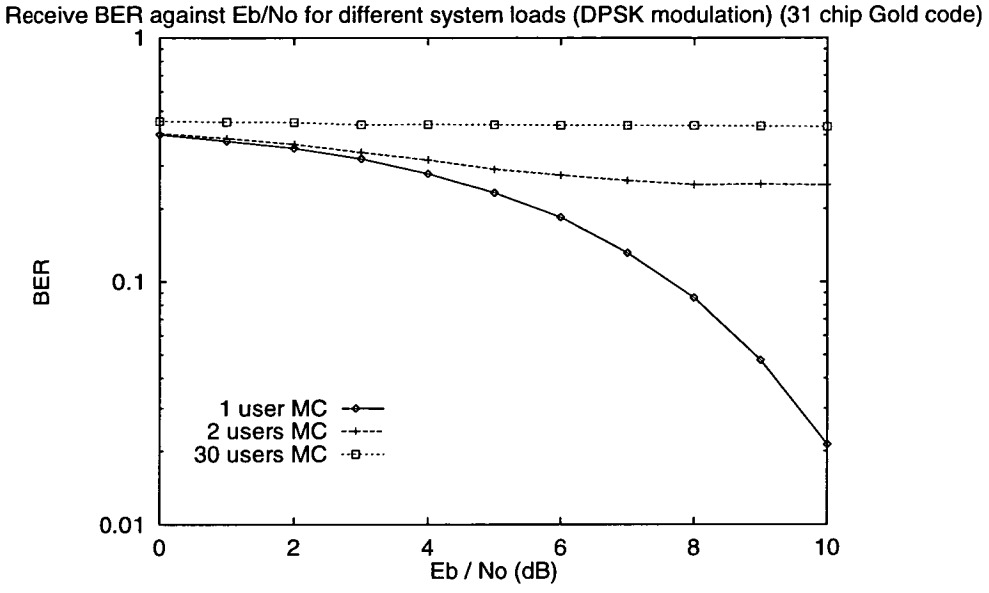

Figure 4.15: DPSK per carrier MC-CDMA receiver in a Gaussian noise channel

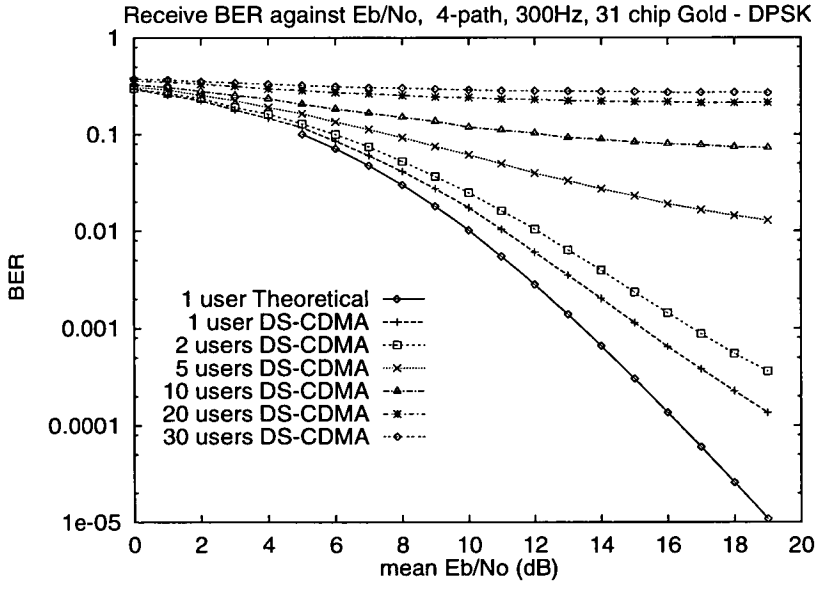

Figure 4.16: DS-CDMA RAKE - 4-path Rayleigh fading

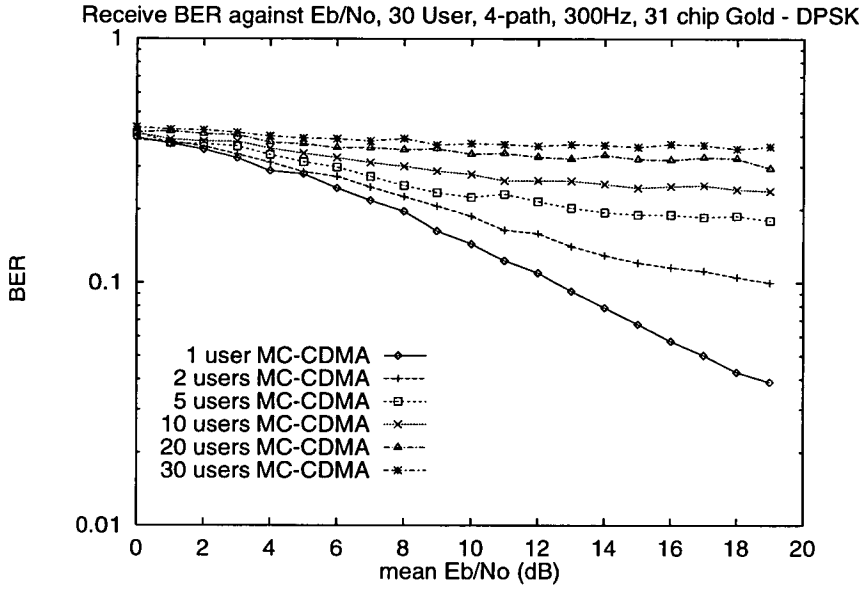

Figure 4.17: MC-CDMA DPSK per data bit receiver - 4-path Rayleigh fading

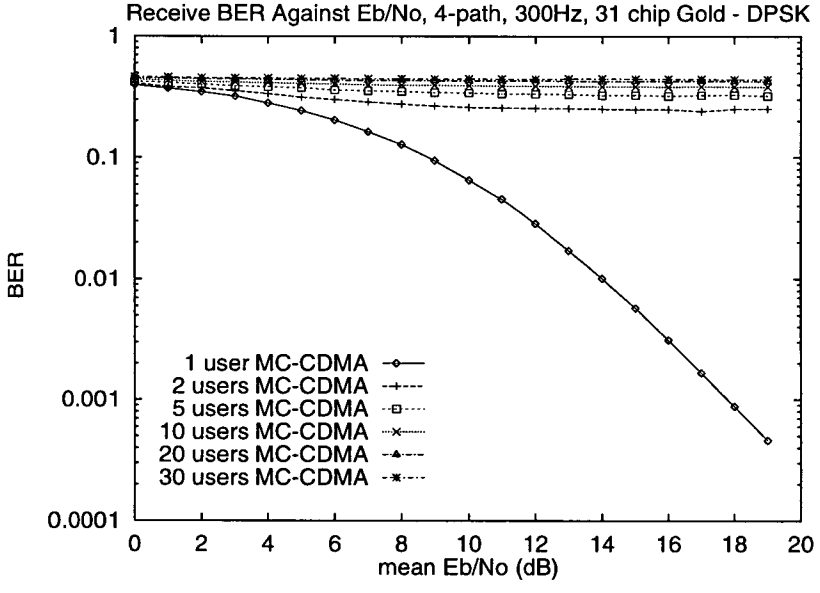

Figure 4.18: MC-CDMA DPSK per carrier - 4-path Rayleigh fading

The BER results of the DS-CDMA system includes the theoretical performance for a single user which is given by Proakis [14]

$$\text{BER} = \frac{1}{2^{2D-1}(D-1)!(1+\gamma_c)^D} \sum_{k=0}^{D-1} q_k (D-1+k)! \left(\frac{\gamma_c}{1+\gamma_c}\right)^k \tag{4.23}$$

where γ_c is E_b/N_0 per tap, D is the diversity and q_k is given by,

$$q_k = \frac{1}{k!} \sum_{n=0}^{D-1-k} \begin{pmatrix} 2D-1 \\ n \end{pmatrix} \tag{4.24}$$

It can be seen that there is approximately a 3 dB difference at a BER of 1×10^{-3} between the theoretical and Monte Carlo simulations for a single user. This is due to the high Doppler (300 Hz) which causes the channel to change from one data bit to the next.

By examining all of the graphs the DPSK DS-CDMA system has the best performance for the single user. The BER of the DS-CDMA system gradually decreases with increasing load. It can be seen for 10 users that the irreducible BER of 7×10^{-2} is reached at an E_b/N_0 of 18 dB.

The performance of the DPSK per carrier MC-CDMA system has worse performance than the DPSK DS-CDMA system for the single user. The performance is approximately 3 dB worse at a receive BER of 1×10^{-3}, but the BER increases rapidly with increasing load. For two users the irreducible BER of 0.25 is already reached at a E_b/N_0 of 10 dB.

The DPSK per data bit has the worst performance for the single user as no effort has been made to equalise the received signal on the different carriers. However, for multiple users the DPSK per data bit has better performance than the DPSK per carrier system. This occurs as the DPSK per carrier system works very well at coherently combining the signals on the different carriers for the single user. However, it also acts as a form of maximal ratio combining on each of the received carriers. The combining more heavily weights the carriers with the most interference. As the processing gain on each of the individual carriers is only one, the technique is unsuitable for more than one user.

4.4.4.3 DPSK conclusions

An examination of two DPSK MC-CDMA systems compared to a DPSK DS-CDMA has been made. For a single user the DPSK per carrier MC-CDMA system performs approximately 5 dB worse than the DS-CDMA system in a Gaussian channel at a BER of 3×10^{-2}.

However in a 4-path channel the DPSK per carrier MC-CDMA system performs approximately 3 dB worse than the DS-CDMA system. To achieve this no knowledge of the channel dispersion is needed.

The performance of the DPSK per carrier can be explained as follows: as the channel delay spread is increased the coherence bandwidth is reduced. Therefore frequency diversity is improved with increasing channel dispersion. To utilise this diversity we have described a MC-CDMA system in which the carriers are individually equalised, unlike the DS-CDMA system no knowledge of the channels dispersion is needed.

With increasing time dispersion the coherence bandwidth is reduced and the system performance is increased for a single user. For this reason we refer to this architecture as a frequency domain RAKE. For more than one user the performance of the frequency domain RAKE decreases. In this situation the performance of the MC-CDMA per data bit system has a better BER performance than the frequency domain RAKE.

The poor performance of the MC-CDMA per data bit system in the multipath channel occurs because dispersion in the channel results in different attenuation and phases for each of the sub-carriers. Received amplitudes and phases of sub-carriers become less correlated if the channel dispersion is increased. The DPSK per data bit would combine the carriers in the optimal sense if all of the carriers were subject to the same phase. This is the case in a Gaussian channel but not in a multipath channel. In a Gaussian channel the DPSK per data bit MC-CDMA system has the same performance as the DPSK DS-CDMA system.

We have examined two types of differential demodulation for MC-CDMA systems. We can conclude therefore that only coherent demodulation schemes are appropriate for MC-CDMA systems in which there is one chip per carrier.

4.5 Adaptive receiver summary

In this section we examine the performance of adaptive receivers for the MC-CDMA system. Throughout this section we shall assume we have perfect knowledge of the channel using pilot tones. In sub-section 4.5.1 we investigate the performance of the system in which the equaliser coefficients are calculated to meet the minimum mean square error (MMSE) criteria. To achieve this, knowledge of the number of active users and the signal to noise ratio is needed. In sub-section 4.5.2 we investigate the performance of adaptive algorithms which use a training period to compute the coefficients.

4.5.1 Calculated MMSE

In this section we can calculate the MMSE criteria for each equaliser coefficient. The MMSE criteria is given by Proakis [14],

$$C_k = \frac{h_k^*}{|h_k|^2 + \frac{\sigma_n^2}{\sigma_a^2}} \tag{4.25}$$

where C_k is the equaliser coefficient, h_k is the complex channel coefficient, σ_n^2 is the variance of the additive noise and σ_a^2 is the variance of the transmitted data symbol. The transmitted data has a +1 or -1 with equal probability. If we apply the MMSE criteria on a per carrier basis the variance of the data (σ_a^2) is given by

$$\sigma_a^2 = \sum_{i=0}^{1} (x_i - \mu_0)^2 \, p(x_i) \tag{4.26}$$

where

$$p(x_1) = p(x_0) = 1/2 \tag{4.27}$$

and

$$\mu_0 = 0; \tag{4.28}$$

therefore

$$\sigma_a^2 = 1. \tag{4.29}$$

However for N_u users $\sigma_a^2 = N_u$. σ_n^2 is the variance of the additive noise per carrier and hence $\sigma_n^2 = NN_0/2E_b$ where $2E_b/N_0$ is the SNR per data bit and N is spreading sequence length. For the MC-CDMA system we are considering the equaliser coefficient $a_k(n)$ is therefore given by

$$a_k(n) = \frac{h_k(n)^*}{|h_k(n)|^2 + \frac{NN_0}{2E_bN_u}} \tag{4.30}$$

To calculate the equaliser coefficients therefore the receiver requires correct knowledge of the channel, the number of active users and the signal to noise ratio.

Due to the complexity of this, a non-optimal MMSE criteria has been proposed by Kaiser [37] in which the number of users N and the signal to noise ratio ($2E_b/N_0$) are fixed to the maximum values in the system. The equaliser coefficients are therefore given by

$$a_k(n) = \frac{h_k(n)^*}{|h_k(n)|^2 + \frac{N}{SNR_{max} \cdot N_u max}} \tag{4.31}$$

4.5.1.1 Performance evaluation in multipath channel

Monte Carlo simulations were conducted under the same conditions as those described in section 4.3.2. The multipath channel is the same as that described in section 4.3.2.1.

BER results for the MC-CDMA MMSE optimal and non-optimal BPSK systems are shown in Figures 4.19 and 4.20 respectively. The number of users in the non-optimal MMSE criteria have been fixed at 30 users with the maximum E_b/N_0 set to 20 dB. It can be seen that for the case of 30 users a BER of 0.01 can be achieved for both systems at a E_b/N_0 of 13 dB.

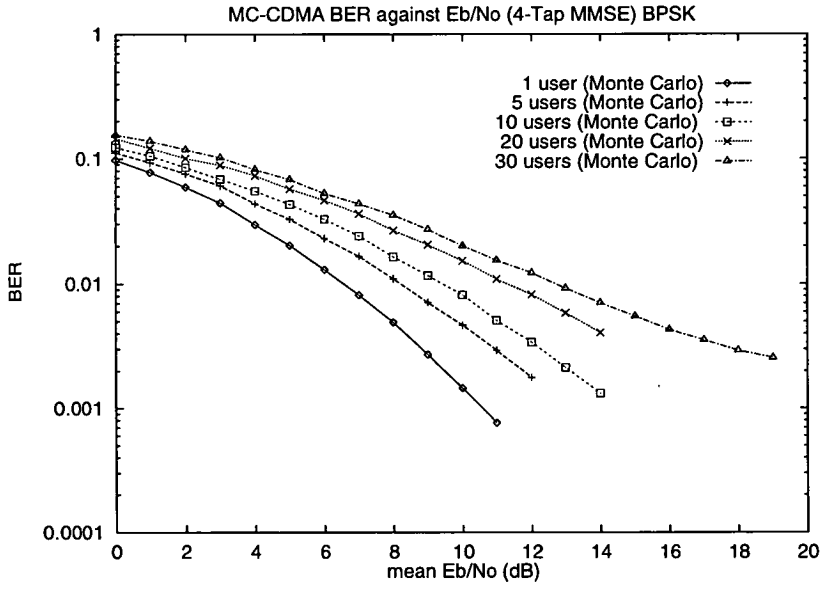

Figure 4.19: MC-CDMA BPSK MMSE

By examining Figure 4.10 it can be seen that 30 users can not be supported at a BER of 0.01 for the case of equal gain combining (EGC). The MMSE criteria therefore offers improved performance.

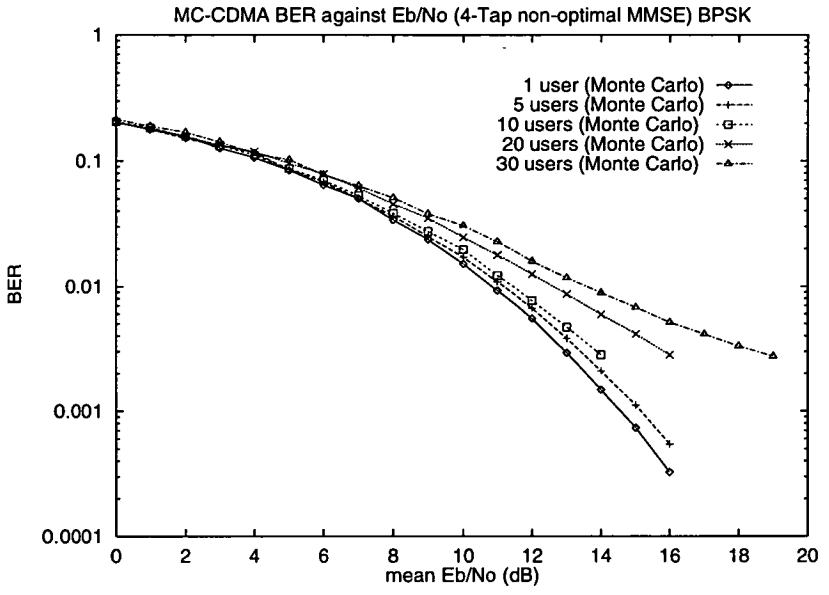

Figure 4.20: MC-CDMA BPSK Non-optimal MMSE

The non-optimal MMSE MC-CDMA system has a lower BER than the optimal MMSE for low numbers of users. This is to be expected as the non-optimal MMSE system only fulfils the MMSE criteria for the case of 30 users and 20 dB E_b/N_0. To support 5 users at a BER of 0.01 the optimal MMSE solution requires a E_b/N_0 of 8 dB compared to 11 dB for the non-optimal MMSE solution and 8 dB for EGC (see Figure 4.10).

4.5.2 Adaptive algorithm

In this section we shall investigate the possibility of using an adaptive algorithm and a training sequence. In this way, knowledge of the number of users and signal to noise ratio is not needed. The algorithms we shall consider here are the least mean square algorithm (LMS) and the recursive least squares (RLS). Both of these algorithms require a training time to converge. During training the adaptive receiver attempts to reduce the mean square error (MSE) between the received data bit and training bit. The adaptive receiver is shown in Figure 4.21. (An adaptive receiver using a complex algorithm which reduces the mean square error on a per carrier basis could also be used but we would only be able to use the LMS algorithm [54]. An algorithm of this type would however not require pilot tones.) After the FFT and channel equalisation the receiver is similar to the adaptive receiver for DS-CDMA investigated by Cruickshank [55]. In our adaptive receiver the spreading sequence is replaced by adaptive coefficients. These adaptive coefficients are trained to minimise the MSE and reduce the multi-user interference. We shall consider the performance of the receiver in a Gaussian channel and a multipath channel. The two adaptive algorithms are described first.

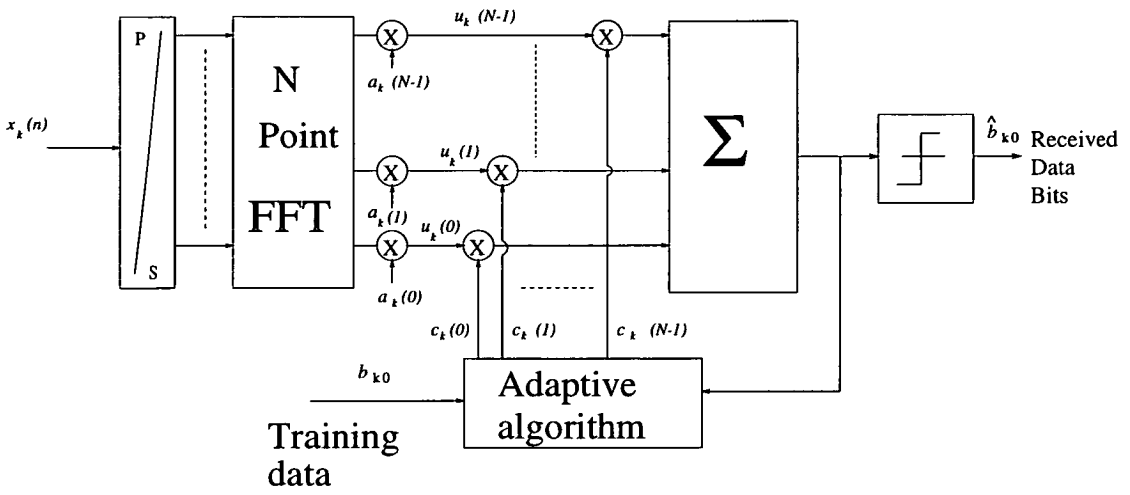

Figure 4.21: MC-CDMA Adaptive BPSK receiver

4.5.2.1 LMS

We shall represent the adaptive coefficients at time interval k by vector $\mathbf{c}_k = (c_k(0), c_k(1), \ldots, c_k(N-1))$,

- Initialisation

  $\mathbf{c}_o$ can be arbitrarily chosen.

- Algorithm

$$e_k = b_{k0} - \widehat{b}_{k0} \tag{4.32}$$

$$= b_{k0} - \mathbf{c}_k^T.\mathbf{u}_k \tag{4.33}$$

$$\mathbf{c}_{k+1} = \mathbf{c}_k + \mu \mathbf{u}_k e_k \tag{4.34}$$

where $\mathbf{r}_k$ is the received vector $(N \times 1)$ at the FFT output after equalisation and μ is the step size.

4.5.2.2 RLS

- Initialisation

$$\mathbf{c}_o = (0, 0, \ldots 0) \tag{4.35}$$

$$\mathbf{P}_o = \delta^{-1}\mathbf{I} \tag{4.36}$$

$$\delta^{-1} = \text{small positive constant} \tag{4.37}$$

where $\mathbf{P}_o$ is a $N \times N$ matrix and $\mathbf{I}$ is the $N \times N$ identity matrix.

- Algorithm

$$\mathbf{f}_k = \frac{\mathbf{u}_k^H \mathbf{P}_{k-1}}{\lambda + \mathbf{u}_k^H \mathbf{P}_{k-1} \mathbf{u}_k} \tag{4.38}$$

$$\alpha = b_{k0} - \mathbf{c}_k^T . \mathbf{u}_k \tag{4.39}$$

$$\mathbf{c}_k = \mathbf{c}_k + \mathbf{f}_k \alpha^* \tag{4.40}$$

$$\mathbf{P}'_{k-1} = \mathbf{f}_k \mathbf{u}_k^H \mathbf{P}_{k-1} \tag{4.41}$$

$$\mathbf{P}_k = \frac{1}{\lambda}(\mathbf{P}_{k-1} - \mathbf{P}'_{k-1}) \tag{4.42}$$

where $\mathbf{f}_k$ is a $N \times 1$ vector, $\mathbf{P}_k$ and $\mathbf{P}_{k-1}$ are $N \times N$ matrices and λ is the forgetting factor.

4.5.2.3 Performance in Gaussian channel

The performance of the adaptive MC-CDMA receiver was conducted in a Gaussian channel. (For the Gaussian channel the equaliser vector $\mathbf{a}_k$ is set to 1 for all values of k.) Initially the convergence of the adaptive algorithms was studied. The convergence of the LMS algorithm for a 30 user system with stepsize (μ) set to 1×10^{-4} is shown in Figures 4.22 and 4.23 for 0 dB E_b/N_0 and 10 dB E_b/N_0 respectively. The convergence results are plotted as mean square error (MSE) against iteration. It can be seen from Figures 4.22 and 4.23 that the LMS algorithm converges within 600 iterations to a MSE which is approximately $1/\text{SNR} = 1/(2E_b/N_0)$. Faster convergence could be obtained by using a larger step size but with extra noise on the convergence characteristic.

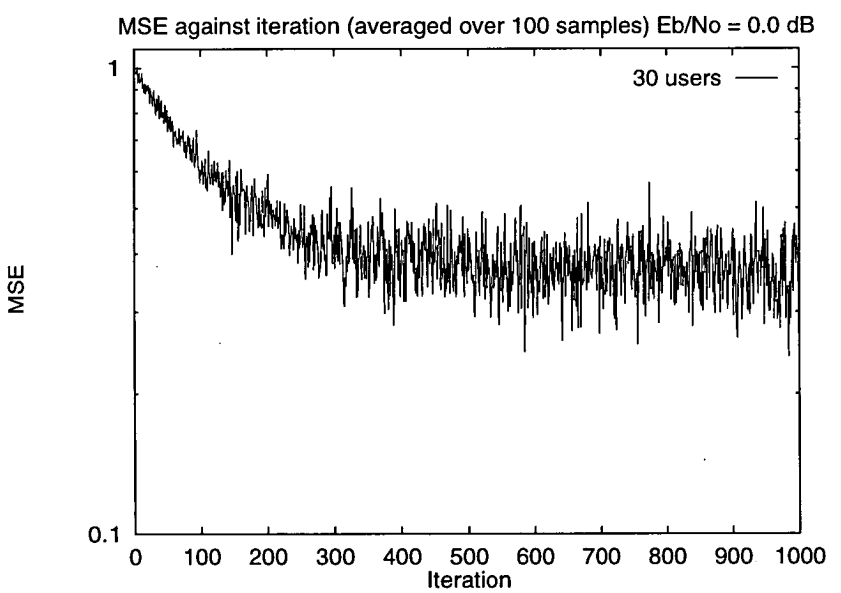

Figure 4.22: LMS convergence for MC-CDMA with 30 users ($\mu = 0.0001$) E_b/N_0 = 0 dB

The convergence of the RLS algorithm for a 30 user system with $\lambda = 1.0$ is shown in Figure 4.24 and 4.25 for 0 dB E_b/N_0 and 10 dB E_b/N_0 respectively. It can be seen that the convergence of the RLS

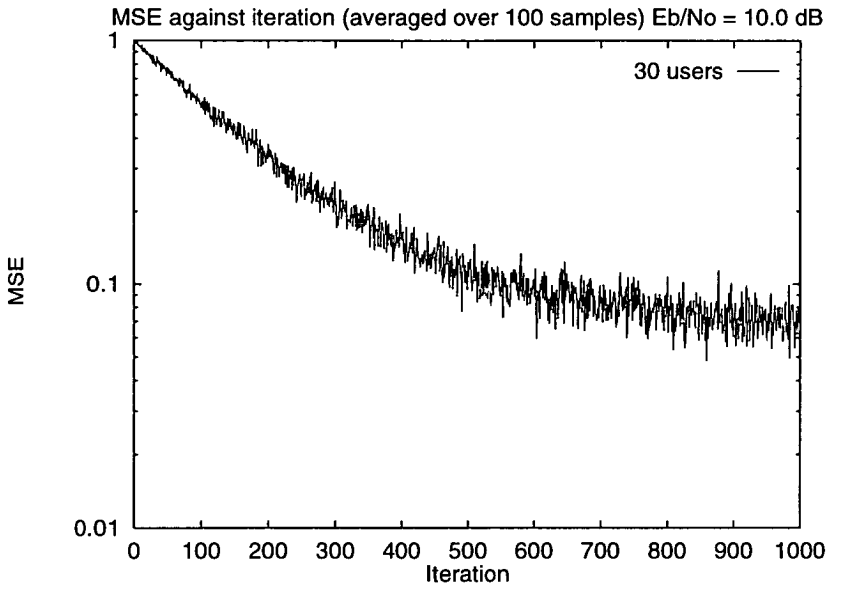

Figure 4.23: LMS convergence for MC-CDMA with 30 users ($\mu = 0.0001$) E_b/N_0 = 10 dB

algorithm occurs within $2N$ iterations where N is the number of adaptive weights. There is however an instability problem associated with the RLS algorithm as can be seen between iterations 20 and 40. This can be reduced by changing the value of δ as seen in equation (4.37).

Received BER curves for the adaptive MC-CDMA receiver are shown in Figures 4.26 and 4.27 for the LMS and RLS algorithm respectively. The BER is measured after 1000 training bits have been sent. Matched filter results are also plotted as a reference. (The receiver acts as a matched filter when the adaptive coefficient vector $\mathbf{c}_k$ is set to the local spreading sequence.) By examining Figure 4.26 it can be seen that for the case of 30 users and E_b/N_0 values greater than 7.5 dB the adaptive receiver has lower BER performance than the matched filter receiver. For values of E_b/N_0 lower than 7.5 dB the adaptive receiver has worse performance than the matched filter because the noise and the multi-user interference cause the algorithm not to converge to the optimal MMSE solution (Wiener solution).

For the case of 10 users, the adaptive receiver has lower BER than the matched filter for values of E_b/N_0 greater than 7 dB. This is 0.5 dB less than the 30 user case because the multi-user interference is reduced.

By examining Figure 4.27 it can be seen that the RLS algorithm has lower BER than the LMS algorithm. For the 30 user case and E_b/N_0 values greater than 5 dB the adaptive filter receiver has lower BER than the matched filter receiver. The RLS algorithm offers better performance than the LMS algorithm because its convergence is accomplished after $2N$ iterations. The MSE which the RLS algorithm achieves after 1000 iterations is therefore much lower than the LMS.

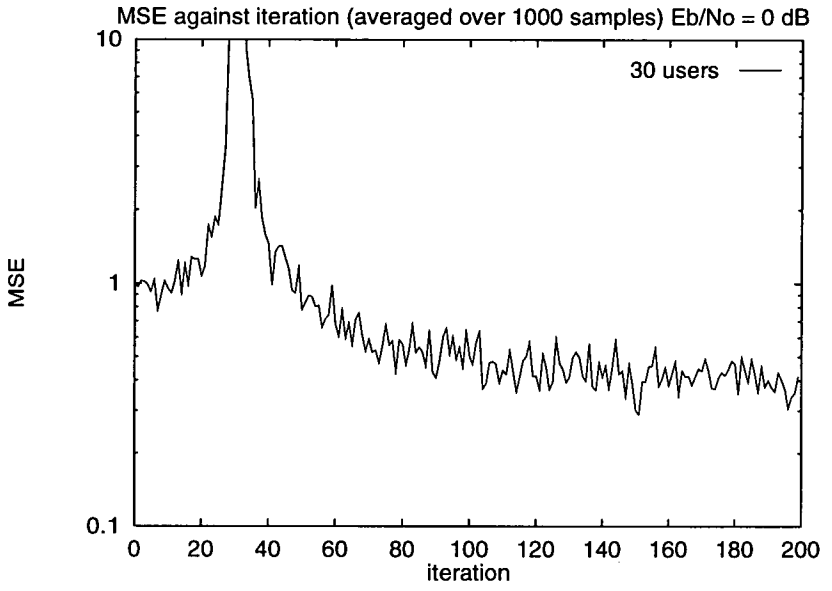

Figure 4.24: RLS convergence for MC-CDMA with 30 users (λ = 1.0) E_b/N_0 = 0 dB

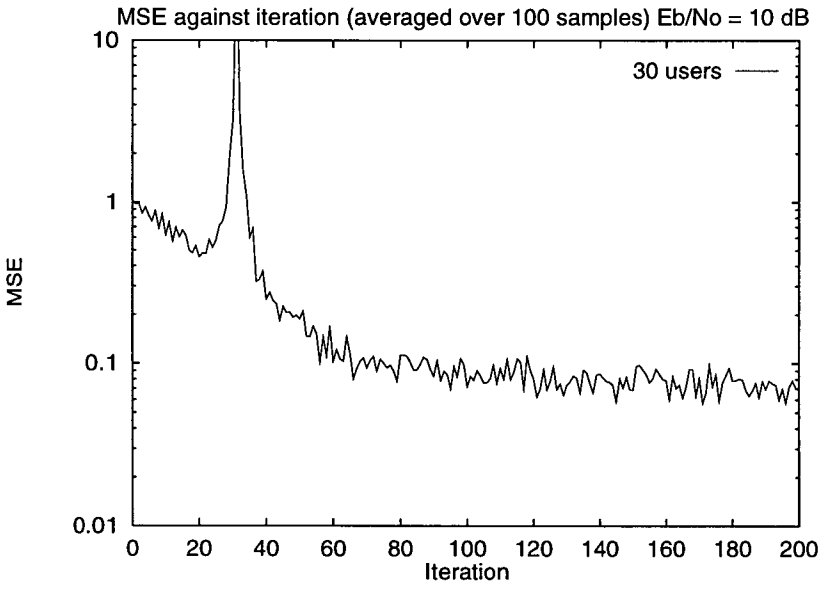

Figure 4.25: RLS convergence for MC-CDMA with 30 users (λ = 1.0) E_b/N_0 = 10 dB

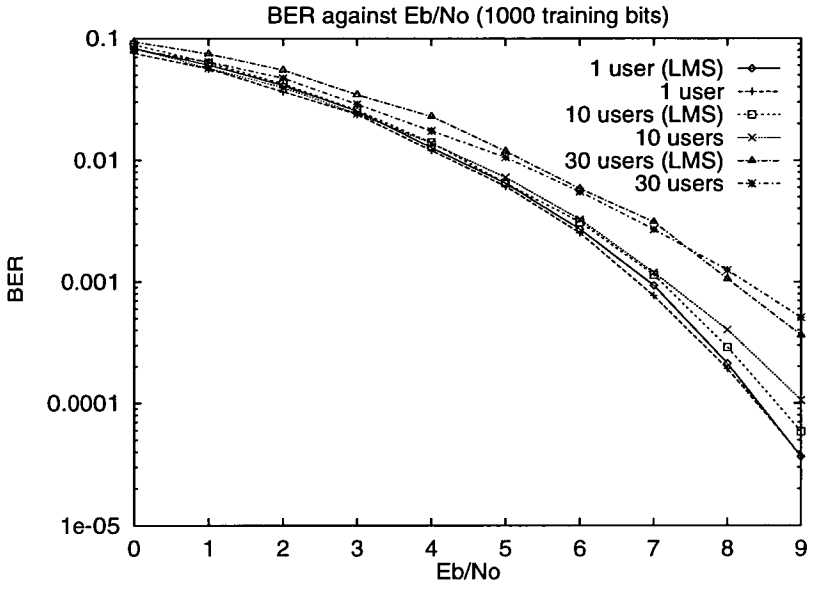

Figure 4.26: MC-CDMA receiver BER after 1000 iterations using the LMS ($\mu = 1 \times 10^{-4}$)

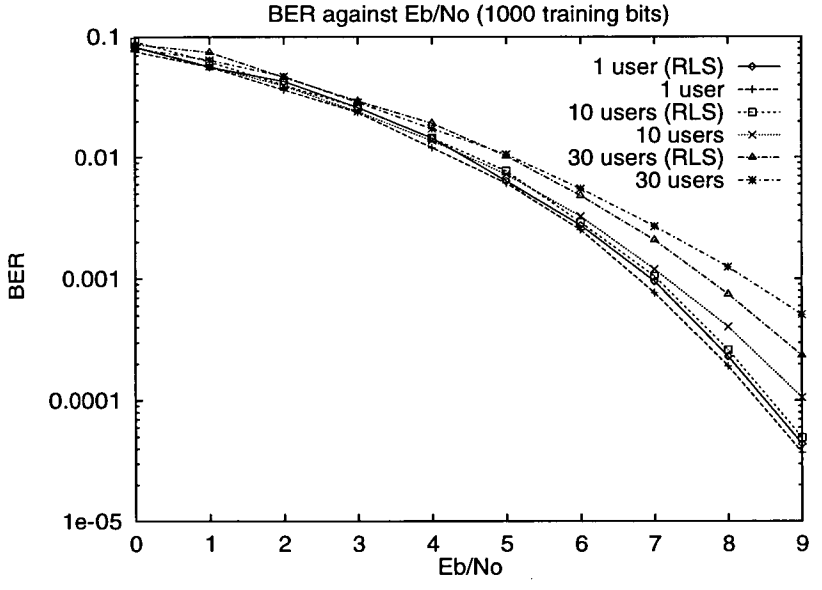

Figure 4.27: MC-CDMA receive BER after 1000 iterations using the RLS ($\lambda = 1.00$)

4.5.2.4 Performance in multipath channel

The performance of the adaptive MC-CDMA receiver was conducted in a multipath channel. Due to the non-stationarity of the fast fading multipath channel, it is important to choose an adaptive algorithm which is sufficiently fast to track the channel variations. We therefore choose to investigate the performance of the RLS algorithm in this channel. For the RLS algorithm it is necessary to have a value of λ less than unity so the algorithm has finite memory and can follow the statistical variations of the received signal. When $\lambda = 1$ the RLS algorithm computes the method of least squares. When λ is less than 1, the RLS algorithm has an exponential decaying memory and the RLS algorithm implements the method of exponentially weighted least square which minimises the cost function,

$$E(n) = \sum_{i=1}^{N} \lambda^{N-1} |e_i|^2 \tag{4.43}$$

where N is the number of adaptive coefficients. The time constant of the RLS algorithm is given by $(1-\lambda)^{-1}T_b$ where T_b is the duration of a data bit. To update the equaliser coefficients at regular intervals it is necessary to use a block training structure as seen in Figure 4.28. This consists of two sections: a training data section which has a duration T_{train} and a useful data section which has duration T_{data}.

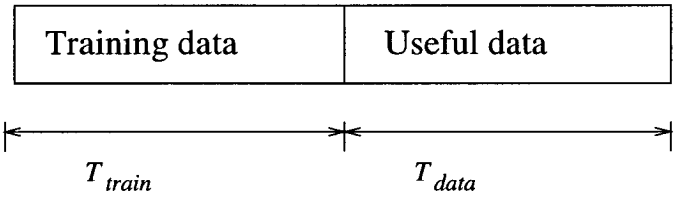

Figure 4.28: Block training structure

To track the channel variations it is important to satisfy the following criteria:

1) The training time of the RLS algorithm must be longer than twice the time it takes to send N data bits.

$$T_{train} \geq 2NT_b \tag{4.44}$$

2) The time constant of the RLS algorithm must be longer than the training time, T_{train}, so all of the training data is used for computation. We must therefore satisfy,

$$(1-\lambda)^{-1}T_b \geq T_{train} \tag{4.45}$$

3) The time duration of the training period and data period ($T_{train} + T_{data}$) must much shorter than the

coherence time of the channel. In this way the received signal is stationary over this period. We must therefore satisfy,

$$T_{train} + T_{data} \ll 1/f_{d_{max}} \tag{4.46}$$

where $f_{d_{max}}$ is the maximum Doppler frequency. The MC-CDMA system we consider in this chapter (see section 4.3.2) has a baseband data rate of 8 kbits/s (T_b = 125 μs). To satisfy the above inequalities we chose a training period of 93 data bits, set λ to 0.99 and limit ourselves to considering channels which have a maximum Doppler rate of 3 Hz. These parameters are summarised in Table 4.1.

Table 4.1: *Parameters*

T_{train}, T_{data}	93 $\times T_b$ = 11.625 $\times 10^{-3}$s
$1/f_{dmax}$	333.33$\times$ 10^{-3}s
$(1 - \lambda)^{-1}T_b$	12.5 $\times$ 10^{-3}s

Before examining the BER of the adaptive receiver we shall examine the convergence of the adaptive receiver in the 4-path channel. (The channel is fully described in section 4.3.2.1.) The convergence of the adaptive receiver is shown in Figures 4.29, 4.30 and 4.31 for an E_b/N_0 of 0 dB, 10 dB and 20 dB respectively. It can be seen that the MSE's after convergence are much higher than those seen in the Gaussian channel. At 10 dB E_b/N_0 (Figure 4.29) a MSE of 0.5 is reached which is much higher than the MSE of 0.05 which is achievable at 10 dB E_b/N_0 in the Gaussian channel (see Figure 4.25). The MSE is much higher in the multipath channel due to the fading and inter-carrier interference.

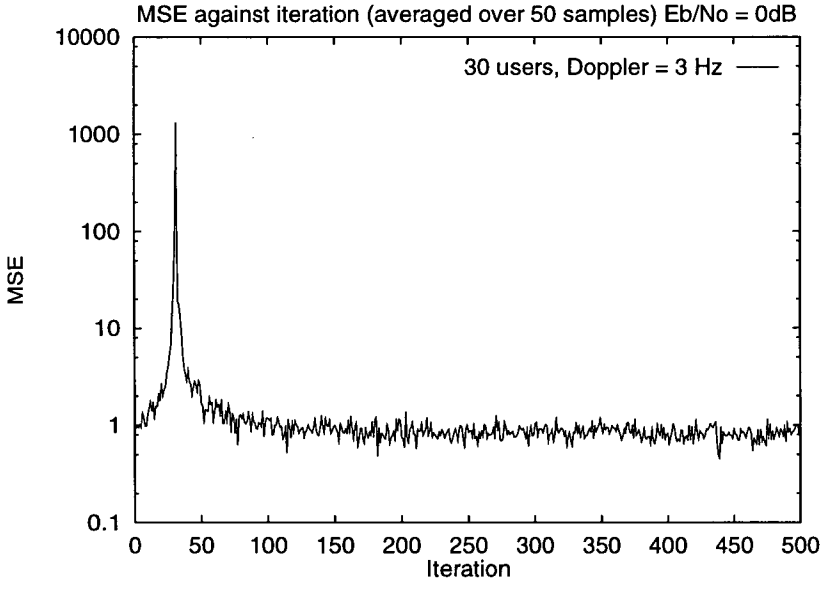

Figure 4.29: RLS convergence for MC-CDMA with 30 users (λ = 0.99), E_b/N_0 = 0 dB

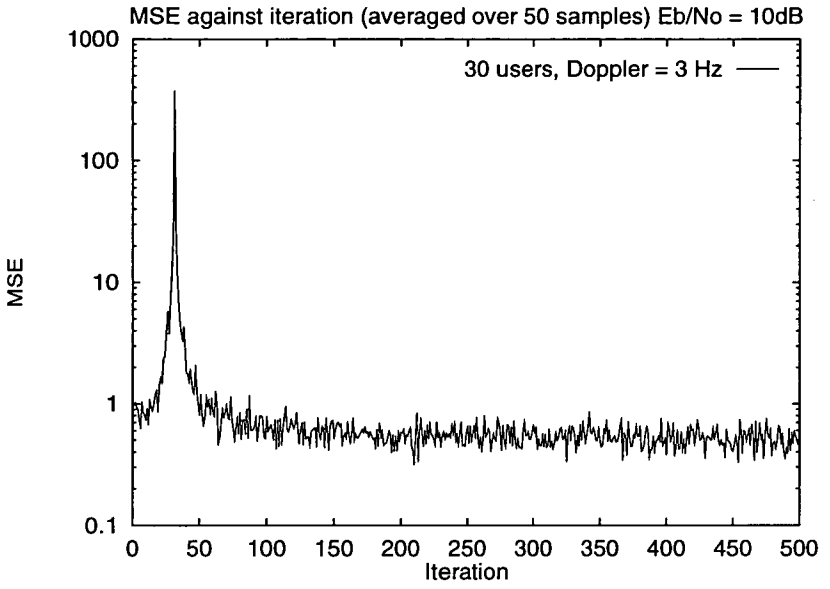

Figure 4.30: RLS convergence for MC-CDMA with 30 users ($\lambda = 0.99$), $E_b/N_0 = 10$ dB

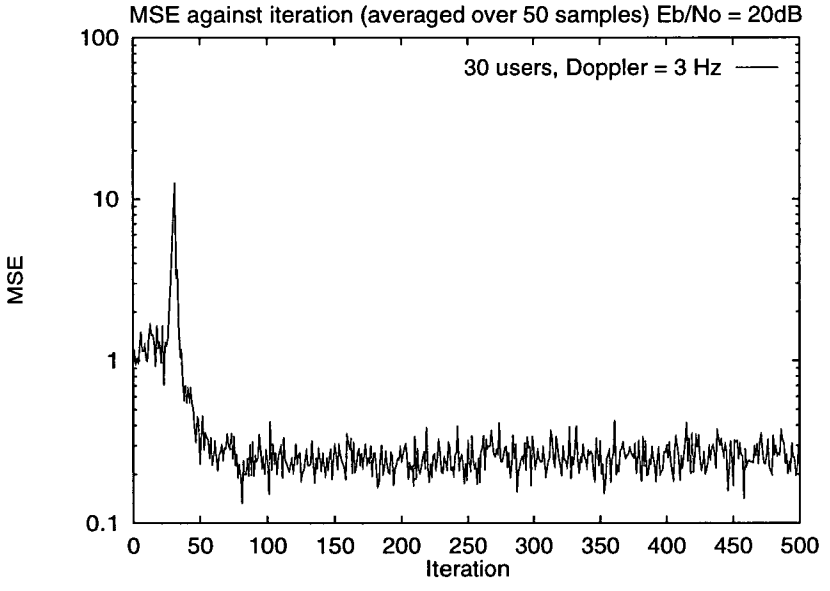

Figure 4.31: RLS convergence for MC-CDMA with 30 users ($\lambda = 0.99$), $E_b/N_0 = 20$ dB

The resulting BER for the adaptive receiver using the parameters in Table 4.1 is shown in Figure 4.32. As can be seen the BER results are much higher for a given number of users than those seen for the calculated MMSE criteria (Figure 4.19). The BER results are also much higher than those for EGC (Figure 4.10) . This is due to the high MSE after convergence.

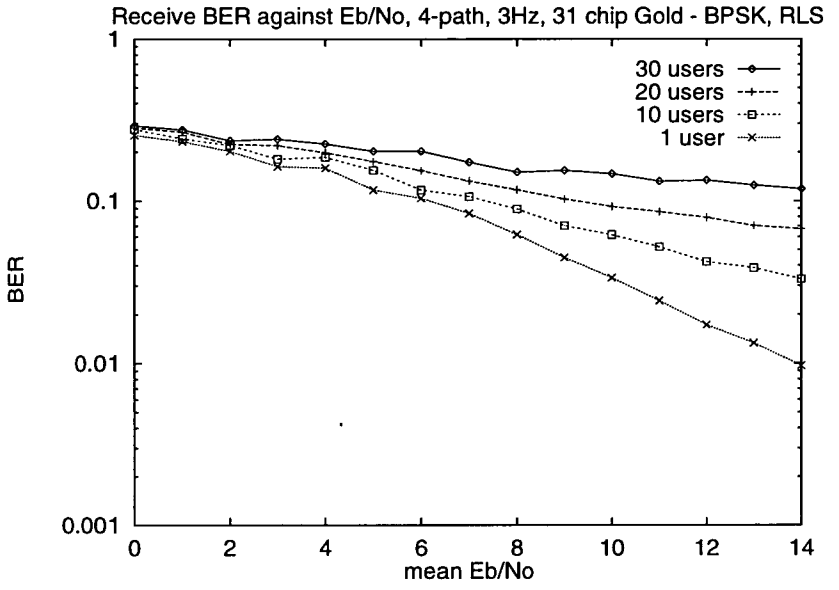

Figure 4.32: Adaptive MC-CDMA receiver BER in multipath with RLS algorithm ($\lambda = 0.99$)

4.5.3 Adaptive summary

We have studied two types of adaptive receivers for our MC-CDMA system. The first is a calculated value based on the MSE per carrier criteria. Its computation relies on correct knowledge of the channel, the number of users and the value of E_b/N_0. With correct knowledge the adaptive receiver supports 30 users at an E_b/N_0 of 13 dB. A calculated non-optimal MMSE per carrier system has also been discussed which requires only channel knowledge.

The second adaptive receiver uses an adaptive algorithm which is based on the MSE per data bit. In this receiver, the channel knowledge is used to phase compensate the carriers (equal gain combining) and the adaptive algorithm optimises the local spreading sequence to reduce the multi-user interference. To achieve convergence quickly in a fading channel we have investigated the RLS algorithm. It is also possible to use an adaptive algorithm based on the MSE per carrier. This would however necessitate the use of the LMS algorithm [54] and thus we would be restricted to static channels due to the long convergence time.

The adaptive algorithm works very well in a Gaussian channel, but due to the fading and inter-carrier interference, a high MMSE is obtained after convergence. The resulting BER is much higher than a receiver with EGC due to this reason.

4.6 Chapter summary

In this chapter we have examined a multi-carrier CDMA system similar to Linnartz. In our system the carriers overlap in the OFDM sense. We have not used a guard interval and therefore the system experiences inter-carrier interference. We have examined BPSK modulation, DPSK modulation and adaptive receiver architectures.

We have shown that EGC has a higher peformance (lower BER) than MRC for the BPSK modulated MC-CDMA system. We have further shown that at a BER of 0.01 the MC-CDMA system using EGC has a 1 dB advantage over DS-CDMA using MRC.

For DPSK modulation we have examined DPSK on a per carrier and per data bit basis. When DPSK is used on a per carrier basis we have shown that the orthogonality of the spreading sequence is destroyed and the system can only support one user. If DPSK modulation is used on a per data bit basis, the carriers are not phase corrected and a high BER is obtained for all users. We conclude that only coherent modulation schemes are possible for a one chip per carrier MC-CDMA system.

We have investigated adaptive receiver architectures using a calculated value based on the MSE per carrier criteria and an adaptive algorithm based on the MSE per data bit criteria. We have shown that the calculated MSE per carrier receiver supports 30 users at a E_b/N_0 of 13 dB for the four path channel. It does however require knowledge of the number of active users and the E_b/N_0 value, in addition to the channel knowledge. The adaptive receiver using the RLS algorithm performs well in a Gaussian channel but in the four path channel the resulting BER is higher than EGC due to the intercarrier interference and fading.

Chapter 5
Orthogonal frequency divison multiplexing CDMA

5.1 Introduction

In this chapter we investigate the performance of an orthogonal frequency division multiplexing CDMA (OFDM-CDMA) system proposed by Fazel [5]. This OFDM-CDMA system is similar to the multi-carrier CDMA system proposed by Linnartz [7] in the sense that both systems are one chip per carrier multi-carrier CDMA systems. In contrast, however, this OFDM-CDMA system utilises many low data rate overlapping orthogonal carriers. After spreading by a sequence of length L, M data bits are serial to parallel converted producing ML parallel streams. In this way the data rate of every carrier is reduced by a factor of M and the number of carriers is increased by M. All parallel streams are multiplexed onto the carriers to gain frequency diversity and a cyclically extended guard interval is introduced to prevent ISI and maintain the orthogonality of the carriers. The system has a high spectral efficiency.

In section 5.2 the system is described and in section 5.3 the performance of different detection schemes are investigated. In section 5.4 we investigate the performance of different channel coding schemes for this type of OFDM-CDMA system with equal gain combining (EGC). In section 5.5 we combine some of these coding schemes with different detection schemes for increased performance. A summary is then presented in section 5.6.

5.2 System description

Fazel [5] proposed two different OFDM-CDMA systems. In system 1 (see Figure 5.1) the transmitted signal of the N_u users data bits (at rate A bits/s) are split into Q sub-systems so that each sub-system supports N_u/Q users. The data bit of every user in each sub-system is spread by a Walsh code of length L/Q where L is the maximum number of users in the whole system. The chip stream of sub system q can be written as a row vector $\mathbf{s}_q$,

$$\mathbf{s}_q = \sum_{m=(N_u/Q)q+1}^{(q+1)(N_u/Q)} b_m \mathbf{c}_m \tag{5.1}$$

where $\mathbf{c}_m$ is a vector representing the Walsh code of length L/Q for user m and b_m is the data bit for user m. After spreading, M data bits are serial to parallel converted producing ML/Q parallel streams

(at rate A/M bits/s) from each of the Q sub-systems. Streams from all sub-systems are fed to the frequency interleaver and passed to the OFDM modulator.

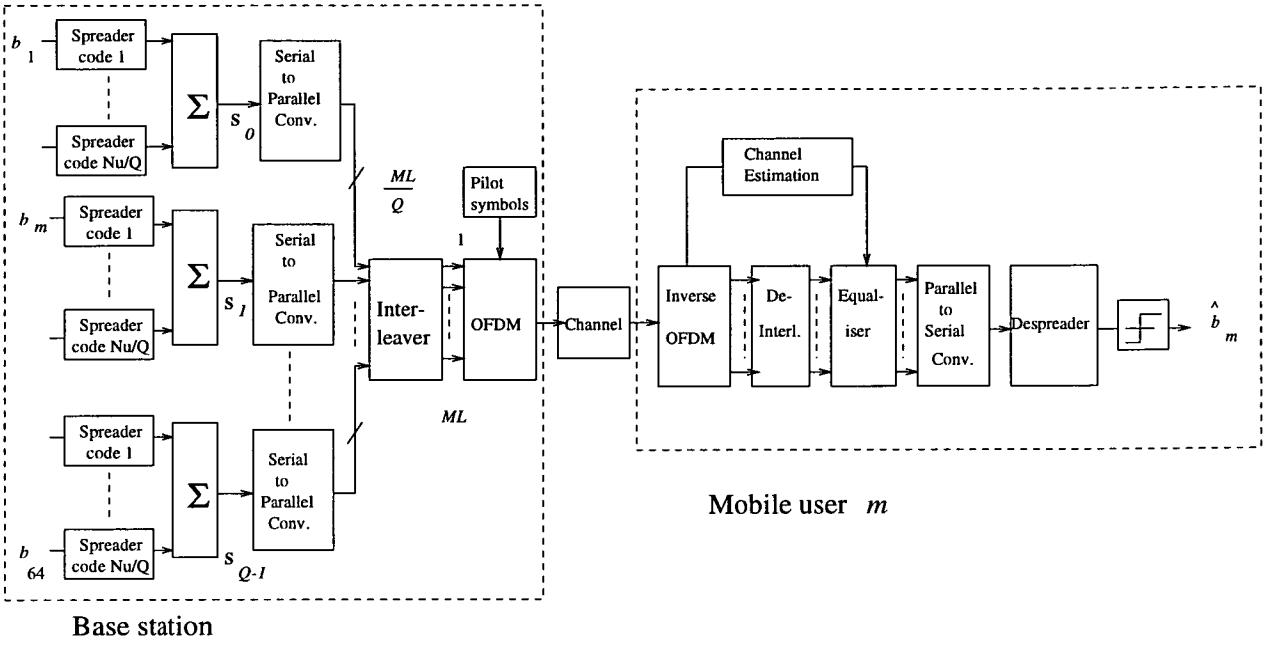

Figure 5.1: OFDM-CDMA system type 1

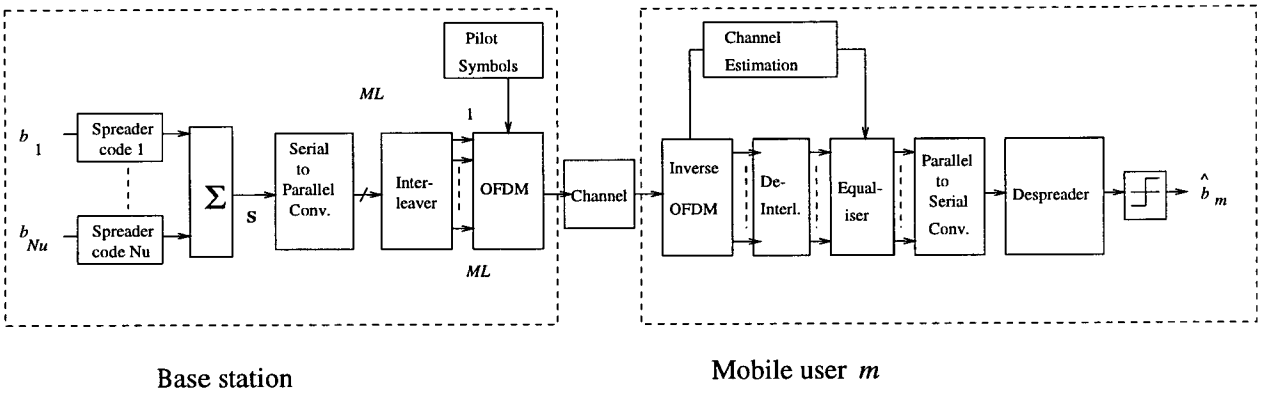

Figure 5.2: OFDM-CDMA system type 2

System 2 (see Figure 5.2) consists of one system using length L Walsh codes. The output of this system can be written as a row vector s,

$$\mathbf{s} = \sum_{m=1}^{N_u} b_m \mathbf{c}_m \tag{5.2}$$

where $\mathbf{c}_m$ is a vector representing the Walsh code of length L for user m. After the users signals are spread, M data bits are serial to parallel converted producing ML parallel streams of A/M bits/s . These streams are then passed to the OFDM modulator.

In both systems $L = 64$ and $M = 8$, the data rate of 16 kbits/s is reduced to 2 kbits/s and there are 512 carriers. In the first system $Q = 8$. A guard interval Δ is inserted into both systems which is longer than the delay spread to prevent ISI and intercarrier interference (ICI). Pilot symbols are also inserted into the OFDM multiplex for channel estimation.

Both of these systems support 64 users. System 1 has the advantage however, that each user experiences multi-user interference from only 7 other users. The 8 chips produced by vectors $\mathbf{s}_0, \ldots, \mathbf{s}_{Q-1}$ are separated in frequency (due to the interleaver) corresponding to the spacing of 64 carriers (128 kHz). As the carriers are subject to flat fading, it is possible to achieve maximum likelihood detection (MLD) by evaluating 256 sequences. The maximum diversity available is however restricted to 8.

System 2 which consists of one subsystem makes MLD unfeasible as 2^{64} sequences have to be evaluated. It does, however, have the advantage that a frequency diversity [2] greater than 8 could be achieved if sufficient bandwidth and channel dispersion are available.

In this chapter we will study in particular the performance of the type 1 system in which length 8 Walsh codes are used and the maximum diversity achievable is 8. We shall assume throughout this chapter that the 8 chips produced by the vectors $\mathbf{s}_0, \ldots, \mathbf{s}_{Q-1}$ are separated much further apart than the coherence bandwidth and thus are subject to independent fading. In the next section we will show that this assumption is reasonable for a typical multipath mobile radio channel.

5.2.1 Independence assumption

The receiver for the OFDM-CDMA system we are considering is shown in Figure 5.3. Assuming the guard interval is longer than the channel dispersion the received signal after the FFT and de-interleaver can be written as a vector r of L/Q components,

$$\mathbf{r} = \mathbf{H}_q . \mathbf{s}_q^T + \mathbf{n} \tag{5.3}$$

[2] An approximate measure of the frequency diversity D' is given by $D' = B/(\Delta f)_c$ where B is transmission bandwidth and $(\Delta f)_c$ is the coherence bandwidth. There are however several different definitions of coherence bandwidth (see Appendix B).

where $\mathbf{H}_q$ is a diagonal matrix representing the fading of the sub-carriers assigned to the qth block. $\mathbf{s}_q^T$ is the transposed transmitted sequence and $\mathbf{n}$ is received the noise vector. The received signal is passed to an equaliser whose output is given by $\mathbf{u}$,

$$\mathbf{u} = \mathbf{G}.\mathbf{r} \tag{5.4}$$

where $\mathbf{G}$ is a diagonal matrix representing the equaliser coefficients.

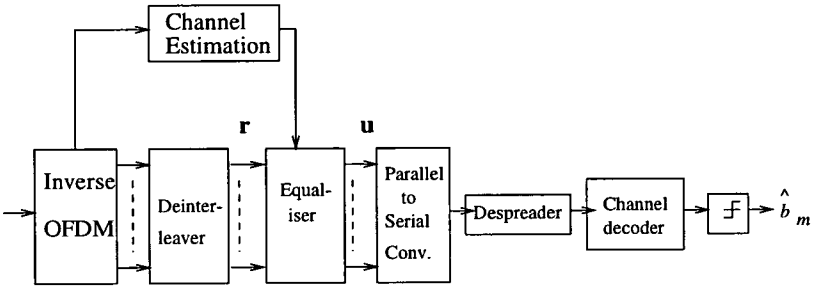

Figure 5.3: OFDM-CDMA receiver

The system can be modelled in the frequency domain as seen in Figure 5.4. The fading of the carriers in each sub section are represented by the diagonal elements $h_{0,0}, \ldots, h_{L/Q-1,L/Q-1}$ of the fading matrix $\mathbf{H}$ and the equaliser coefficients are represented by the diagonal elements $g_{0,0}, \ldots, g_{L/Q-1,L/Q-1}$ of the equaliser matrix $\mathbf{G}$. The variables representing the fading of the sub-carriers $h_{0,0}, \ldots, h_{L/Q-1,L/Q-1}$ are correlated variables with Rayleigh statistics. In the case when the carriers are separated much further apart than the coherence bandwidth, the correlation between these variables is low and a diversity of L/Q (8 in this case) is achieved.

To examine this assumption we investigate the performance of the system shown in Figure 5.1 for different multipath fading channels. We shall use an interleaver which separates the adjacent chips from the same data bit by 64 carriers. A 512 point IFFT is used at the transmitter (a corresponding 512 point FFT is used at the receiver) with a cyclically extended guard interval of 17.5 μs (18 samples). At the receiver the guard interval is removed before the FFT is performed. We assume to have perfect channel knowledge and use equal gain combining (EGC) at the receiver. The performance of a single user will be studied. The structure of the multipath channel is the same as that seen in Figure 4.5. We simulate a 4, 8 and 16 path channel. The 4 path channel has scaling factors (see Figure 4.5) $a_1 = a_2 = a_3 = a_4 = 0.5$, the 8 path channel has scaling factors $a_1, \ldots, a_8 = 0.3536$ and the 16 path channel has scaling factors $a_1, \ldots, a_{16} = 0.25$. The BER results are shown in Figure 5.5. Also shown in Figure 5.5 are the results for the case of 8 independent fading channels as seen in Figure 5.4.

As can be seen from Figure 5.5 the 4 path channel does not have sufficient dispersion (maximum delay

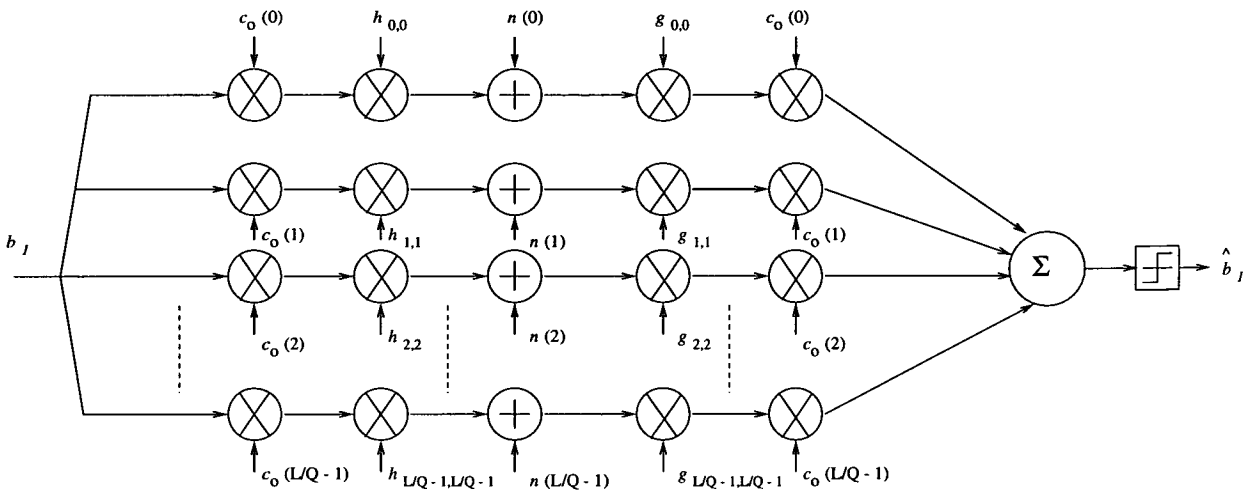

Figure 5.4: Single user OFDM-CDMA system modelled in the frequency domain

spread 3.6 μs) for the system to be modelled as 8 independent channels. The 8 path (maximum delay spread 7.2 μs) and 16 path (maximum delay spread 14.4 μs) channels have much better performance. Their performance is very close to that of the 8 independent channels. For mobile radio channels which have a dispersion in excess of 10 μs it is therefore reasonable to model the OFDM-CDMA system as seen in Figure 5.4 with 8 independent fading channels. For the rest of this chapter this OFDM-CDMA system will be modelled in this way. This also alleviates the large simulation burden of the 512 point FFT and IFFT's. (In Chapter 6 the modelling of the OFDM-CDMA system will again use the 512 point FFT and IFFT's for synchronisation and channel estimation purposes.)

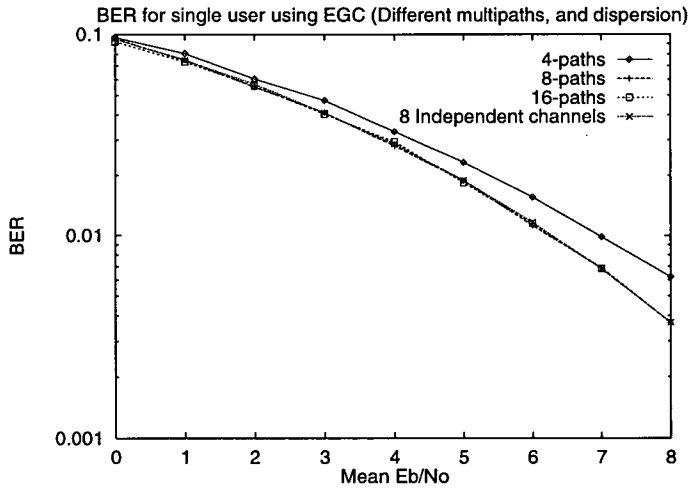

Figure 5.5: BER performance for single user with EGC for different channels

5.3 Detection techniques

In this section we examine the performance of different detection schemes for the OFDM-CDMA system. These detection schemes have different levels of complexity and therefore any of the detection

schemes could be selected for a given complexity/performance compromise. Throughout this section we shall refer to the diagonal elements $g_{0,0}, \ldots, g_{L/Q-1,L/Q-1}$ of the matrix $\mathbf{G}$ as $g_0, \ldots, g_{L/Q-1}$ and the diagonal elements $h_{0,0}, \ldots, h_{L/Q-1,L/Q-1}$ of the diagonal matrix $\mathbf{H}$ as $h_0, \ldots, h_{L/Q-1}$. In this section we shall assume we have perfect knowledge of the channel and all comparisons will be made at a BER of 2×10^{-3}. Equal gain combining (EGC) and maximal ratio combining (MRC) have already been described in section 4.3. To perform EGC the equaliser coefficient g_l is given by,

$$g_l = \frac{h_l^*}{|h_l|} \tag{5.5}$$

and to perform MRC the equaliser coefficient g_l is given by

$$g_l = h_l^* \tag{5.6}$$

The Monte Carlo performance of the OFDM-CDMA system for EGC and MRC are shown in Figures 5.6 and 5.7 respectively. As we have previously discussed in section 4.3.2.3, EGC is the preferred technique for a one chip per carrier MC-CDMA system. As can be seen from Figure 5.6 with EGC a BER of 2×10^{-3} can be supported for 32 users at 17 dB E_b/N_0. By examining Figure 5.7 it can be seen that 32 users can not be supported with MRC at a BER of 2×10^{-3}. For the single user with MRC, however only 8 dB is required compared to 9 dB to support a BER of 2×10^{-3}.

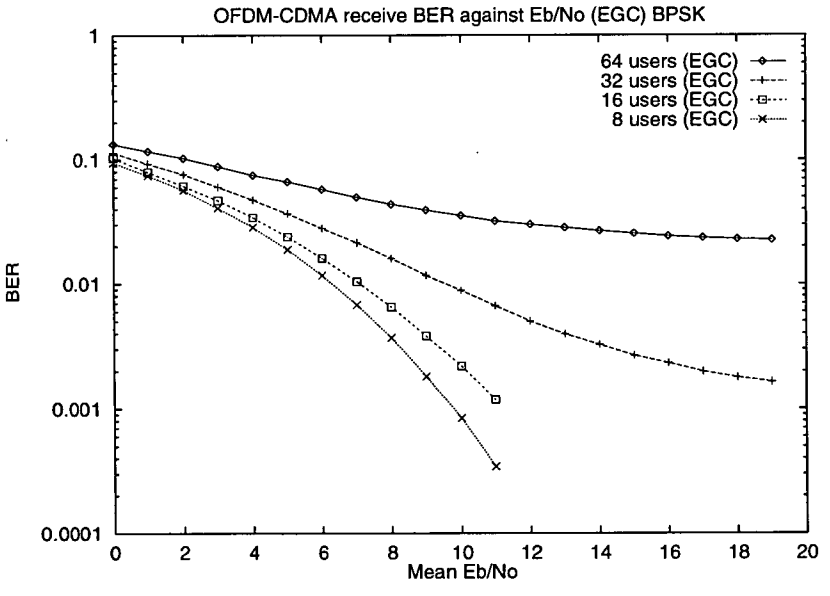

Figure 5.6: Equal gain combining (EGC)

The orthogonality of the spreading sequence can be maintained if a zero forcing equaliser is used. To perform the zero forcing solution the equaliser coefficient g_l is given by,

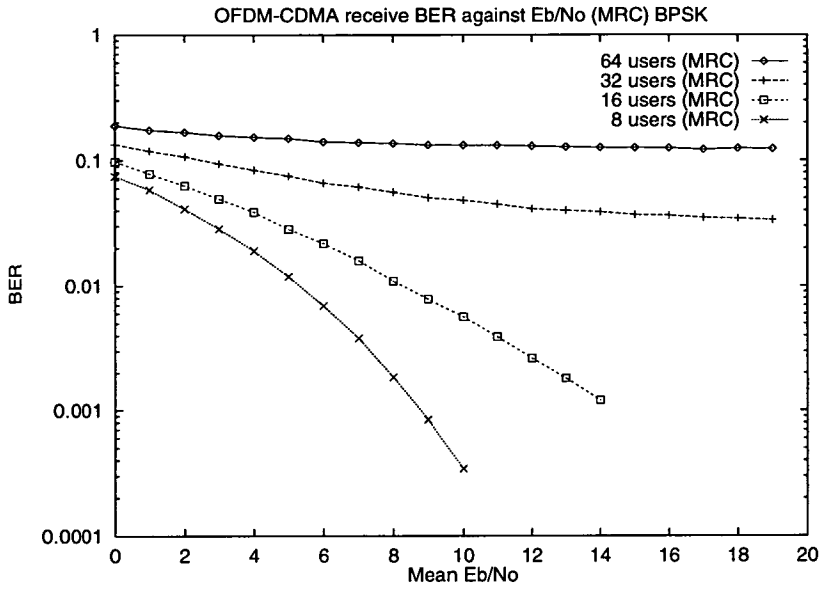

Figure 5.7: Maximal ratio combining (MRC)

$$g_l = \frac{1}{h_l} \tag{5.7}$$

The results using the zero forcing approach are shown in Figure 5.8. It may be seen that, although orthogonality is maintained, an E_b/N_0 of 21 dB is required to support 1 (or any number of users up to 64 users) for a BER of 2×10^{-3}.

An improvement on this method can be obtained if the zero forcing equaliser approach is applied when the fading signal on each carrier is greater than a given threshold. If the fading is below this threshold the equal gain combining criteria is used. This method is called controlled equalisation and was first introduced by Linnartz [7]. The equaliser coefficient g_l is given by,

$$g_l = \begin{cases} \frac{1}{h_l} & : \quad |h_l| \geq p_{thres} \\ \frac{h_l^*}{|h_l|} & : \quad |h_l| \leq p_{thres} \end{cases}$$

Results for controlled equalisation with a threshold p_{thres} of 0.168 are shown in Figure 5.9. As can be seen a BER of 2×10^{-3} can be supported for 64 users at 15 dB E_b/N_0.

For increased performance the MMSE criteria can be used. To calculate the equaliser coefficients to fulfil the MMSE criteria, knowledge of the channel, the number of active users and the signal to noise ratio is required. The equaliser coefficient g_l (as derived in section 4.5.1) is given by,

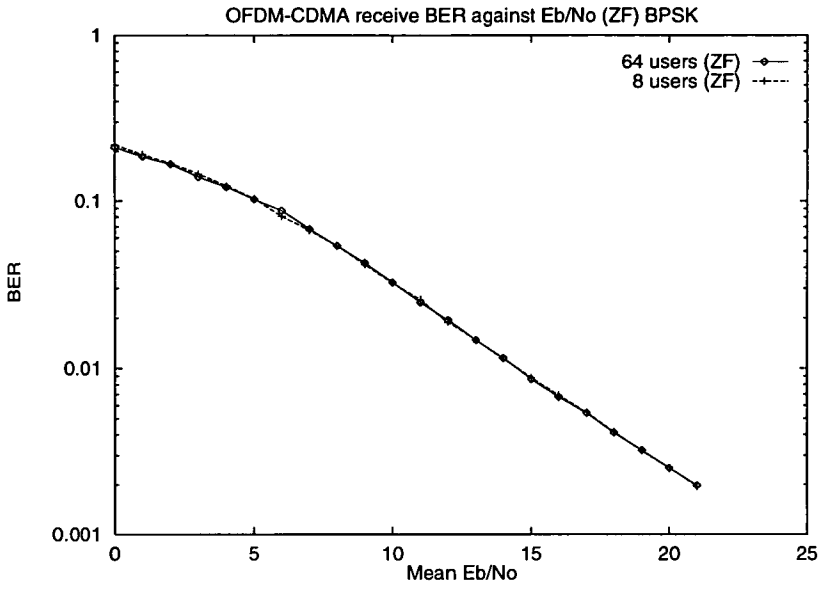

Figure 5.8: Zero forcing (ZF)

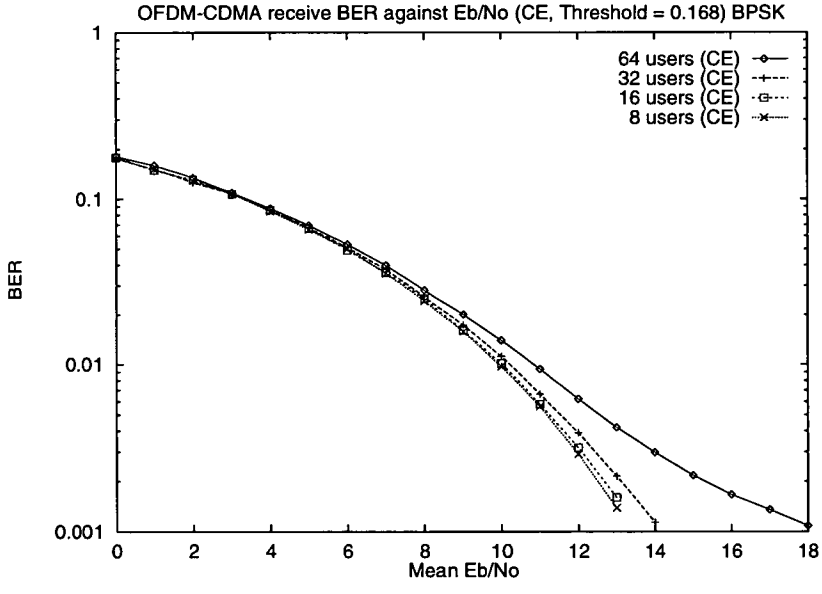

Figure 5.9: Controlled equalisation (CE), threshold = 0.168

$$g_l = \frac{h_l^*}{|h_l|^2 + \frac{LN_0}{2E_bN_u}} \tag{5.8}$$

where L is the spreading sequence length ($L = 8$) and N_u is the number of active users. The performance of the system using the MMSE criteria is shown in Figure 5.10. As can be seen from Figure 5.10 a BER of 2×10^{-3} can be supported for 64 users at 14 dB E_b/N_0. To support a BER of 2×10^{-3} for 8 users, 8 dB is required.

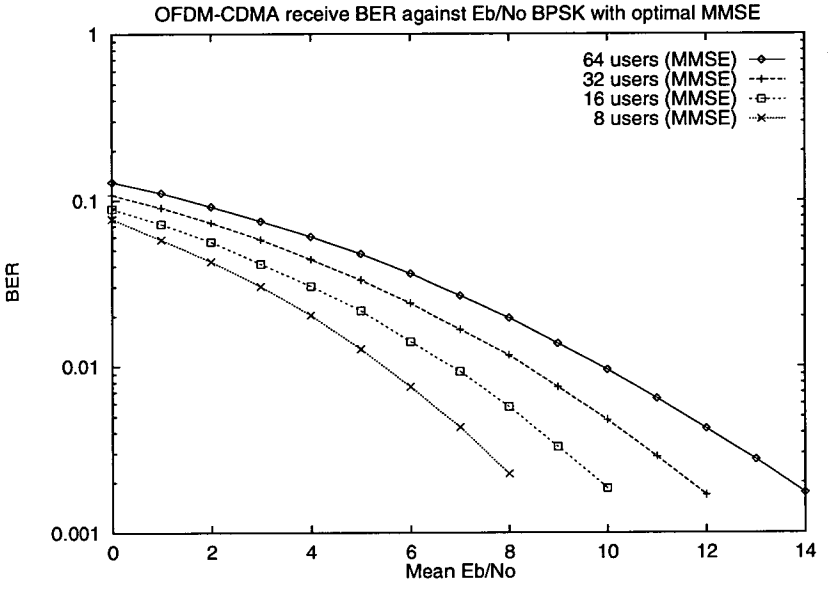

Figure 5.10: Optimal MMSE

When only channel information is available the non-optimal MMSE criteria can be used. The equaliser coefficient g_l is given by

$$g_l = \frac{h_l^*}{|h_l|^2 + \frac{L}{SNR_{max} \cdot N_{u_{max}}}} \tag{5.9}$$

where SNR_{max} is the maximum signal to noise ratio ($2E_b/N_0$) and $N_{u_{max}}$ is the maximum number of users. BER results are shown in Figure 5.11 with the maximum E_b/N_0 set to 20 dB and N_{max} set to 64. By examining Figure 5.11 it can be seen that 64 users can be supported at 14 dB. For low numbers of users the non-optimal MMSE criteria requires a higher E_b/N_0 than the optimal MMSE for a given BER. For the case of 8 users the non-optimal MMSE criteria requires 13 dB E_b/N_0 to support a BER of 2×10^{-3}.

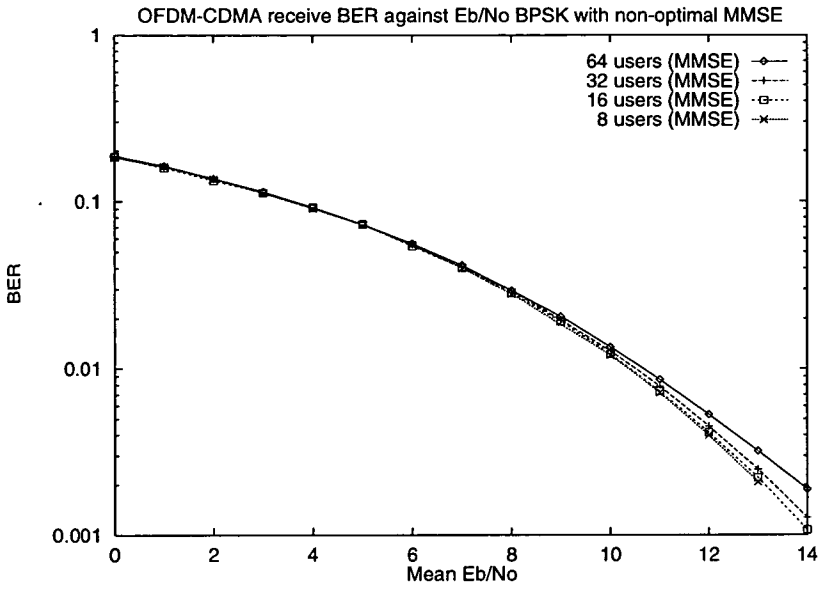

Figure 5.11: Non-optimal MMSE

Interference cancellation can be used for OFDM-CDMA. Several different interference cancellation schemes have been studied. Fazel [5] has investigated a single stage canceller in which EGC is used. A two stage canceller has also been suggested by Kaiser [37] in which MMSE is used as the first stage and the EGC is used for subsequent stages. A simpler two stage interference canceller has been suggested by Kalofonos [38] which uses a controlled equaliser as the first stage. (In the paper this is referred to as threshold orthogonalising combining (TORC)). The second stage uses MRC. We shall examine a canceller which uses EGC for every stage. In this way only knowledge of the number of users and the channel is needed. A single stage interference canceller is seen in Figure 5.12.

The interference canceller may also be increased to two stages for increased performance but the system delay is then increased by a factor of two. BER curves for the one and two stages of interference cancellation are seen in Figures 5.13 and 5.14 respectively. The two stage canceller provides a marginal improvement over the single stage canceller. It can be seen that for low numbers of users the MMSE criteria has a lower BER for a given E_b/N_0 than the two stage canceller. For 32 users the single stage interference cancellation and the MMSE have similar performance both requiring 12 dB E_b/N_0 to support a BER of 2×10^{-3}. For 64 users the two stage interference canceller reaches an irreducible BER of 8×10^{-3} at 13 dB E_b/N_0.

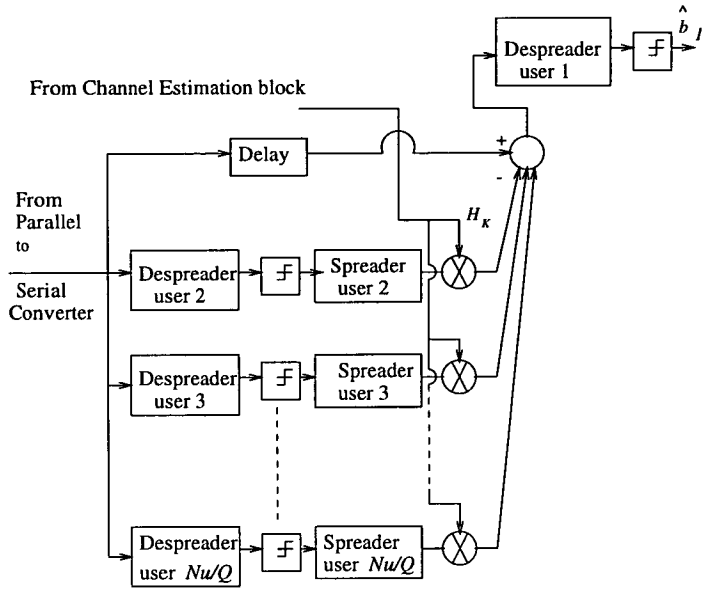

Figure 5.12: Receiver with single stage interference cancellation

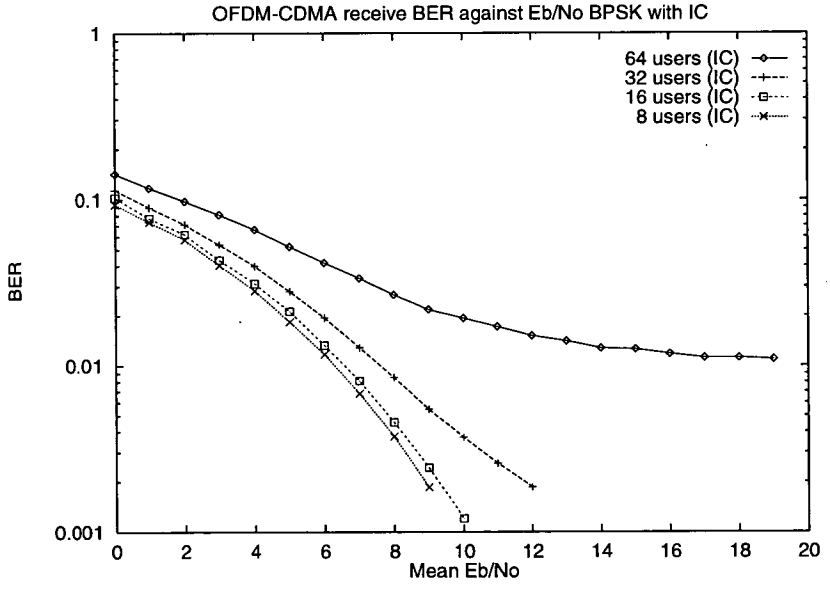

Figure 5.13: One stage interference cancellation

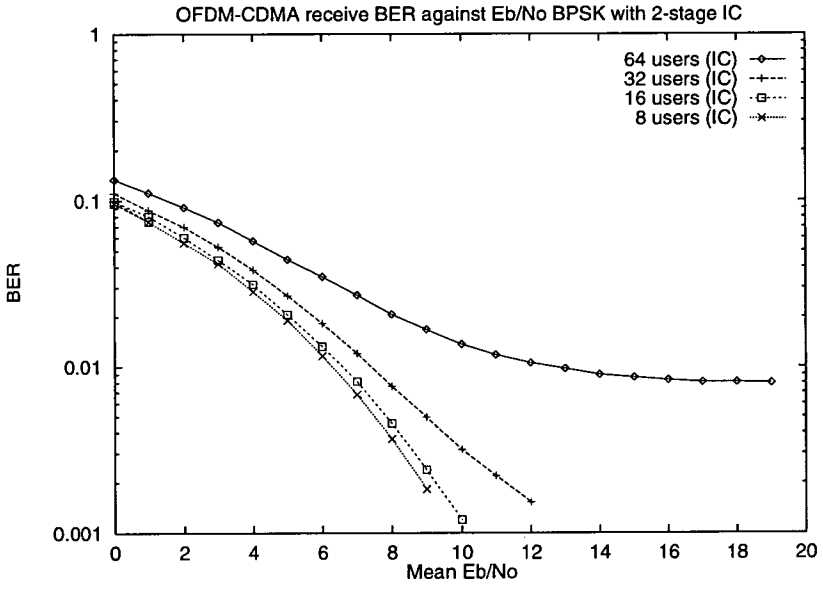

Figure 5.14: Two stage interference cancellation

With knowledge of the number of users and the channel, it is possible to perform maximum likelihood detection (MLD) for this OFDM-CDMA system. To achieve this, the distances δ_j^2 between the received vector $\mathbf{r}$ and all sent sequences $\mathbf{v}_j$ ($j = 0, \ldots, 2^{L/Q}$) multiplied by the channel matrix $\mathbf{H}$ are evaluated. In this way the most likely sent sequence $\mathbf{v}_n$ is found. The minimum distance δ_n^2 is given by

$$\delta_n^2 = \min||\mathbf{r} - \mathbf{H}\mathbf{v}_j||^2 \tag{5.10}$$

For the OFDM-CDMA system considered here there are a maximum number of 256 sequences to evaluate. (The number of sequences to evaluate depends on the number of users.) When the most likely sequence is found it is then despread by the local spreading code. A sign decision is then made on the resulting signal to form the received data bit $\widehat{b}_m$. BER curves for MLD are shown in Figure 5.15. As can be seen in Figure 5.15 a BER of 2×10^{-3} can be supported for 64 users at 11 dB E_b/N_0. This compares with the MMSE criteria which requires 14 dB E_b/N_0 (see Figure 5.10 page 68). It is important to note, that although MLD offers the best performance it is not as robust as the optimal MMSE criteria. If the knowledge of the number of users is incorrect the performance is very poor. If the number of users is incorrect in the case of the MMSE criteria conversely it has already been shown that moderate performance can be obtained with the non-optimal MMSE criteria.

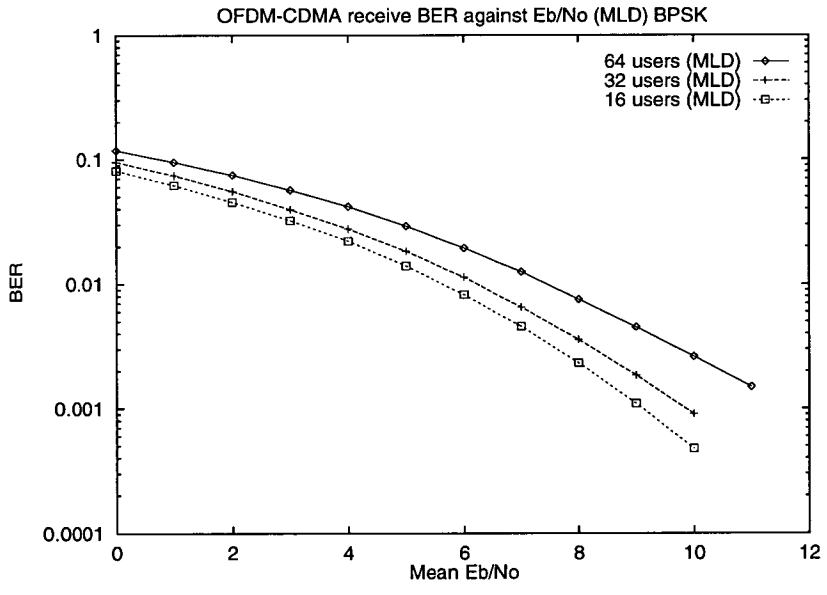

Figure 5.15: Maximum likelihood detection (MLD)

5.3.1 Detection summary

In this section we have examined the performance of the different detection schemes for the type 1 OFDM-CDMA system. The performance of the different detection schemes and the knowledge required at the receiver is shown in Table 5.1. If only channel information is available, the non-optimal MMSE criteria is the best detection scheme to choose for 64 users. If the number of users is also available the MLD is the best choice. The spectral efficiencies of the different schemes are shown in Figure 5.16. In the calculation for spectral efficiencies we have assumed that 15 % of the data is needed for channel sounding (see Chapter 5).

Table 5.1: *Performance of different detection schemes*

Detection scheme	E_b/N_0 for BER of 2×10^{-3}		Knowledge required
	8 users	64 users	at receiver
EGC	9 dB	-	Channel
MRC	8 dB	-	Channel
Zero forcing (ZF)	21 dB	21 dB	Channel
Control. Eq. (CE)	12.5 dB	16 dB	Channel
Two stage IC	9 dB	-	Channel, no. of users
MMSE	8 dB	14 dB	Channel, no. of users, E_b/N_0
Non-opt. MMSE	13 dB	14 dB	Channel
MLD	8 dB	11 dB	Channel, no. of users

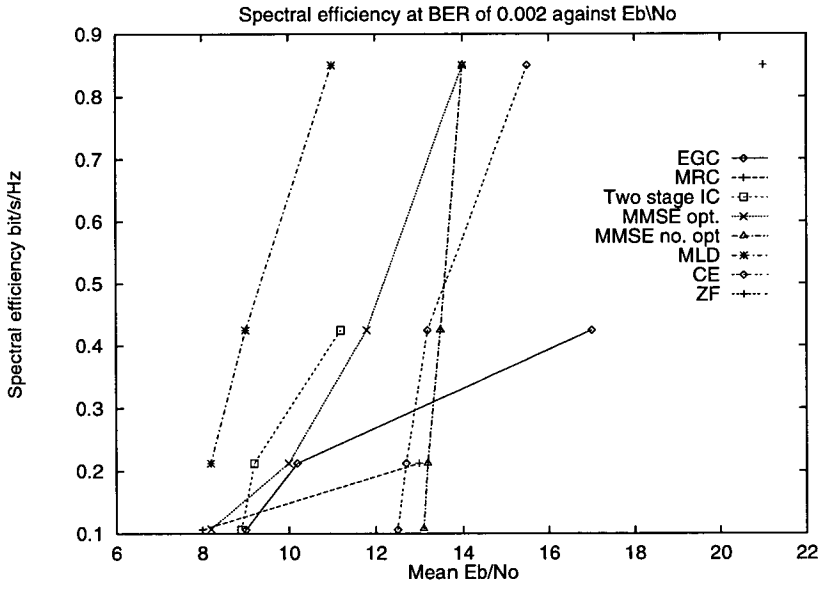

Figure 5.16: Spectral efficiency for different detection schemes

5.4 Channel coding

In this section we examine the performance of different channel coding schemes for this OFDM-CDMA system. It is important to differentiate channel coding from source coding. Source coding removes redundancy from certain data sources such as images or speech. (These are commonly referred to as speech and image coding respectively.) There are two broad categories of channel coding: block coding and convolutional coding. Both of these categories can be split into many different types. However, broadly speaking a block code consists of a block of k information bits followed by a group of r check bits that are derived from the block of information bits. At the receiver the check bits in the block are used to verify the information bits in the same block. In convolutional coding, code words are formed which depend on the present and $K-1$ previous data bits, where K is the constraint length.

These two channel coding schemes can also be combined to form a powerful concatenated coding scheme [56]. In this section however we will deal exclusively with convolutional coding due to the relative ease with which the channel decoder can be implemented by using a Viterbi decoder.

5.4.1 Convolutional coding

A convolutional code (CC) is generated by passing the uncoded data bits through a finite shift register. In general the shift register consists of K stages (of k bits) and n linear algebraic functions. A general k/n rate convolutional coder is shown in Figure 5.17.

The input data is shifted through the register k bits at a time. For every k information bits the switch moves from position 1 to position n producing n encoded data bits. The value of the encoded data bits depends on the value of the inputs in the K stages, due to the connections to the modulo 2 adders. These connections can be written as a vector of Kk elements for each adder. By examining Figure 5.17 the connection for the first and second adder can be written as vectors $\mathbf{g}_1$ and $\mathbf{g}_2$ of length Kk,

$$\mathbf{g}_1 = [1, 1, \overbrace{0, \ldots, 0}^{Kk-2}] \tag{5.11}$$

$$\mathbf{g}_2 = [0, 1, \underbrace{0, \ldots, 0}_{2k-3}, 1, \underbrace{0, \ldots, 0}_{Kk-2k}] \tag{5.12}$$

These connections are often quoted in octal format for convenience. They form the output sequence for any input sequence and therefore affect the Hamming distance between any two output sequences which were generated by different input sequences. The connections therefore determine the error correcting properties of the code. For a given convolutional code of rate k/n and constraint length K, there are connections which optimise the minimum Hamming distance of the code [57,58] and therefore optimise the error correcting property of the code. This minimum Hamming distance is also referred as the *minimum free distance* [1].

[1] The *minimum free distance* can easily be evaluated by calculating the Hamming distance between an encoded sequence generated by all zeros at the input and an encoded sequence generated by a 1 followed by all zeros at the input.

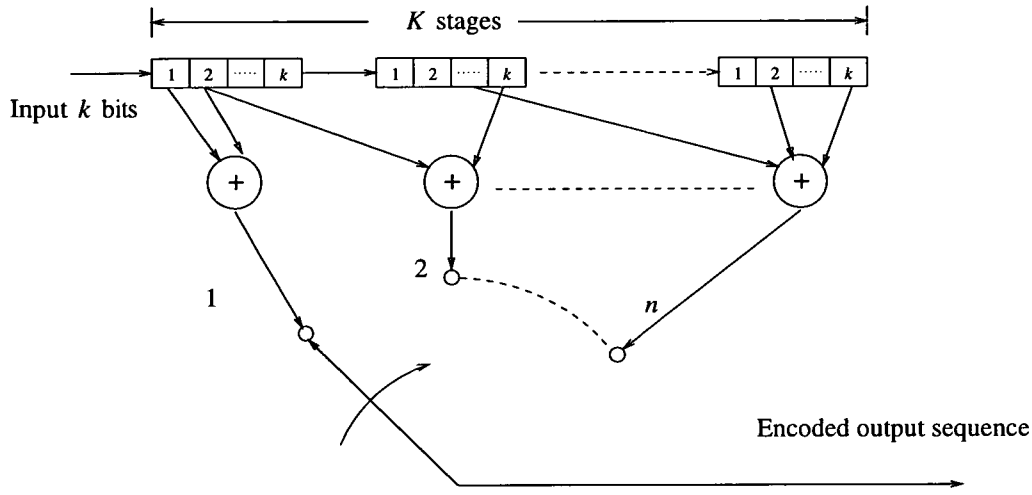

Figure 5.17: General constraint length K, k/n rate convolutional coder

To decode the encoded data, a trellis is used which has $2^{k(K-1)}$ states for each step as seen in Figure 5.18. Each of these states can be reached by 2^k paths or transitions. For a coder of a given constraint length and adder connections, the possible transitions in the trellis can be calculated and the Viterbi decoder designed. The Viterbi algorithm evaluates the most likely sent sequence through the trellis. To implement the Viterbi algorithm a sliding window is used and the received data is compared against the values contained in the trellis. At the first stage in the trellis all the $2^{k(K-1)}$ states are assigned a *state metric* of zero. For step 2 of the trellis n received data bits are multiplied by the data values seen in the trellis, forming a *transition metric*. The *transition metric* is then added to the *state metric* from where the transition came from so the metric for that path can be evaluated. For every state in step 2 the metric of the merging paths are compared and the one with the highest metric is chosen.

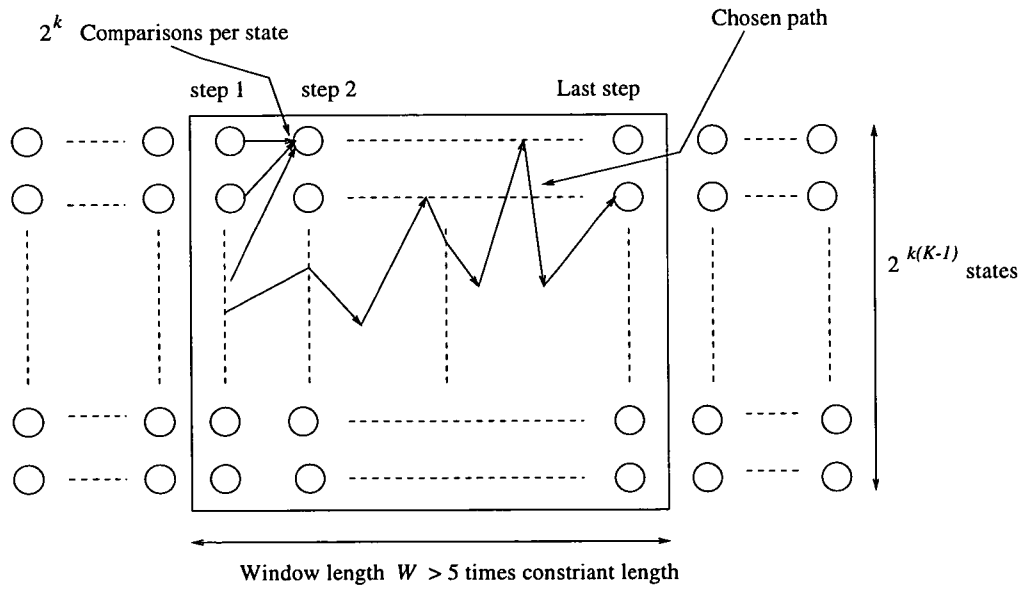

Figure 5.18: Viterbi decoder trellis

The procedure continues iteratively along the trellis until the end of the window is reached. The length of the window (W) is determined by the memory capacity of the system and the processing time available. If the length of the window is less than five times the constraint length, the performance starts to degrade [59]. At the end of the trellis the state with the highest metric is selected and the path associated with this state is then deemed the path of maximum likelihood. A decision is then made on the first data bits which occurred on the transition between step 1 and step 2 on the chosen path. The trellis is then moved along one stage and the process repeated.

By representing the state metric of the ith state from the kth step by *state metric* $[i, k]$ and the transition metric from state x to i as *transition metric* $[x, i]$ where $i, x \in \{1, \ldots, 2^{k(K-1)}\}$ and $k \in \{1, \ldots, W\}$ we can describe this decoding process in the following steps:

1) *state metric* $[i,0] = 0$ for all i.

2) for $k = 1$ to window length
{ for $i = 0$ to $2^{k(K-1)}$
{ *state metric* $[i, k]$ = max (*transition metric* $[x, i]$ + *state metric* $[x, k-1]$)
}
}

3) choose path which corresponds to final state.
Final state = max (*state metric* $[i$, window length])

4) Output data bits corresponding to transition between step 1 and step 2 of chosen path.

5) Move trellis along one step and repeat steps 1 to 4.

5.4.2 Convolutionally coded OFDM-CDMA

In this section we shall examine the BER performance of the OFDM-CDMA system in conjunction with convolutional coding. We have already investigated the performance of different detection schemes for the OFDM-CDMA system and all of these schemes can be used in conjunction with coding.

It is important however, that the input of the Viterbi decoder receives a soft input to enable a soft decision Viterbi decoder to be used. Soft decision Viterbi decoding is about 3 dB better than hard decision Viterbi decoding in Gaussian channels, however, in Rayleigh fading channel the performance difference between soft and hard decoding is much larger and increases with decreasing BER. The soft input must represent the quality or reliability of the received signal. If MLD is used as a detection technique, the values produced at the despreader output can only be considered to be optimal soft values when the correct sent sequence has been chosen. This will only occur at very high values of E_b/N_0. At low values of E_b/N_0 the incorrect sent sequence will be chosen and the output values will be incorrect. The output of the MLD detector therefore has to be supplemented with reliability information so the

optimal soft output can be formed. This requires knowledge of the signal to noise ratio and is achieved by using the log-likelihood function on the despreader output [39,40].

In this section, however, we investigate the performance of different channel coding schemes for the OFDM-CDMA system in conjunction with EGC. Although, EGC is not the best choice of detection scheme for an uncoded system (see Table 5.1), the output of the despreader using EGC is the optimal soft value. Channel decoding can therefore be implemented without a log-likelihood detector and without knowledge of the SNR. The OFDM-CDMA receiver with channel coding is shown in Figure 5.19.

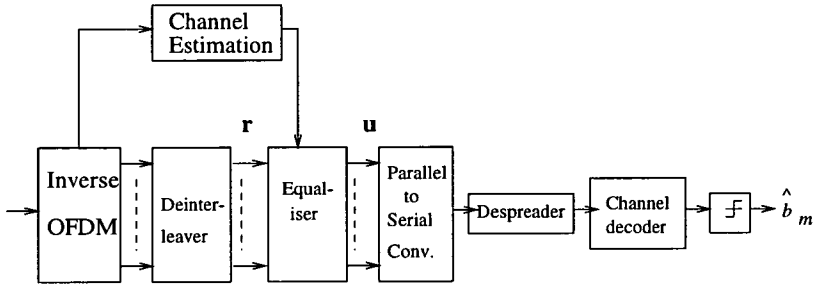

Figure 5.19: OFDM-CDMA receiver with channel decoding

5.4.2.1 1/2 rate convolutionally coded OFDM-CDMA with EGC

In this section we investigate the performance of the OFDM-CDMA system with 1/2 rate convolutional coding. The performance of convolutional coders with constraint length K = 3 and constraint length K = 7 are studied. The selected connections in the coder have the maximal free distance for their constraint length [58]. For the K = 3 coder the connections are given by (5,7) in octal format and for K = 7 the connections are (131,171).

In a Gaussian noise channel, the theoretical BER performance of a convolutional code is upper bounded by

$$\text{BER} \leq \sum_{d=d_{free}}^{\infty} \omega_d P(d) \tag{5.13}$$

where $P(d)$ is the probability that the wrong path at distance d is selected and ω_d is the distance spectra of the code. The distance spectra of the code is defined as the distance profile weighted by the number of bit errors per error event with distance d. $P(d)$ is given by,

$$P(d) = \frac{1}{2}\text{erfc}\left(\sqrt{\frac{E_b d R_c}{N_o}}\right) \tag{5.14}$$

where d is the distance and R_c is the rate of the code. The performance of the two 1/2 rate convolutional coders in Gaussian noise are shown in Figure 5.20. It can be seen that the simulated results approach the upper bounds [1] at low BER values less than 1×10^{-3}. The simulated results in multipath are seen in Figures 5.21 and 5.22 for the $K = 3$ and $K = 7$ codes respectively.

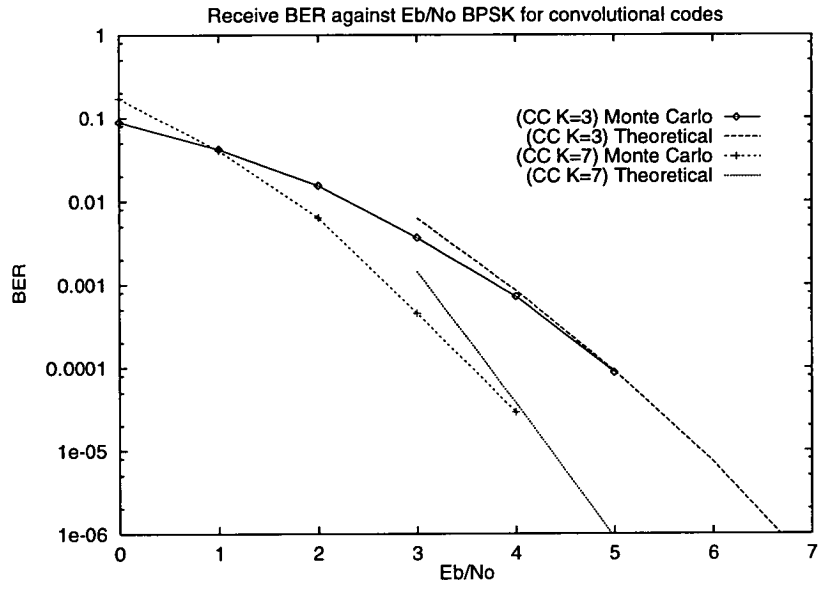

Figure 5.20: BER results for 1/2 rate coder in Gaussian noise

These results assume the data rate for each user is fixed at 16 kbits/s and that the transmitted bandwidth is 2 MHz. From the figures it can be seen that 8 dB E_b/N_0 is required to support 64 users at a BER of 2×10^{-3} for the $K = 3$ coder which compares to 6 dB E_b/N_0 for the $K = 7$ coder.

[1] It is important to note that due to the infinte upper bound in equation 5.13 it is only possible to form an approximation. The first 17 values of ω_d given by Conan [58] were used.

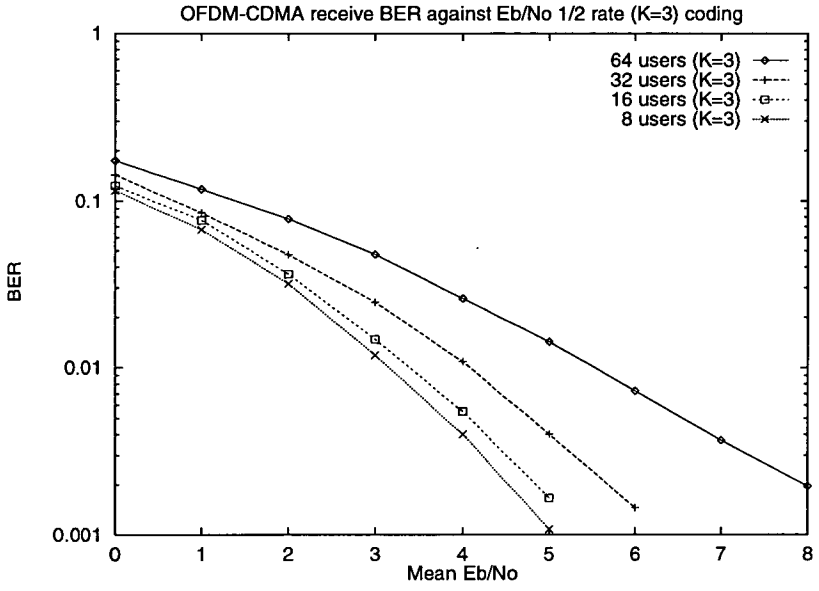

Figure 5.21: BER results for 1/2 rate coder ($K = 3$) in multipath

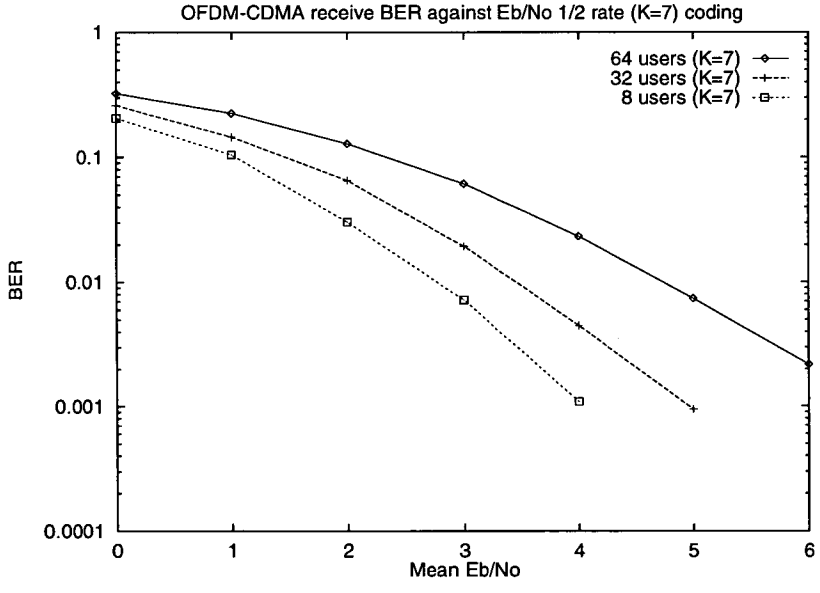

Figure 5.22: BER results for 1/2 rate coder ($K = 7$) in multipath

5.4.3 1/2 rate convolutionally coded DS-CDMA

In this section we examine the performance of a convolutionally coded BPSK DS-CDMA system occupying the same bandwidth as the convolutionally coded OFDM-CDMA system described in section 5.4.2.1. The DS-CDMA uses the same uncoded data rate and the same channel coding scheme. The DS-CDMA system with a RAKE receiver is shown in Figure 5.23.

The RAKE receiver uses maximal ratio combining (MRC) as explained in section 4.3.1. To incorporate coding into DS-CDMA, the binary information sequence is first convolutionally coded at the transmitter before being multiplied by the spreading sequence. We consider a half rate convolutional coder of constraint length 7. The interleaver reduces the fading correlation between adjacent data bits, reducing burst errors and enabling the Viterbi decoder to work more efficiently. We assume the fading is fast enough to implement a perfect interleaver. This provides us with an upper bound on performance. The soft output of the RAKE receiver is passed to a soft decision Viterbi decoder. A hard decision is then made at the Viterbi decoders output to obtain the received data bit $\widehat{b}_m$.

The coded DS-CDMA system uses an uncoded data rate of 16 kbits/s and a length 63 Gold code. This yields a coded bandwidth of 2.010 MHz. This compares with 2.048 MHz for the coded OFDM-CDMA system. We shall investigate the performance of a 4 tap RAKE receiver in a 4 path channel which has 10 μs delay spread. The Monte Carlo results for the coded DS-CDMA system are shown in Figure 5.24. The theoretical results for a single user are also shown. The theoretical results for a single user is taken from the upper bound derived by Schramm [60] given by

$$\text{BER} \leq \frac{1}{2\sqrt{\pi K}} \sqrt{\frac{1+\frac{R_c E_b}{D N_0}}{\frac{R_c E_b}{D N_0}}} \sum_{d=d_{min}}^{\infty} \omega_d \frac{\Gamma(d_{min} D - 1/2)}{\Gamma(d_{min} D)} \frac{1}{\left(\frac{R_c E_b}{D N_0}+1\right)^{dD}} \tag{5.15}$$

where Γ () is the gamma function, D is the number of multipath components, d_{min} is the minimum free distance of the code and ω_d is the spectra of the code [58]. It can be seen from Figure 5.24 that the DS-CDMA RAKE supports a BER of 2×10^{-3} for 32 users at 20 dB E_b/N_0. The spectral efficiency of the coded OFDM-CDMA and the coded DS-CDMA systems are seen in Figure 5.25. For the calculation of spectral efficiency we shall assume that 15 % of the 16 kbits/s is needed for channel sounding in the OFDM-CDMA case. For channel sounding in the DS-CDMA case one user is used as a pilot tone. Therefore when N_u are active, N_u - 1 users send useful data. The OFDM-CDMA coded system yields a spectral efficiency of 0.42 bits/s/Hz (64 users) at 6 dB E_b/N_0 compared to the coded DS-CDMA system which yields a spectral efficiency of 0.11 bits/s/Hz.

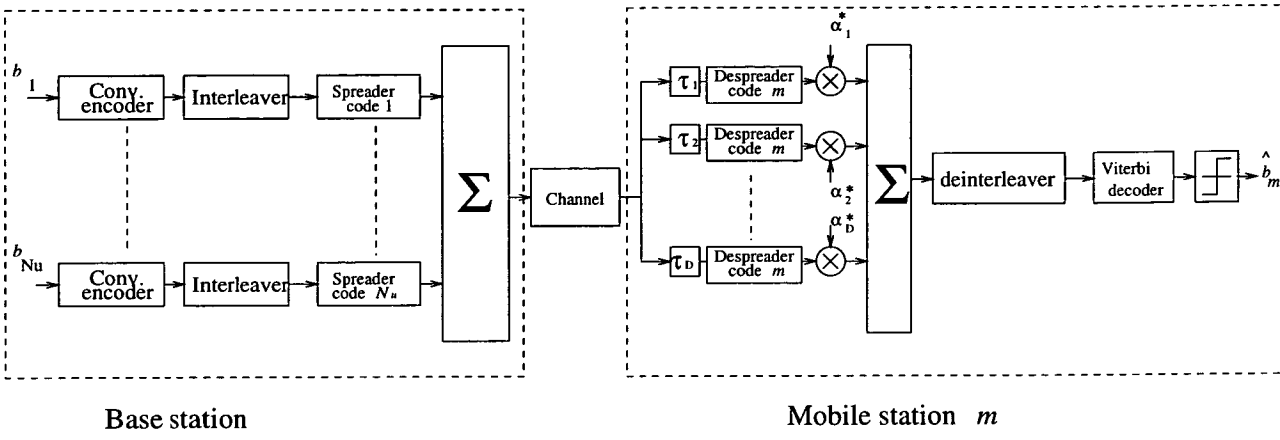

Figure 5.23: Transmision scheme for DS-CDMA for downlink

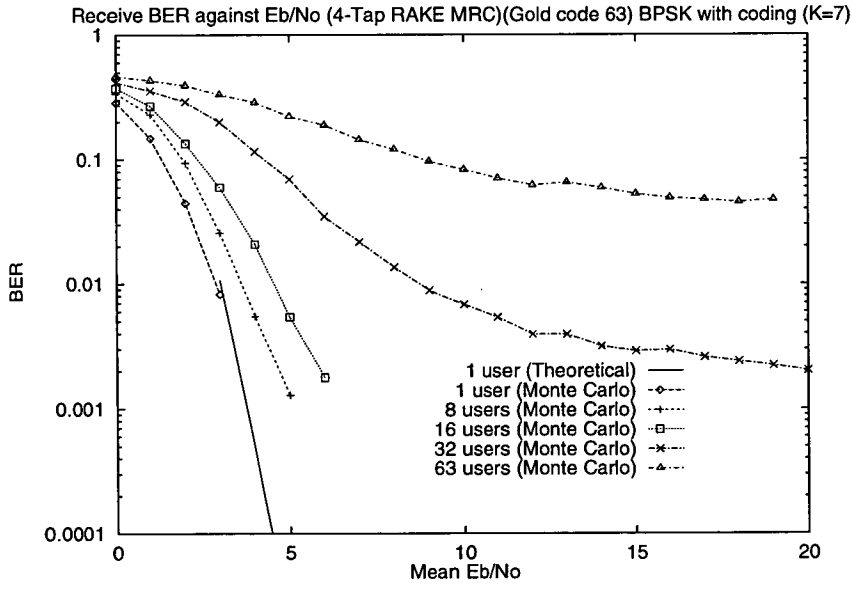

Figure 5.24: BER results for 1/2 rate ($K = 7$) in multipath

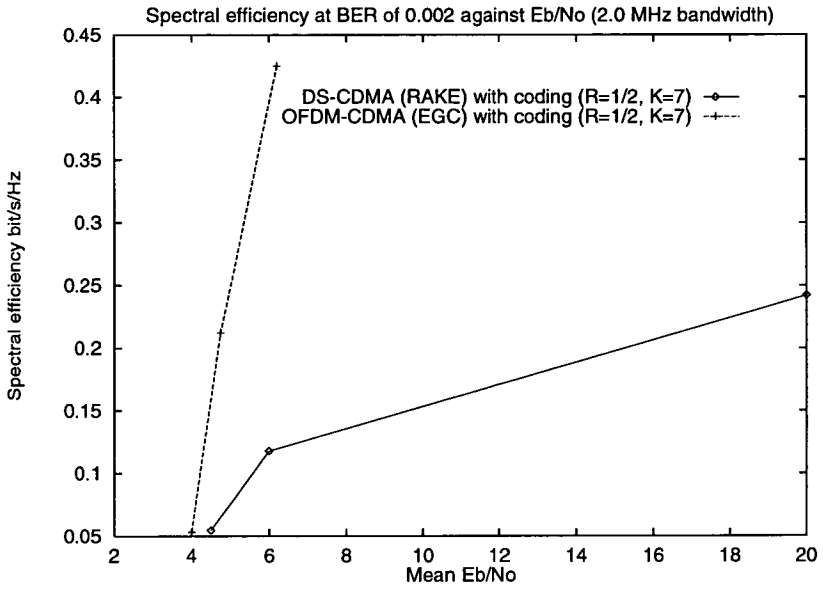

Figure 5.25: Spectral efficiency of coded DS-CDMA and coded OFDM-CDMA systems

5.4.4 Alternative coding schemes for OFDM-CDMA

We have shown in the previous section that at a BER of 2 $\times 10^{-3}$ 64 users can be supported at 6 dB E_b/N_0 for the 1/2 rate convolutionally coded (K = 7) OFDM-CDMA system. The maximum spectral efficiency achievable is 0.425 bits/s/Hz. In this section we examine coding schemes which have lower bandwidth expansions and therefore achieve higher spectral efficiencies. In particular we examine higher rate codes and orthogonal coding.

5.4.4.1 Punctured convolutional coding

For a convolutional code of rate $R_c = k/n$ there are 2^k merging paths at each node in the trellis. The number of comparisons that have to be made at each node in the decoding trellis is therefore 2^k. For higher rate codes ($k > 1$) the decoding complexity is therefore much greater than lower rate codes ($k = 1$). A punctured convolutional code is a modification of a standard $1/n$ convolutional code in which bits of the output encoder are periodically deleted, generating a higher rate code. The number of comparisons at each node is the same as the standard convolutional code, thereby reducing complexity. There is however a reduction in the *minimum free distance* due to the puncturing. We consider the performance of a 3/4 rate K = 7 punctured convolutional code which has the highest *minimum free distance* for this constraint length [61, 62].

For a punctured convolutional code the upper bound is given by [61],

$$\text{BER} \leq \frac{1}{p} \sum_{d=d_{free}}^{\infty} \omega_d P(d) \tag{5.16}$$

where p is the puncturing period, ω_d is the distance spectra of the code and $P(d)$ is given by equation 5.14. The performance of the convolutional code in Gaussian noise is shown in Figure 5.26. It can be seen that the simulated results match with the upper bounds. The simulated results in multipath are shown in Figure 5.27. These results assume the data rate for each user is fixed at 16 kbits/s and that the transmitted bandwidth is 1.33 MHz. From Figure 5.27 it can be seen that 19 dB E_b/N_0 is needed to support 64 users at a BER of 2×10^{-3}. The resulting spectral efficiency is shown in Figure 5.28. It can be seen that the punctured convolutional coding reaches a higher spectral efficiency than the 1/2 rate convolutional code due to the lower bandwidth expansion. However, to achieve a given spectral efficiency less than 0.5 the punctured convolutional code requires a higher value of E_b/N_0 than the 1/2 rate convolutional code. A non-punctured convolutional 3/4 rate code would achieve better performance but at the expense of increased decoder complexity.

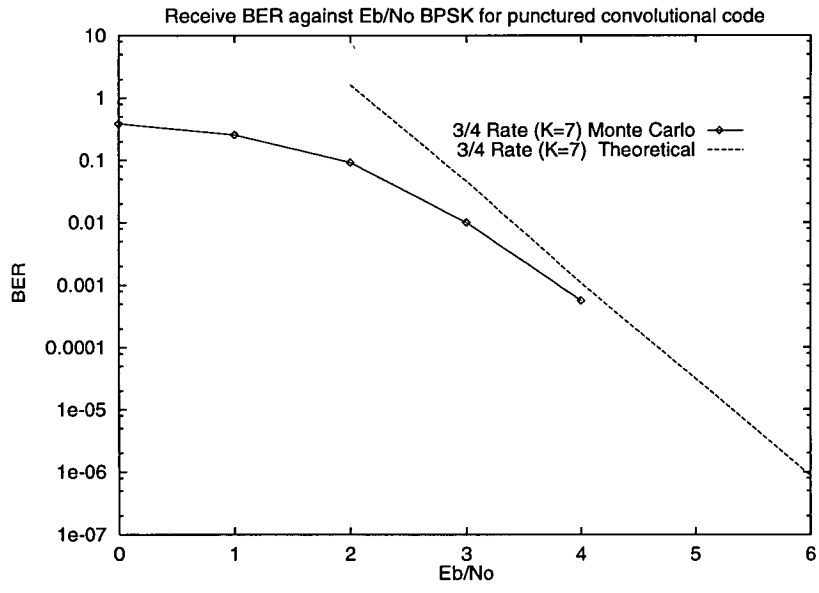

Figure 5.26: BER results for 3/4 rate punctured convolutional coder in Gaussian noise

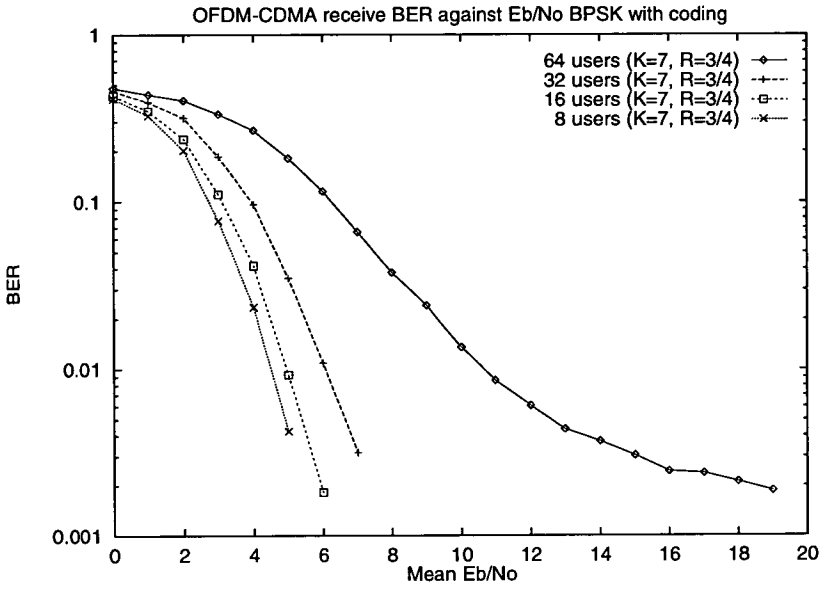

Figure 5.27: BER results for 3/4 rate punctured convolutional in multipath

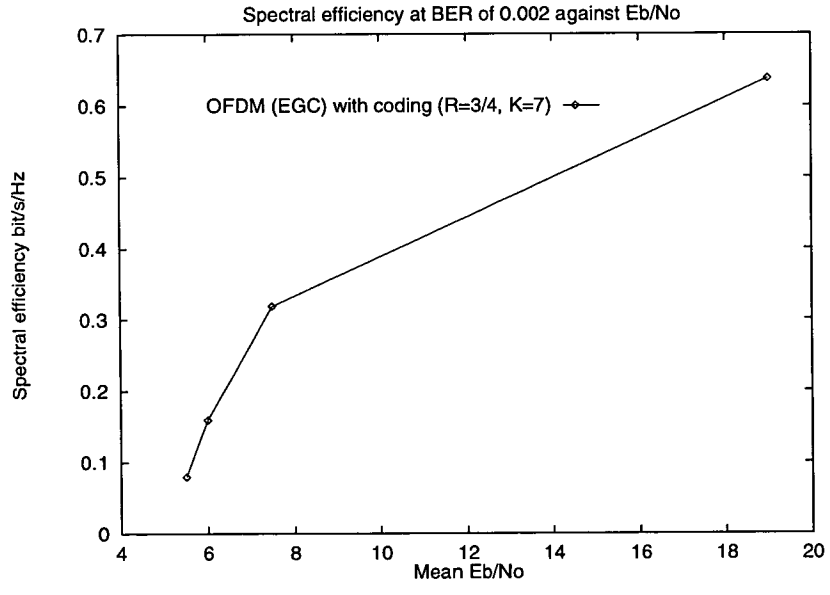

Figure 5.28: Spectral efficiency for 3/4 rate punctured convolutional code in multipath

5.4.4.2 Orthogonal coding

In the following sections we examine the performance of the OFDM-CDMA system with coding schemes that produce orthogonal Walsh codes which depend on the present and previous data bits. The combination of orthogonal coding schemes with OFDM-CDMA is a new idea. By choosing a suitable length orthogonal coder, the length 8 Walsh code normally produced by the spreader operation at the transmitter (see Figure 5.1) can be produced by the coder, thus combining coding and spreading. The advantage of this coder is that the orthogonal coder has the same bandwidth expansion as an uncoded system with spreading only.

5.4.4.3 Orthogonal convolutional coding

The orthogonal coder (or Hadamard encoder) [63, 64] is shown in Figure 5.29. It consists of two shift registers of length K in which the K parallel outputs of the first shift registers are connected to the second via a connector assignment block. The first shift register has K - 1 delay blocks. Each delay block has a delay of T, where T is the uncoded data bit duration. The second shift register contains switches, modulo 2 adders and K delay blocks. The output of the second shift register forms the coder output. Each delay block in the second shift register has a delay which is a multiple of T_c, the chip duration. The first delay is T_c the second is $2T_c$, the third is $4T_c$ and so on. The switches toggle at rate 1,2,4 etc, so that for each data bit at the input of the first shift register a unique 2^K length Walsh code is produced. There is a fixed relationship between the code rate R_c and the constraint length K given by $R_c = 1/2^K$. Figure 5.29 shows a K = 3, R_c = 1/8 coder. With this coder spreading and coding are combined resulting in a bandwidth expansion of 8.

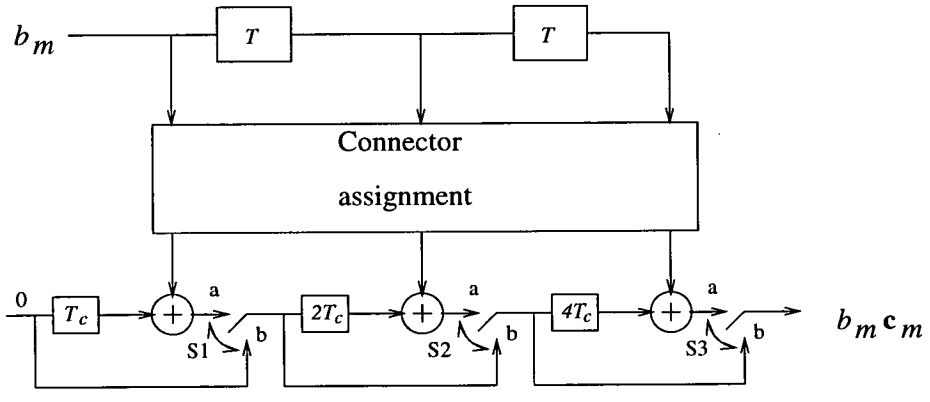

Figure 5.29: Orthogonal coder (K = 3)

Table 5.2 shows the position of the three switches S1, S2 and S3 for each chip of the produced Walsh code from the K = 3 orthogonal coder.

To obtain multiple access two different schemes can be adopted. The first schemes uses different connector assignments for each user. For the K = 3 coder, 6 possible combinations are available using

Table 5.2: *Switch positions for orthogonal coder (K=3)*

Chip No.	S1	S2	S3
1	a	a	a
2	b	a	a
3	a	b	a
4	b	b	a
5	a	a	b
6	b	a	b
7	a	b	b
8	b	b	b

all connections and thus 6 different coders can be formed. With this scheme the different coders will produce a different Walsh code for the same set of input data bits. However, the different coders may produce the same Walsh code for different sets of input data bits. For these instances the users signals will not distinguishable. To reduce the probability of this event, this scheme can be modified by multiplying the output of each coder by a spreading code of the same rate.

In the second scheme every user has the same connector assignment and the output of the coder is multiplied by a separate spreading sequence at the same rate for each user. The performance of these schemes will now be investigated.

The BER performance of these different schemes is seen in Figure 5.30. The worst multi-access performance is obtained if each user has a different coder. (This is obtained by each user having a different connection in the connector assignment block.)

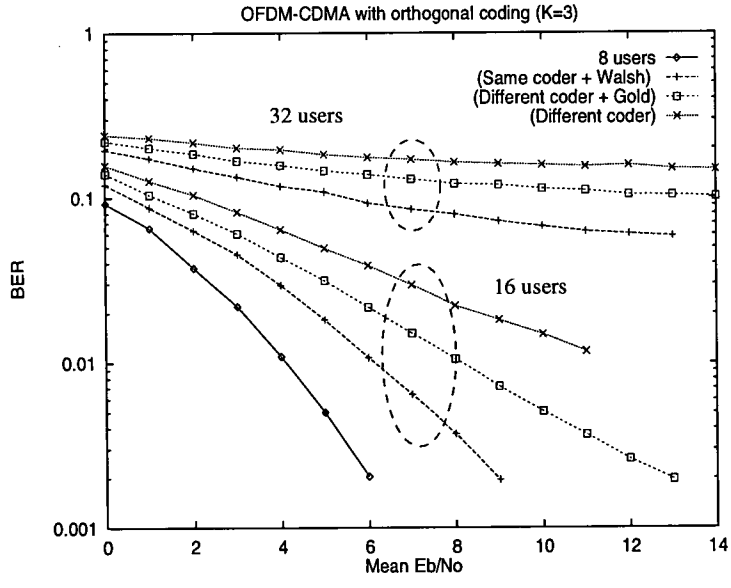

Figure 5.30: BER performance for orthogonal coder (K = 3) in multipath

An improvement on this can be made if the output of every coder for each user is multiplied by an extended (length 8) Gold code. The best performance however is obtained if each user has the same

coder and the output of the coder is multiplied by a unique length 8 Walsh code. With this arrangement a BER of 2×10^{-3} can be maintained for 16 users at a E_b/N_0 of 9 dB.

5.4.4.4 Super orthogonal convolutional coding

The super orthogonal coder [64] is shown in Figure 5.31. This is an extension of the orthogonal coder in which the relationship between the code rate and the constraint length is given by $R_c = 1/2^{K-2}$. Therefore for a given code rate R_c a larger constraint length K can be used compared to the orthogonal coder, improving error correction. Figure 5.31 shows a $K = 5$, $R_c = 1/8$ coder.

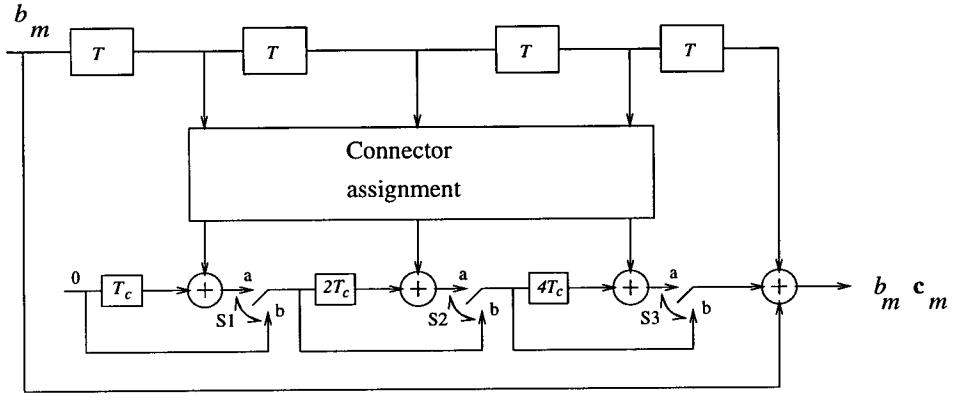

Figure 5.31: Super orthogonal coder ($K = 5$)

Multiple access performance is obtained in the same way as the orthogonal coder. Both enhanced multiple access schemes were investigated. The first method uses a different coder for every user whose output is multiplied by an unique extended (length 8) Gold code. The second method uses the same coder for every user whose output is multiplied by a unique length 8 Walsh code. For the super orthogonal coder there was found to be no difference in BER performance between these two schemes.

The BER performance of the second scheme is shown in Figure 5.32. By examining Figure 5.32 it can be seen that a BER of 2×10^{-3} can be achieved for 16 users at a E_b/N_0 of 6 dB. This is 3 dB lower than the orthogonal coder.

The spectral efficiencies of the two different orthogonal coding schemes are shown in Figure 5.33 for a BER of 2×10^{-3}. It can be seen that the super orthogonal coder achieves a spectral efficiency of 0.2125 bits/s/Hz at 6 dB E_b/N_0. This spectral efficiency is not very high when compared to the high spectral efficiency achieved by the punctured convolutional code. The super orthogonal coder however achieves coding with no bandwidth expansion or necessary reduction in data rate for a given bandwidth.

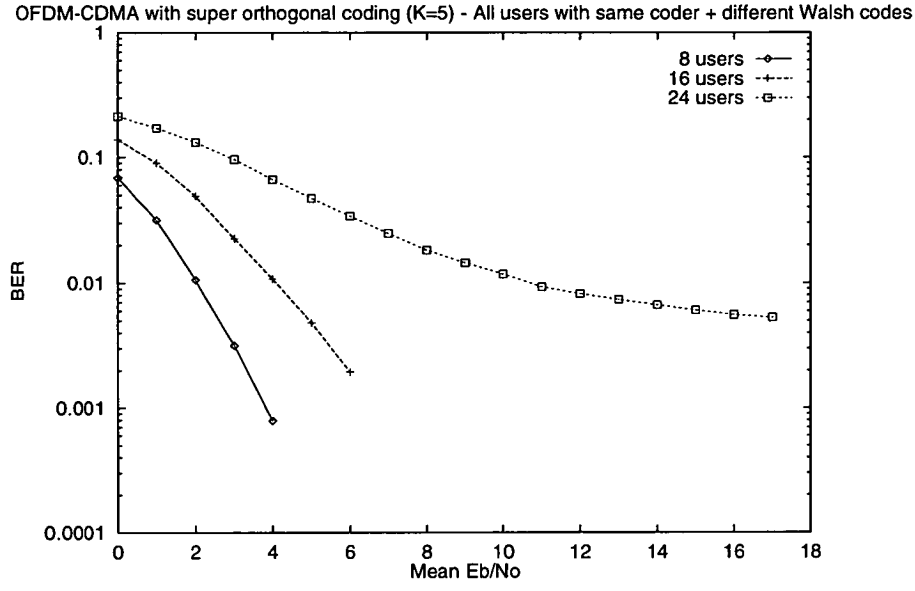

Figure 5.32: BER performance for super orthogonal coder ($K = 5$) in multipath

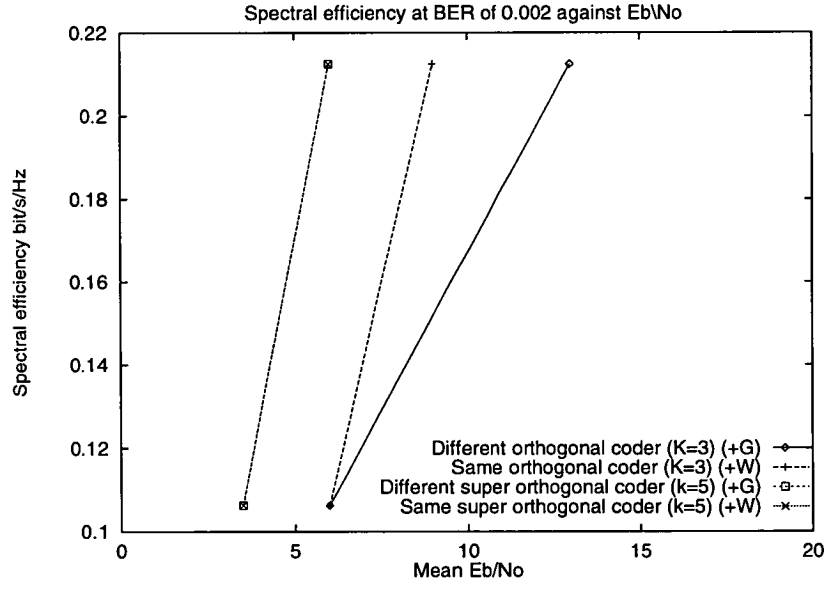

Figure 5.33: Spectral efficiency for the orthogonal and super orthogonal coder

5.4.5 Summary

In this section we have examined the BER and spectral efficiency performance of different channel coding schemes for the OFDM-CDMA system with EGC. The 1/2 rate convolutional coding scheme has the best BER performance enabling a BER of 2×10^{-3} to be supported for 64 users at 6 dB E_b/N_0. Due to its bandwidth expansion however the maximum spectral efficiency achievable is 0.425 bits/s/Hz. The 3/4 rate punctured convolutional coding scheme requires 19 dB E_b/N_0 to support a BER of 2×10^{-3} for 64 users. It can however achieve a spectral efficiency of 0.65 bits/s/Hz due to its lower bandwidth expansion.

In theory the orthogonal coding scheme could achieve a high spectral efficiency but its BER performance is very poor. This is primarily due to the lack of orthogonality between the sequences generated from any two coders. The orthogonality is improved slightly by multiplying the output of the each coder by another unique Walsh code.

We conclude that the best spectral efficiency performance is achieved by using a higher rate code. A non-punctured high rate code would have better BER and spectral efficiency performance but with increased decoding complexity. This conclusion is also valid when the OFDM-CDMA system is used with other detection schemes because the other schemes (MLD, MMSE etc.) have higher performance.

5.5 Combination of channel coding and different detection techniques

5.5.1 MLD with punctured convolutional coding (PCC)

MLD with punctured convolutional coding (PCC) has already been investigated by Fazel [39] and Kaiser [40]. We will examine it here so that its performance can be compared to other combinations of coding and detection schemes which will be described later in this section. As already described in section 5.4.2, to provide a soft output from the MLD detector, the log-likelihood function is applied on the MLD output. An approximation of the log-likelihood function for this OFDM-CDMA system to the MLD is given by Fazel [39]

$$L(j) = \frac{1}{\sigma^2}\min(\Delta_j^i)v_j \tag{5.17}$$

where v_j is the soft output from the MLD despreader operation and σ depends on the SNR. Δ_j^i is the difference in Euclidian distance between the ith possible transmitted sequence and the chosen ML sequence if the sequences make an error. Simulation results of the MLD detection scheme using the log likelihood detection approximation given in equation (5.17) and a 3/4 rate ($K = 7$) punctured convolutional code are shown in Figure 5.34.

These results assume the receiver has perfect knowledge of the SNR. As can be seen from Figure 5.34 a BER of 2×10^{-3} can be supported for 64 users at 7.75 dB E_b/N_0. This compares to 19 dB E_b/N_0 for

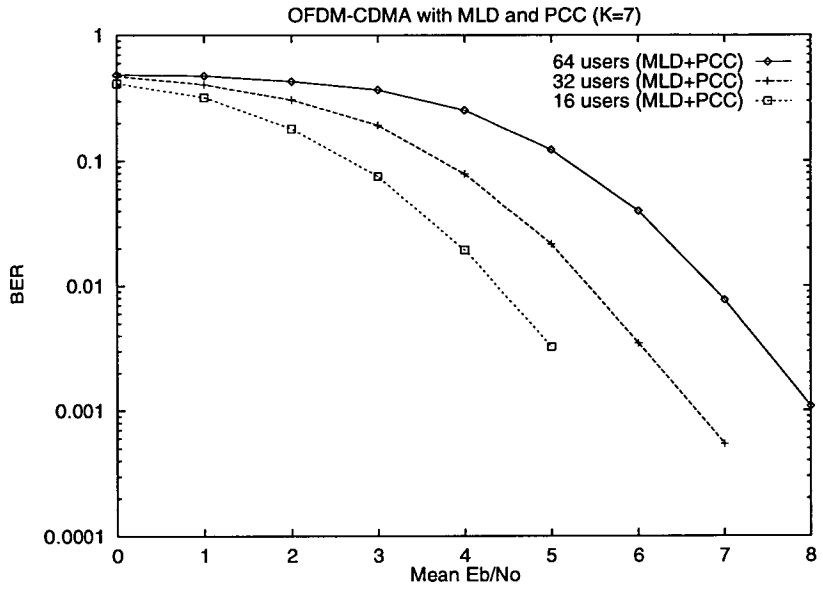

Figure 5.34: BER results for MLD receiver with punctured convolutional coding (PCC)

the combination of EGC with punctured convolutional coding (see Figure 5.27). These results assume an uncoded data rate of 16 kbits/s.

5.5.2 Interference cancellation with convolutional coding

In this section we investigate the performance of an OFDM-CDMA receiver in which an interference canceller (IC) is used at the receiver with EGC. The interference estimates made by the canceller are improved by Viterbi decoding before being subtracted from a delayed version of the received signal. This is a new approach for OFDM-CDMA. The coding schemes we consider in conjunction with this canceller are ones which have a low bandwidth expansion and so, with a fully loaded system, a high spectral efficiency can be achieved. The coding schemes considered are orthogonal coding and punctured convolutional coding.

The combined channel decoder and interference canceller is shown in Figure 5.35. This part of the receiver replaces the two rightmost blocks of Figure 5.3. After each of the active users signals are despread, channel decoding is performed which enables a better estimate of the sent data for each user to be obtained. The estimated data bits are then re-encoded and respread to form the interference estimates. These estimates are then subtracted from the received signal. The resulting signal is then despread and decoded before a sign decision is made. This receiver therefore requires knowledge of the number of active users and the channel. It does not however require knowledge of the signal to noise ratio unlike the combination of MLD with channel coding (see section 5.5.1).

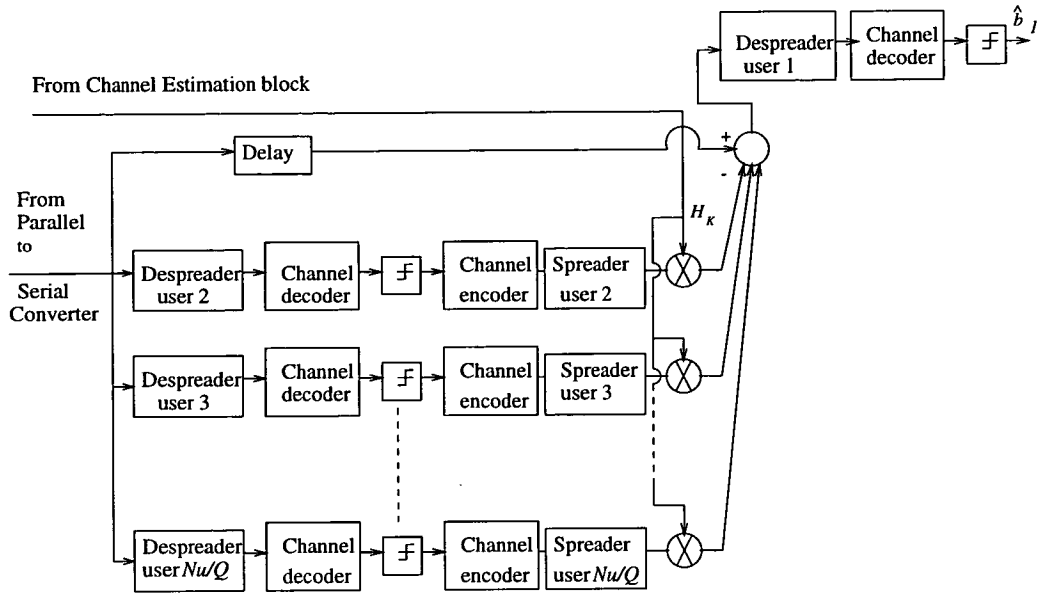

Figure 5.35: Receiver with convolutional decoding and interference cancellation

5.5.2.1 Interference cancellation with punctured convolutional coding

The BER performance of the OFDM-CDMA system with punctured convolutional coding is shown in Figure 5.36. The BER performance with and without cancellation is shown. It can be seen that for a fully loaded system of 64 users a BER of 2×10^{-3} can be achieved at 9 dB E_b/N_0 which is a gain of 10 dB over no cancellation. The spectral efficiency of the system is shown in Figure 5.37 which also shows the the spectral efficiency of EGC with punctured convolutional coding and MLD with punctured convolutional coding.

It can be seen that the MLD with punctured convolutional coding has a similar spectral efficiency performance to IC with coding. For the case of 32 users (0.325 bits/s/Hz), IC with coding requires a lower E_b/N_0 than MLD with coding. For the case of 64 users (0.65 bits/s/Hz) the situation is reversed. If the large processing delays of IC with coding can be tolerated, this technique offers an alternative to MLD with coding.

5.5.3 Interference cancellation with orthogonal convolutional coding

The BER performance of orthogonal coding and super orthogonal coding with and without cancellation are shown in Figures 5.38 and 5.39 respectively. For the orthogonal coder we have chosen a $K = 3$ coder whose output is multiplied by a user specific Walsh code of length 8. Every user has a separate Walsh code. The super orthogonal coder uses a $K = 5$ coder whose output is again multiplied by a unique Walsh code of length 8.

By examining Figure 5.38 it can be seen that the orthogonal coder with cancellation can support a BER

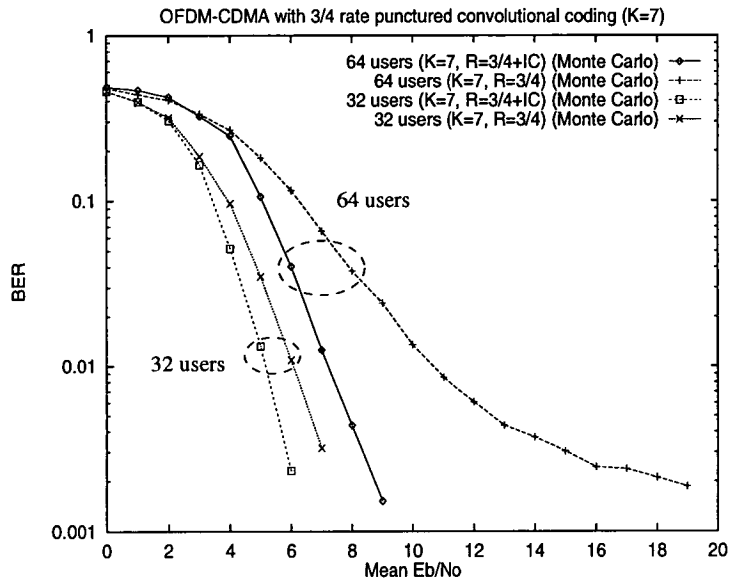

Figure 5.36: BER results for 3/4 rate punctured convolutional coding with interference cancellation

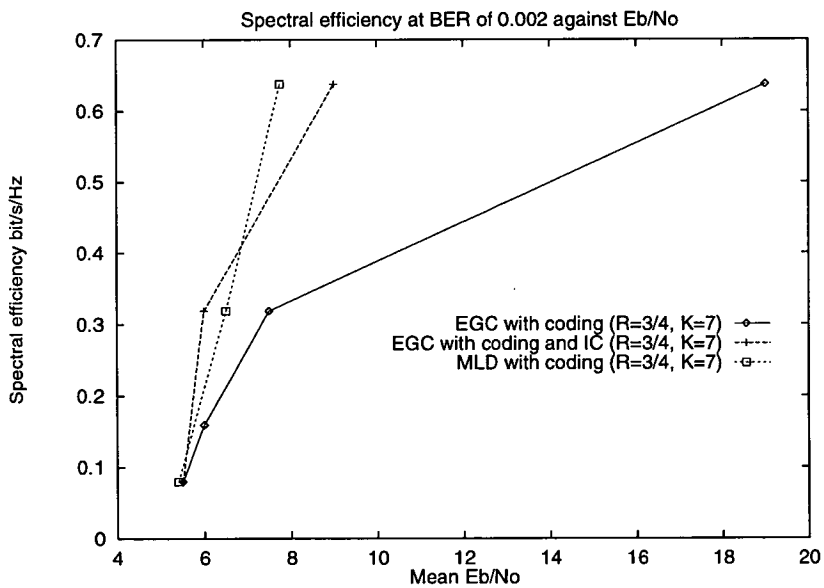

Figure 5.37: Spectral efficiency for 1.3 MHz bandwidth

of 2×10^{-3} for 16 users at 7 dB E_b/N_0. This compares to 9 dB with no cancellation. A smaller improvement is seen for the case of 24 users.

From Figure 5.39 it can be seen that the interference canceller with super orthogonal coding reduces the required E_b/N_0 by 1.5 dB to support 16 users at a BER of 2×10^{-3}. Smaller improvements are seen for the case of 24 users.

The spectral efficiency at a BER of 2×10^{-3} for the OFDM-CDMA system with the orthogonal coding schemes and interference cancellation is shown in Figure 5.40. Also shown in Figure 5.40 are the coding schemes without cancellation, MLD and IC. All systems occupy the same bandwidth and the same data rate of 16 kbits/s. It can be seen that super orthogonal coding offers the possibility to support a spectral efficiency of 0.2125 bits/s/Hz at 6 dB E_b/N_0 which compares to 8 dB E_b/N_0 for MLD. Super orthogonal coding is however unable to support a higher spectral efficiency than 0.2125 bits/s/Hz. With interference cancellation the BER performance of both orthogonal and super orthogonal coding are improved. For the super orthogonal coding with canceller a spectral efficiency of 0.2125 bits/s/Hz is achieved at an E_b/N_0 of 4.75 dB. Despite these improvements neither orthogonal coding scheme with canceller can support a higher spectral efficiency than 0.2125 bits/s/Hz for a BER of 2×10^{-3}.

By referring to Figure 5.37 it can be seen that the improvements achieved by the punctured convolutional code with cancellation are much higher than those by the two orthogonal coding schemes. This is because the signal SNR at the input of the channel decoder inside the canceller is higher for the case of the punctured convolutional coding than for the other two schemes. The additional Walsh code, which is combined with the orthogonal coding schemes to increase performance does not increase the processing gain of the system. It does however improve the multiple access properties.

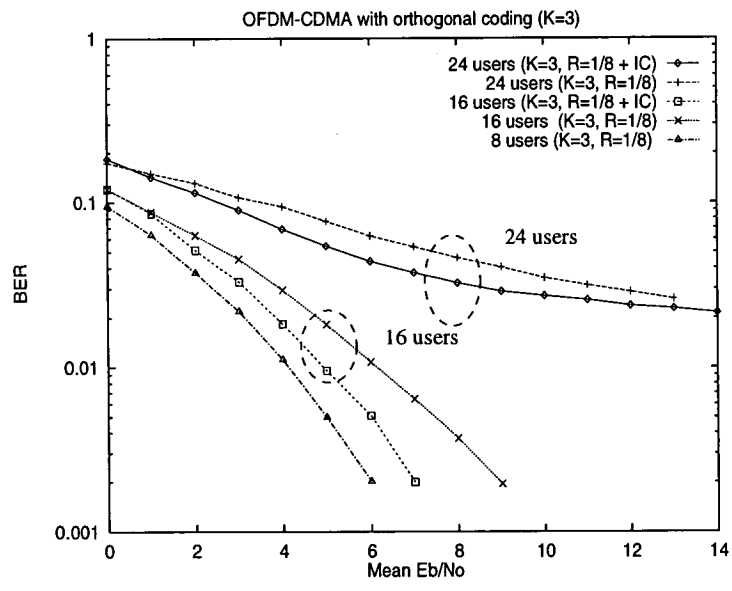

Figure 5.38: BER results for orthogonal convolutional coding with interference cancellation

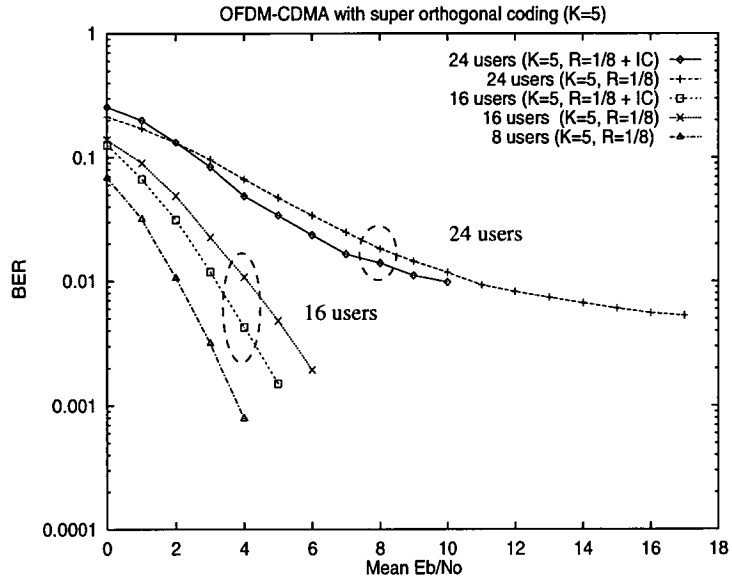

Figure 5.39: BER results for super orthogonal convolutional coding with interference cancellation

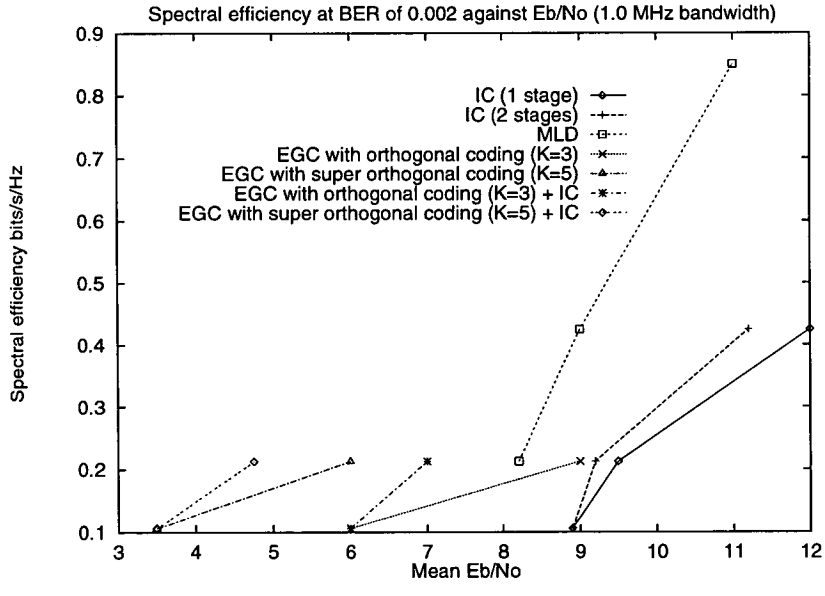

Figure 5.40: Spectral efficiency results for 1 MHz bandwidth

5.6 Chapter summary

In this chapter we have studied the performance of the OFDM-CDMA concept proposed by Fazel. We have in particular studied the performance of the OFDM-CDMA system with 8 sub-systems and length 8 Walsh codes. The system has been studied with and without channel coding.

Without channel coding we have investigated the performance of different detection schemes. We have shown, that if knowledge of the number of users and the channel are available at the receiver, MLD offers the best performance. When only channel information is available the non-optimal MMSE offers the better solution.

The performance of different channel coding schemes were investigated in conjunction with EGC. EGC was chosen as it provides a soft input to the soft decision Viterbi decoder without requiring knowledge of the SNR. The performance of four different channel coding schemes were investigated. These were 1/2 rate convolutional coding, 3/4 rate punctured convolutional coding, orthogonal coding and super orthogonal coding.

The OFDM-CDMA system with EGC and 1/2 rate (K = 7) convolutional coding enables a BER of 2×10^{-3} to be supported for 64 users (each users transmitting 16 kbits/s) at 6 dB E_b/N_0 however, the maximal spectral efficiency achievable is however only 0.425 bits/s/Hz. To achieve higher spectral efficiencies channel coding schemes with lower bandwidth expansions were investigated, namely higher rate convolutional coding and orthogonal coding.

To reduce the complexity of the Viterbi decoder for higher rate convolutional coding we investigated the performance of punctured convolutional coding. The OFDM-CDMA system with EGC and 3/4 rate punctured convolutional coding enables a BER of 2×10^{-3} to be supported for 64 users at 19 dB E_b/N_0. The maximum spectral efficiency achievable is 0.65 bits/s/Hz at 19 dB E_b/N_0.

The performance of the orthogonal coding and super orthogonal coding schemes were also investigated. The BER performance of both coding schemes were however relatively poor due to the orthogonality of the encoded sequences. The OFDM-CDMA system with EGC and super orthogonal coding enables a BER of 2×10^{-3} to be supported for 16 users at 6 dB E_b/N_0. The spectral efficiency achieved is 0.2125 bits/s/Hz at 6 dB E_b/N_0. The maximum spectral efficiency achievable by the orthogonal coding scheme is worse than the other two schemes. Despite this poor performance the two orthogonal coding schemes do offer a method of channel coding which does not require more bandwidth than an uncoded scheme for the same data rate. Alternatively for a given transmission bandwidth the data rate does not have to be reduced to accommodate coding.

Finally in this chapter we studied the performance of an interference canceller with channel coding. This canceller was investigated in conjunction with punctured convolutional coding, orthogonal coding and super orthogonal coding. The canceller only provided small improvements in BER for the orthogonal and super orthogonal coding schemes. For the punctured convolutional coding scheme a performance advantage of 10 dB is achieved at a BER of 2×10^{-3} compared to a system with no cancellation.

With punctured convolutional coding the performance of the interference canceller was shown to have comparable performance to MLD with punctured convolutional coding. If the large processing delays of IC with coding can be tolerated, IC with coding offers an alternative to MLD with coding. Unlike MLD with coding, IC with coding does not require knowledge of the SNR.

Chapter 6
Synchronisation and channel estimation

6.1 Introduction

In the previous chapters, we assumed the receivers for the MC-CDMA and OFDM-CDMA systems were perfectly synchronised and had perfect knowledge of the channel. The results and discussions made in these chapters are therefore valid on a relative basis. However, the absolute performance values shown in these chapters represent lower bounds on realistic BER performance. It is, therefore, important to investigate algorithms to achieve synchronisation and channel estimation for these multi-carrier CDMA systems.

In this chapter, we investigate in particular the performance of synchronisation and channel estimation algorithms for the OFDM-CDMA system described in Chapter 5. This chapter is split into two sections. Section 6.2 examines methods for achieving synchronisation whereas section 6.3 examines methods to obtain a channel estimate.

6.2 Synchronisation

Synchronisation for an OFDM-CDMA receiver can be split into frequency and timing synchronisation. Frequency synchronisation is necessary to compensate for the frequency offset between the transmitter and receiver. Timing synchronisation is needed to provide the FFT block at the receiver with the useful part of the transmitted symbol. Each of these aspects will be examined.

6.2.1 Frequency synchronisation

One of the disadvantages of a multi-carrier communication system compared to one with a single carrier is the increased BER sensitivity of the system to frequency offsets between the transmitted and received signals. One of the most important functions of the OFDM-CDMA receiver is, therefore, frequency synchronisation.

Frequency synchronisation can be split into two steps acquisition and tracking. Whereas during tracking only small frequency offsets are encountered, the frequency offsets during acquisition are much higher. For this OFDM-CDMA system we shall transfer from acquisition to tracking when the acquisition

scheme has identified the frequency offset to within an FFT bin. (For this OFDM-CDMA system a FFT bin is 2 kHz wide.) Tracking will then reduce the frequency offset still further. To establish if tracking is necessary, we shall first investigate the sensitivity of the OFDM-CDMA system to frequency offsets.

6.2.1.1 Frequency offset sensitivity

The frequency offset between the transmitted and received signal may be caused, by the Doppler effect or alternatively it may arise from the drift [1] of the reference source [2] (for a mobile terminal this is typically a quartz crystal) which is used for the local oscillator at the receiver. The OFDM-CDMA system we shall investigate is the same as that described in section 5.2. In this system a 512 point IFFT is used at the transmitter and a 512 point FFT is used at the receiver. A cyclically extended guard interval is used at the transmitter and each carrier transmits data at a rate of 2 kbits/s. We shall investigate the sensitivity of the system in a Gaussian channel and an 8-path channel. (The 8-path channel is described in section 5.2.1.) For the case of the multipath channel we shall assume the receiver has perfect knowledge of the channel. Due to the presence of the frequency offset and the method by which the channel estimates are traditionally obtained (see section 6.3), the BER results for the multipath channel are a little optimistic.

BER results for the Gaussian channel and the 8-path channel are shown in Figures 6.1. As can be seen

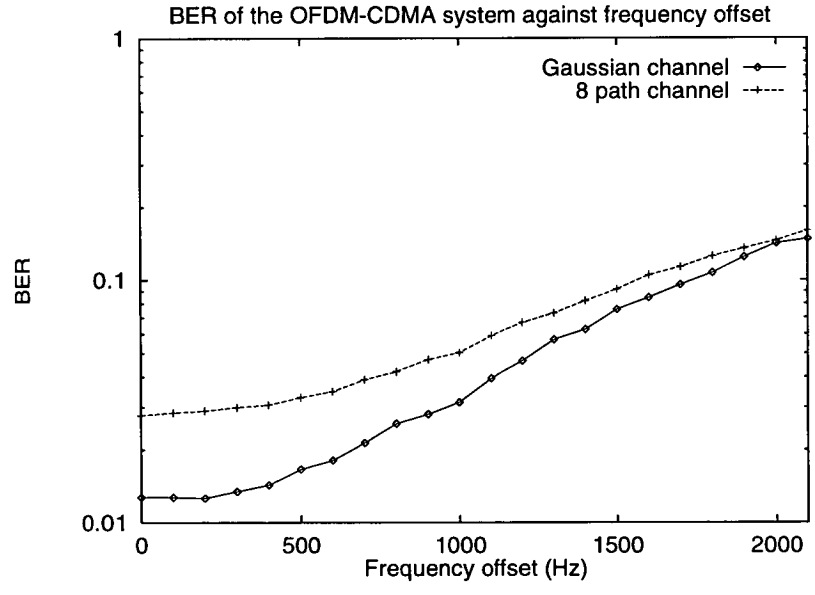

Figure 6.1: *BER against frequency offset for the OFDM-CDMA system in a Gaussian channel and the 8 path channel at 4 dB E_b/N_0*

from Figure 6.1 the BER degradation for the Gaussian channel across the frequency offset from 0 to

[1] This problem is combatted in GSM by the use of the frequency correction burst which is sent from the base station to the mobile. The base station contains a highly accurate frequency reference source. In a cellular OFDM-CDMA system this method could also be used.

[2] Typical frequency stability of high quality quartz crystal = ± 10 parts per million (ppm).

2000 Hz is approximately a factor of ten. However, the BER degradation for the 8-path channel over the same frequency range is only approximately a factor of five. This is mainly due to the inherent diversity in the system.

The frequency range shown in Figure 6.1 is over 2 kHz and therefore illustrates the BER degradation which will occur if tracking is not performed after acquisition. We can conclude from these results that if high performance is to be maintained a tracking algorithm is required to correct for frequency offsets less than one FFT. Before investigating methods for tracking we shall examine methods for frequency acquisition.

6.2.1.2 Frequency acquisition

A typical OFDM frame structure is shown in Figure 6.2. In this frame structure there are three kinds of transmitted symbol: a null period, a pilot period and a data period. In the null period which is used to identify the start of the frame, no symbols are transmitted. In the pilot period no useful data symbols are transmitted. The data period contains data and pilot symbols.

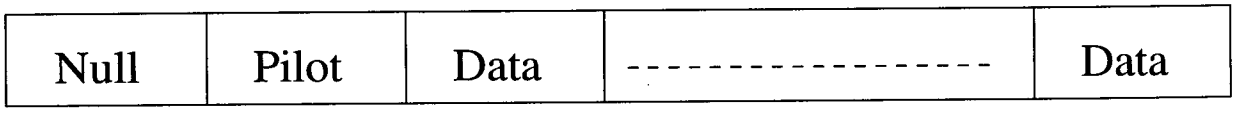

Figure 6.2: Transmission frame structure from Nogami [65]

In the data portion of the frame there are various ways of inserting these pilot tones into the OFDM multiplex [66]. In a practical OFDM system [19] different kinds of pilot tones are used. We shall consider the simple pilot tone arrangements shown in Figures 6.3 and 6.4. Figures 6.3 and 6.4 only show a subset of the 512 carriers to illustrate the pattern of pilot tones and data bits.

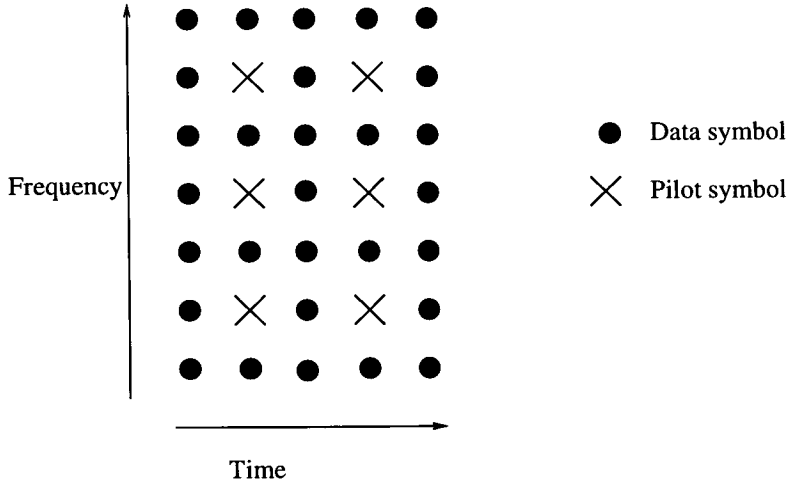

Figure 6.3: Pilot tone arrangement in data portion of frame (18 % overhead)

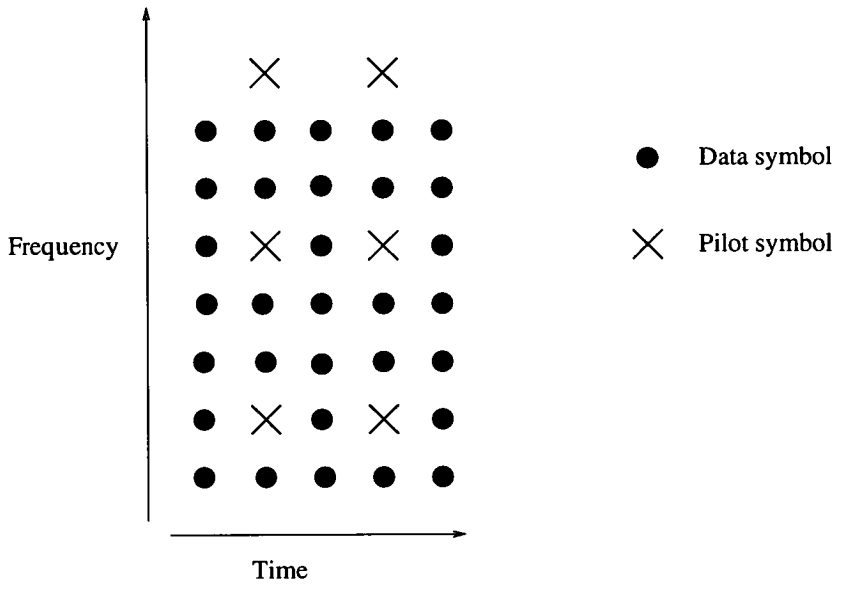

Figure 6.4: Pilot tone arrangement in data portion of frame (13 % overhead)

For large frequency offsets (greater than one FFT bin) these pilot tones are shifted in frequency (see Figure 6.5). The shift of the pilot tones can therefore be measured at the receiver (to an accuracy of one FFT bin) to achieve frequency acquisition.

If, however, the value of these pilot tones are all fixed at +1, it is difficult in the data portion of the frame to obtain an estimate of the frequency offset ($\widehat{f}_{offset}$) because the shifted pilot tones cannot be distinguished from the shifted data bits. For this arrangement, therefore, the estimated frequency offset can only be measured in the pilot portion of the frame and is calculated by averaging the measured frequency offsets (Δf_i) of each pilot tone.

$$\text{frequency offset estimate } \widehat{f}_{offset} = \frac{\sum_{i=1}^{L_f} \Delta f_i}{L_f} \tag{6.1}$$

where L_f is the total number of pilot tones in the frequency domain.

Figure 6.6 shows the estimated frequency offset against the actual frequency offset in a Gaussian channel using conventional pilot tones (all pilot tones fixed at +1) spaced 16 carriers apart. The frequency offset was calculated using equation 6.1. The results shown are only obtained from one symbol. (More accurate results can be obtained by averaging over several frames assuming the frequency offset does not change in this time.) As can be seen from Figure 6.6 at E_b/N_0 values less than 20 dB these estimates are subject to large errors. To improve this the number of pilots could be increased in the frequency domain, but this would decrease the range of acquisition.

To improve this technique the pilot tones can be modulated by a PN-sequence. This method has been adopted by the Digital Broadcasting standard ETSI 300 744 [19] and has also been suggested by Nogami

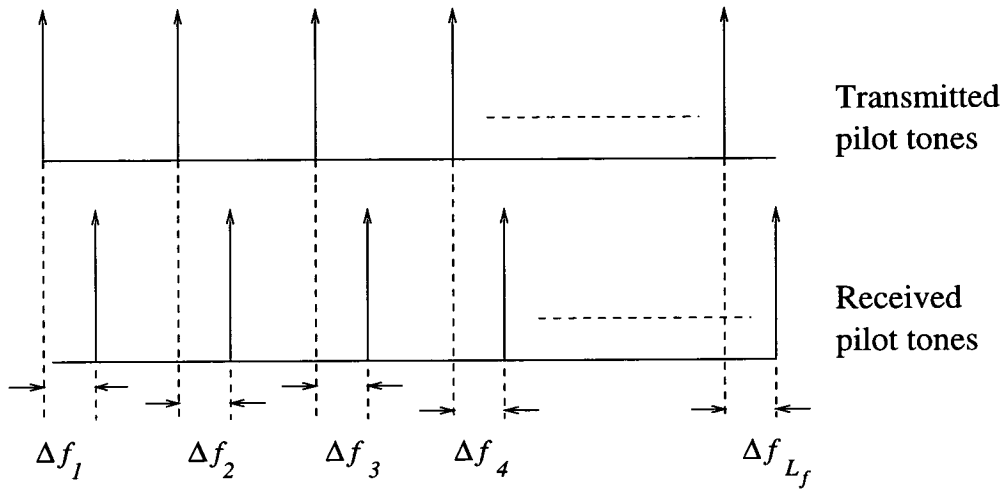

Figure 6.5: Frequency shifted pilot tones

[65]. This scheme has several advantages over using conventional pilot tones:

1) The frequency offset between the receiver and the transmitter can be identified in the data portion of the frame by using a sliding correlator at the receiver.

2) The range of frequency acquisition is increased. (If the value of the pilot tones are all fixed at +1, the frequency range of acquisition is limited to the frequency spacing between the tones.)

3) The frequency offset is easier to identify in high noise/deep fade situations due to the processing gain achieved by the PN code.

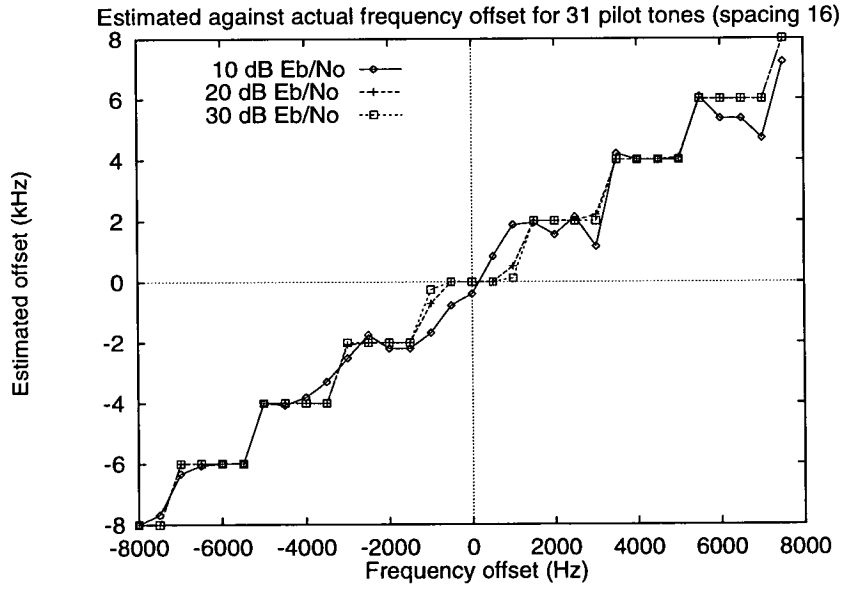

Figure 6.6: Estimated against actual frequency offset for 31 pilot tones spaced 16 carriers apart

Figure 6.7 shows the estimated frequency offset for the same 31 tones when they are modulated by a length 31 m-sequence (generator polynomial = 45 in octal notation). The results are, again, only obtained from one symbol. As can be seen from Figure 6.7 at 10 dB E_b/N_0 the estimates are better than those shown in Figure 6.6 for 10 dB E_b/N_0. The large error at +14 kHz in Figure 6.7 for 0 dB and 5 dB is due to the cyclic nature of the frequency estimator. Figure 6.8 shows the same results as Figure 6.6 but the frequency step for the simulation is set to 500 Hz. It can be seen that the errors made at low E_b/N_0 mainly occur when the offset frequency is between the FFT bins.

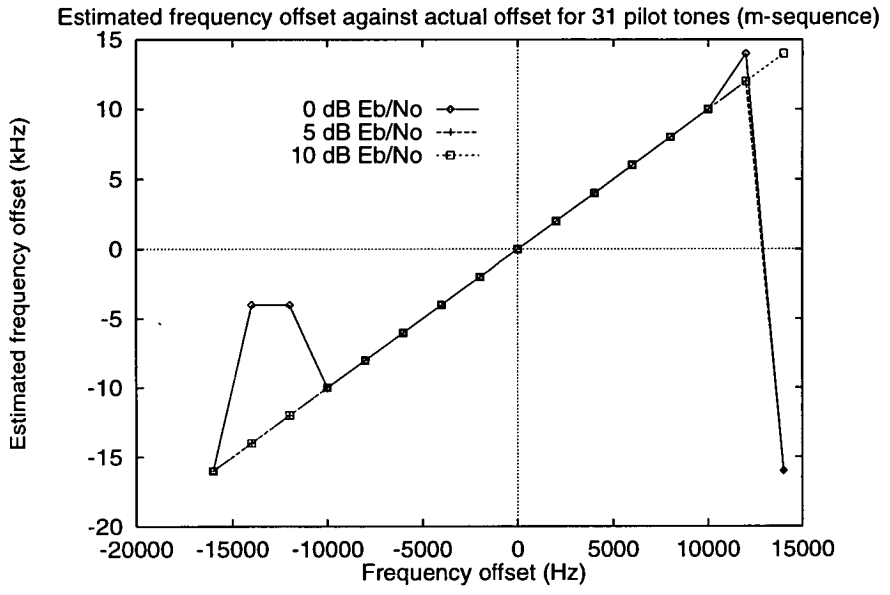

Figure 6.7: *Estimated against actual frequency offset for 31 pilots modulated by length 31 m-sequence (frequency step 2kHz)*

The results presented in Figures 6.6, 6.7 and 6.8 all show the frequency estimates from a single one shot simulation. Although they illustrate the acquisition range of the different frequency estimators, they are not good indicators of accuracy. A better measure of accuracy is the frequency estimation variance σ_f^2, given by

$$\sigma_f^2 = E\left[(\widehat{f}_{offset} - E[\widehat{f}_{offset}])^2\right] \tag{6.2}$$

Figure 6.9 shows the frequency estimation variance against E_b/N_0 for the frequency detector formed by the 31 pilot tones all fixed at amplitude 1 and the 31 pilot tones modulated by the length 31 m-sequence. The frequency offset was set to 5000 Hz. The frequency estimation variance was measured over 10000 runs for every value of E_b/N_0. As can be seen from Figure 6.9 an estimation variance of 1×10^{-5} can be obtained by the 31 pilot tones modulated by the m-sequence. This compares with the fixed amplitude 31 pilot tones which require greater than 25 dB E_b/N_0 to achieve the same estimation variance.

In the above a length 31 m-sequence was chosen to modulate the pilot tones so a comparison could be made between the 31 pilot tones fixed at +1 and the 31 pilot tones modulated by the m-sequence. For

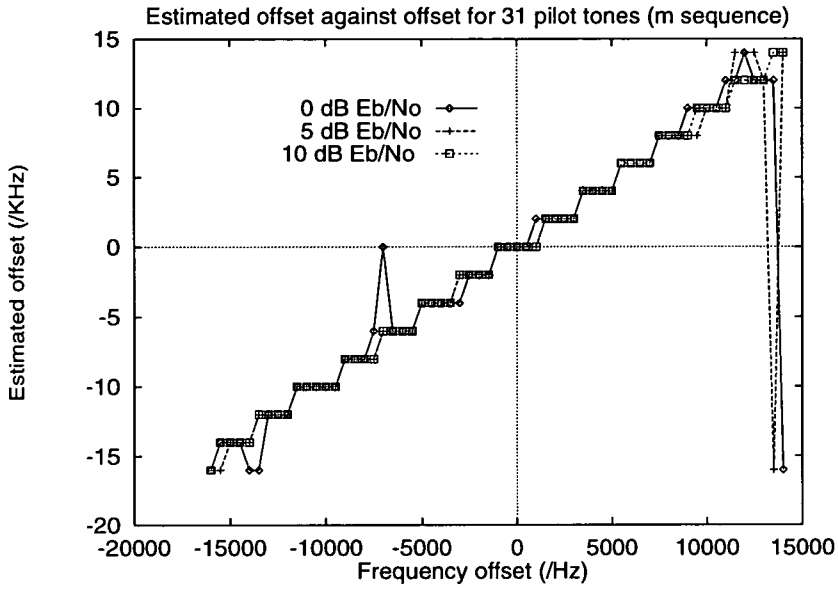

Figure 6.8: *Estimated against actual frequency offset for 31 pilots modulated by length 31 m-sequence (frequency step 500 Hz)*

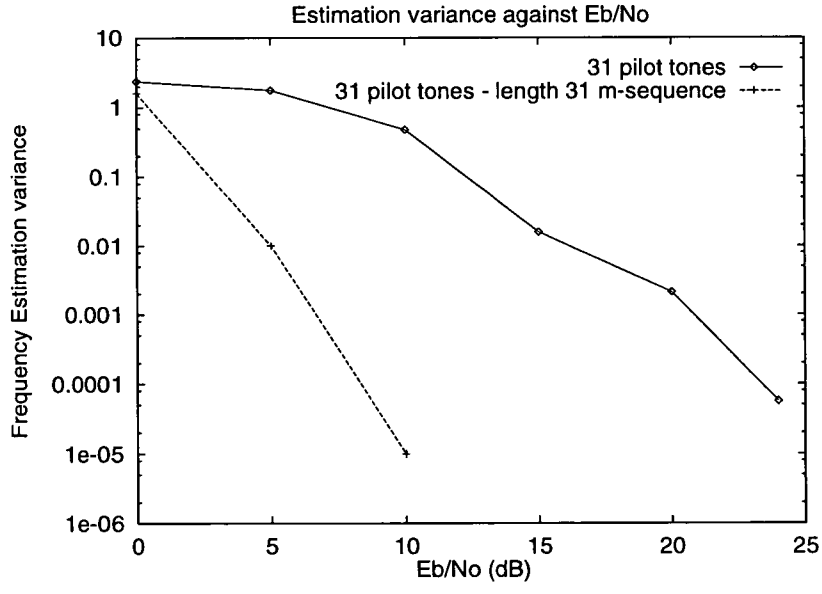

Figure 6.9: Frequency estimation variance against E_b/N_0

the pilot tone arrangement shown in Figure 6.3 for which there are 255 pilot tones for the 512 carriers a length 255 m-sequence (generator polynomial = 435 in octal notation) could be used for increased performance.

6.2.1.3 Frequency tracking

In this section we shall describe two methods which have been proposed for tracking and present results for one of them.

The first method described by Daffara and Adami [67] uses the fact that samples in the useful part of the transmitted symbol are repeated in the cyclically extended guard interval. To explain this, it is possible to represent samples of the received signals, $x(t)$, before the FFT by x_n $(-N_g \leq n \leq ML-1)$. The first N_g samples of the block $(-N_g \leq n \leq -1)$ belong to the guard interval, while the other samples $(0 \leq n \leq ML-1)$ represent the useful part of the symbol. When there is no frequency offset the product $x_{ML-i}x^*_{-i}$ $(i = 1, 2, \ldots, N_g)$ is a real number. However, in the presence of a frequency error the two samples are affected by a different rotation and the imaginary part of the symbol contains information about the frequency offset. By averaging over L_{error} samples the error signal E may be obtained,

$$E = \frac{1}{L_{error}} \sum_{i=1}^{L_{error}} \mathrm{Im}\left[x_{ML-i}x^*_{-i}\right] \quad 1 \leq L_{error} \leq N_g \tag{6.3}$$

In the system described by Daffara and Adami, the error signal E is the output of the frequency detector for a frequency recovery loop. If only a frequency estimate is required, equation 6.3 can be modified to obtain the frequency estimate $\widehat{f}_{offset}$

$$\widehat{f}_{offset} = \frac{1}{2\pi T_u L_{error}} \sum_{i=1}^{L_{error}} \arg\left[x_{ML-i}x^*_{-i}\right] \quad 1 \leq L_{error} \leq N_g \tag{6.4}$$

where T_u is the time duration of the useful part of the symbol which consists of ML samples and arg is the argument of the complex number. The main drawback of this technique is that the cyclically extended guard interval is subject to ISI. To improve the performance of this technique in multipath, it has been suggested by Daffara and Adami to only perform averaging on the last part of the guard interval ($L_{error} < N_g$). This part of the guard interval is not subject to ISI if the guard interval is longer than the delay spread.

Figure 6.10 shows the value of E for the OFDM-CDMA system as described in Chapter 5 (with the length 18 guard interval) against frequency with no added AWGN. As can be seen, the output is very distorted as only 18 samples have been used to form E. Figure 6.11 shows the value of the E against frequency for the same OFDM-CDMA system with a length 64 guard interval. Here in Figure 6.11 the

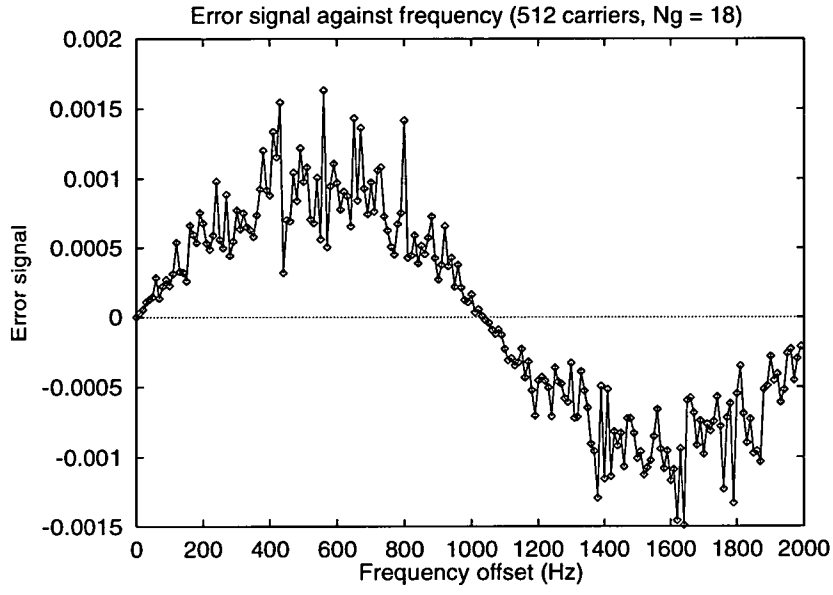

Figure 6.10: Error signal E against frequency for system with length 18 guard interval

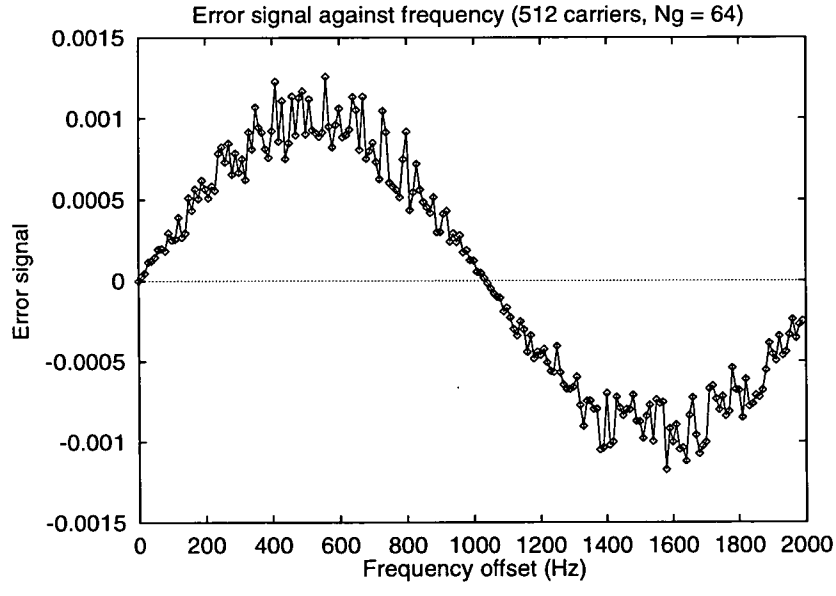

Figure 6.11: Error signal E against frequency for system with length 64 guard interval

value of E is less distorted compared to Figure 6.10 due to the increased number of samples. Both these waveforms will, however, degrade in the presence of noise and multipath.

An alternative tracking strategy, and one which is perhaps more robust to the effects of ISI, has been suggested by Classen and Meyr [68, 69]. In this scheme, the phase change between two subsequent sub-channel samples (after the FFT and de-interleaver) are examined. It is possible to represent the received signal after the FFT and de-interleaver for bit l as a vector $\mathbf{r_l}$. The vector $\mathbf{r_l}$ has 512 elements $r_1(l) \ldots r_{512}(l)$ corresponding to the 512 sub-carriers. Two subsequent sub-channel samples can therefore be represented by $r_n(l)$ and $r_n(l+1)$. These sub-channel samples are chosen to be in the same position as the pilot tones so the effect of data modulation can be removed. This phase change estimate can be averaged over all the pilot tones in the frequency domain to form an improved estimate.

The frequency estimate $\widehat{f}_{offset}$ is given by

$$\widehat{f}_{offset} = \frac{1}{2\pi T_{sym} S_{pilots} L_f} \arg\left(\sum_{j=0}^{L_f-1} (r_{p(j)}(l + S_{pilots}) r_{p(j)}(l)^*)(t_j(0)^* t_j(1)) \right) \tag{6.5}$$

where T_{sym} is the time duration of the data symbol (useful part and guard interval) and S_{pilots} is an integer representing the number of data symbols between pilot symbols. L_f is the number of pilot tones in the frequency domain. The function $p(j)$ gives the position of the jth sub-channel which carries one of the L_f pilot tones. $t_j(0)$ is the pilot tone transmitted on carrier j and $t_j(1)$ is the pilot tone transmitted on the same carrier but at the $(l + S_{pilots})$th time periods.

6.2.2 Timing acquisition

Timing acquisition is needed to enable the correct part of the received signal to be processed by the FFT. For this function, we shall investigate the performance of two types of correlators. There appears to be no open literature on these methods for timing acquisition. These correlators operate by virtue of the fact that the data in the useful part of the symbol is repeated in the guard interval to cyclically extend the symbol.

6.2.2.1 Linear correlator

The linear correlator is seen in Figure 6.12. The received samples in the useful part of the symbol are multiplied by the received samples delayed by T_u seconds where T_u is the time duration of the useful part of the symbol.

By adopting the same notation as in section 6.2.1.3 the received signal (before the FFT) $x(t)$ can be sampled to give x_n $(-N_g \leq n \leq ML-1)$. The first N_g samples of the block $(-N_g \leq n \leq -1)$ belong to the guard interval, while the other samples $(0 \leq n \leq ML-1)$ represent the useful part of the

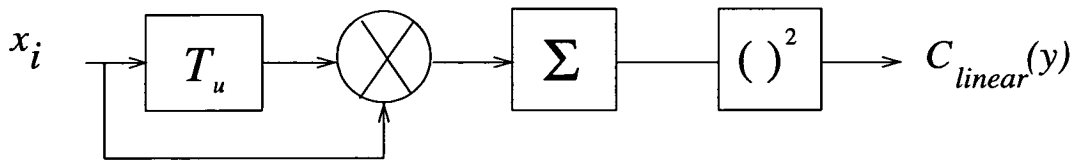

Figure 6.12: Linear correlator

symbol. By examining Figure 6.12 it can be seen that a total number of N_g multiplications are made. In this way, a correlation peak is observed when the timing is such that the first sample is taken at the end of the useful part of symbol.

Denoting the first sample by

$$x_i = a_i + iz_i \tag{6.6}$$

and the delayed sample by

$$x_{i-ML} = a_{i-ML} + iz_{i-ML} \tag{6.7}$$

Then the real part is

$$R_i = a_i a_{i-ML} - z_i z_{i-ML} \tag{6.8}$$

and the imaginary part is

$$I_i = z_i a_{i-ML} + a_i z_{i-ML} \tag{6.9}$$

A total number of N_g samples are summed forming the linear correlator function $C_{linear}(y)$

$$C_{linear}(y) = \sqrt{\left(\left(\sum_{i=y}^{i=y+N_g} R_i\right)^2 + \left(\sum_{i=y}^{i=y+N_g} I_i\right)^2\right)} \tag{6.10}$$

Figure 6.13 shows the plot of the linear correlator function $C_{linear}(y)$ against y the timing offset for the OFDM-CDMA system with the length 18 guard interval. Probability of detection results for the OFDM-CDMA system with a guard interval length of 18 are shown in Figure 6.14 for different levels of normalised thresholds against output E_b/N_0. The threshold level is normalised to the maximum value of the linear correlator function. By examining Figure 6.13 it can be seen that the maximum value is 0.02. It can be seen that at high threshold values the probability of detection increases very rapidly with increasing E_b/N_0. A detection probability of 0.9 can be obtained at an output E_b/N_0 of 13 dB for a normalised threshold value of 1. The probability of false alarm for the linear correlator is determined by the bandwidth of the baseband receiver filter.

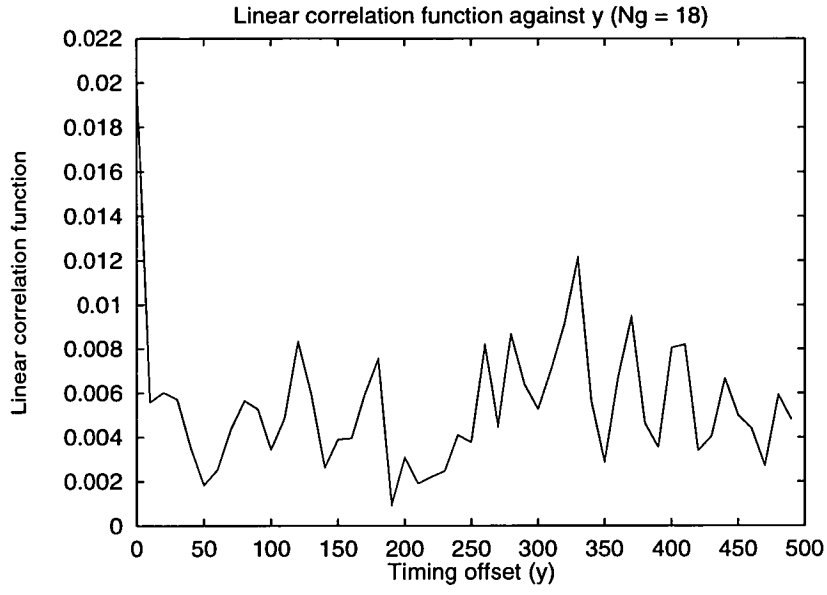

Figure 6.13: Correlation against timing offset for linear correlator

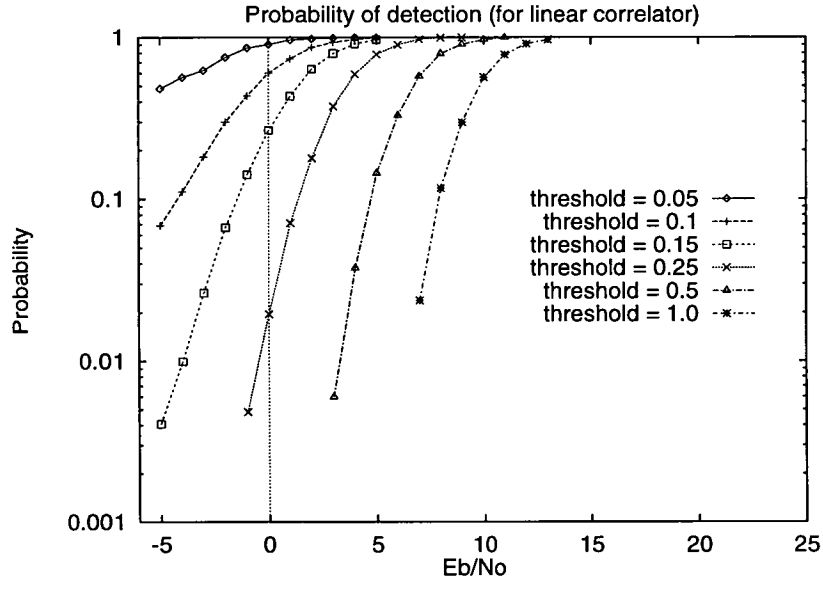

Figure 6.14: *Probability of detection for linear correlator in a Gaussian channel (threshold is normalised to maximum value of linear correlator function.)*

6.2.2.2 Sign-only correlator

The sign only correlator is shown in Figure 6.15. This correlator is similar to the linear correlator except that a sign decision is made on the real (a_i) and imaginary (z_i) parts of the received signal.

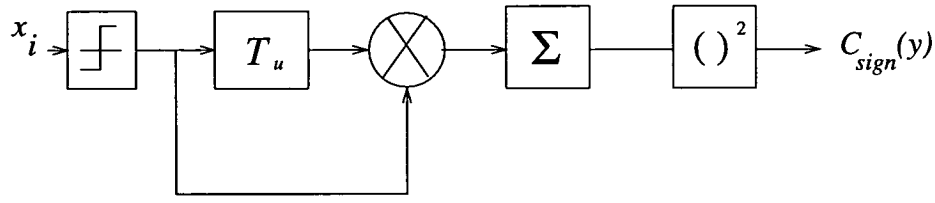

Figure 6.15: Sign only correlator

In this way, implementation complexity is reduced since only binary signals need to be processed after the limiter. The multiplier can be implemented in hardware as a negated version of an exclusive OR gate. The output variable of the correlator is given by $C_{sign}(y)$

$$C_{sign}(y) = \sqrt{\left(\left(\sum_{i=y}^{i=y+N_g} R_{i_{sign}}\right)^2 + \left(\sum_{i=y}^{i=y+N_g} I_{i_{sign}}\right)^2\right)} \tag{6.11}$$

where $R_{i_{sign}}$ is given by

$$R_{i_{sign}} = \text{sgn}(a_i)\text{sgn}(a_{i-ML}) - \text{sgn}(z_i)\text{sgn}(z_{i-ML}) \tag{6.12}$$

and $I_{i_{sign}}$ is given by

$$I_{i_{sign}} = \text{sgn}(z_i)\text{sgn}(a_{i-ML}) + \text{sgn}(a_i)\text{sgn}(z_{i-ML}) \tag{6.13}$$

The maximum value of $C_{sign}(y)$ is, therefore, given by N_g, the guard interval length. Probability of detection results for the OFDM-CDMA system with a guard interval length of 18 are shown in Figure 6.16 against E_b/N_0. The threshold level is normalised to the maximum value of the sign only correlator function. It can be seen that at high normalised threshold levels the detection probability for the sign only correlator does not change as rapidly with E_b/N_0 as the linear correlator (Figure 6.14).

This is because at low values of E_b/N_0 the output of the multiplier in the sign only correlator produces high values since the inputs have been hard limited. This has three effects :

1) At low values of E_b/N_0, the sign only correlator has a higher probability of detection than the linear correlator for a comparative threshold level.

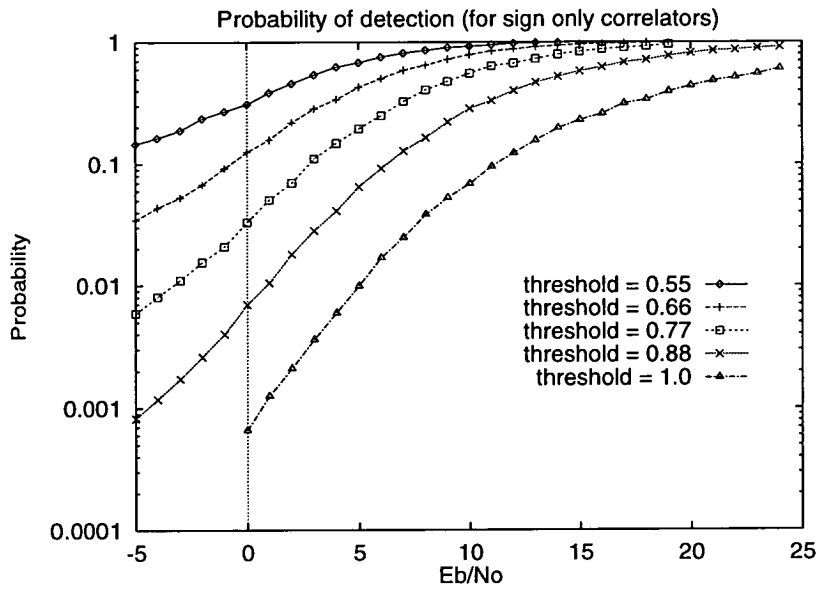

Figure 6.16: *Probability of detection for sign-only correlator (threshold is normalised to maximum value of sign-only correlator function)*

2) To achieve a high probability of detection at high thresholds levels, the sign only correlator requires a higher value of E_b/N_0 than the linear correlator. By examining Figure 6.14, a detection probability of 0.6 can be achieved at a normalised threshold level of 1.0 for the linear correlator at 11 dB E_b/N_0. This compares with the sign only correlator which at a normalised threshold level of 1.0 requires 24 dB to achieve the same detection probability of 0.6 .

3) The sign only correlator has a higher probability of false alarm for the same probability of detection value.

The probability of false alarm for the OFDM-CDMA system with 18 length guard interval (N_g) is shown in Figure 6.17. Both the theoretical probability of false alarm (P_{false}), given by

$$P_{false} = e^{-\frac{threshold^2}{4.N_g}} \tag{6.14}$$

and the Monte Carlo simulation are shown. Equation 6.14 is derived in Appendix C, based on the assumption that the summations of the binomial variables $R_{i_{sign}}$ and $I_{i_{sign}}$ in equation 6.11 form Gaussian variables due to the central limit theorem. It can be seen from Figure 6.17, that the theoretical and Monte Carlo results are in agreement. For a normalised threshold value of 0.88 the theoretical results yield a probability of false alarm of 2×10^{-2}.

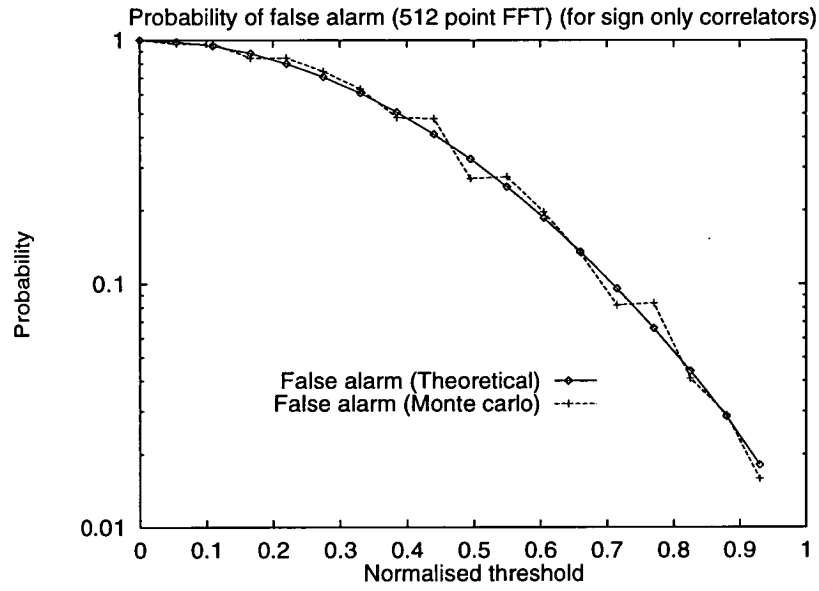

Figure 6.17: Probability of false alarm for sign-only correlator

6.2.3 Synchronisation conclusions

In the previous sections, we have examined the performance of different schemes for synchronisation, tracking and timing. For synchronisation we investigated measuring the shift of the pilot tones in the frequency domain as a frequency offset estimator. To increase the performance, the pilot tones are modulated by a PN sequence. This improves the acquisition range and enables the offset to be measured at a lower E_b/N_0 than fixed amplitude pilot tones. By using a length 31 m-sequence, the received signal can be acquired within a range of +14 kHz to -16kHz. This acquisition range could be improved still further by using a length 255 m-sequence.

By examining the BER degradation for the OFDM-CDMA system in the 8-path fading channel at 4 dB E_b/N_0 we showed that the BER degrades by a factor of 5 for frequency offsets of 2000 Hz (half an FFT bin). It is, therefore, necessary to reduce the frequency offset still further by using tracking after acquisition. Two methods have been described for achieving this. The first method uses a complex correlator and measures the phase change between the samples in the guard interval and the same samples in the useful part of the data bit. The performance of this method will, however, degrade when the guard interval is short or when the guard interval is subject to ISI. Measuring the phase change between two pilot tones may, therefore, be more robust for this OFDM-CDMA system with the 18 length guard interval. More work should be conducted here in multipath to confirm this result.

The performance of two correlators for timing acquisition was also investigated. The simplest of these correlators, the sign only correlator, achieves a probability of detection of 0.5 with a normalised threshold level of 0.88 at 14 dB E_b/N_0 in a Gaussian channel. This corresponds with a probability of false alarm for the same threshold level of 0.03. Initial results, therefore, are promising, but further simulations should be conducted in a multipath channel.

6.3 Channel estimation

Once the OFDM-CDMA receiver is synchronised and tracking is in progress, the channel must be estimated so the equaliser can operate and the received data bits can be formed. To perform a channel estimate, the received signal transmitted by the pilot tones can be used to form a channel estimate. Several authors have studied channel estimators for OFDM systems. Hoeher [70] has suggested using a 2-dimensional Wiener filter but the computation complexity of this is very high requiring the inverse of a $N \times N$ matrix, where N is the size of the IFFT/FFT. For the OFDM-CDMA system considered here this would require the inverse of a 512×512 matrix. A simpler estimator can formed using the least square (LS) estimator which only requires the inverse of a $N \times N$ diagonal matrix. The performance of the LS estimator, however, has been shown for OFDM systems to suffer from high mean square error [71]. A reduced complexity version of the MMSE channel estimator and an enhanced version of the LS estimator has been studied by Beck et al. [71]. In this section, we shall study the performance of a simple channel estimator suggested by Tomba and Krzymin [72] for the OFDM-CDMA system. This channel estimator is based on the LS estimator. To describe this technique, we shall examine the OFDM-CDMA receiver as shown in Figure 6.18.

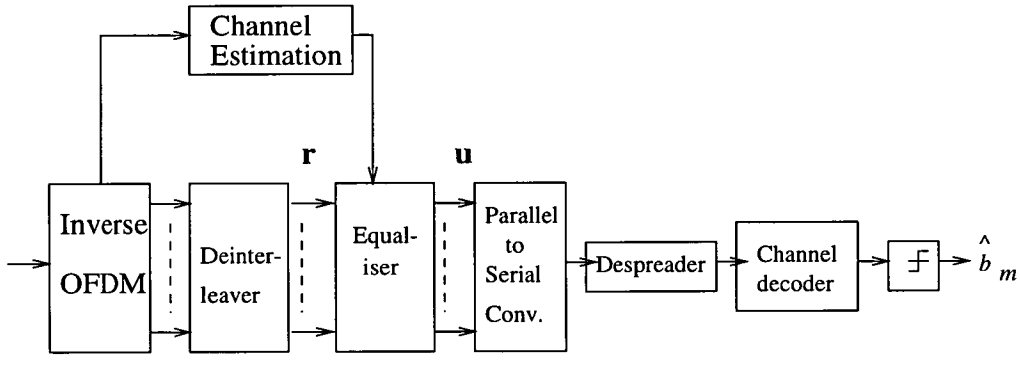

Figure 6.18: OFDM-CDMA receiver

By assuming that the guard interval is longer than the channel dispersion, the received signal for the lth input data block after the FFT and de-interleaver can be written as a vector $\mathbf{r}_l$

$$\mathbf{r}_l = \mathbf{H}.\mathbf{a}_l^T + \mathbf{n}_l \tag{6.15}$$

where $\mathbf{H}$ is a diagonal matrix representing the fading of the sub-carriers, $\mathbf{a}_l^T$ is the transposed transmitted sequence and $\mathbf{n}_l$ is the noise vector. We shall represent the diagonal elements of $\mathbf{H}$ by $h_{1,1} \ldots h_{512,512}$, the elements of vector $\mathbf{a}_l$ by $a_1(l) \ldots a_{512}(l)$ and the elements of vector $\mathbf{r}_l$ by $r_1(l) \ldots r_{512}(l)$. The channel estimate $\widehat{h}_{i,i}$ of $h_{i,i}$ for carrier i can be written as

$$\widehat{h}_{i,i} = \frac{1}{N_A} \sum_{l=1}^{N_A} \frac{r_i(l)}{a_i(l)} \tag{6.16}$$

where $a_i(l)$ has been assumed known and $h_{i,i}$ is assumed constant over N_A data blocks. $\widehat{h}_{i,i}$ is an unbiased estimate of $h_{i,i}$ and the variance of this estimation error is given by $\frac{1}{N_A}\sigma^2_{n,l}$ where $\sigma^2_{n,l}$ is the variance of the noise, $\mathbf{n}$. The position (in time and frequency) and amplitude of the transmitted pilot tones are known (once frequency synchronisation is achieved), and therefore equation 6.16 can be applied on all of the received symbols which correspond to pilot tones. By examining Figure 6.3 it can be seen that the pilot tones are transmitted in a regular pattern. To obtain an estimate for the data symbols between two pilot tones, a linear interpolation in frequency is performed.

Figures 6.19, 6.20 and 6.21 show the BER results for the OFDM-CDMA system with the channel estimators for N_A values of 1, 2 and 3. For each value of N_A, we have studied the performance of the channel estimators for 3 different Doppler rates. By examining Figure 6.19 (N_A = 1), it can be seen that at a BER of 0.1 that the OFDM-CDMA system with the channel estimator requires 19 dB more than a system with perfect channel knowledge. For the three different Doppler rates (50 Hz, 100 Hz and 300 Hz) there are only small differences in performance. This is to be expected as no averaging is performed.

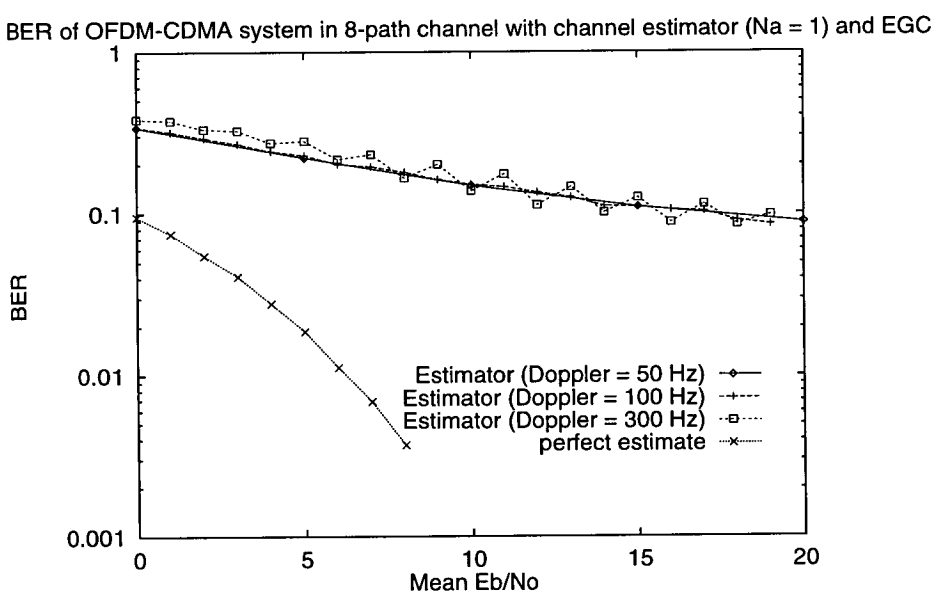

Figure 6.19: BER with EGC with perfect and estimated channel response N_A = 1

Figure 6.20 shows the performance of the channel estimators for N_A = 2. It can be seen that for the case of 50 Hz Doppler and a BER of 0.1 that the OFDM-CDMA system with the channel estimator requires 10 dB more than a system with perfect channel knowledge. (This is 9 dB lower than N_A = 1.) As the Doppler frequency increases the improvement of the N_A = 2 estimator over the N_A = 1 decreases. This is to expected as the channel is no longer stationary over the channel estimation period. For the case of N_A = 2 the channel estimation period is 5 data bits.

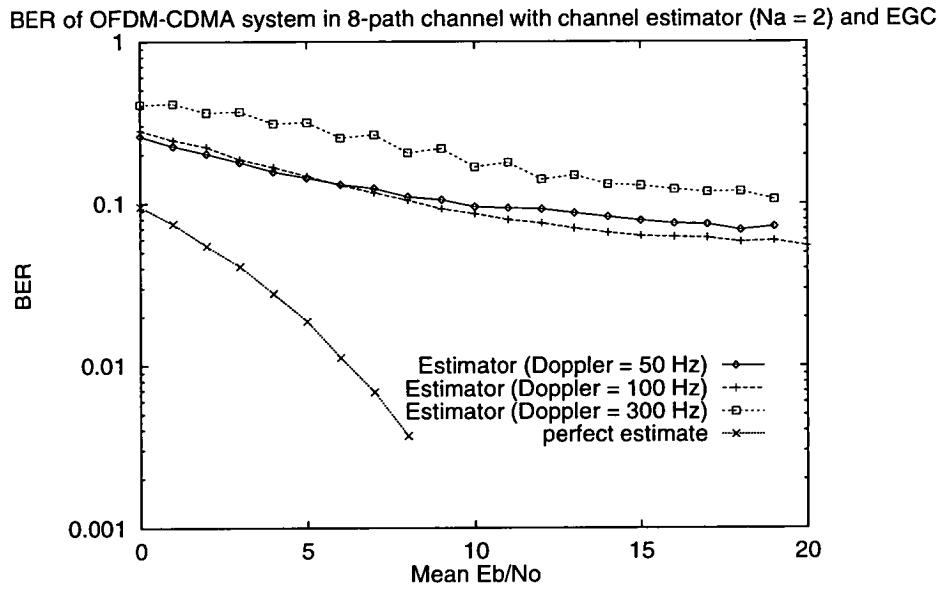

Figure 6.20: BER with EGC with perfect and estimated channel response $N_A = 2$

Figure 6.21 shows the performance of the channel estimator for $N_A = 3$. Similar trends to the results shown in Figures 6.19 and 6.20 are seen in Figure 6.21. It can be seen for the case of 50 Hz, that the channel estimator requires 8 dB more than the system with perfect channel knowledge to support a BER of 0.1. This is 2 dB lower than $N_A = 2$. For 300 Hz Doppler the BER results are considerably worse than $N_A = 2$, this is be expected. There is also an interesting effect at low E_b/N_0 values the results for 50 Hz Doppler have a lower BER than the results for 100 Hz Doppler. However, at high E_b/N_0 values the situation changes and the 100 Hz Doppler yields a lower BER than 50 Hz. The crossover point occurs at 7 dB for $N_A = 2$ and 10 dB for $N_A = 3$. It is unknown at the time of writing the cause of this effect, however at higher values of N_A it is anticipated that the BER results for 50 Hz will be less than 100 Hz for the range of E_b/N_0 values seen in these figures.

It can be concluded, therefore, from this relatively simple channel estimator that when $N_A = 1$, the channel estimates made are very noisy. As N_A is increased the estimation period is lengthened and the variance of the estimates are reduced. To achieve improvements in BER for increased values of N_A it is, however, important that the channel is stationary over the averaging period. This simple channel estimator would have a good performance for low Doppler environments where a high value of N_A could be used. An improved channel estimator could be formed by a Wiener filter in the time domain and linear interpolation in the frequency domain. This is a modification of the 2-dimensional Wiener filter suggested by Hoeher. By using a Wiener filter with delays corresponding to the location of the pilot tones, it would be relativity simple to calculate the crosscorrelation and autocorrelation matrices required to calculate the Wiener solution.

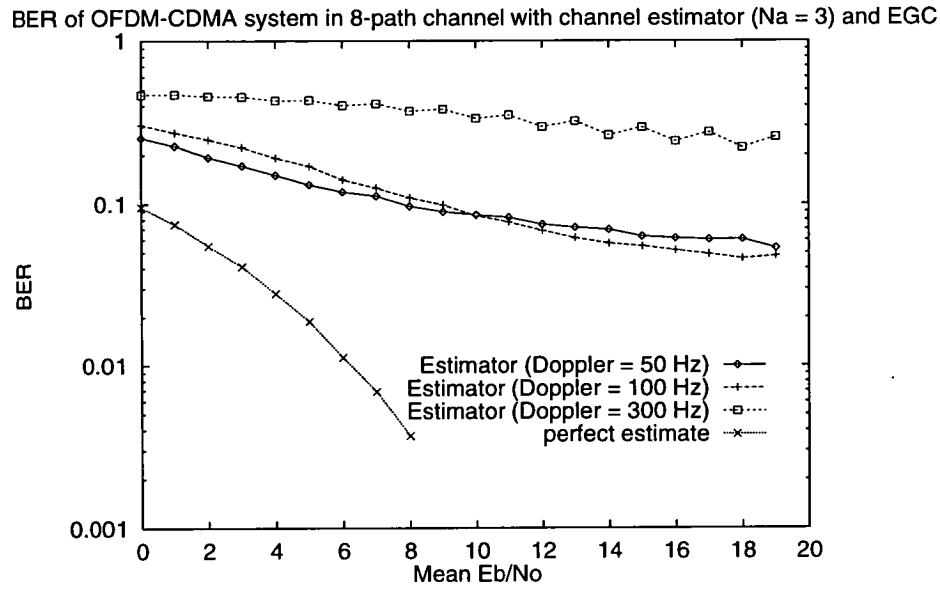

Figure 6.21: BER with EGC with perfect and estimated channel response $N_A = 3$

6.4 Conclusions

In this section we have investigated synchronisation and channel estimation algorithms for the OFDM-CDMA receiver described in Chapter 4. Synchronisation for the receiver can be split into two aspects: frequency and timing.

Initial investigations into frequency synchronisation showed that due to the BER sensitivity of the OFDM-CDMA system a frequency offset estimator with an accuracy of less than one FFT bin is required. To achieve this, synchronisation for the OFDM-CDMA receiver is split between acquisition and tracking. The acquisition algorithm measures and corrects the frequency offset to an accuracy of one FFT bin (2 kHz). The tracking algorithm is then initiated which further reduces the frequency offset.

For frequency acquisition the shift of the pilot tones was investigated as a frequency offset estimator. In terms of acquisition range and accuracy, modulating the pilot tones by a PN sequence was shown to provide better performance than fixed value pilot tones.

Two methods have been described for tracking. The first method measures the phase change between received samples in the guard interval and received samples in the useful part of the data bit. The guard interval is a cyclic extension and thus the transmitted samples in the guard interval are repeated versions of the samples in the useful part of the symbol. By measuring the phase changes between these repeated samples it is possible to measure the frequency offset. To achieve this the imaginary output of a complex correlator is used. The performance of this method may, however, degrade when the guard interval is short or subject to ISI. The second tracking method measures the phase change between two pilot tones. This second method may prove more robust for the OFDM-CDMA system with a guard interval of 18 samples in the presence of multipath. More work should be done here, to study the performance of these

tracking mechanisms in the presence of multipath.

For timing synchronisation the performance of two types of correlator were studied. Both correlators operate on a similar principle to the correlator described above for tracking. As samples in the guard interval are repeated versions of the samples in the useful part of the symbol a correlation peak is formed when the timing is correct. The simplest of these correlator, the sign correlator has promising performance but further work should be conducted in a multipath channel to confirm these results.

Finally in this chapter the performance of a simple channel estimator algorithm has been investigated. This technique forms a channel estimate based on the received signal from each of the pilot tones. Interpolation is then performed in frequency. This channel estimator has high BER performance for low Doppler situations. Due to the time needed to achieve channel estimates of lower variance, this estimation technique has poorer performance at higher Doppler. This channel estimation technique may be suitable for static channels as the averaging time (value of N_A) could be made very long. An alternative solution has been suggested by using a Wiener filter in the time domain and linear interpolation in the frequency domain.

Chapter 7
Conclusions

In this chapter we shall summarise the main findings of this thesis. Suggestions for possible future work will also be made.

7.1 Summary of the work

The work throughout this thesis has been investigating the performance of a communication system based on combining multi-carrier modulation with CDMA. In Chapter 3 we identified three possible combinations of multi-carrier modulation with CDMA. Subsequently, the work in chapters 4, 5 and 6 has concentrated on examining one of these combinations, namely a one chip per carrier multi-carrier CDMA system.

Initially, a multi-carrier CDMA system similar to the one proposed by Linnartz was examined in Chapter 4. The system proposed by Linnartz modulates a set of N carriers (the number of carriers is the same as the spreading sequence length) where each carrier is separated further apart than the coherence bandwidth to achieve maximum diversity. This however, requires a large bandwidth and is not spectrally efficient. In our study, the carriers were made to overlap in the OFDM sense, to reduce the transmission bandwidth and to enable the system to be compared to a DS-CDMA system of the same bandwidth. Contrary to a traditional OFDM system a guard interval was not used. Despite the lack of guard interval and subsequent intercarrier interference, the multi-carrier CDMA system still showed a small advantage over the DS-CDMA system (1 dB at a BER of 0.01). Further, to alleviate the requirement for pilot tones which are needed for channel estimation, the use of DPSK modulation was examined. At the receiver DPSK demodulation was investigated on a per carrier and per data bit basis. The per carrier DPSK demodulation yielded the correct phase compensation for each carrier but the orthogonality of the spreading sequence set was destroyed. The system could, therefore, only support one user. The per data bit DPSK demodulation scheme did not correctly phase compensate the carriers and so yielded high BER performance. We can conclude, therefore, that for a multi-user one chip per carrier multi-carrier CDMA system, only coherent modulation schemes should be used.

One of the advantages of a multi-carrier CDMA system over a DS-CDMA system is that equalisation can be accomplished using N one tap equalisers compared to one N tap equaliser needed for DS-CDMA. In Chapter 4, we showed that it is, therefore, simple to calculate the equaliser coefficients to perform the MMSE criteria. In contrast, to compute the MMSE criteria for an N tap equaliser it is required to calculate the inverse of an $N \times N$ matrix. This was shown to be considerably more effective than using an adaptive algorithm.

In Chapter 5 a different one chip per carrier multi-carrier CDMA system was investigated. This is referred to as an OFDM-CDMA system and utilises 512 low data rate overlapping orthogonal carriers. After spreading, the data streams are interleaved onto 512 carriers so adjacent chips from the same data bits are separated in frequency by a distance of 64 carriers. A cyclically extended guard interval is then inserted which is longer than the channel delay spread eliminating intersymbol interference and ensuring orthogonality of the carriers. For this system, we initially investigated the performance of various detection schemes. The system facilitates the practical implementation of MLD since only 256 sequences need to be evaluated to support 64 users. This compares with the $2^{3\times 64}$ sequences needed to be evaluated for a comparable DS-CDMA system. (In this calculation for DS-CDMA the factor 3 arises due to the presence of ISI in the DS-CDMA system.) MLD was shown to offer the best detector solution if knowledge of the number of users and the channel are available at the receiver. When only channel information is available the non-optimal MMSE criteria offers the best solution.

The performance of different channel coding schemes were also investigated in conjunction with EGC. This detection scheme was chosen as it provides a soft input to the soft decision Viterbi decoder without requiring knowledge of the SNR. The performance of the 1/2 rate, $K = 7$ coded OFDM-CDMA system with EGC was compared to a 1/2 rate, $K = 7$ coded 4-tap DS-CDMA system of the same bandwidth. We have shown that the coded OFDM-CDMA system can support a BER of 2×10^{-3} for a fully loaded (64 users) system at 6 dB E_b/N_0. This compares with the DS-CDMA system which at a BER of 2×10^{-3} and 6 dB E_b/N_0 can only support 16 users. The spectral efficiency of the 1/2 rate coded OFDM-CDMA system is however limited to 0.425 bits/s/Hz.

To increase spectral efficiency, higher rate channel coding schemes were investigated. The OFDM-CDMA system in conjunction with a 3/4 rate, $K = 7$ convolutional code was shown to support 64 users at a BER of 2×10^{-3} yielding a spectral efficiency of 0.65 bits/s/Hz. The coding scheme does, however, require 19 dB E_b/N_0 to achieve this. Both orthogonal and super orthogonal coding schemes were also investigated. These schemes enabled coding and spreading to be combined while only requiring the bandwidth expansion due to spreading. The maximum spectral efficiency of the OFDM-CDMA system with these coding schemes was however relatively poor. The main advantage envisaged by these coding schemes, for the OFDM-CDMA system, is that they do not require a reduction in data rate or an expansion in bandwidth to accommodate coding. Finally in the performance of a combined interference canceller/decoder was investigated. For the 3/4 rate punctured convolutional coding $K = 7$ scheme a performance advantage of 10 dB is achieved at a BER of 2×10^{-3} compared to a system with no cancellation. The resulting performance was shown to have comparable performance to MLD with punctured convolutional coding. Unlike MLD with coding, IC with coding does not require knowledge of the SNR.

The work in chapters 4 and 5 assumed the multi-carrier receivers were perfectly synchronised and had perfect knowledge of the channel. As such, these results represent a lower bound on BER performance. In Chapter 6 synchronisation and channel estimation algorithms were investigated. In particular the performance of these methods were considered in conjunction with the OFDM-CDMA system described in Chapter 5. The work of this chapter is split into two sections. The first section, synchronisation,

addresses the issue of frequency and timing synchronisation. For coarse frequency synchronisation (acquisition), modulating the pilot tones by an m-sequence and measuring the frequency shift of the pilot tones yielded frequency estimates with low estimation variance. For finer synchronisation (tracking) two techniques were suggested. The first of these methods measures the phase difference between samples in the guard interval and samples in the useful part of the symbol. The performance of this method may, however, degrade when the guard interval is short or subject to ISI. The second method measures the phase change between subsequent received pilot tones. The second method may prove to be more robust for the OFDM-CDMA system in the presence of multipath. For timing synchronisation two types of correlators were studied. To identify the useful part of the received signal to pass on to the FFT, both correlators compare samples in the guard interval to samples in the useful part of the symbol. The simplest of these correlators, the sign only correlator has promising performance. However as samples in the guard interval are used, further work should be conducted in a multipath channel.

Finally in Chapter 6, the performance of a simple channel estimator was investigated. This technique forms a channel estimator based on the received signal from each of the pilot tones. This simple channel estimator has high BER performance. Further, due to the time needed to achieve channel estimates of lower variance, the estimation technique has very poor performance for high Doppler spreads. This channel estimation technique would be suitable for a static channel. Suggestions for more sophisticated techniques have been made.

7.2 Summary of main points

The main points of this research can be summarised by the following points:

- Three combinations of multi-carrier modulation with CDMA have been identified.
- For a multi-user one chip per carrier multi-carrier CDMA system only coherent modulation schemes can be used. A channel estimation is therefore needed and this is normally obtained using pilot tones.
- The multi-carrier CDMA system described in Chapter 4 does not have a significant BER performance advantage over a DS-CDMA system for EGC or MRC combining techniques. However, the equaliser for a multi-carrier CDMA receiver consists of N one tap equalisers compared to one N tap equaliser for DS-CDMA. It is therefore easier with multi-carrier CDMA to calculate the necessary coefficients at the receiver to fulfil the MMSE criteria.
- The OFDM-CDMA system described in Chapter 5 does have a performance advantage (both in terms of spectral efficiency and BER) over a DS-CDMA system with the same bandwidth. A practical form of MLD is also possible. Although high spectral efficiencies can be achieved with no coding, to achieve a high spectral efficiency with coding, a high rate coding scheme should be chosen.
- A coded OFDM-CDMA system with an EGC equaliser at the receiver and combined canceller/decoder can attain similar spectral efficiency performance to a coded OFDM-CDMA with MLD. Unlike

coding with MLD, the combined canceller/decoder does not require knowledge or an estimate of the SNR.

- To achieve high performance, the OFDM-CDMA system requires a sophisticated channel estimation algorithm.

7.3 Suggestions for further work

7.3.1 Cellular analysis

It has been shown that the OFDM-CDMA system can achieve a high spectral efficiency. The work so far has concentrated on a downlink single cell system. For a cellular system, it is important to take into account the influence of the interference from the surrounding cells. A possible avenue for new research could therefore be identifying any problems that the OFDM-CDMA system may encounter in a cellular environment and ascertaining the achievable cellular capacity for a given outage probability. Some work has been carried out in this direction by Toskala et al. [73] and it may be useful to build on this work.

7.3.2 Power amplifier non-linearities

An area which has not been considered in this thesis is the influence of the power amplifier non-linearities on the received BER. In this thesis, it is assumed that the operating point of the amplifier is sufficiently below the 1dB compression point [1] so that, any harmonic products produced from the amplifier have little influence on the received BER. As the OFDM signal has a high peak to mean value this means the amplifier is not being used efficiently. It may be interesting to examine the reduction in BER for the OFDM-CDMA system as this operating point is moved closer to the 1 dB compression point.

7.3.3 Improvement in combined canceller/decoder

The performance of the combined canceller/decoder showed very promising performance. It may be possible to increase its performance by using 'soft' decisions at all stages in the architecture. This may require knowledge of the SNR, but its performance may be superior to the that of MLD with channel coding.

[1] The 1 dB compression point is the power level (quoted as an input or output power) for which the power gain of the amplifier is 1 dB lower than expected due to compression.

7.3.4 Synchronisation

In this thesis the performance of the timing and tracking mechanisms in Chapter 6 have only been examined in Gaussian channels. In multipath fading channels the guard interval is subject to ISI and this may cause a performance degradation. It would be useful for the performance of these correlators to be simulated in a multipath channel to finish the work started in this thesis.

7.3.5 Channel estimation

The performance of the channel estimator in Chapter 6 was very poor. An interesting field of future research could be an investigation of other channel estimation algorithms. In particular the performance of the suggested channel estimation algorithm using a Wiener filter in the time domain and interpolation in frequency could be investigated.

7.3.6 Other multi-carrier CDMA systems

The main work contained in this thesis has concentrated on one chip per carrier multi carrier CDMA systems. As highlighted in Chapter 3 there are two other types of multi-carrier CDMA systems. These systems facilitate the use of DPSK modulation and therefore channel estimation and equalisation are not necessary. A possible avenue for future research could be investigating the performance of these systems.

References

[1] TIA/EIA/IS-95, *Mobile Station-Base Station Compatibility Standard for Dual Mode Wide-Band Spread Spectrum Cellular Systems.* Telecommunication Industry Association, 1993.

[2] W. H. W. Tuttlebee, "Cordless personal communications," *IEEE Communications Magazine*, pp. 42–53, December 1992.

[3] P. Andermo and L. Ewerbring, "A CDMA–based radio access design for UMTS," *IEEE Personal Communications Magazine*, vol. Vol 2, pp. pp48–53, February 1995.

[4] J. Padgett, C. Gunther, and T. Hattori, "Overview of wireless personal communications," *IEEE Communications Magazine*, vol. Vol 33, pp. pp28–42, January 1995.

[5] K. Fazel, "Performance of CDMA/OFDM for Mobile Communications," *IEEE Int. Conference on Universal Personal Communications*, pp. 975–979, October 1993.

[6] A. Chouldy, A. Brajal, and S. Jourdan, "Orthogonal Multicarrier Techniques Applied to Direct Sequence Spread Spectrum CDMA systems," *IEEE Globecom 93*, vol. 3, pp. 1723–1728, November 1993.

[7] N. Yee and J. P. Linnartz, "Controlled Equalisation of Multi-carrier CDMA in an Indoor Rician Fading Channel," *Proceedings IEEE Vehicular Technology Conference (VTC), Stockholm*, pp. 1665–1669, June 1994.

[8] C. E. Shannon, "Communication Theory of Secrecy Systems," *Bell Systems Technical Journal*, pp. 656–715, October 1949.

[9] G. Cooper and C. McGillem, *Modern Communications and Spread Spectrum.* London: McGraw-Hill Book Co., international ed., 1986.

[10] G. L. Turin, "Introduction to Spread Spectrum Anti-multipath Techniques and their Application to Urban Digital Radio," *Proceedings of the IEEE*, vol. 68, pp. 328–353, March 1980.

[11] K. S. Gilhousen, I. M. Jacobs, R. Padovani, A. J. Viterbi, L. A. Weaver, and C. E. Wheatly, "On the Capacity of a Cellular CDMA System," *IEEE Trans. Veh. Tech.*, vol. VT-40, pp. 303–312, May 1991.

[12] R. Gold, "Maximal Recursive Sequences with 3-valued Recursive Cross-correlation Functions," *IEEE Trans. Inf. Theory*, vol. IT-14, pp. 154–156, January 1968.

[13] M. Failli, ed., *Digital Land Mobile Radio Communications - COST 207 : Final Report.* Luxembourg: Commision of the European Communities, 1989.

[14] J. G. Proakis, *Digital Communications.* New York: McGraw-Hill, 2nd ed., 1983.

[15] M. Doelz and E. T. Heald, "Binary Data Transmission Techniques for Linear Systems," *IEE Proc. Radio Eng.*, vol. 45, pp. 656–661, May 1957.

[16] B. R. Salzberg, "Performance of an Efficient Parallel Data Transmission System," *IEEE Trans. Commun.*, vol. COM-15, pp. 803–811, December 1967.

[17] S. Weinstein and P. Ebert, "Data Transmission by Frequency Division Multiplexing Using The Discrete Fourier Transform," *IEEE Trans. Commun.*, vol. COM-29, pp. 628–634, July 1981.

[18] European Telecomunication Standard, *Radio broadcasting system: Digital Audio Broadcasting (DAB) to mobile, portable and fixed receivers*, November 1994. pr ETS 300 401.

[19] European Telecomunication Standard, *Digital Broadcasting Systems for television and data services; Framing structure, channel coding and modulation for digital television*, Feburary 1996. pr ETS 300 744.

[20] H. Sari, G. Karam, and I. Jeanclaude, "Transmission Techniques for Digital Terrestrial TV Broadcasting," *IEEE Communications Magazine*, pp. 100–109, Feburary 1995.

[21] M. O. Polley, W. F. Schreiber, and S. J. Wee, "Comments on "Transmission Techniques for Digital Terrestrial TV Broadcasting"," *IEEE Communications Magazine*, pp. 22–26, November 1995.

[22] M. Saito, S. Moriyama, *et al.*, "Transmission Characteristics of DQPSK - OFDM for Terrestrial Broadcasting Systems," *IEICE Trans. Commun.*, vol. E77-B, pp. 1451–1459, December 1994.

[23] H. Rohling and V. Engels, "Differential Amplitude Phase Shift Keying (DAPSK) - A New Modulation Methods for DTVB," *IEE International Broadcasting Convention*, pp. 102 – 108, September 1995.

[24] V. Mignone, A. Morello, and M. Visintin, "CD3-OFDM: A New Channel Estimation Method to Improve the Spectrum Efficiency in Digital Terrestrial Television Systems," *IEE International Broadcasting Convention*, pp. 122 – 128, September 1995.

[25] E. Sourour and M. Nakagawa, "Performance of Orthogonal Multi-Carrier CDMA in Nonfading Nonselective Fading Channels," *Proceedings of the IEEE Int. Symposium on Spread Spectrum Techniques and Applications, Oulu, Finland*, pp. 203–207, July 1994.

[26] E. Sourour and M. Nakagawa, "Two Stage Co-Channel Interference Cancellation in Orthogonal Multi-Carrier CDMA in a Frequency Selective Fading Channel," *IEEE International Symposium on Personal, Indoor and Mobile Radio Communications (PIMRC), The Hague, The Netherlands*, pp. 189–193, September 1994.

[27] E. Sourour and M. Nakagawa, "Performance of Orthogonal Multi-carrier CDMA in a Multipath Fading Channel," *IEEE Trans. Commun.*, vol. 44, pp. 356–367, March 1996.

[28] Q. Chen, E. S. Sousa, and S. Pasupathy, "Performance of a Coded Multi-Carrier DS-CDMA System in Multi-Path Fading Channels," *Wireless Personal Communications Journal*, vol. 2, no. 1-2, pp. 167–183, 1995.

[29] Q. Chen, E. S. Sousa, and S. Pasupathy, "Multi-Carrier DS-CDMA with Adaptive Sub-Carrier Hopping for Fading Channels," *IEEE International Symposium on Personal, Indoor and Mobile Radio Communications (PIMRC), Toronto, Canada*, pp. 76–80, September 1995.

[30] S. Kondo and L. B. Milstein, "Performance of Multicarrier DS-CDMA Systems," *IEEE Trans. Commun.*, vol. 44, pp. 238–246, February 1996.

[31] S. Kondo and L. B. Milstein, "Multicarrier CDMA System With Cochannel Interference Cancellation," *Proceedings IEEE Vehicular Technology Conference (VTC), Stockholm*, pp. 1640–1644, June 1994.

[32] N. Yee, J. Linnartz, and G. Fettweis, "Multi-Carrier CDMA in Indoor Wireless Radio Networks," *IEICE Trans. Commun.*, vol. E77-B, pp. 900–904, July 1994.

[33] Y. Bar-Ness, J. P. Linnartz, and X. Liu, "Synchronous Multi-user Multi-carrier CDMA Communication System with Decorrelating Interference Canceller," *IEEE International Symposium on Personal, Indoor and Mobile Radio Communications (PIMRC), The Hague, The Netherlands*, vol. 1, pp. 184–188, September 1994.

[34] K. Fazel, S. Kaiser, and M. Schnell, "A Flexible and High Performance Cellular Mobile Communications System Based on Orthogonal Multi-Carrier SSMA," *Wireless Personal Communications Journal*, vol. 2, no. 1-2, pp. 121–144, 1995.

[35] S. Kaiser, "OFDM-CDMA versus DS-CDMA: Performance Evaluation for Fading Channels," *IEEE Int. Conference on Communications (ICC), Seatle, USA*, pp. 1722–1726, June 1995.

[36] S. Kaiser, "Analytical Performance Evalution of OFDM-CDMA Mobile Radio System," *European Personal and Mobile Communications Conference (EPMCC), Bologna, Italy*, pp. 215–220, November 1995.

[37] S. Kaiser, "On the Performance of Different Detection Techniques for OFDM-CDMA in Fading Channels," *IEEE Globecom*, pp. 2059–2063, November 1995.

[38] D. N. Kalofonos and J. G. Proakis, "Performance of the Multi-stage Detector for a MC-CDMA System in a Rayleigh Fading Channel," *IEEE Globecom*, pp. 1784–1788, November 1996.

[39] K. Fazel, "Performance of Convolutionally Coded CDMA/OFDM in a Frequency-Time Selective Fading Channels and its Near-Far Resistance," *IEEE Int. Conference on Communications (ICC), New Orleans, USA*, pp. 1438–1442, May 1994.

[40] S. Kaiser and L. Papke, "Optimal detection when Combining OFDM-CDMA with Convolutional and Turbo Channel Coding," *IEEE Int. Conference on Communications (ICC), Dallas, USA*, pp. 343–348, June 1996.

[41] K. Fazel, "Narrow-Band Interference Rejection in Orthogonal Multi-carrier Spread-Spectrum Communications," *IEEE Int. Conference on Universal Personal Communications*, pp. 46–50, September 1994.

[42] L. Vandendorpe, "Multitone Spread Spectrum Multiple Access Communications System in a Multipath Rician Fading Channel," *IEEE Trans. Veh. Tech.*, vol. 44, pp. 327–337, May 1995.

[43] O. van de Wiel and L. Vandendorpe, "Analysis of Residual Interference after DFE equilization of multitone DS/SS systems over multipath channels," *IEEE Int. Conference on Communications (ICC), Seatle, USA*, vol. 1, pp. 394–398, June 1995.

[44] O. van de Wiel and L. Vandendorpe, "Adaptive Equalisation Structures for Multitone CDMA Systems," *IEEE International Symposium on Personal, Indoor and Mobile Radio Communications (PIMRC), The Hague, The Netherlands*, vol. 1, pp. 253–257, September 1994.

[45] L. Vandendorpe and O. van de Wiel, "Performance Analysis of Linear Joint Multiple Access Interference Cancellation-Equalization for Asynchronous Multitone CDMA," *IEEE International Symposium on Personal, Indoor and Mobile Radio Communications (PIMRC), Toronto, Canada*, vol. 2, pp. 537–541, September 1995.

[46] R. Prasad and S. Hara, "An Overview of Multi-carrier CDMA," *Proceedings of the IEEE Int. Symposium on Spread Spectrum Techniques and Applications, Mainz, Germany*, pp. 107–114, September 1996.

[47] L. Vandendorpe and O. van de Wiel, "Fractionally Spaced Decision Feedback Joint Detection for Multitone CDMA Systems," *Proceedings of the IEEE Int. Symposium on Spread Spectrum Techniques and Applications, Mainz, Germany*, pp. 1361–1365, September 1996.

[48] P. Robertson and S. Kaiser, "Analysis of the Effects of Phase-Noise in Orthogonal Frequency Division Multiplex (OFDM) Systems," *IEEE Int. Conference on Communications (ICC), Seatle, USA*, pp. 1652–1657, June 1995.

[49] T. Pollet, M. Moenclay, I. Jeanclaude, and H. Sari, "Effect of Carrier Phase Jitter on Single-Carrier and Multi-Carrier QAM Systems," *IEEE Int. Conference on Communications (ICC), Seatle, USA*, pp. 1046–1050, June 1995.

[50] M. Alard and R. Lasselle, "Principles of Modulation and Channel Coding For Digital Broadcasting for Mobile Receivers," *EBU Review*, pp. 168–190, August 1987.

[51] M. Alard, R. Halbert, B. L. Floch, and D. Pomminer, "A New System of Sound Broadcasting to Mobile Receivers," *IEEE European Conference On Electrotechnics*, pp. 416–420, June 1988.

[52] H. Sari, G. Karam, and I. Jeanclaude, "An Analysis of Orthogonal Frequency-Division Multiplexing for Mobile Radio Applications," *Proceedings IEEE Vehicular Technology Conference (VTC), Stockholm*, pp. 1635–1639, June 1994.

[53] G. J. R. Povey, P. M. Grant, and R. D. Pringle, "A decision-directed spread spectrum rake receiver for fast fading mobile channels," *Proceedings IEEE Vehicular Technology Conference (VTC), Stockholm*, pp. 742–746, June 1994.

[54] M. Dentino, J. McCool, and B. Widrow, "Adaptive Filtering in the Frequency Domain," *Proceedings of the IEEE*, vol. 66, pp. 1658–1659, December 1978.

[55] D. G. M. Cruickshank, "Optimal and Adaptive FIR Filter Receivers for DS-CDMA," *IEEE International Symposium on Personal, Indoor and Mobile Radio Communications (PIMRC), The Hague, The Netherlands*, pp. 1339–1345, September 1994.

[56] K. Liu and J. Lee, "Recent Results on the Use of Concatenated Reed-Solomon/Viterbi Channel Coding and Data Compression for Space Communications," *IEEE Trans. Commun.*, pp. 518–523, May 1984.

[57] K. J. Larsen, "Short Convolutional Codes with Maximal Free Distance for Rates 1/2, 1/3, and 1/4," *IEEE Trans. Inf. Theory*, pp. 371–372, May 1973.

[58] J. Conan, "The Weight Spectra of Some Short Low-Rate Convolutional Codes," *IEEE Trans. Commun.*, vol. 32, pp. 1050–1053, September 1984.

[59] J. Heller and I. Jacobs, "Viterbi Decoding for Satellite and Space Communication," *IEEE Trans. Commun.*, vol. COM-19, pp. 835–848, October 1971.

[60] P. Schramm, "Tight Upper Bound on the Bit Error Probability of Convutionally Encoded Spread Spectrum Communications Over Frequency-Selective Rayleigh-Fading Channels," *IEEE Int. Conference on Communications (ICC), Seatle, USA*, pp. 1727–1731, June 1995.

[61] D. Haccoun and G. Begin, "High-Rate Punctured Convolutional Codes for Soft Decision Viterbi Decoding," *IEEE Trans. Commun.*, vol. COM-37, pp. 1113–1125, November 1989.

[62] G. Begin, D. Haccoun, and C. Paquin, "Further Results on high-Rate Punctured Convolutional Codes for Soft Decision Viterbi Decoding," *IEEE Trans. Commun.*, vol. COM-37, pp. 1922–1928, November 1989.

[63] A. J. Viterbi, "Very Low Rate Convolutional Codes for Maximum Theoretical Performance of Spread Spectrum Multiple Access Channels," *IEEE Journal Sel. Areas Commun.*, vol. 8, pp. 641–649, May 1990.

[64] A. J. Viterbi, *Chapter 5 ,CDMA Principles of Spread Spectrum Communications*. Massachusetts: Addison-Wesley, 1st ed., 1995.

[65] H. N. T. Nagashima, "A Frequency and Timing Period Acquistion Technique for OFDM Systems," *IEEE International Symposium on Personal, Indoor and Mobile Radio Communications (PIMRC), Toronto, Canada*, pp. 1010–1015, September 1995.

[66] F. Tufvesson and T. Maseng, "Pilot Assisted Channel Estimation for OFDM in Mobile Cellular Systems," *Proceedings IEEE Vehicular Technology Conference (VTC), Phoenix*, pp. 1639–1643, May 1997.

[67] F. Daffara and O. Adami, "An New Frequency Detector for Orthogonal Multicarrier Transmission Techniques," *Proceedings IEEE Vehicular Technology Conference (VTC), Chicago*, pp. 804–809, June 1995.

[68] F. Classen and H. Meyr, "Frequency Synchronisation Algorithms for OFDM Systems suitable for Communications over Frequency Selective Fading Channels," *Proceedings IEEE Vehicular Technology Conference (VTC), Stockholm*, pp. 1655–1659, June 1994.

[69] F. Classen and H. Meyr, "Synchronisation Algorithms for an OFDM Systems for Mobile Communications," *Proc. of ITG Conference on Source and Channel Coding, Munich*, vol. 130, pp. 105–113, 1994.

[70] P. Hoeher, "TCM on Frequency-Selective Land-Mobile Fading Channels," *Proc. of the Tirrneia Intern. Workshop on Digital Communications, Elsevier Science Publishers*, pp. 317–327, September 1992.

[71] J. van de Beek, O. Edfors, M. Sandell, S. K. Wilson, and P. O. Borjesson, "On channel estimation in OFDM Systems," *Proceedings IEEE Vehicular Technology Conference (VTC), Chicago*, pp. 815–819, June 1995.

[72] L. Tomba and W. Krzymin, "Downlink Detection Schemes for MC-CDMA Systems in Indoor Environments," *IEICE Trans. Commun.*, vol. E79-B, pp. 1351–1360, September 1996.

[73] A. Toskala, J. Castro, L. Chalard, S. Haemaelaeinern, and K. Kalliojaervi, "Cellular OFDM/CDMA Downlink Performance in the Link and System Levels," *Proceedings IEEE Vehicular Technology Conference (VTC), Phoenix*, pp. 855–859, May 1997.

[74] R. Prasad, *CDMA for Wireless Personal Communications*. Artech House, 1996.

[75] W. C. Y. Lee, *Mobile Cellular Telecommunication Systems - International Edition*. McGraw Hill Book Company, 1st ed., 1990.

Appendix A
Original Publications

The author of this thesis has the following publications:

- † R. A. Stirling-Gallacher, G. J. R. Povey, "*Different channel coding strategies for OFDM-CDMA*", Proceedings IEEE Vehicular Technology Conference (VTC), Phoenix, pp. 845-849, 4-7 May 1997.
- R. A. Stirling-Gallacher, G. J. R. Povey, "*Performance of an OFDM-CDMA System with Orthogonal Convolutional Coding and Interference cancellation*", Proceedings IEEE Vehicular Technology Conference (VTC), Phoenix, pp. 860-864, 4-7 May 1997.
- † Y. H. Ng, P. M. Grant, R. A. Stirling-Gallacher, "*Carrier tracking technique for OFDM signal transmissions*", IEE Electronics Letters, no. 22, Vol 32, pp. 2047-2048, 24th October 1996.
- R. A. Stirling-Gallacher, A. P. Hulbert, G. J. R. Povey, "*A fast acquisition technique in the presence of a large Doppler shift*", Proceedings of the IEEE Int. Symposium on Spread Spectrum Techniques and Applications, Mainz, Germany, pp. 156-160, 22-25 September 1996.
- † R. A. Stirling-Gallacher, G. J. R. Povey, "*Comparison of MC-CDMA and DS-CDMA using frequency and time-domain RAKE receivers*", Wireless Personal Communications, **2**, No. 1-2, pp. 105-119, Kluwer Academic Publishers, 1995.
- R. A. Stirling-Gallacher, G. J. R. Povey, "*Performance of a multi-carrier code division multiple access frequency domain RAKE receiver*", Proceedings of IEE conference on Radio Receivers and Associated Systems, Bath, pp. 86-90, 26-27th September 1995.

† Reprinted in this appendix.

Different Channel Coding Strategies for OFDM-CDMA

R.A. Stirling-Gallacher, G.J.R. Povey

Signals and Systems Group
Dept. of Electrical Engineering,
University of Edinburgh,
Scotland EH9 3JL, UK.
Email: rasg@ee.ed.ac.uk

Abstract - In this paper the performance of different channel coding schemes are presented for an OFDM-CDMA system. The different channel coding schemes are shown for a receiver using equal gain combining on the carriers in a multipath channel. As such the only information needed at the receiver is the phase of the sub-carriers. Two new channel coding schemes for OFDM-CDMA are presented, orthogonal and super orthogonal convolutional coding. These are compared against a $1/2$ rate $K = 7$ convolutional code and a $3/4$ rate $K = 7$ punctured convolutional code. A comparison is made of the spectral efficiency of the different coding schemes, the bandwidth required and the receiver complexity tradeoffs.

I. INTRODUCTION

Orthogonal frequency division multiplexing (OFDM) is a parallel data transmission scheme. Within a bandwidth B high data rates $R = B$ can be realised by transmitting N bits simultaneously using N orthogonal subcarriers. The orthogonal sub-carriers are spaced by B/N in frequency and overlap resulting in optimum bandwidth efficiency. With OFDM the frequency selectivity of the channel can be combatted by a simple one tap equaliser. To prevent intersymbol interference (ISI) and inter carrier interference (ICI) a guard interval is inserted between adjacent symbols which is longer than the multipath delay spread T_m of the channel.

To combat fading, OFDM can be combined with direct sequence spread spectrum, where the signal is spread over several carriers to achieve frequency diversity. Multiple access is possible by having different users transmitting on the same subcarrier. This technique was introduced as OFDM-CDMA or multi-carrier CDMA [1, 2].

The aim of this paper is to investigate the performance of OFDM-CDMA with different channel coding schemes. These channel coding schemes are examined in conjunction with equal gain combining (EGC). Various detection schemes have been examined for OFDM-CDMA systems [3] which range in complexity from EGC to maximum likelihood detection (MLD) and maximum mean square error (MMSE). Although the performance of MLD and MMSE for OFDM-CDMA are far superior to EGC, these detection schemes require information at the receiver which may not always be available. Further, when combining MLD or MMSE with channel coding, reliability information is needed to provide a soft output value to the soft decision Viterbi decoder. This requires knowledge of the signal to noise ratio [4].

In the system we analyse here the only information required at the receiver is the phase of the sub-carriers. We introduce two new coding schemes for OFDM-CDMA, namely orthogonal and super orthogonal coding. The performance of these are compared against a 1/2 rate ($K = 7$) convolutional code and a 3/4 rate ($K = 7$) punctured convolutional code.

The paper is structured as follows: In section II the OFDM-CDMA system is described. The different channel coding schemes are then described in section III. In section IV the system parameters are described and the performance of the channel coding schemes are presented in a Gaussian noise channel. These are compared against theoretical results. Monte Carlo results are then presented in a multipath channel. Conclusions are made in section IV.

II. SYSTEM DESCRIPTION

The transmission scheme for the downlink of the OFDM-CDMA system with channel coding is shown in figure 1. The transmitted signal of the N_u data bits are split into Q sub-systems. Each sub-system has a maximum capacity of L/Q users where L is the maximum number of users that can be supported in the whole system. The N_u user data streams are convolutionally encoded with code rate R. The encoded data bit for user i is denoted by b_i which has a duration of $T_b = RT_d$, where T_d is the duration of the uncoded data bit. Each code bit b_i is then spread by a spreading code $\mathbf{c}_i$ of length L/Q with the chip streams of all users being added synchronously. In this way each sub-system is effectively a DS-CDMA system. The spreading sequence used is a Walsh code to maintain orthogonality. The chip streams of all users in the qth sub-system can therefore be written as vector $\mathbf{s}_q$

$$\mathbf{s}_q = \sum_{i=(N_u/Q)q+1}^{(N_u/Q)(q+1)} b_i \mathbf{c}_i \qquad (1)$$

From each sub-system M data bits are serial to parallel converted producing ML/Q parallel output streams of duration MT_b seconds. These streams are sent to the frequency interleaver which scrambles all of the outputs and passes them onto the OFDM modulator. The frequency interleaver attempts to separate chips from the same data bit further apart than the coherence bandwidth to achieve frequency diversity. The total number of carriers is ML. A guard interval Δ, is then inserted which is longer than the delay spread in the channel to prevent ISI and ICI. This gives a total symbol duration of $T = MT_d + \Delta$.

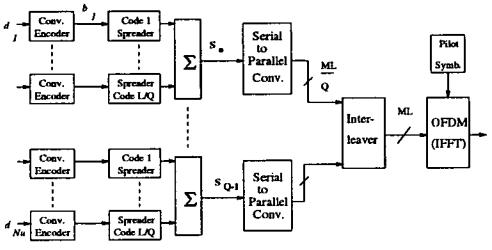

Figure 1: OFDM-CDMA transmitter with channel coding

The receiver is shown in figure 2. The received signal after the FFT and de-interleaving can be written as a vector $\mathbf{r}$ of L/Q components.

$$\mathbf{r} = \mathbf{H}_q.\mathbf{s}_q^T + \mathbf{n} \tag{2}$$

where $\mathbf{H}_q$ is a diagonal matrix representing the fading of the sub-carriers assigned to the qth block. $\mathbf{s}_q^T$ is the transposed transmitted sequence and $\mathbf{n}$ is the noise vector.

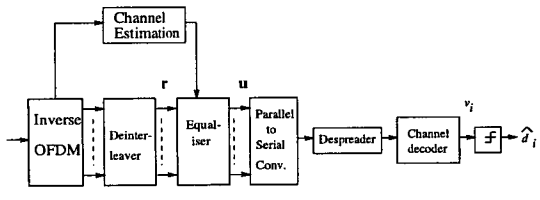

Figure 2: OFDM-CDMA receiver with channel decoding

The received signal is then passed to an equaliser. The output of the equaliser is given by,

$$\mathbf{u} = \mathbf{G}.\mathbf{r} \tag{3}$$

where $\mathbf{G}$ is a diagonal matrix representing the equaliser coefficients. By representing the diagonal element $h_{l,l}$ of $\mathbf{H}$ by h_l and the diagonal element $g_{l,l}$ of $\mathbf{G}$ by g_l, the equaliser coefficients to perform equal gain combining are given by

$$g_l = \frac{h_l^*}{|h_l|} \qquad l = 1 \ . \ . \ L/Q \tag{4}$$

$\mathbf{u}$ is then despread by the local spreading code $\mathbf{c}_i$ to form the soft output v_i which is passed to the soft-decision Viterbi decoder. A sign decision is then made on the output of the soft decision Viterbi decoder to form the decoded output data bit $\hat{d}_i$.

III. CHANNEL CODING

In this paper we will consider four possible channel coding schemes for OFDM-CDMA.

Orthogonal Convolutional Coding

The orthogonal (or Hadamard encoder) [5] [6] is shown in figure 3. It consists of two shift registers of length K in which the parallel outputs of the first shift registers are connected to the second via a connecting block. The second shift register contains switches and modulo 2 adders and the output of this shift register forms the coder output. The switches toggle at rate 1,2,4 etc, so that for each data bit at the input of the first shift register a unique 2^K length Walsh code is produced. There is a fixed relationship between the code rate R and the constraint length K given by $R = 1/2^K$. Figure 3 shows a $K = 3$, $R = 1/8$ coder. With this coder spreading and coding are combined resulting in a bandwidth expansion of 1.

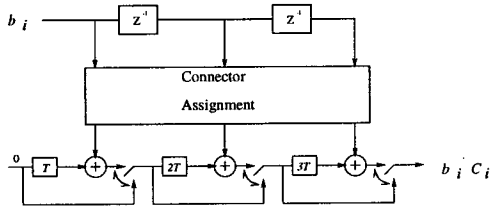

Figure 3: Orthogonal coder

To obtain multiple access two different schemes can be adopted. The first schemes has different connector assignments for each user. For the $K = 3$ coder, 6 possible combinations are available using all connections. The second scheme is that every user has the same connector assignment but the output of the coder is multiplied by a seperate spreading sequence of the same rate for each user. The performance of both schemes will be investigated.

Super Orthogonal Convolutional Coding

The super orthogonal coder [6] is shown in figure 4. This is an extension of the orthogonal coder in which the relationship between the code rate and the constraint length is given by $R = 1/2^{K-2}$ and thus for a given code rate a larger constraint length is achieved than the orthogonal coder. Figure 4 shows a $K = 5$, $R = 1/8$ coder. Multiple access performance is obtained in the same way as the orthogonal coder.

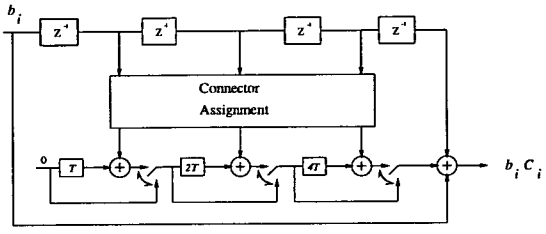

Figure 4: Super orthogonal coder

Standard Convolutional Coding

Channel coding with standard $1/2$ rate convolutional codes of constraint lengths $K = 7$ and $K = 3$ will be considered. The coders used have the maximal free distance for constraint length $K = 7$ and $K = 3$ [7].

Punctured Convolutional Coding

For a convolutional code of rate k/m there are 2^k merging paths at each node in the trellis. The number of comparisons that have to be made at each node is therefore 2^k in the decoding trellis. For higher rate codes ($k > 1$) the decoding complexity is very high. A punctured convolutional code is a modification of a standard convolutional code in which bits of the output encoder are periodically deleted, generating a higher rate code. The number of comparisons at each node is the same as the standard convolutional code, thereby reducing complexity. There is however a reduction in the minimum free distance due to the puncturing. We consider the performance of a $3/4$ rate $K = 7$ punctured convolutional code which has minimal free distance for this constraint length [8].

IV. PERFORMANCE EVALUATION

Gaussian Noise Channel

In a Gaussian noise channel, the theoretical BER performance of a convolutional code is upper bounded by

$$\text{BER} \leq \sum_{d=d_{free}}^{\infty} c_d P(d) \tag{5}$$

where $P(d)$ is the probability that the wrong path at distance d is selected. c_d is the distance spectra of the code. $P(d)$ is given by,

$$P(d) = \frac{1}{2}\text{erfc}\left(\sqrt{\frac{E_b.d.R}{N_0}}\right) \tag{6}$$

where d is the distance and R is the rate of the code. For a punctured convolutional code the upper bound is given by [8],

$$\text{BER} \leq \frac{1}{p} \sum_{d=d_{free}}^{\infty} c_d P(d) \tag{7}$$

where p is the puncturing period. The Gaussian noise performance of these coding schemes are shown in figure 5 for a single user to verify performance. It can be seen that the Monte Carlo simulations are close to the theoretical upper bounds.

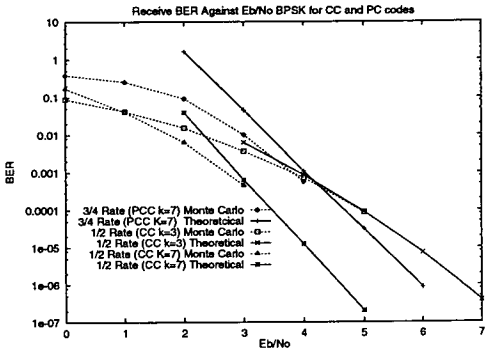

Figure 5: Gaussian noise performance for single user

For the orthogonal code the BER rate is obtained by a looser bound given by differentiating the code transfer function $T(W, B)$ [6]

$$\text{BER} \leq \frac{1}{2}\frac{dT(W,B)}{dB}\bigg|_{B=1, W=Z^{\frac{1}{2r}}, Z=e^{-\frac{E_b}{N_0}r}} \tag{8}$$

For the orthogonal coder the derivative of the code transfer function is given by,

$$\frac{dT(W,B)}{dB} = \frac{W^K(1-W)^2}{(1-2W+W^K)^2} \tag{9}$$

and for the super orthogonal coder,

$$\frac{dT(W,B)}{dB} = \frac{W^{K+2}}{(1-2W)^2}\left(\frac{1-W}{1-W^{K-2}}\right)^2 \tag{10}$$

where K is the constraint length and r is the reciprocal of the code rate R.

System Parameters

The OFDM-CDMA transmitter uses a 512 point IFFT with $Q = 8$ and $M = 8$ in which we have 8 sub-systems using a 8 length Walsh codes. For a uncoded data rate of 16 kbits/s the data rate per carrier is 2 kbits/s with a transmit bandwidth of 1.025 MHz.

We assume there is sufficient dispersion in the channel so that the interleaver can achieve perfect interleaving. This is achievable in our system if the channel dispersion is greater than 14 μs. Each of the eight chips from the same

data bit will therefore be subject to independent Rayleigh fading. The Rayleigh fading channel is characterised by the presence of the Doppler filter. A classic Doppler spectrum is used with a Doppler rate of 300 Hz which corresponds to a mobile speed of 162 km/h for a frequency of 2 GHz.

We also assume the guard interval T_m is longer than the channel dispersion and that the receiver has perfect channel knowledge and is perfectly synchronised.

When comparing different coding methods the uncoded data rate is fixed at 16 kbits/s and thus the different coding schemes occupy different bandwidths. We could compare system with the same transmission bandwidth, but this would require different uncoded data rates or different levels of processing gain. Making a comparison with different uncoded date rates is difficult due to the different performance of the required speech coders. Making a comparison with different processing gains in OFDM-CDMA is difficult due to the different levels of diversity.

Performance in Multipath

The performance of the OFDM-CDMA system with orthogonal coding for different multi-access schemes is shown in figure 6. An orthogonal coder of length 3 is chosen so that a 8 length Walsh code is produced and the system occupies the same bandwidth as the uncoded system. By examining figure 6 the worse multi-access performance is obtained if each user has a different coder. (This is obtained by each user having different connections in the connector block.) An improvement can be made if the output of every coder for each user is multiplied by an extended (length 8) Gold code. The best performance is obtained if each user has the same coder and the output of the coder is multiplied by a unique 8-length Walsh code for each user. With this arrangement a BER of 2×10^{-3} can be maintained for 16 users at a E_b/N_0 of 9 dB.

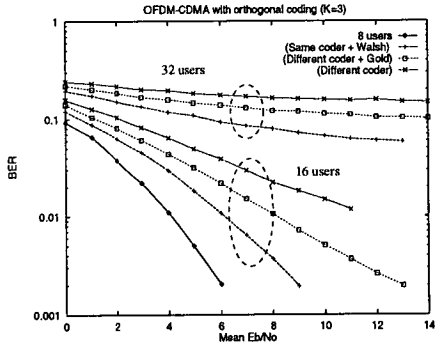

Figure 6: BER performance for orthogonal coder (K=3)

The performance of the OFDM-CDMA system with super orthogonal coding is shown in figure 7. A constraint length K of 5 is chosen so that 8 length Walsh codes are produced. For this coder there was very little difference between the two improved multi-access methods described above. For clarity, therefore only one arrangement is shown, the same coder for every user with a different Walsh code. It can be seen that at a BER of 2×10^{-3}, 16 users can be supported at a E_b/N_0 of 6 dB. This is 3 dB lower than the orthogonal coder.

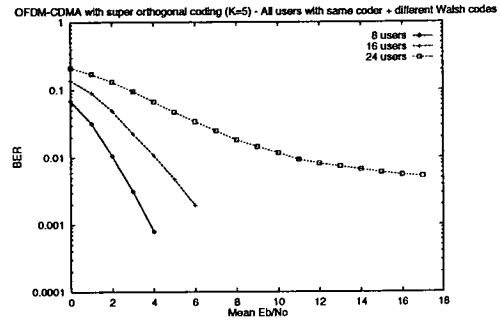

Figure 7: BER performance for super orthogonal coder (K=5)

Results for the fully loaded (N_u = 64 users) OFDM-CDMA system with standard and punctured convolutional codes are shown in figure 8. The OFDM-CDMA system with the 1/2 rate convolutional codes (K = 3 and K = 7) both occupy 2 MHz. It can be seen that at a BER of 2×10^{-3} the 1/2 rate $K = 7$ code is only 2 dB better than the $K = 3$ code despite it's higher complexity (64 states compared to 4 states.) The 3/4 rate $K = 7$ punctured convolutional code requires 19 dB E_b/N_0 to support 64 users at a BER of 2×10^{-3}.

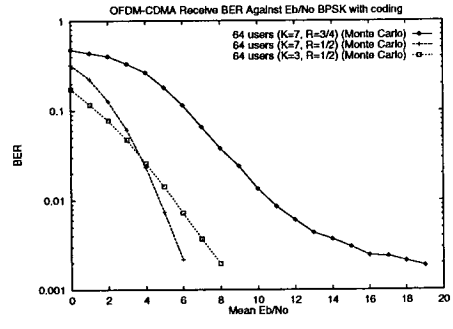

Figure 8: BER performance for standard and punctured convolutional codes (N_u = 64)

The spectral efficiencies of the OFDM-CDMA system with orthogonal and super orthogonal coding are shown in figure 9. (For all spectral efficiencies 15 % of the data is assumed to be needed for channel sounding.) Results are also provided for two uncoded detection schemes EGC and MLD. All systems require the same bandwidth. It can be seen that at a spectral efficiency of 0.2125 bits/s/Hz the super orthogonal coding scheme is 4.2 dB better than

EGC and 2.2 dB better than MLD. The super orthogonal coding scheme is however unable to support higher spectral efficiencies due to the orthogonality of the codes produced.

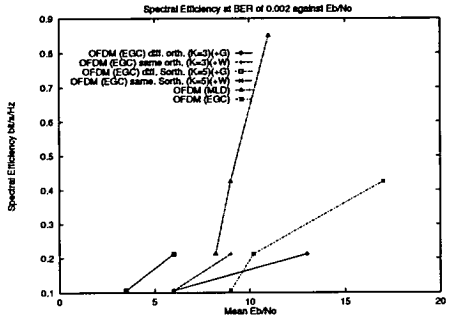

Figure 9: 1.0 MHz bandwidth

The spectral efficiencies of the standard and punctured convolutional codes are shown in figure 10 and 11 respectively. Due to the lower bandwidth expansion of the punctured convolutional code a higher spectral efficiency is achieved. However, below a spectral efficiency of 0.425 bits/s/Hz the punctured convolutional code requires a higher E_b/N_0 than the standard convolutional code to achieve a given spectral efficiency.

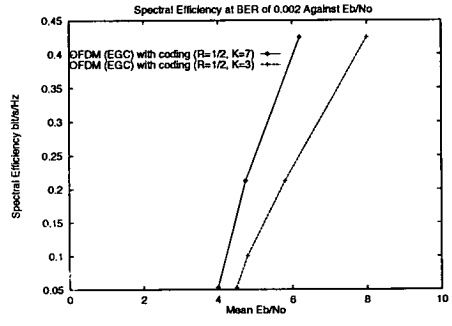

Figure 10: 2.0 MHz bandwidth

V. CONCLUSIONS

We have examined an OFDM-CDMA system with different forms of channel coding in conjunction with EGC. It has been shown that for a BER of 2×10^{-3} with a spectral effeciency of 0.212 bits/s/Hz, super orthogonal coding requires a E_b/N_0 2.2 dB lower than MLD. By improving the orthogonality of the generated codes higher spectral efficiencies will be achieved. In it's present form, super orthogonal coding is a good choice in a channel with a low E_b/N_0, where coding is not an option due to bandwidth restrictions. Both standard and punctured convolutional codes with EGC offer low complexity solutions which require more bandwidth. A non-punctured higher rate code

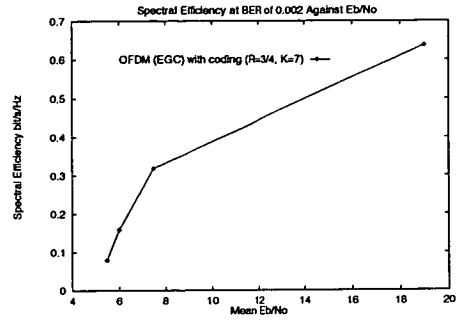

Figure 11: 1.33 MHz bandwidth

would offer higher performance but at increased decoding complexity.

ACKNOWLEDGMENTS

The authors would like to thank the Engineering and Physical Sciences Research Council (EPSRC) and Roke Manor Research Ltd. for funding this research.

REFERENCES

[1] K.Fazel, "Performance of CDMA/OFDM for Mobile Communications," *IEEE Int. Conference on Universal Personal Communications*, pp. 975–979, October 1993.

[2] N. Yee, J. Linnartz, and G. Fettweis, "Multi-Carrier CDMA in Indoor Wireless Radio Networks," *IEICE Trans. Commun.*, vol. E77-B, pp. 900–904, July 1994.

[3] S. Kaiser, "On the Performance of Different Detection Techniques for OFDM-CDMA in Fading Channels," *IEEE Globecom*, pp. 2059–2063, Nov 1995.

[4] S. Kaiser, "Trade-off between Channel Coding and Spreading in Multi-Carrier CDMA Systems," *Proceedings of the IEEE Int. Symposium on Spread Spectrum Techniques and Applications, Mainz, Germany*, pp. 1366–1370, September 1996.

[5] A. Viterbi, "Very Low Rate Convolutional Codes for Maximum Theoretical Performance of Spread Spectrum Multiple Access Channels," *IEEE Journal Sel. Areas Commun.*, vol. 8, pp. 641–649, May 1990.

[6] A. J. Viterbi, *Chapter 5 ,CDMA Principles of Spread Spectrum Communications*. Massachusetts: Addison-Wesley, 1st ed., 1995.

[7] J. Conan, "The Weight Spectra of Some Short Low-Rate Convolutional Codes," *IEEE Trans. Commun.*, vol. 32, no. 9, pp. 1050–1053, 1984.

[8] D. Haccoun and G. Begin, "High-Rate Punctured Convolutional Codes for Soft Decision Viterbi Decoding," *IEEE Trans. Commun.*, vol. COM-37, no. 11, pp. 1113–1125, 1989.

Wireless Personal Communications 2: 105–119, 1995.

Comparison of MC-CDMA with DS-CDMA Using Frequency Domain and Time Domain RAKE Receivers

R.A. STIRLING-GALLACHER and G.J.R. POVEY
Signals and Systems Group, Department of Electrical Engineering, University of Edinburgh, Edinburgh EH9 3JL, Scotland, U.K. (Tel.: 131-650-5659; Fax: 131-650-6554)

Abstract. In this paper a multicarrier CDMA (MC-CDMA) system with a soft decision differential phase shift keying (DPSK) frequency domain RAKE receiver is described. We compare a MC-CDMA system with a direct sequence CDMA system using RAKE receivers. In contrast with previous MC-CDMA systems, guard intervals are not used and the carriers are spaced at the reciprocal of the bit rate, optimising the usage of the bandwidth. In this way a comparison can be made between the multicarrier CDMA system described and a direct sequence (DS-CDMA) system with the same bandwidth. The results presented are received bit error rates from Monte Carlo simulations. The simulations are conducted in a multipath channel with Rayleigh fading and 300 Hz Doppler spectrum with additive white Gaussian noise. It is shown that the multicarrier CDMA matched filter receiver performs favourably compared to the direct sequence CDMA matched filter receiver for 1-path fading. For a single user at a receive bit error rate of 1×10^{-3} in the 4-path fading channel the multicarrier RAKE receiver requires no knowledge of the channel delay spread and performs 3 dB worse than the DS-CDMA RAKE receiver simulated. The performance of the MC-CDMA RAKE receiver for a single user increases with increasing channel dispersion. The performance of the DS-CDMA RAKE receiver for multiple user is superior to that of the MC-CDMA RAKE receiver.

Key words: Multi-carrier, spread-spectrum, RAKE.

1. Introduction

Orthogonal frequency division multiplexing (OFDM) has been used to combat the delay spread experienced by a multipath channel. An OFDM system considered by Cimini [1] converts a incoming data stream (of rate l/T_b) into a parallel data stream by use of a N output serial to parallel converter. The output of each symbol of the serial to parallel converter therefore occur at a rate of l/NT_b, thereby increasing the symbol duration. These symbols are then modulated by N sinusoidal carriers. As the symbol duration on the individual carriers is increased the effects of intersymbol interference (ISI) in a multipath channel are reduced.

To eliminate the effects of ISI and to maintain the orthogonality of the separate carriers in a multipath channel, OFDM systems have been considered with a cyclically extended guard interval on the individual carriers. This guard interval has a duration longer than the maximum delay spread in the channel. Reiners and Rohlings [2] have considered a system of this type in a multipath channel with a Doppler spectrum. An OFDM system of this type has also been adopted in the European Digital Audio Broadcasting (DAB) project [3] in conjunction with interleaving and channel coding.

Recently, OFDM has been investigated in various forms in connection with direct sequence spread spectrum (DS-SS). Chouldy et al. [4] considered a downlink CDMA system where the users DS-SS signals are first combined before serial to parallel conversion. An interleaver,

Inverse Fast Fourier Transform (IFFT) and a guard interval are then used at the transmitter. (Receiver architectures using a complex channel equalizer based on the MSE criteria are then investigated.) Fazel considered [5–7] a downlink CDMA system of a similar nature using Hadamard codes and various detection algorithm including Maximum Likelihood Detection (MLD). The performance of MLD is also analysed in the presence of narrowband interference [5] and non ideal power control [7]. Linnartz et al. [8] considered an OFDM/CDMA system referred to as MC-CDMA. In this system one data symbol is duplicated into N parallel copies. Each branch of the data stream is then multiplied by a chip from a spreading code of length N. The outputs of these multipliers then modulate a set of N carriers. In this system the carriers are separated at a distance greater than the coherence bandwidth, thereby experiencing independent fading.

In this paper we consider an orthogonal MC-CDMA system in which the carriers are spaced at $1/T_b$ requiring the minimum bandwidth for transmission. We will not incorporate an interleaver or a guard interval, so the bandwidth requirement of the described MC-CDMA system is the same as a DS-CDMA system.

In our MC-CDMA system therefore, dispersion in the channel results in different attenuation and phases for each subcarrier. Received amplitudes and phases of adjacent subcarriers are correlated but become less so if the channel delay spread is large. Hence the coherence bandwidth is reduced as the time dispersion in the channel is increased. Therefore frequency diversity is improved with increasing channel dispersion. To utilise this diversity, we describe a RAKE receiver, implemented in the frequency domain for our MC-CDMA system, in which the individual carriers are differentially equalised. With increasing time dispersion the coherence bandwidth is reduced and the system performance is increased for a single user.

This is in contrast to direct sequence CDMA (DS-CDMA) where channel dispersion leads to the reception of several resolvable paths. RAKE receivers have been successfully applied in combining these resolvable paths [9] in order to combat the effect of multipath fading on mobile radio channels. A RAKE receiver has been investigated by Fettweiss et al. [10] in the frequency domain by extending the input of the FFT as the transmit bandwidth is increased due to the Doppler shift. In our system this is not necessary as the maximum Doppler frequency is much less than the carrier spacing. The performance of our MC-CDMA RAKE receiver will be compared with that of a DS-CDMA RAKE receiver which has perfect knowledge of the channel dispersion. The paper is organized as follows: Section 2 introduces differential Phase Shift Keying (DPSK) DS-CDMA and MC-CDMA techniques. We describe architectures on which the simulations are based.

Section 2.1 describes a single path DS-CDMA matched filter receiver, Section 2.2 describes the time domain DS-CDMA RAKE receiver, Section 2.3 describes the MC-CDMA matched filter receiver and finally in Section 2.4 the frequency domain MC-CDMA RAKE receiver is described. Section 3 describes the Gaussian and frequency selective Rayleigh multipath channels. Simulation results are then presented in Section 4 showing receive error probability results for the RAKE receivers simulated in these channels under different loading conditions. Conclusion from these results are then presented in Section 5.

2. Receiver Architectures

2.1. DPSK DS-CDMA Receiver

For a DPSK DS-CDMA transmitter, the data is first differentially encoded.

$$d_k = b_k d_{k-1} \qquad \{d_k, b_k\} \in \{1, -1\}, \tag{1}$$

where b_k is the kth information bit, and d_k is the kth differentially encoded bit. The encoded data is then modulated by a high speed spreading code and modulated onto a radio carrier. We will only consider baseband signals for a system with M users. Each users has a spreading code of length N chips. The simulation will assume that the users are chip and data bit synchronous and that all users signals go through the same channel. For a cellular mobile radio system this would be equivalent to simulating a synchronous downlink i.e. the link between the base station and the mobile. The resultant transmitted signal is given by

$$y_k(n) = \sum_{m=0}^{M-1} d_{km} c_m(n) \qquad n \in \{0 \ldots N-1\}, \tag{2}$$

where $y_k(n)$ is the composite output signal at chip n within bit k. d_{km} is kth differentially encoded bit transmitted from the mth user. $c_m(n)$ is the nth chip from the mth user.

At the receiver the signal is downconverted from the RF carrier and the base-band signal $r_k(n)$ is received in the presence of Gaussian noise.

$$r_k(n) = \sum_{m=0}^{M-1} d_{km} c_m(n) + W(n) \qquad n \in \{0 \ldots N-1\}, \tag{3}$$

where $W(n)$ is the noise on chip n. This signal is then correlated with the wanted spreading code for the mth mobile. The post correlation signal for the mth mobile, $x_m(k)$ is therefore obtained,

$$x_m(k) = \sum_{m=0}^{N-1} r_k(n) c_m(n), \tag{4}$$

where the signal $x_m(k)$ represents the kth received post correlation symbol obtained from the mth mobile. We will assume the wanted signal was transmitted from mobile 0, and hence we will only consider the case of $m = 0$. This signal $x_0(k)$ is complex and can be split into real and imaginary components

$$x_0(k) = x_0(k)_I + j x_0(k)_Q, \tag{5}$$

where $x_0(k)_I$ is the real component and $x_0(k)_Q$ is the complex component. From this complex signal $x_0(k)$, the received bit $\hat{b}_{k0}$ is to be obtained. ($\hat{b}_{k0}$ represents the kth received bit from mobile 0.) The original sent bit b_{k0} was differently encoded with the previous bit $d_{(k-1)0}$ to form the transmitted bit d_{k0}. The received bit $\hat{b}_{k0}$ is therefore obtained by evaluating the sign of the real part of the product of $x_0(k)$ and the complex conjugate of $x_0(k-1)$. This effectively implements the DPSK demodulation [11].

$$\begin{aligned} b_{k0} &= \operatorname{sgn}\left[\operatorname{Re}\{x_0(k) x_0^*(k-1)\}\right] \\ &= \operatorname{sgn}\left[\{x_0(k))_I x_0(k-1)_I + x_0(k)_Q x_0(k-1)_Q\}\right], \end{aligned} \tag{6}$$

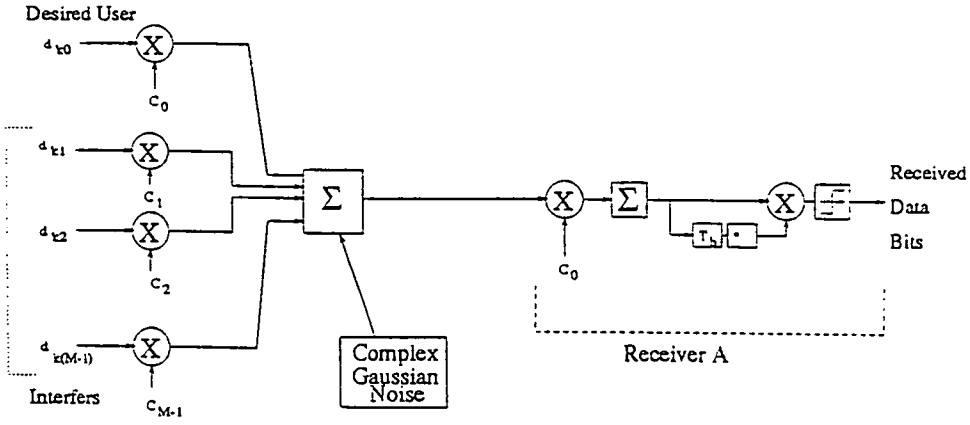

Fig. 1. DS-CDMA system in Gaussian noise using receiver architecture A.

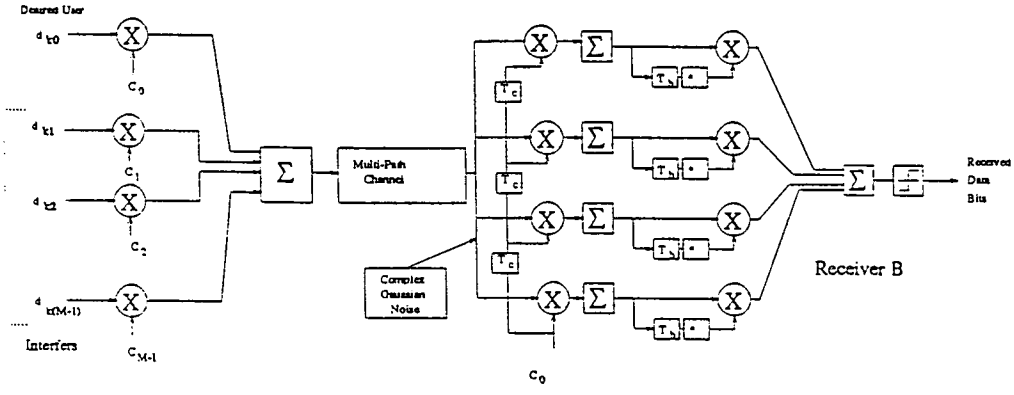

Fig. 2. DS-CDMA system in the 4-path channel using receiver architecture B.

where sgn $[x]$ is the Signum function of x. If the received bit $\hat{b}_{k0}$ does not equal the sent bit b_{k0} an error has occurred. The described DPSK DS-CDMA system is shown in Fig. 1. This receiver is suitable when the transmission channel contains only one path. In situations where the transmission medium is a multipath, a time domain RAKE receiver can be used.

2.2. The DPSK DS-CDMA Time Domain RAKE Receiver

If the multipath channel has a delay spread of D, the DS-SS RAKE receiver can resolve and combine $1 + D/T_c$ multipath components, where T_c represents the duration of a chip. We shall use a channel with a delay spread of $3T_c$. This is shown in Fig. 9. (The channel is explained in more detail in Section 3.2.) The time domain RAKE Receiver can therefore resolve 4 paths in this channel and is shown in Fig. 2. Here the received signal is multiplied by 3 delayed versions of the local spreading code, each delayed by multiples of the chip duration T_c. The received data bit is for mobile 0 and is therefore given by,

$$\hat{b}_{k0} = \operatorname{sgn} \sum_{l=0}^{L-1} [\mathrm{Re}\{x_{l0}(k) x_{l0}^*(k-1)\}] \tag{7}$$

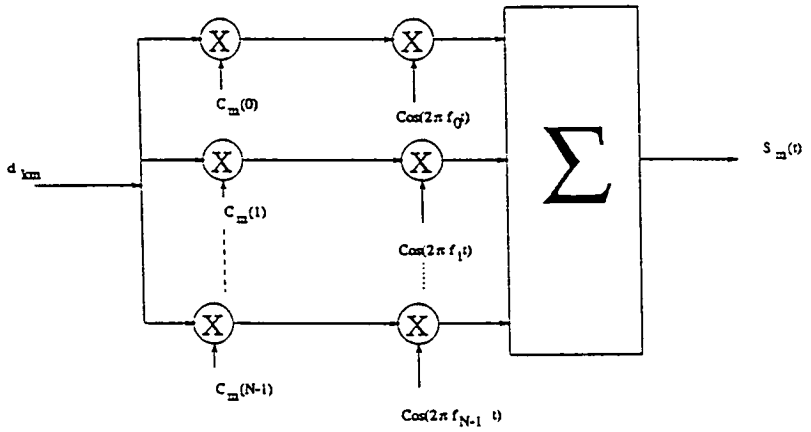

Fig. 3. MC-CDMA transmitter.

$$= \operatorname{sgn} \sum_{l=0}^{L-1} [\{x_{l0}(k)_I x_{l0}(k-1)_I + x_{l0}(k)_Q x_{l0}(k-1)_Q\}], \tag{8}$$

where $x_{l0}(k)$ is the kth decorrelated symbol for mobile 0 on the lth transmitted path. L is the total number of taps contained in the RAKE receiver. (Equation (5) reduces to equation (4) for $L = 1$.) In this way the multipath signals after decorrelation are combined using differential phase combining (DPC) [11, 12]. In this simulation we will consider $L = 1$ and $L = 4$ corresponding to a single path and 4-path channel.

2.3. The DPSK MC-CDMA Receiver

A MC-CDMA transmitter is shown in Fig. 3. Here each data bit b_k is first differentially encoded in the same way as the DS-CDMA system to form the transmitted symbol d_k. This data symbol is then simultaneously transmitted on N narrowband subcarriers, each separated by $1/T_b$ where T_b is the symbol duration. Each of the N subcarriers is further multiplied by a single chip of the spreading code of length N. The continuous-time signal representation of the baseband signal produced by the mth user, is given by

$$S_m(t) = d_{km} P_{T_b}(t - kT_b) \sum_{n=0}^{N-1} c_m(n) \cos\left(2\pi \left(f_c + \frac{n}{T_b}\right)^t\right), \tag{9}$$

where d_{km} is the kth symbol transmitted from the mth user. $P_{T_b}(t)$ is a unit amplitude pulse which is non-zero in the interval of $[0, T_b]$. f_c represents the carrier frequency of the system. We will only consider baseband signals, thus $f_c = 0$. It is important to note that this MC-CDMA does not use a guard interval. To reduce the number of RF mixers required, the bank of mixers can be implemented by sampling the signal and using the Inverse Fast Fourier Transform (IFFT). The output of this IFFT is then transmitted in a serial format. This is shown in Fig. 4. The discrete time representation of the baseband signal produced by the mth user in this system is given by

$$S_m(i) = d_{km} P_{T_b}(i - kN) \operatorname{Re}\left[\sum_{n=0}^{N-1} c_m(n) e^{j2\pi(ni/N)}\right]. \tag{10}$$

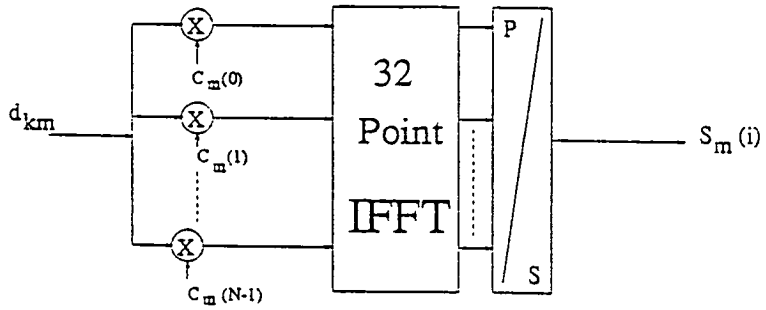

Fig. 4. MC-CDMA serial transmitter.

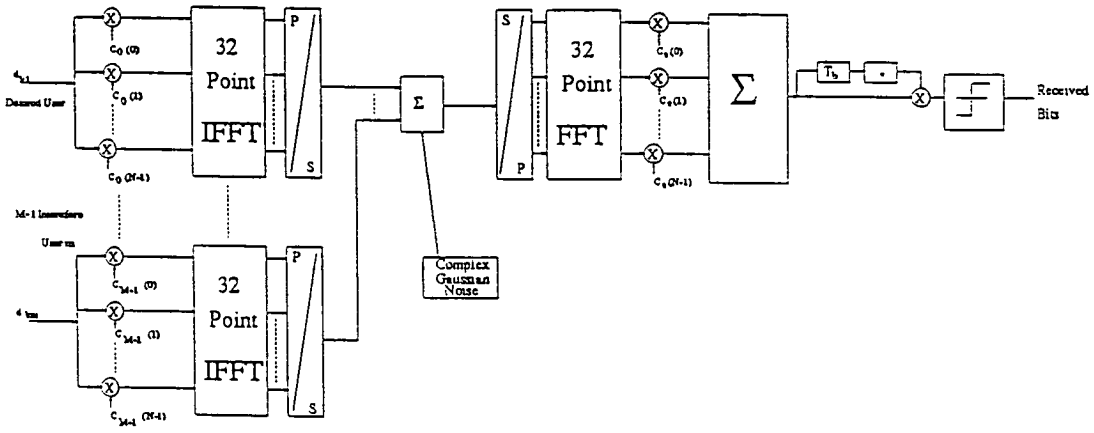

Fig. 5. MC-CDMA system in Gaussian noise using receiver architecture C.

The received MC-CDMA signal is downconverted to baseband and sampled at the chip rate to form the incoming signal $r_k(n)$, which represents the nth chip from the kth transmitted bit. The signal is then serial to parallel converted. These parallel samples are the inputs to an N-point FFT. The outputs of the FFT operation are multiplied by the receiver spreading code to form $\hat{d}_{k0}(n)$ which represents the decorrelated chips from the kth symbol for mobile 0.

$$\hat{d}_{k0}(n) = c_0(n) \sum_{m=0}^{N-1} r_k(n-m) e^{-j\pi(mi/N)} \qquad n \in \{0 \ldots N-1\}. \tag{11}$$

These are then summed to from the kth decorrelated symbol $x_0(k)$.

$$x_0(k) = \sum_{n=0}^{N-1} \hat{d}_{k0}(n). \tag{12}$$

The decision variable is therefore obtained as in the DS-CDMA receiver by multiplying $x_0(k)$ by the complex conjugate of $x_0(k-1)$,

$$\hat{b}_{k0} = \text{sgn}\,[\text{Re}\{x_0(k)x_0^*(k-1)\}]. \tag{13}$$

This receiver architecture with Gaussian noise is shown in Fig. 5.

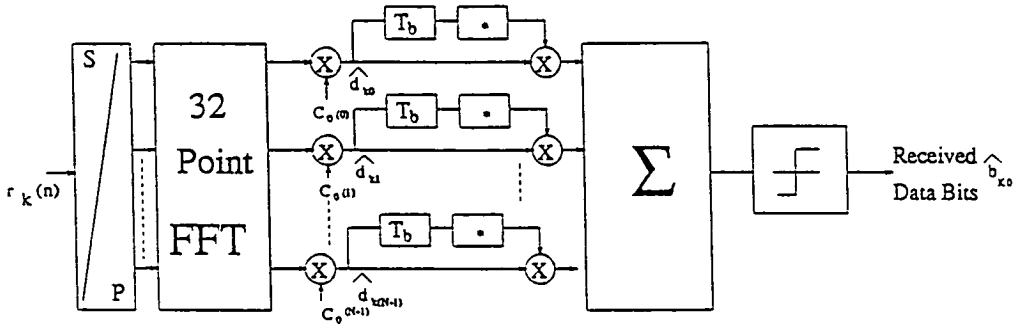

Fig. 6. Receiver architecture D – MC-CDMA frequency domain RAKE receiver.

2.4. The MC-CDMA Frequency Domain RAKE Receiver

Our MC-CDMA frequency domain RAKE receiver is shown in Fig. 6. As in architecture C the received signal is downconverted to baseband and sampled at the chip rate to form the incoming signal $r_k(n)$. These parallel samples are the inputs to a N-point FFT. The outputs of the FFT operation are multiplied by the receiver spreading code. The effects of the multipath channel are then equalised out by multiplying each chip sample (sent on a different carrier) of the kth transmitted symbol $\hat{d}_{k0}(n)$, by its previous value $\hat{d}_{(k-1)0}(n)$. In this way a soft DPSK demodulation is performed for each carrier and the effects of the channel are equalised, once the signals are combined. If the channel does not change between two successive received bits, the results of this operation will yield a value with no complex component (ignoring the effects of noise). In a frequency selective channel different carriers will experience different attenuations. The results of the DPSK soft decisions are summed to form the decision variable

$$\hat{b}_{k0} = \operatorname{sgn}\left[\sum_{n=0}^{N-1} \operatorname{Re}\{\hat{d}_{k0}(n)\hat{d}^*_{(k-1)0}(n)\}\right] \tag{14}$$

$$= \operatorname{sgn}\left[\sum_{n=0}^{N-1} \{\hat{d}_{k0}(n)_I\hat{d}_{(k-1)0}(n)_I + \hat{d}_{k0}(n)_Q\hat{d}_{(k-1)0}(n)_Q\}\right], \tag{15}$$

where d_{k0} is given by equation (11).

3. Simulation Results

Monte Carlo simulations were conducted for both the MC-CDMA and the DS-CDMA systems. Both systems use a 31-length Gold code as the spreading sequence. (In a traditional multicarrier system a guard interval is used, which absorbs the multipath. In these systems orthogonal sequence such as Walsh codes are used as the orthogonality is maintained in the single path channel. The performance of Walsh codes is similar to Gold codes for a matched filter receiver in a multipath channel as the orthogonality is not maintained.) A 32-point IFFT and FFT were used in the case of MC-CDMA with the last point zero padded. The baseband data rate in both systems was fixed at 8 kbits/s, yielding a chip rate of 248 kbits/s for the DS-CDMA system. Random data was transmitted and a minimum of 1000 errors were logged for every point plotted on the bit error rate (BER) graphs.

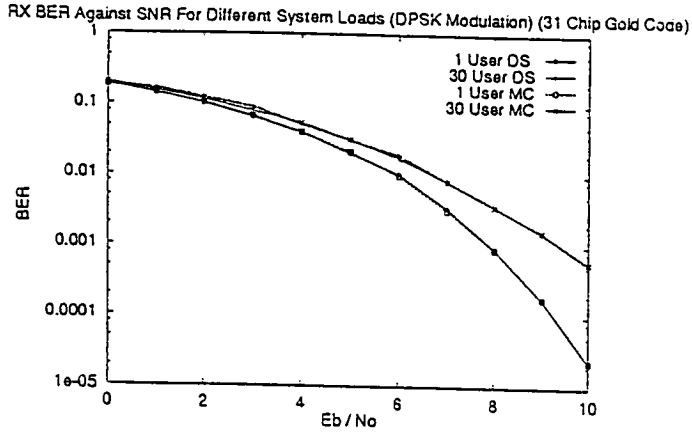

Fig. 7. Receivers A and C (DS and MC matched filter) in Gaussian noise channel.

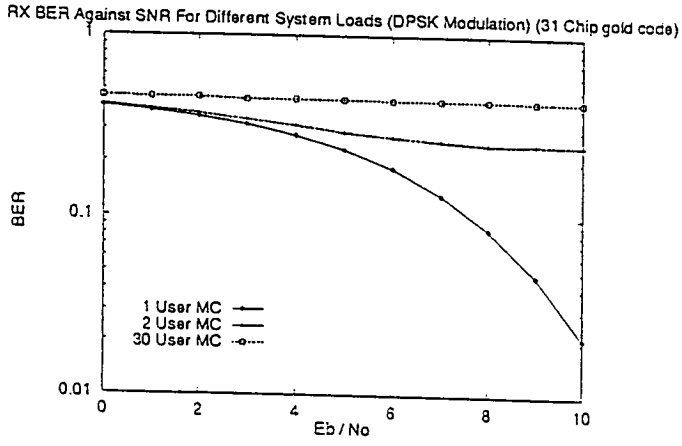

Fig. 8. Receiver D (frequency domain RAKE receiver) in Gaussian noise channel.

3.1. Simulation Results in Gaussian Noise

Receiver architectures A, C and D are simulated in the presence of Gaussian noise and multi-user interference. The results for receivers A and C (the DS and MC matched filter receivers) are seen in Fig. 7, and in Fig. 8 for receiver D (the frequency domain RAKE). As can be seen in Fig. 7, architectures A and C perform identically in the presence of white Gaussian noise for 1 and 30 users. The performance of receiver architecture D (Fig. 8), for the single user at a bit error rate of 2×10^{-2} is, however, approximately 5 dB worse than architectures A and C. The irreducible BER of 3×10^{-1} has already been reached at an E_b/N_o value of 7 with only two users. For a single user the frequency domain RAKE receiver performs worse than architectures A and C, because the 31 'soft' decision DPSK demodulators produce excess noise. The orthogonality of the code sequence is also destroyed. We will however show that the performance improves in a multipath channel.

3.2. The Multipath Channel

For the simulations conducted in a multipath channel (architectures A, B, C and D) we have adopted 1 and 4-path channel models with additive white Gaussian noise (AWGN). The mean

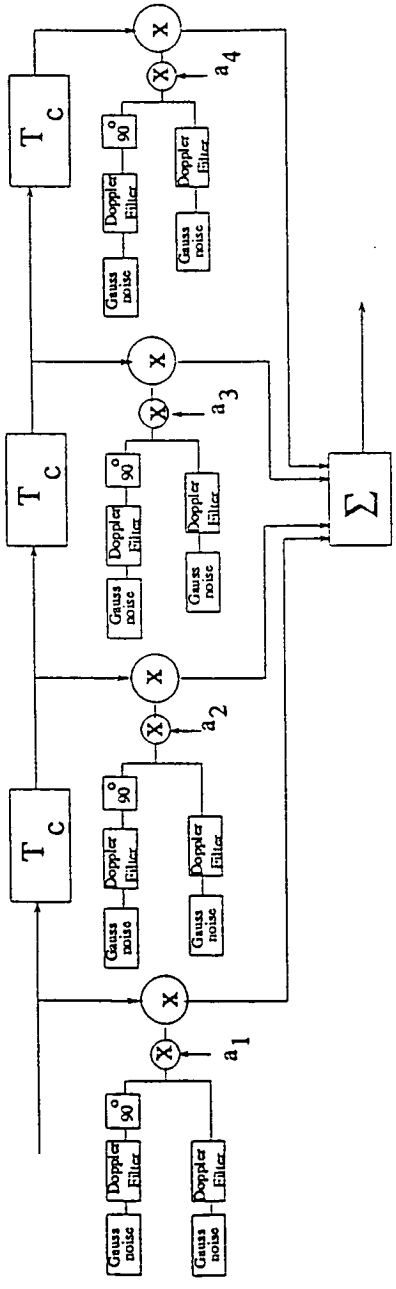

Fig. 9. 4-path time domain multipath channel.

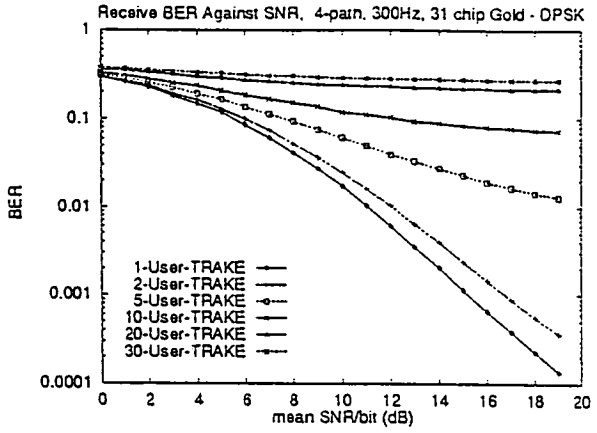

Fig. 10. Architecture B – time domain RAKE – 4-path Rayleigh fading.

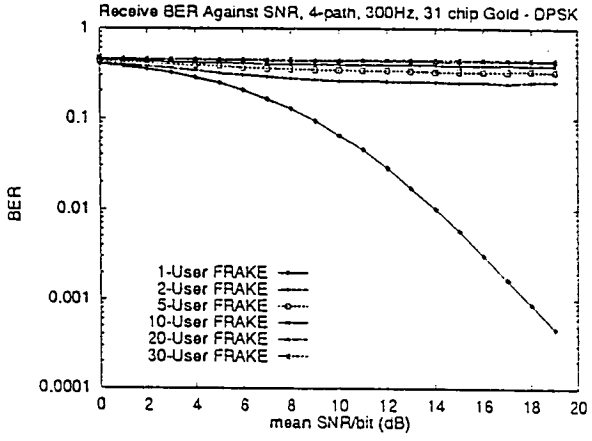

Fig. 11. Architecture D – frequency domain RAKE - 4-path Rayleigh fading.

power for all channels is assumed to be 1. The 4-path channel model is seen in Fig. 9. In this model the scaling factors are set to $a_1 = a_2 = a_3 = a_4 = 0.5$. For the single path channel $a_1 = 1.0$. In the 4-path channel the tap delays are equally spaced at the chip duration, T_c, with independent Rayleigh fading on each path. The Rayleigh fading is characterized by the presence of the Doppler filter. The sampling rate of the Doppler filter was fixed at 992 Hz which is 250 times slower than the chip rate of 248 kbits/s. Therefore linear interpolation is performed between successive outputs of the digital filter. This ensures that the characteristics of the channel are updated at the chip rate. A classical Doppler spectrum [13] is used with a maximum Doppler rate of 300 Hz which corresponds to a mobile speed of 162 km/h for a carrier frequency of 2 Ghz. In all multipath simulation architectures A, B, C and D were compared.

3.3. Error Probability in 4-Path Fading

Results for architectures A, B. C and D are seen in Figs. 12, 10, 13 and 11 respectively, for the 4-path fading model with 300 Hz maximum Doppler shift. Architecture B, the time domain RAKE receiver (TRAKE) achieves the best performance for the single user (see

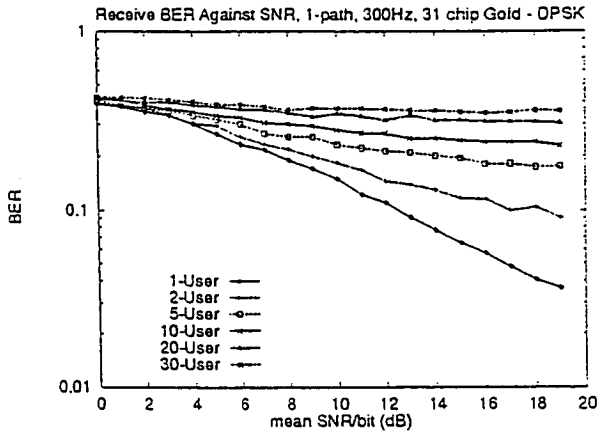

Fig. 12. Architecture A – DS-CDMA receiver – 4-path Rayleigh fading.

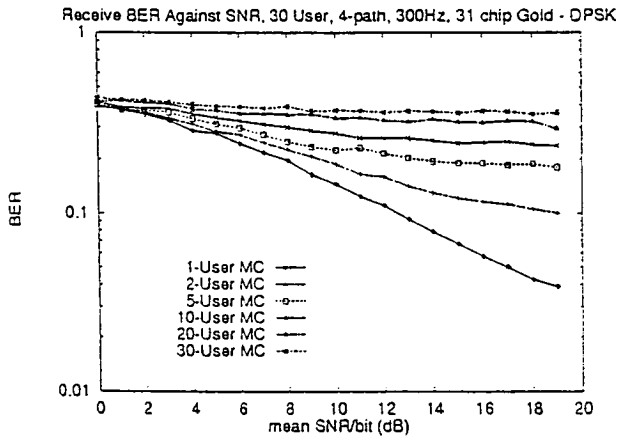

Fig. 13. Architecture C – MC-CDMA receiver – 4-path Rayleigh fading.

Fig. 10). The BER increases gradually with increasing load. It can be seen for 10 users, that the irreducible BER of 7×10^{-2} is reached at an SNR of 18 dB. The performance of architecture D, the frequency domain RAKE (FRAKE) has worse performance than the time domain RAKE, for the single user. The performance is approximately 3 dB worse at a receive BER of 1×10^{-3}, but the received BER increases rapidly with increasing load. For two users the irreducible the BER of 0.25 is already reached at an SNR of 10 dB. Architectures A and C have much worse performance than B and D for the single user, as no effort has been made to equalise the received signals on the different carriers. The performance of these architectures would improve if a guard interval is used. The performance of architectures A and C are however better than architecture D for multiple users. This occurs as the soft decision DPSK demodulated in architecture D, works very well in coherently combining the signals on the different carriers for the single user. However, it also acts a form of maximal ratio combining (MRC) on each of the individual carriers. When multi-user interference is present on each of the individual carriers, this combining will more heavily weight the carriers with the most interference as the processing gain on each of the individual carriers is one.

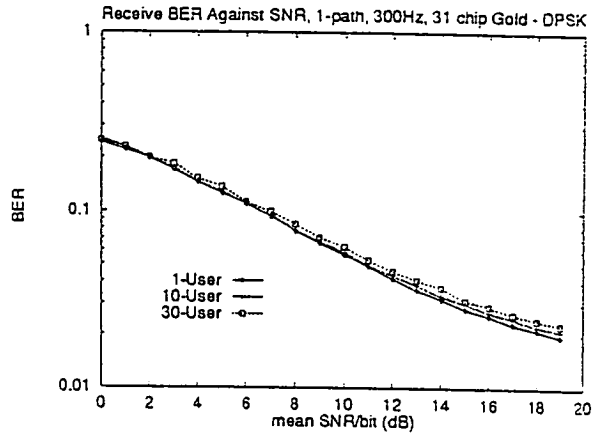

Fig. 14. Architectures A/B – time domain RAKE - 1-path Rayleigh fading.

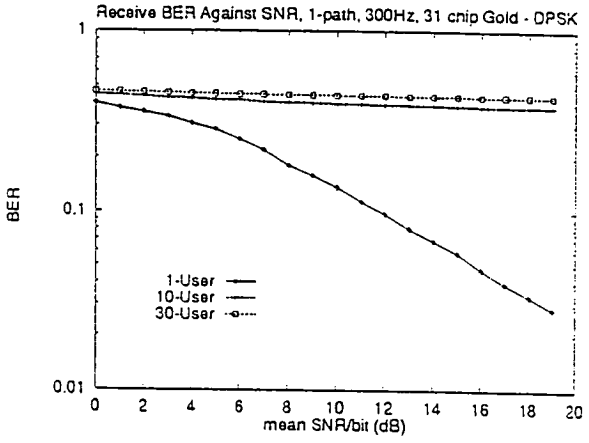

Fig. 15. Architecture D – frequency domain RAKE – 1-path Rayleigh fading.

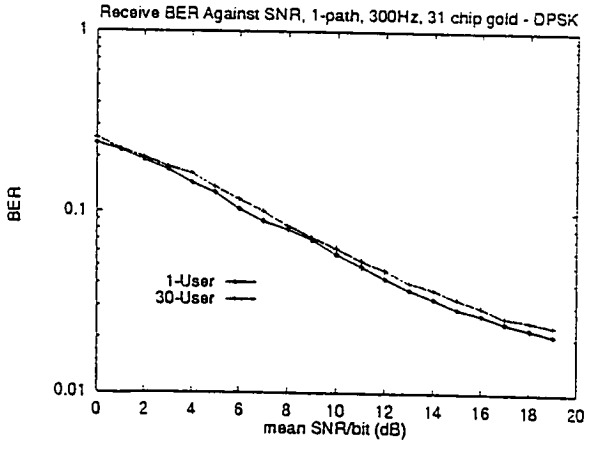

Fig. 16. Architecture C – MC-CDMA receiver – 1-path Rayleigh fading.

3.4. Error Probability in 1-Path Fading

The results in the 1-path Rayleigh fading channel are seen in Figs. 14, 16 and 15 for architectures A, C and D respectively. Architecture B reduces to architecture A for the 1-path fading case. By referring to Fig. 14, it can be seen that architecture B for a single user, has higher BER than in the 4-path fading channel (Fig. 10). This results is to be expected. For a load of 30 users however the received BER is lower than in the 4-path channel. This results is also to be expected and illustrates that the channel imperfections caused by the Rayleigh fading dominate those caused by the multi-user interference.

By referring to Fig. 15, it can be seen that FRAKE has higher BER than in the 4-path (Fig. 11) channel. The difference in performance between architecture D and C is 5 dB at a receive BER of 3×10^{-2}. This difference is the same as observed in the Gaussian channel and occurs because the "soft" decision produces more noise than the hard decision. It can be seen that architecture C (Fig. 16) has comparable performance to the TRAKE (Fig. 14). This again illustrates that architecture D is superior to architecture C, for multi-user interference, but cannot combine multipath signals.

4. Conclusions

MC-CDMA has been used in conjunction with a frequency domain RAKE (FRAKE) receiver. This has been compared to a time domain RAKE receiver which is matched to the time spread of the channel. The MC-CDMA RAKE receiver is used without a guard interval and the channel dispersion relates to a correlation between the fading of the carriers (coherence bandwidth). An increase in time dispersion in the channel results in a reduced coherence bandwidth and a increase in diversity. To use this effect the frequency domain RAKE receiver differentially equalises the individual carriers. The performance of the frequency domain RAKE receivers increases with increasing channel dispersion. We have shown that, for a single user, in both the Gaussian and single path Rayleigh fading channels the frequency domain RAKE receiver performs approximately 5 dB worse than DS matched filter receiver at a BER of 3×10^{-2}. However, in the 4-path channel the frequency domain RAKE receiver performs approximately 3 dB worse than the time domain RAKE receiver for the single user at a BER of 1×10^{-4}. To achieve this no knowledge of the channel dispersion is needed. This is in contrast to a time domain RAKE receiver, which requires channel dispersion information. For more than one user, however, the performance of the frequency domain RAKE receiver rapidly decreases. In high load conditions the performance of the MC receivers with hard decision DPSK demodulation have lower BER performance than the FRAKE (architecture D). The performance of the MC receiver (architecture C) would improve if a guard interval is used, but the frequency domain RAKE receiver will not operate in the manner described if a guard interval is used.

Acknowledgement

The authors would like to thank the Engineering and Physical Sciences Research Council and Roke Manor Research Ltd. in supporting this research programme.

References

1. L. Cimini, "Analysis and simulations of a digital mobile channel using orthogonal frequency division multiplexing," IEEE Trans. Commun., Vol. COM-33, pp. 665–675, 1985.
2. C. Reiners and H. Rohling, "Multicarrier/transmission technique in cellular mobile communications systems," Proceedings IEEE VTC'94, pp. 1645–1649, 1994.
3. M. Alard and R. Lasselle, "Principles of modulation and channel coding for digital broadcasting for mobile receivers," EBU Review, pp. 168–190, 1987.
4. A. Chouldy, A. Brajal, and S. Jourdan, "Orthogonal multicarrier techniques applied to direct sequence spread spectrum CDMA systems," IEEE Globecom 93, Vol. 3, pp. 1723–1728, 1993.
5. K. Fazel, "Narrow-band interference rejection in orthogonal multi-carrier spread-spectrum communications," IEEE Int. Conference on Universal Personal Communications, pp. 46–50, 1994.
6. K. Fazel, "Performance of CDMA/OFDM for mobile communications," IEEE Int. Conference on Universal Personal Communications, pp. 975–979, 1993.
7. K. Fazel, "Performance of convolutional coded CDMA/OFDM in a frequency-time selective fading Channel and its near–far resistance," IEEE Int. Conference on Communications (ICC), New Orleans, USA, pp. 1438–1442, 1994.
8. N. Yee, J. Linnartz, and G. Fettweiss, "Multi-carrier CDMA in indoor wireless radio networks," IEICE Trans. Commun., Vol. E77-B, pp. 900–904, 1994.
9. G. Turin, "The effects of multipath and fading on the performance of direct sequence CDMA systems," IEEE Journal Sel. Areas Commun., Vol. SAC-2, pp. 597–603, 1984.
10. G. Fettweiss, A. Bahnai, and K. Anvari, "On multi-carrier code division multiple access (MC-CDMA) modem design," Proceedings IEEE VTC'94, pp. 1670–1674, 1994.
11. J. Proakis, Digital Communications. New York: McGraw-Hill, 2nd ed., 1983.
12. G. Povey, P. Grant, and R. Pringle, "A decision-directed spread spectrum rake receiver for fast fading mobile channels," Proceedings IEEE VTC'94, pp. 742–746, 1994.
13. M. Failli, ed., Digital Land Mobile Radio Communications – COST 207: Final Report. Luxembourg: Commission of the European Communities, 1989.

Richard A. Stirling-Gallacher was born in Kent, England in 1968. He received a MEng from Southampton University in 1990. Between 1990 and 1993 he worked as a Development Engineer at Motorola in the UK and Philips Kommunikations Industrie, Germany. In 1994 he was Research Associate at the University of Edinburgh. He is currently studying towards a PhD in spread spectrum communications. His research interests include multicarrier CDMA, spread spectrum communications and satellite communications. Mr. Stirling-Gallacher is an associate member of the IEE and a student member of the IEEE.

Gordon J.R. Povey was born in Glasgow, Scotland in 1963. He received a BSc honours degree in 1989 and a PhD from the University of Edinburgh in 1993. Between 1990 and 1992 he was a research associate at University of Edinburgh in the Department of Electrical Engineering where he studied novel spread spectrum receiver architectures for the British Ministry of Defence. He subsequently became a lecturer in this department in 1992. His research interests include mobile radio systems, spread spectrum communications, satellite communications, traffic telematics and signal processing. He worked with BT Laboratories as a Research Fellow in 1993, and is currently acting as a consultant to the Finnish company Elektrobit. Dr. Povey is a Chartered Engineer and serves on two local Institution of Electrical Engineers committees.

Carrier tracking technique for OFDM signal transmissions

Y.H. Ng, P.M. Grant and R.A. Stirling-Gallacher

Indexing terms: Digital communications, Frequency division multiplexing

Coded orthogonal frequency division multiplex is an attractive technique for broadcast to mobiles. The authors describe a method to identify the frequency offset, due to Doppler etc., and subsequently permit offset compensation to be incorporated in the receiver, prior to performing the data demodulation.

Introduction: This Letter addresses the operation of orthogonal frequency division multiplexed (OFDM) systems. These systems are becoming widely used for digital audio broadcast to mobiles [1, 2] and digital TV distribution [3].

One problem in OFDM systems is that, with Doppler frequency shift, the OFDM carriers alter in frequency and this introduces errors in the receiver. This Letter describes a tracking technique which uses one or more unmodulated pilot tones within the OFDM composite spectrum. These frequencies are measured in the receiver, with an oversize FFT processor, and then offset correction is applied prior to the demodulation of the received OFDM signal. This improves the bit error ratio.

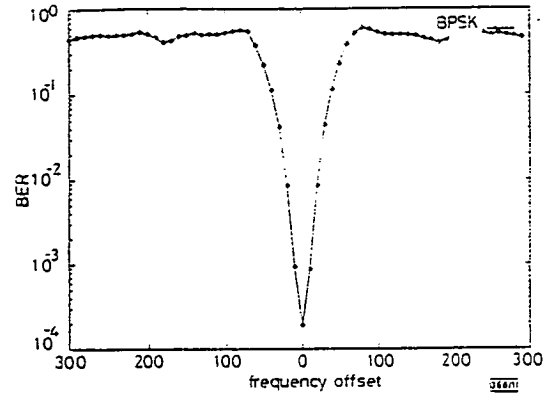

Fig. 1 *Bit error ratio when an offset frequency is introduced onto a 16 channel 32 kbit/s OFDM signal*

Technique: We have investigated techniques to construct a high accuracy spectrum analyser which can identify the movement in unmodulated pilot tone frequencies within an OFDM signal. Fig. 1 shows the increase in bit error ratio (BER) when an offset frequency is introduced onto a simple (uncoded) OFDM signal. The test signal comprised a 16 channel OFDM which was modulated at a 32kbit/s data rate. Here, a frequency offset of only 70Hz reduces the BER from 2×10^{-4} to 0.5.

Initially our investigations concentrated on examining systems which used a synchronisation period where the data were disabled and only unmodulated pilot tones were transmitted on selected OFDM channels, to avoid interference with the data. To measure offset in the pilot tones, the received data vectors were zero padded, and a larger size of receiver FFT [4] was deployed to achieve interpolation and measure, more accurately, the precise frequency of the shifted pilot tones within these synchronisation transmissions. This was successful in our 16 channel demonstration and simulation results showed that when using a 1024-point FFT, with frame-to-frame averaging to reduce noise effects, we could identify the frequency offset from the largest output of the FFT. A frequency correction was then applied in the receiver, by multiplying the input with the identified offset frequency, to enable the data to be demodulated, alleviating the errors in Fig. 1.

This technique suffered from degradation from theoretical performance at low SNR as the post-FFT averaging did not provide sufficiently accurate Doppler estimates.

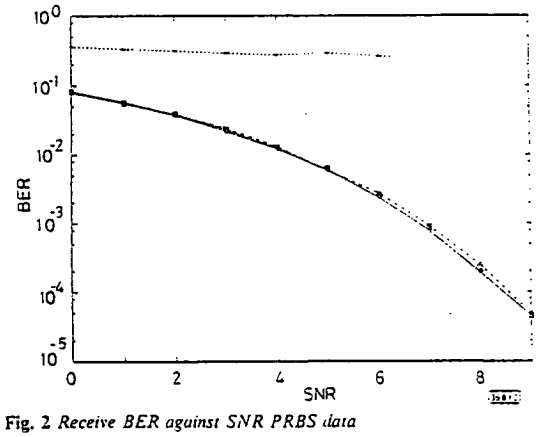

Fig. 2 *Receive BER against SNR PRBS data*

a ◇ PRBS: BER operation without frequency offset
b + no_comp: BER operation with a 50Hz offset but no correction
c □ comp.(4): operation with offset correction for 4 pilot tones
d × comp.(1): one pilot tone only
e - - - theoretical performance without offset

Improved technique: The initial success with the above zero-padded FFT receiver compensation method prompted the investigation of a second technique for achieving corrections within the data traffic, which was simulated using a pseudo-random bit sequence (PRBS). The method also uses an oversize FFT (e.g. 128-point for the 16channel system) and transforms several (e.g. 8) concatenated frames of OFDM traffic which comprises data plus selected channels with unmodulated pilot tones. When performing such a spectrum analysis, the pilot tone(s) sum over the eight frames but the +1/−1 random data traffic is suppressed with respect to the pilot tones. Also the larger 128-point FFT provides the accuracy to measure the Doppler offset and allow this to be applied as a correction at the input of the smaller 16-point FFT, used for data demodulation.

Fig. 2 shows a simulation on our 16-channel system for: *a* BER operation without frequency offset in curve labelled PRBS; *b* BER operation with a 50 Hz offset but no correction (no_comp); *c* operation with offset correction for four pilot tones; *d* operation with offset correction for one pilot tone only; and *e* the theoretical BER performance without offset. Fig. 2*b*, without correction, simply repeats the 50Hz offset result of Fig. 1. With the four pilot tones the offset measured on each tone was averaged over all the pilot tones to give the overall offset correction value to use in the receiver. The 50Hz offset pilot tone had a deviation of 3.3FFT output 'bins' from the zero offset case. The correction system showed that adequate performance is achieved with a single pilot tone, Fig. 2*d*. This system was found not to operate effectively with a smaller 64-point FFT, as the signal record was not long enough to suppress the data with respect to the pilot tone. Even larger sizes of FFT than the 128-point used here may eventually be required to provide sufficient measurement accuracy to identify correctly, arbitrary frequency offset values.

Conclusion: This Letter has described a correction technique for OFDM transmission which uses a larger than normal FFT in the receiver to process over several concatenated frames to measure any frequency offsets. This then permits the effects of frequency offset in the channel to be compensated for, subsequently, in the receiver. Simulations have been performed on a simple 16-channel OFDM system to verify the operation of these techniques over a range of SNR values. These results are promising and now need to be extended to the typical complexities of the practical OFDM systems which will be used for audio and TV broadcast.

9 August 1996

Electronics Letters Online No: 19961361

Y.H. Ng, P.M. Grant and R.A. Stirling-Gallacher (*Department of Electrical Engineering, University of Edinburgh, The King's Buildings, Mayfield Road, Edinburgh EH9 3JL, United Kingdom*)

References

1 SHELSWELL, P.: 'The COFDM modulation system: the heart of digital audio broadcasting', *IEE ECEJ*, 1995, 7, (3), pp. 127–136

2 ALARD, M., and LASSALLE, R.: 'Principles of modulation and channel coding dor digital broadcast to mobile receivers', EBU collected papers on concepts of broadcast into the 21st century, August 1988, pp. 47–69

3 GLEDHILL, J., ANIKHINDI, S.V., and AVON, P.: 'The transmission of digital television in the UHF band using orthogonal frequency division multiplexing', IEE Conf. Proc., September 1991, No. 340, pp. 175–180

4 WEINSTEIN, S.B., and EBERT, P.M.: 'Data transmission by frequency-division multiplexing using the discrete Fourier transform', *IEEE Trans.*, October 1971, COM-19, (5), pp. 628–634

Appendix B
Coherence bandwidth

There are serveral different definitions of coherence bandwidth $(\Delta f)_c$. In this appendix three different defintions are explained and calculations presented for two multipath channels. The purpose of this is to illustrate the ambigiuty of the coherence bandwidth term.

The power spectral density of a multipath channel is characterised by D multipath components. Each multipath component has a delay τ_l and a power β_l. The maximum delay spread is given by T and the RMS delay spread is given by T_m

T_m is given by

$$T_m = \sqrt{E(\tau^2) - E^2(\tau)} \tag{B.1}$$

where $E(\tau^2)$ and $E^2(\tau)$ are given by,

$$E(\tau) = \frac{\sum_{l=1}^{D} \tau_l \beta_l}{\sum_{l=1}^{D} \beta_l} \tag{B.2}$$

$$E(\tau^2) = \frac{\sum_{l=1}^{D} \tau_l^2 \beta_l}{\sum_{l=1}^{D} \beta_l} \tag{B.3}$$

There are serveral different definitions of coherence bandwidth. Prasad [74] defines the coherence bandwith $(\Delta f)_{c1}$ as the reciprocal of the RMS delay spread T_m

$$(\Delta f)_{c1} \approx 1/T_m \tag{B.4}$$

Proakis [14] defines the coherence bandwidth $(\Delta f)_{c2}$ as the reciprocal of the maximum delay spread T

$$(\Delta f)_{c2} \approx 1/T \tag{B.5}$$

Lee [75] defines the coherence bandwidth $(\Delta f)_{c3}$ as the separation in frequency of two carriers so that their correlation is 0.5. $(\Delta f)_{c3}$ is given by

$$(\Delta f)_{c3}1 \approx 1/4\pi T_m \tag{B.6}$$

If we consider a Bad Urban channel (as defined by COST207 [13]) whoose power delay profile is shown in Table B.1,

Table B.1: *BU-12 Delay profile*

Tap No.	Delay μ s	Power (lin)
1	0	0.2
2	0.2	0.5
3	0.4	1
4	0.8	1
5	1.6	0.63
6	2.2	0.25
7	3.2	0.2
8	5.0	0.79
9	6.0	0.63
10	7.2	0.2
11	8.2	0.1
12	10.0	0.03

the different definitions of coherence bandwidth have the following values.

$$(\Delta f)_{c1} \approx 410kHz \tag{B.7}$$

$$(\Delta f)_{c2} \approx 100kHz \tag{B.8}$$

$$(\Delta f)_{c3} \approx 63.91kHz. \tag{B.9}$$

If we consider a channel with 10 taps in which every path has equal power as seen in Table B.2, the different definitions of coherence bandwidth have the following values.

$$(\Delta f)_{c1} \approx 187kHz \tag{B.10}$$

$$(\Delta f)_{c2} \approx 100kHz \tag{B.11}$$

$$(\Delta f)_{c3} \approx 14.87kHz. \tag{B.12}$$

Table B.2: *Delay profile*

Tap No.	Delay μ s	Power (lin)
1	0	0.1
2	1	0.1
3	2	0.1
4	3	0.1
5	4	0.1
6	5	0.1
7	6	0.1
8	7	0.1
9	8	0.1
10	9	0.1

Appendix C

Probability of false alarm

In the presence of no signal and zero mean Gaussian noise the multiplier output of the sign-only correlator is given by

$$\begin{aligned} R_{i_{sign}} + jI_{i_{sign}} = & \quad \text{sgn}(a_i)\text{sgn}(a_{i-ML}) - \text{sgn}(z_i)\text{sgn}(z_{i-ML}) \\ + & \quad j(\text{sgn}(z_i)\text{sgn}(a_{i-ML}) + \text{sgn}(a_i)\text{sgn}(z_{i-ML})) \end{aligned} \tag{C.1}$$

where $\text{sgn}(a_i)$, $\text{sgn}(a_{i-ML})$, $\text{sgn}(z_i)$ and $\text{sgn}(z_{i-ML})$ are all binomial variables with equal probability of ± 1. Both $R_{i_{sign}}$ and $I_{i_{sign}}$ have three possibilities +2.0, 0 and -2.0. Both +2 and -2 have a probability of 0.25 and 0 has a probability of 0.5.

The means of $R_{i_{sign}}$ and $I_{i_{sign}}$ are therefore zero with variance ,

$$\sigma^2 = \sum (z-\mu)^2 p(x) \tag{C.2}$$

$$= 2.0 \tag{C.3}$$

The output of the correlator is given by

$$C_{sign}(y) = \sqrt{\left(\left(\sum_{i=y}^{i=y+N_g} R_{i_{sign}}\right)^2 + \left(\sum_{i=y}^{i=y+N_g} I_{i_{sign}}\right)^2\right)} \tag{C.4}$$

By using the central limit theorem we can assume the sum of the real and imaginary components leads to Gaussian variables of zero mean and variance $2N_g$. The variable $C_{sign}(y)$ is therefore Rayleigh distributed. The probability of false alarm is given by

$$P_{false} = e^{-\frac{threshold^2}{4.N_g}} \tag{C.5}$$